SYSTEMS ANALYSIS OF INTEGRATED BIOMASS TORREFACTION AND DENSIFICATION TECHNOLOGY

by

MARYAM MANOUCHEHRINEJAD

(Under the Direction of Sudhagar Mani)

ABSTRACT

Biomass is a promising renewable energy source for providing a significant contribution to an ever-increasing global energy demand, reducing the GHG emissions, and improving the energy security. However, it is necessary to overcome challenges related to using biomass as a solid biofuel. Torrefaction is a thermal treatment process, where the biomass constituents, mainly hemicellulose, are thermally decomposed under atmospheric pressure. This results in reducing the biomass heterogeneity, changing the fibrous biomass to a more brittle structure like coal, and removing volatiles including hydroxyl and carboxyl groups from the biomass structure. The remaining torrefied solid has higher energy content and hydrophobic nature. The densification process such as pelletization would further increase the energy density of the torrefied pellets, reducing the costs of handling, storage, and transportation. The final torrefied pellet is a potential feedstock for several processes but specifically suited for co-firing with coal in power generation plants.

Since the conventional combined torrefaction and pelletization (TOP) plant has not fully developed yet, in this study, an integrated torrefaction and pelletization process with a new configuration of torrefaction after pelletization (TAP) was proposed and investigated. A

comprehensive process simulation framework was modeled with detailed unit operations, incorporating thermochemical conversion kinetics to study different lignocellulosic biomass feedstocks. The model was validated with the experimental data from torrefaction of two types of commercial wood pellets at a temperature range of 200 to 300°C and process data from the literature. The developed model was used to explore the mass and energy balances, system efficiencies, design parameters for unit operations, and emissions to the environment at different industrial scales.

The techno-economic analysis showed that for a 100,000 Mg yr^{-1} production capacity torrefied pellet plant, the total capital investment of a TAP configuration was around $29.6 million, which was 12% lower than the TOP approach. The production cost and minimum selling price were $166 Mg^{-1} ($6.9 GJ^{-1}) and $197 Mg^{-1} ($8.1 GJ^{-1}) respectively. If the price of torrefied pellets were equivalent to price of wood pellets ($185 Mg^{-1}), the return on investment (ROI) was 15% for a torrefied pellet plant capacity of 200,000 Mg yr^{-1}.

INDEX WORDS: Torrefied pellets, Torrefaction after pelletization, Process simulation, Torrefaction by-products, Techno-economic analysis

SYSTEMS ANALYSIS OF INTEGRATED BIOMASS TORREFACTION AND DENSIFICATION TECHNOLOGY

by

MARYAM MANOUCHEHRINEJAD

B.Sc., Iran University of Science and Technology, Iran, 2004

M.Sc., Iran University of Science and Technology, Iran, 2008

A Dissertation Submitted to the Graduate Faculty of The University of Georgia in Partial Fulfillment of the Requirements for the Degree

DOCTOR OF PHILOSOPHY

ATHENS, GEORGIA

2018

SYSTEMS ANALYSIS OF INTEGRATED BIOMASS TORREFACTION AND DENSIFICATION TECHNOLOGY

by

MARYAM MANOUCHEHRINEJAD

Major Professor:	Sudhagar Mani
Committee:	K.C. Das
	Jim Kastner

Electronic Version Approved:

Suzanne Barbour
Dean of the Graduate School
The University of Georgia
August 2018

DEDICATION

This dissertation is dedicated to women everywhere who still have to work harder for the same recognition of achievement, to international scientists who leave everything behind in the service of the global community and pursuit of truth, and to me who endeavored the last eighteen years dreaming of a better life.

And to my husband and loving family for their true support and motivation.

This is the first step in my new life.

“You yourself are your own obstacle, rise above yourself.”- Hafez.

ACKNOWLEDGEMENTS

I would like to express my gratitude to my supervisor, Dr. Sudhagar Mani, for his support, guidance, and insight throughout this research project. I would like to thank Dr. Jim Kastner, Dr. K.C. Das, and Dr. Dalia Abbas for serving on my committee, and for all of their inputs and advice. I express my deepest appreciation to Dr. Kaveh Rayat for his help and consultancy on development of the process simulation model. I am very thankful to Dr. Nalladurai Kaliyan for discussion and advice on various aspects of this project.

And finally, I would like to thank all my close friends and family. You have all encouraged and believed in me.

TABLE OF CONTENTS

Page

LIST OF TABLES

Page

LIST OF FIGURES

Page

CHAPTER 1

INTRODUCTION AND RESEARCH OBJECTIVES

Introduction

Global population growth, economic development, and living standard advances have dramatically increased the worldwide energy demand in power, transportation, and other sectors over the past few decades, especially in non-OECD countries (countries outside of the Organization for Economic Cooperation and Development). According to the International Energy Outlook 2016 (IEO2016), an estimated 48% rise in worldwide energy demand from 2012 to 2040 will intensify fossil fuel consumption [1], leading to fossil fuel depletion as well as causing significant environmental impacts such as climate change, and health hazards. Several countries have established environmental policies to reduce greenhouse gas (GHG) emissions according to the Kyoto protocol objectives [2–5]. The United States has set targets to reduce greenhouse gas (GHG) emissions up to 17% by 2020 and to 26%-28% by 2025 [6]. In addition to aforementioned reasons, fluctuations in fossil fuel price and economic and political instability in oil-producing regions further drives the need for alternative sources of energy. Among all the renewable energy types, biomass energy has the ability to store and utilize on-demand, contrary to discontinuous solar and wind energies [7]. Biomass is a carbon carrier with the highest share (about 45% in 2017) of the total renewable energy consumed in the United States [8].

The types of biomass available for energy use include wood and wood wastes, agricultural plants, energy crops, aquatic plants, manures, etc. [9]. Despite serious concerns about deforestation and food security, the availability of forest residues and the potential to grow energy crops in

marginal lands promote the sustainable use of biomass for bioenergy applications [10]. Conventional timber and pulp wood harvesting practices in the US leaves excessive amount of forest residues (more than 30%), which affects the forest health by disease spreading and potential for wildfire. Between 2005 and 2014, approximately 628,000 wildfire events occurred in the United States causing a total forest land loss of 65 million acres [11]. Harvesting forest residue can mitigate disastrous wildfires, while also serving as a feedstock to produce biomass pellets for biopower. Removing forest residue can also decrease environmental challenges due to wildfires and pile burnings, while increasing forest health and local job opportunities [12]. The US Billion ton 2016 report by US Department of Energy has estimated that the availability of secondary mill residues, urban wood waste, and other removal residues ranged from 130-141 million dry tons per year [11]. Moreover, biomass grown on marginally fertile lands is another potential sources of biomass, which could reduce the competition with arable lands available for food production [13,14].

The United States total GHG emissions was about 6,511 million metric tons CO_2 in 2016 mainly from transportation, power generation, industries, commercial and residential, and agriculture [15]. Power generation sector is one of the largest contributors (28%) of total GHG emissions with more than 30% of the electricity is generated from coal-fired power generation plants [16]. In order to reduce the GHG emission, biomass co-firing with coal in the existing power generation facilities is one of the least expensive options. For example, a significant number of power generation plants in Europe adapted a co-firing technology (10 to 100%) to mitigate GHG emissions [17]. In the United States, despite the current low percentage of biomass usage (less than 2%) for the power generation, the biomass co-firing power generation plants will be prospered if

high biomass availability, competitive biomass price with high and consistent quality, low transportation costs, and lastly the influential environmental regulations get established [18].

In general, biomass consists of cellulose (30-50% dry basis), hemicellulose (20–40%), lignin (15–25%) and other inorganic fractions, also called as ash (3–10%)[19]. Biomass can be used as a feedstock to produce solid, liquid, and gaseous biofuels [20]. However, it has a number of inherent challenges that prevent its efficient and economic use for producing biofuels, biopower and biochemicals. The non-uniform shape and size, low bulk density, low calorific value, and high moisture content of biomass pose major challenges during handling, transportation and storage for bioenergy application. Moreover, biomass is fibrous and hard to grind, causing increased energy required for size reduction and is highly susceptible to spoilage due to hydrophilic nature [2,4,21,22]. To overcome the above challenges, biomass needs to be preprocessed and pretreated.

Densification, the most common preprocessing method is commercially used, where biomass is dried, size reduced, and extruded or compacted into pellet and briquettes for long-distance transport. Pelletizing and briquetting are two mechanical densification processes that compact ground biomass into a more uniform dense shape, improving energy density and facilitating the flowability and handling of the biomass. Densification can improve the bulk density of biomass about ten times [23]. Type of feedstock, chemical composition, particle size, moisture content, addition of a binder, preheating or steam injection, temperature, type of densification machine, and applied pressure are the major variables that contribute to the quality of densified materials [24,25,34,35,26–33]. So far, pelletizing process produces the only source of globally developed solid biofuels (i.e., pellet) [36]. The United States is one of the largest producers of wood pellets for renewable feedstock purposes [37,38]. The total amount of produced wood pellets in the United States in 2017 were about 8.9 million tons, out of that about 5.2 million tons (more

than 58%) were exported to the United Kingdom and Europe [39]. Although wood pellets can be used in small boilers and heating systems as well as for domestic usages, it is increasingly utilized for co-firing with coal or direct conversion in power generation plants in European utilities mainly due to governmental incentives [38]. However, the differences in compositions and structural variations biomass and coal, and in particular, the higher energy required for size reduction and the lower energy content of biomass compared to that of coal pose major challenges for the advanced development of co-firing technology for the existing power plant facilities in the US [40,41].

Torrefaction is a low temperature pyrolysis process where biomass is heated to a temperature between 200–300°C in an inert environment under atmospheric pressure [42–45]. During torrefaction, hemicellulose content of biomass is thermally decomposed mostly removed the OH functional groups present in biomass, which caused the increased carbon content and calorific value of the remaining biomass, called torrefied biomass[45]. Torrefaction transforms the biomass into a brittle and non-fibrous structure. Furthermore, the removal of polar hydroxyl and carbonyl groups change the biomass from hydrophilic to hydrophobic nature to a certain extend. The hydrophobicity of torrefied biomass reduces the microbial degradation and storage losses. The torrefied biomass with a common characteristics with coal can be used as a solid drop-in biofuel in all relevant applications such as power generation plants, industrial heating services, and domestic usages [42–45]. The most suited application of the torrefied biomass is co-firing with coal in power generation plants that allows the high replacement of coal with torrefied biomass even by 100%, without significant decrease in the system efficiencies [46]. Torrefied biomass is also an attractive precursor for other thermal conversion methods such as pyrolysis and gasification to produce bioenergy.

Gasification is the process of converting biomass to synthesis gas or syngas (i.e., H_2+CO) under a control amount of oxygen. The produced syngas can be combusted directly or used for production of ethanol, methanol, hydrogen, or converted to liquid biofuel through Fischer-Tropsch process [47]. Torrefied biomass with higher calorific value and lower volatiles content would increase the gasification temperature that consequently decreases tar formation and improves the quality of syngas and its conversion efficiency [48–50].

Pyrolysis, and specifically fast pyrolysis, is a thermal treatment similar to torrefaction that takes place at higher temperatures, where the main product is bio-oil. In slow pyrolysis the gaseous and solid products are also produced [20]. Bio-oil contains heavier hydrocarbon molecules of biomass including acetic acid, formaldehyde, formic acid, acetol, furfural, hydroxyl acetaldehyde, levoglucosan, and etc. that can be burned as mixtures in boilers or upgraded to many chemicals [51]. The bio-oil, produced from fast pyrolysis of the torrefied biomass, contains less acidity with higher calorific value and higher stability [52].

Although biomass benefits from several improved properties after torrefaction, the bulk density of the torrefied material still remains poor and, in some cases, lower than the initial raw biomass. A low density adversely affects the handling and flowability as well as the efficient and economical transportation and storage of treated biomass [36,53–55]. Thus, torrefied biomass should be densified to enhance the effective usage of torrefied biomass as a "tradable energy commodity" [56,57]. An integration of torrefaction with proper densification processes offers a synergistic pathway in biomass processing that yields a higher value torrefied biomass with an inherent ease of handling, storage, and transportation.

Integrated torrefaction and pelletizing, known as the TOP process (also called the BO_2 process), was initially developed by Energy Research Centre Netherlands (ECN) [58] to provide

the appropriate feedstock for power plants. In this process, biomass is initially dried and torrefied. The torrefied biomass is sent to the grinding section to reduce the particle size and finally is densified into pellet or briquette (Figure 1.a). The commercial development of torrefaction is currently in its early phase; however, some torrefaction technologies have been tested at pilot scale, and they could penetrate into the commercial market. For instance; a Solvay torrefaction plant in Meridian, MS is operated to produce 40,000 tonne/year of torrefied pellet [59]. Technological advancements in combined torrefaction and pelletizing, specifically focused on reactor types, are developing around the world, especially in Europe, Canada, and North America [59]. There are several publications on modeling torrefaction kinetics and mechanisms [42,60–62], reactor types [63–66], process simulations [67–72], and integrated torrefaction and pelletizing [2,3,73,74]. However, in most cases, torrefaction is implemented before pelletizing. Densification of torrefied material is an energy intensive process. Torrefaction can hinder densification process by weakening the bonding forces between particles; hence, a high die temperature, more compressive pressure, or binding agent is necessary for the densification step [34,75,76]. Most of the earlier studies were dedicated to optimizing the combined torrefaction and pelletizing process to achieve a high-quality product with reasonable energy consumption. Nevertheless, another potential pathway is torrefaction after pelletizing (Figure 1.b).

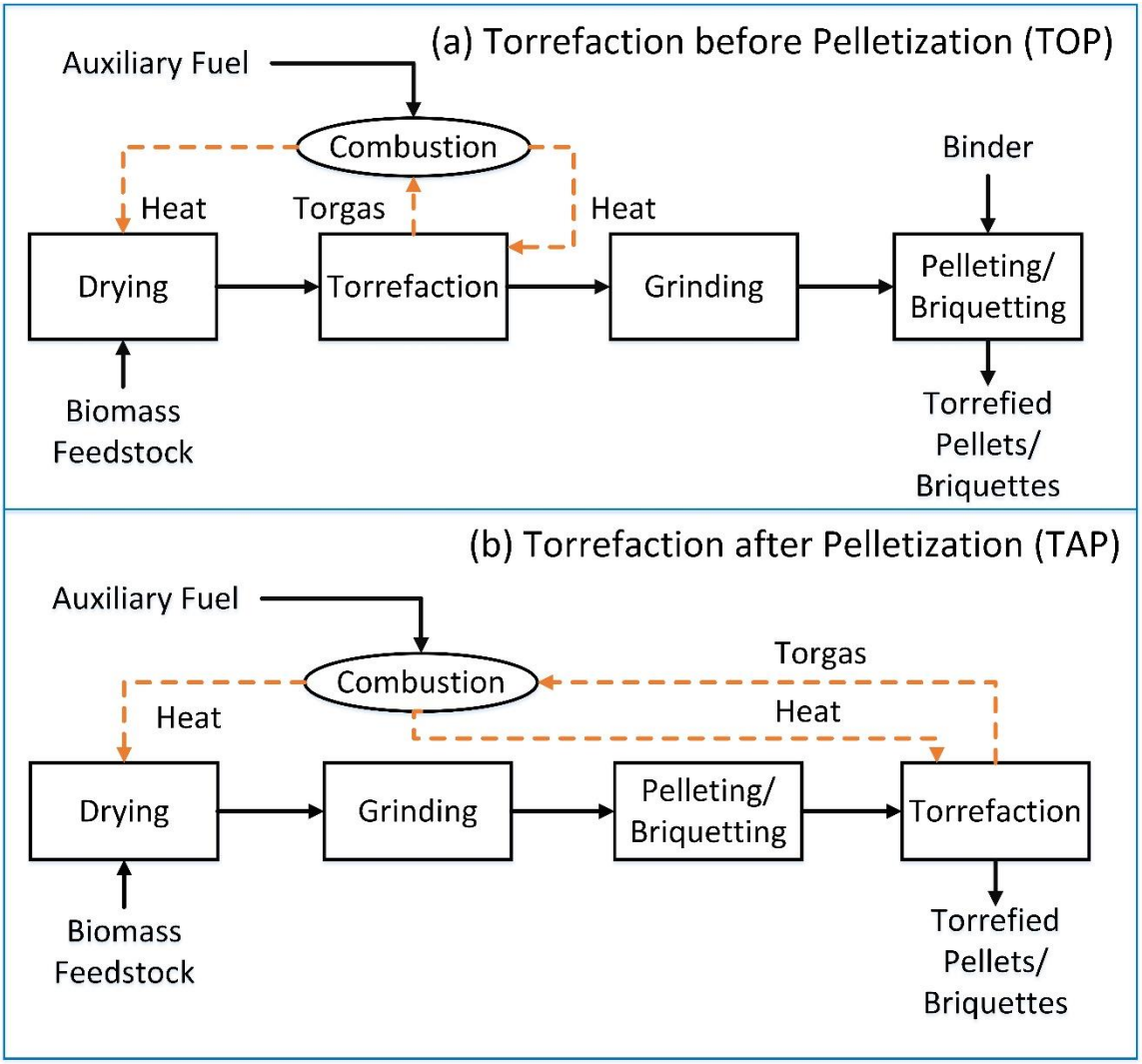

Figure 1-1. Block flow diagram of torrefied pellet production, (a) torrefaction before pelletization (TOP), (b) torrefaction after pelletization (TAP).

Torrefaction after pelletizing could potentially be an easier [56,77] and more cost efficient pathway in producing torrefied pellets. In such a combined scenario, a "dual purpose plant" capable of producing two products (untreated pellet and torrefied pellet) can be achieved or the torrefaction section can be carried out individually at power generation/boiler facilities. Torrefied pellets need to be produced at high quality while the energy consumption is minimized. Nevertheless, the studies on torrefaction after pelletizing are limited [21,36,56,77,78].

Ghiasi et al. [56] studied the torrefaction of wood pellets at a lab scale. They showed that "pelletized and subsequently torrefied materials" have a higher energy/carbon value, reduced

moisture content, and higher stability in water in comparison with pre-torrefied wood pellets. In addition, the traditional method of torrefaction followed by pelletizing without a binding agent is energy intensive [56] while a TAP method was a more promising pathway to reduce the costs of torrefied pellet production. Doassans-Carrère et al. [77] investigated pre- and post torrefaction on several biomass types (wood chips, coniferous barks, olive pits, straw, and pine pellets) and reported that the pre-torrefaction enhanced the grindability of wood chips and olive pits by reducing the cost of the grinding , but by increasing the energy required for densification. On the other hand, the pre-torrefaction method had low impacts on grindability of coniferous barks and straw. The extremely low density straw caused a lower mass flow rate inside the reactor and increases the torrefaction cost per kilogram. Therefore, post-torrefaction (TAP) of straw pellets seemed to be more suitable. In conclusion, they reported that the choice between pre-torrefaction and post-torrefaction was inconclusive, but depends on the feedstock type or integration possibilities [77]. Peng et al. [78] examined the thermal treatment of two commercial pellets and one type of lab-made control pellets at different temperature ranging 270-450°C and compared their properties with conventional torrefied pellets (pellets from torrefied sawdust). Although the calorific value and energy yield of post torrefied pellets were slightly higher and water uptake was lower than that of conventional torrefied pellets, the bulk density and volumetric energy density of post torrefied pellets were lower. Recently, Chen et al. [21] studied the torrefaction of oil palm fiber pellets at temperature range of 275-350°C under inert and oxidative conditions. They also analyzed the condensed liquid product generated during the torrefaction of pellets. The previous literature review suggests further study on the properties of post-torrefied pellets, their energy consumption, and the evaluation of the associated costs.

Depending on the type of biomass, initial moisture content, temperature, and the duration of torrefaction treatment, the mass and energy yield of produced product can be changed. Thus, developing a process model to determine the key torrefaction parameters is essential. Process model is used for optimizing the process to obtain high mass and energy yields along with effective utilization of torgas heat [70]. Furthermore, the design specification of each unit operation are to be analyzed for a complete economic assessment of the process. The main challenges in the simulation of torrefaction are the indeterminate chemical makeup of biomass and complex chemistry of torrefaction [72]. Once the process simulation is done and equipment type, and relevant process parameters are identified together with the mass and energy balance, the process costs analysis can be evaluated.

The economic evaluation of conventional integrated torrefaction and the pelletizing plant was initially carried out by ECN [58] and developed later by Topell Energy [59]. Topell Energy estimated that the total investment cost, including costs of collecting wood, drying equipment, grinding mills, pellet mills, storage, civil workers, and a reactor for torrefaction was approximately \$29 million USD for production of annual 100,000 Mg torrefied pellet [59] which was higher than the previous estimation for ECN model by Bergman et al. [40]. The Batidzirai et al. [70] evaluated the short and long term economic performance of the specific torrefaction concept based on available information of the pilot plants and pre-commercialized technologies. They estimated that short-term production costs for woody biomass torrefied pellets are between \$3.3 and \$4.8 GJ_{LHV}^{-1}, and \$2.1-5.1 GJ_{LHV}^{-1} in the long term. The U.S. Department of Energy at Idaho National Laboratory has recently studied the biomass thermal treatment and production costs of torrefied woodchips by USA southeastern pine feedstock [72]. The process simulation in Aspen Plus and cost evaluation for the production of 20 ton h^{-1} torrefied biomass (southeastern pine) in the field

was conducted within a temperature range of 180°C to 270°C. The total capital cost was about $25 million USD in all cases. The thermal processing cost considering the capital recovery charge was $3.6-7.2 million USD per year corresponds to 24-48 $ ton^{-1} of products for 270°C to 180°C torrefaction temperature.

The main goal is to develop an inclusive model, applicable for both woody material and energy crops and, eventually evaluate the process parameters and cost issues to produce value-added torrefied products.

Objectives

The specific objectives of this research are:

1. To experimentally investigate the torrefaction of biomass to determine products yield, compositions and the grinding properties of solid product.
2. To develop a process based plant simulation model to determine the mass and energy balances for the integrated torrefaction and pelleting plant (both TOP and TAP pathways). The model would apply to a wide range of feedstock types through woody biomass to energy crops.
3. To conduct a techno-economic assessment of integrated torrefaction and densification plant (TOP and TAP pathways) to estimate capital investment, production cost and minimum selling price of torrefied solid fuel for heat and power generation.

This study will provide a clear understanding of torrefaction energy consumptions, product quality, and cost issues of producing torrefied solid biofuel. The plant simulation model will be used to evaluate the effects of various process parameters on the production cost and environmental impacts. The developed model could be used to conduct process hazard analysis (PHA) to improve plant performances and process/product safety.

Dissertation organization

This dissertation focused on the experimental analysis and process simulation of the torrefied wood pellet production for the main goal of co-firing with coal in power generation plants. The organization of dissertation is outlined as below:

In Chapter 2, the literature is reviewed for biomass properties, densification process, torrefaction process, and integrated torrefaction and pelletization process. The various torrefaction kinetics and reactor types are studied. The reports on process simulation, life cycle analysis, and economical evaluation are investigated. Moreover, the key technical standards and potential hazard of solid biofuels are explored.

Chapters 3 to 7 are manuscript-based chapters and manuscripts are either submitted or to be submitted to peer-reviewed international journals. The experimental investigation of torrefaction of two commercial wood pellets and studying the products yields and properties are discussed in Chapter 3. Chapter 4 contains the grindability of the torrefied wood pellets compared to that of torrefied wood chips to determine the grinding parameters and Hardgrove Grindability Index (HGI). The process simulation framework for the integrated torrefaction and pelletization process is discribed in Chapter 5. In the same chapter, the mass and energy balance and system efficiency of the conventional TOP process at different torrefaction temperatures are validated and discussed. Chapter 6 discusses the techno-economic analysis of the integrated torrefaction and pelletization in both TOP and TAP configurations. The process simulation results of the TOP and TAP are compared at different torrefaction temperatures and different plant capacities. In the same chapter, the capital cost, production cost, and minimum selling price of the torrefied pellet production are evaluated including the sensitivity analysis and profitability study in detail.

Chapter 7 contains the main conclusions and recommendations for future works. The supplementary information of the manuscripts are attached in the Appendix section.

References

[1] U.S. Energy Information Administration. International Energy Outlook 2016. vol. 0484(2016). 2016. doi:www.eia.gov/forecasts/ieo/pdf/0484(2016).pdf.

[2] Chen WH, Peng J, Bi XT. A state-of-the-art review of biomass torrefaction, densification, and applications. Renew Sustain Energy Rev 2015;44:847–66. doi:10.1016/j.rser.2014.12.039.

[3] Agar D, Gil J, Sanchez D, Echeverria I, Wihersaari M. Torrefied versus conventional pellet production – A comparative study on energy and emission balance based on pilot-plant data and EU sustainability criteria. Appl Energy 2015;138:621–30. doi:10.1016/j.apenergy.2014.08.017.

[4] Chew JJ, Doshi V. Recent advances in biomass pretreatment–Torrefaction fundamentals and technology. Renew Sustain Energy Rev 2011;15:4212–22.

[5] Nations U. Kyoto Protocol To the United Nations Framework Kyoto Protocol To the United Nations Framework. vol. 7. 1998. doi:10.1111/1467-9388.00150.

[6] Mccarthy JE, Ramseur JL, Leggett JA, Wyatt AM, Dolan AM. EPA's Clean Power Plan for Existing Power Plants: Frequently Asked Questions. U.S.: 2016.

[7] Mcnamee P, Adams PWR, Mcmanus MC, Dooley B, Darvell LI, Williams A, et al. An assessment of the torrefaction of North American pine and life cycle greenhouse gas emissions. Energy Convers Manag 2016;113:177–88. doi:10.1016/j.enconman.2016.01.006.

[8] U.S. Energy Information Administration. Monthly Energy Review April 2018. US Dep

Energy, Washington, DC 2018.

[9] McKendry P. Energy production from biomass (part 1): Overview of biomass. Bioresour Technol 2002;83:37–46. doi:10.1016/S0960-8524(01)00118-3.

[10] Gao Y, Skutsch M, Masera O, Pacheco P. A global analysis of deforestation due to biofuel development 2011;68.

[11] U.S. Department of Energy. 2016 Billion-Ton Report: Advancing Domestic Resources for a Thriving Bioeconomy, Volume 1: Economic Availability of Feedstocks. M H Langholtz, B J Stokes, L M Eat (Leads), Oak Ridge Natl Lab Oak Ridge, TN 2016;I:448. doi:ORNL/TM-2016/160.

[12] Mitchell KA, Collaborative CB, Davis U, Parker NC. Draft Report: Potential for Biofuel Production from Forest Woody Biomass 2015.

[13] Sims REH, Hastings A, Schlamadinger B, Taylor G, Smith P. Energy crops: current status and future prospects. Glob Chang Biol 2006;12:2054–76.

[14] FAO Forestry Paper. Forestry for a low-carbon future; Integrating forests and wood products in climate change strategies. Rome: 2016.

[15] U.S. Environmental Protection Agency. Inventory of U.S. Greenhouse Gas Emissions and Sinks 1990-2016. n.d.

[16] EIA Energy Information Administration- Independent Statistics and Analysis. International Energy Outlook 2017 Overview. US Energy Inf Adm 2017;IEO2017:143. doi:www.eia.gov/forecasts/ieo/pdf/0484(2016).pdf.

[17] Roni MS, Chowdhury S, Mamun S, Marufuzzaman M, Lein W, Johnson S. Biomass co-firing technology with policies, challenges, and opportunities: A global review. Renew Sustain Energy Rev 2017;78:1089–101. doi:10.1016/j.rser.2017.05.023.

[18] Goerndt ME, Aguilar FX, Skog K. Drivers of biomass co-firing in U.S. coal-fired power plants. Biomass and Bioenergy 2013;58:158–67. doi:10.1016/j.biombioe.2013.09.012.

[19] Lee D, Owen VN, Boe A, Jeranyama P. Composition of Herbaceous Biomass Feedstocks. 2007.

[20] Basu P. Biomass gasification, pyrolysis and torrefaction: practical design and theory. Academic press; 2013.

[21] Chen W-HH, Zhuang Y-QQ, Liu S-HH, Juang T-TT, Tsai C-MM. Product characteristics from the torrefaction of oil palm fiber pellets in inert and oxidative atmospheres. Bioresour Technol 2016;199:367–74. doi:10.1016/j.biortech.2015.08.066.

[22] van der Stelt MJC, Gerhauser H, Kiel JHA, Ptasinski KJ. Biomass upgrading by torrefaction for the production of biofuels: A review. Biomass and Bioenergy 2011;35:3748–62. doi:10.1016/j.biombioe.2011.06.023.

[23] Wright CT, Kenny KL, Hess JR, Tumuluru JS. A Review on biomass densification technologies for energy application. Idaho Natl Lab Idaho Falls, Idaho 83415 2010:96. doi:INL/EXT-10-18420.

[24] Križan P, Beniak J, Šooš Ľ, Matúš M. Influence of densification process and material properties on final briquettes quality from fast-growing willows. Energy 2015;577:37194.

[25] Kaliyan N, Morey RV. Natural binders and solid bridge type binding mechanisms in briquettes and pellets made from corn stover and switchgrass. Bioresour Technol 2010;101:1082–90. doi:10.1016/j.biortech.2009.08.064.

[26] Muazu RI, Stegemann J a. Effects of operating variables on durability of fuel briquettes from rice husks and corn cobs. Fuel Process Technol 2015;133:137–45. doi:10.1016/j.fuproc.2015.01.022.

[27] Felfli FF, Mesa P JM, Rocha JD, Filippetto D, Luengo C a, Pippo WA. Biomass briquetting and its perspectives in Brazil. Biomass and Bioenergy 2011;35:236–42. doi:http://dx.doi.org/10.1016/j.biombioe.2010.08.011.

[28] Carroll JP, Finnan J. Physical and chemical properties of pellets from energy crops and cereal straws. Biosyst Eng 2012;112:151–9. doi:10.1016/j.biosystemseng.2012.03.012.

[29] Yumak H, Ucar T, Seyidbekiroglu N. Briquetting soda weed (Salsola tragus) to be used as a rural fuel source. Biomass and Bioenergy 2010;34:630–6. doi:10.1016/j.biombioe.2010.01.006.

[30] Kaliyan N, Morey RV. Densification characteristics of corn cobs. Fuel Process Technol 2010;91:559–65. doi:10.1016/j.fuproc.2010.01.001.

[31] Liu Y, Wang X, Xiong Y, Tan H, Niu Y. Study of briquetted biomass co-firing mode in power plants. Appl Therm Eng 2014;63:266–71. doi:10.1016/j.applthermaleng.2013.10.041.

[32] Theerarattananoon K, Xu F, Wilson J, Ballard R, Mckinney L, Staggenborg S, et al. Physical properties of pellets made from sorghum stalk, corn stover, wheat straw, and big bluestem. Ind Crops Prod 2011;33:325–32. doi:10.1016/j.indcrop.2010.11.014.

[33] Zamorano M, Popov V, Rodríguez ML, García-Maraver A. A comparative study of quality properties of pelletized agricultural and forestry lopping residues. Renew Energy 2011;36:3133–40. doi:10.1016/j.renene.2011.03.020.

[34] Mani S, Tabil LG, Sokhansanj S. Effects of compressive force, particle size and moisture content on mechanical properties of biomass pellets from grasses. Biomass and Bioenergy 2006;30:648–54. doi:10.1016/j.biombioe.2005.01.004.

[35] Adapa PK, Schoenau GJ, Tabil LG, Sokhansanj S, Crerar B. Pelleting of fractionated

alfalfa products. 2003 ASAE Annu. Meet., American Society of Agricultural and Biological Engineers; 2003, p. 1.

[36] Shang L, Nielsen NPK, Dahl J, Stelte W, Ahrenfeldt J, Holm JK, et al. Quality effects caused by torrefaction of pellets made from Scots pine. Fuel Process Technol 2012;101:23–8. doi:10.1016/j.fuproc.2012.03.013.

[37] Verhoest C, Ryckmans Y. Industrial wood pellets; Report Pellcert 2014:24. doi:IEE/10/463/SI2.592427.

[38] Goetzl A. Developments in the global trade of wood pellets. Work Pap Ind No ID-039, US Int Trade Comm Washington, DC 2015.

[39] EIA Energy Information Administration- Independent Statistics and Analysis. Densified biomass fuel manufacturing facilities in the United States by state, region, and capacity. US Dep Energy, Washington, DC 2017.

[40] Bergman PCA, Boersma AR, Zwart RWR, Kiel JHA. Torrefaction for biomass co-firing in existing coal-fired power stations. Energy Cent Netherlands, Rep No ECN-C-05-013, Petten, Netherlands 2005.

[41] Kumar L, Koukoulas AA, Mani S, Satyavolu J. Integrating torrefaction in the wood pellet industry: A critical review. Energy and Fuels 2017;31:37–54. doi:10.1021/acs.energyfuels.6b02803.

[42] Prins MJ, Ptasinski KJ, Janssen FJJG. Torrefaction of wood: Part 1. Weight loss kinetics. J Anal Appl Pyrolysis 2006;77:28–34.

[43] Chen D, Zhou J, Zhang Q. Effects of torrefaction on the pyrolysis behavior and bio-oil properties of rice husk by using TG-FTIR and Py-GC/MS. Energy & Fuels 2014:140824102646000. doi:10.1021/ef501189p.

[44] Peng JH, Bi XT, Sokhansanj S, Lim CJ. Torrefaction and densification of different species of softwood residues. Fuel 2013;111:411–21. doi:10.1016/j.fuel.2013.04.048.

[45] Tumuluru JS, Sokhansanj S, Hess JR, Wright CT, Boardman RD. A review on biomass torrefaction process and product properties for energy applications. Ind Biotechnol 2011;5. doi:10.1089/ind.2011.0014.

[46] Li J, Brzdekiewicz A, Yang W, Blasiak W. Co-firing based on biomass torrefaction in a pulverized coal boiler with aim of 100% fuel switching. Appl Energy 2012;99:344–54. doi:10.1016/j.apenergy.2012.05.046.

[47] Kumar A, Jones DD, Hanna MA. Thermochemical Biomass Gasification: A Review of the Current Status of the Technology. Energies 2009;2:556–81. doi:10.3390/en20300556.

[48] Prins MJ, Ptasinski KJ, Janssen FJJG. More efficient biomass gasification via torrefaction. Energy 2006;31:3458–70. doi:10.1016/j.energy.2006.03.008.

[49] Deng J, Wang G jun, Kuang J hong, Zhang Y liang, Luo Y hao. Pretreatment of agricultural residues for co-gasification via torrefaction. J Anal Appl Pyrolysis 2009;86:331–7. doi:10.1016/j.jaap.2009.08.006.

[50] Couhert C, Salvador S, Commandré J-M. Impact of torrefaction on syngas production from wood. Fuel 2009;88:2286–90. doi:10.1016/j.fuel.2009.05.003.

[51] Isahak WNRW, Hisham MWM, Yarmo MA, Yun Hin T. A review on bio-oil production from biomass by using pyrolysis method. Renew Sustain Energy Rev 2012;16:5910–23. doi:10.1016/j.rser.2012.05.039.

[52] Boateng AA, Mullen CA. Fast pyrolysis of biomass thermally pretreated by torrefaction. J Anal Appl Pyrolysis 2013;100:95–102. doi:10.1016/j.jaap.2012.12.002.

[53] Larsson SH, Rudolfsson M, Nordwaeger M, Olofsson I, Samuelsson R. Effects of

moisture content, torrefaction temperature, and die temperature in pilot scale pelletizing of torrefied Norway spruce. Appl Energy 2013;102:827–32. doi:10.1016/j.apenergy.2012.08.046.

[54] Basu P, Rao S, Acharya B, Dhungana A. Effect of torrefaction on the density and volume changes of coarse biomass particles. Can J Chem Eng 2013;91:1040–4. doi:10.1002/cjce.21817.

[55] Phanphanich M, Mani S. Impact of torrefaction on the grindability and fuel characteristics of forest biomass. Bioresour Technol 2011;102:1246–53. doi:10.1016/j.biortech.2010.08.028.

[56] Ghiasi B, Kumar L, Furubayashi T, Lim CJ, Bi X, Kim CS, et al. Densified biocoal from woodchips: Is it better to do torrefaction before or after densification? Appl Energy 2014;134:133–42. doi:10.1016/j.apenergy.2014.07.076.

[57] Tumuluru JS, Wright CT, Kenney KL, Hess JR. A technical review on biomass processing: densification, preprocessing, modeling, and optimization. 2010 ASABE Annu. Int. Meet., vol. 1009401, 2010.

[58] Bergman PCA. Combined torrefaction and pelletisation the TOP process. Energy Cent Netherlands, Rep No ECN-C-05-073, ECN, Petten, Netherlands 2005.

[59] Koppejan J, Sokhansanj S, Melin S, Madrali S. Status overview of torrefaction technologies, a review of the commercialisation status of biomass torrefaction. IEA Energy Technol Network, IEA Bioenergy Task 32 2015.

[60] Peng J, Bi XT, Lim J, Sokhansanj S. Development of torrefaction kinetics for British Columbia softwoods. Int J Chem React Eng 2012;10.

[61] Bates RB, Ghoniem AF. Biomass torrefaction: Modeling of reaction thermochemistry.

Bioresour Technol 2013;134:331–40. doi:10.1016/j.biortech.2013.01.158.

[62] Bates RB, Ghoniem AF. Modeling kinetics-transport interactions during biomass torrefaction: The effects of temperature, particle size, and moisture content. Fuel 2014;137:216–29. doi:10.1016/j.fuel.2014.07.047.

[63] Doassans-Carrère N, Muller S, Mitzkat M. REVE - A new industrial technology for biomass torrefaction: Pilot studies. Fuel Process Technol 2014;126:155–62. doi:10.1016/j.fuproc.2014.04.026.

[64] Mei Y, Liu R, Yang Q, Yang H, Shao J, Draper C, et al. Torrefaction of cedarwood in a pilot scale rotary kiln and the influence of industrial flue gas. Bioresour Technol 2015;177:355–60. doi:10.1016/j.biortech.2014.10.113.

[65] Strandberg M, Olofsson I, Pommer L, Wiklund-Lindström S, Åberg K, Nordin A. Effects of temperature and residence time on continuous torrefaction of spruce wood. Fuel Process Technol 2015;134:387–98. doi:10.1016/j.fuproc.2015.02.021.

[66] Karlsson J. Evaluation of Torrefaction Pilot Plant in 2013.

[67] Joshi Y, de Vries H, Woudstra T, de Jong W. Torrefaction: Unit operation modelling and process simulation. Appl Therm Eng 2014;74:83–8. doi:10.1016/j.applthermaleng.2013.12.059.

[68] Kambo HS, Dutta A. Strength, storage, and combustion characteristics of densified lignocellulosic biomass produced via torrefaction and hydrothermal carbonization. Appl Energy 2014;135:182–91. doi:10.1016/j.apenergy.2014.08.094.

[69] Arteaga-Perez LE, Segura C, Espinoza D, Radovic LR, Jimenez R. Torrefaction of Pinus radiata and Eucalyptus globulus: A combined experimental and modeling approach to process synthesis. Energy Sustain Dev 2015;29:13–23. doi:10.1016/j.esd.2015.08.004.

[70] Batidzirai B, Mignot a. PR, Schakel WB, Junginger HM, Faaij APC. Biomass torrefaction technology: Techno-economic status and future prospects. Energy 2013;62:196–214. doi:10.1016/j.energy.2013.09.035.

[71] Syu FS, Chiueh PT. Process simulation of rice straw torrefaction. Sustain Environ Res 2012;22:177–83.

[72] Cherry RS, Wood R a, Westover TL. Analysis of the Production Cost for Various Grades of Biomass Thermal Treatment. US Dep Energy, Idaho Natl Lab INL/EXT-13-30348, Idaho Falls, Idaho 2013.

[73] Archarya B. Torrefaction and Pelletization of Different Forms of Biomass of Ontario. University of Guelph, 2013.

[74] Cao L, Yuan X, Li H, Li C, Xiao ZZ, Jiang L, et al. Complementary effects of torrefaction and co-pelletization: Energy consumption and characteristics of pellets. Bioresour Technol 2015;185:254–62. doi:10.1016/j.biortech.2015.02.045.

[75] Peng JH, Bi HT, Lim CJ, Sokhansanj S. Study on density, hardness, and moisture uptake of torrefied wood pellets. Energy & Fuels 2013;27:967–74. doi:10.1021/ef301928q.

[76] Stelte W, Nielsen NPK, Hansen HO, Dahl J, Shang L, Sanadi AR. Pelletizing properties of torrefied wheat straw. Biomass and Bioenergy 2013;49:214–21.

[77] Doassans-Carrère N, Muller S, Mitzkat M. REVE: Versatile Continuous Pre/Post-Torrefaction Unit for Pellets Production 2015:14386. doi:10.1007/978-3-658-04355-1.

[78] Peng J, Wang J, Bi XT, Lim CJ, Sokhansanj S, Peng H, et al. Effects of thermal treatment on energy density and hardness of torrefied wood pellets. Fuel Process Technol 2015;129:168–73.

CHAPTER 2

LITERATURE REVIEW

Biomass feedstock

Biomass is generally referred to any organic materials originated from plants or animals containing the energy stored from sunlight photosynthesis. This definition does not encompass the fossil fuels like coal or petroleum which takes millions of years to produce [1]. Biomass can be divided into woody materials like tree, forest residue, and short rotation woody crops and non-woody materials comprise agricultural residues, energy crops, herbaceous products, and animal wastes [2]. Lignocellulosic biomass refers to non-food biomass feedstock with a major application in bioenergy production [3]. Biomass is intended to be a carbon-neutral fuel since the carbon taken from the atmosphere during biomass growth would release within the energy production and thereby not increasing the greenhouse gases concentration [4].

Biomass components

Biomass constituents include cellulose (30-50% dry basis), hemicellulose (20–40% dry basis, lignin (15–25% dry basis), ash (3–10% dry basis) (which is composed of inorganics like silicon, potassium, sodium, magnesium, and calcium), and extractives include resins, fatty acids, phenolic, salts, etc. [5]. Cellulose, hemicellulose, and lignin are major components of biomass which bring up the name of lignocellulosic [6] and their abundance differs from one type to other type of biomass. During the torrefaction each component undergoes different reactions transforming the structure of initial biomass. Therefore, understanding the structure and

composition of these components is beneficial to comprehend the biomass degradation behavior during thermal treatments as well as densification characteristics.

Cellulose is a heavy molecular weight linear homopolysacharide with monomer unit of $\beta-(1 \rightarrow 4)-$D-glucopyranose and general formula $(C_6H_{10}O_5)_m$ [7,8], where subscript m is the degree of polymerization. Cellulose has a crystalline structure making up the fibers in biomass. It contains several hydroxyl group that form hydrogen bond with neighboring chain, resulting a microfibrils with high tensile strength [9]. Hemicellulose is a branched multi-structure polymer with lower molecular weight compare to cellulose [9]. The general formula of hemicellulose structure can be defined as $(C_5H_8O_4)_m$ [7]. The monosaccharides of hemicellulose comprise xylose, mannose, galactose, rhamnose, and arabinose that might vary differently among biomass types. Lignin is a highly branched, amorphous polyphenolic resin with random structure $(C_9H_{10}O_3.(OCH_3)_{0.9-1.7})_m$ [7] . It forms covalent bonds with hemicellulose molecule, cross links different polysaccharides and provide mechanical strength for the biomass. Thermal decomposition of lignin leads to produce phenolic and aromatic compounds and it is hardly dehydrated [9]. Hemicellulose is the most degradable component in biomass structure while the frim crystalline structure of cellulose resists thermal decomposition compared to hemicellulose.

Biomass drawbacks

Apart from numerous advantages of biomass, there are some drawbacks that pose challenges in application of biomass in bioenergy production. The not uniform shape and size of biomass is one of the primary issues of biomass that leads to bringing difficulty in handling and flowability as well as affecting the efficiency of combustion and other conversation processes [10]. The non-spherical particles of biomass influence char burnout since irregular shape biomass does not melt and retained during combustion [11]. The second major issue of biomass is high moisture content

which reduces the efficiency of the biomass conversions, provoking natural degradation and intensifying the problems associated with transportation and storage. However, it might be beneficial in some processes to some extent. Low bulk density is the other disadvantage of biomass that increase the cost of transportation as well as making problems in co-firing with coal within co-milling and feeding into burner due to the difference in densities of biomass and coal [10].

The chemical composition of biomass is very different from fossil fuels, especially due to high content of oxygen in carbohydrate polymers of biomass. The higher oxygen and hydrogen content in biomass resulting a lower energy value of biomass rather fossil fuel which is coming from the lower energy contained in C-O and C-H bonds than in C-C bonds [12]. Formation of smoke and the large volume of flue gas are because of high oxygen content of biomass [4]. The presence of polar compounds (such as hydroxyl, carboxyl, carbonyl) implies the hydrophilic nature resulting biodegradation and reduce the reliability of biomass storage. The biomass drawbacks might have synergic effects on final properties of biomass include flowability, grindability, low calorific value, and hydrophilicity. Moreover, the current energy producing plants and facilities are adapted for fossil fuels that limit the extensive usage of biomass [13]. In order to alleviate these barriers, pre-treatment processes such as torrefaction and pelletizing are required.

The pretreatment processes can be mechanical, chemical, or thermal to produce a suitable drop-in biofuel as a fossil fuel alternative. Densification (mechanical pretreatment) and torrefaction (thermal pretreatment) are the key processes involved in producing torrefied pellets.

Densification

Densification is an efficient pretreatment to improve the density and flowability of biomass. After drying and grinding (size reduction) the biomass, the physical force is applied to compact the ground biomass into the dense shape such as pellet, briquette, or cube. The extruded densified

biomass is then cooled down and stored. During compression process, different mechanisms of particulate binding might be presented. Rumpf and Knepper [14] categorized the mechanisms of binding into following five groups:

1. *Solid bridges:* solid bridges might be formed due to several reasons such as diffusion of molecules from one particle to another when the particles are in a close proximity of each other, crystallization of some elements, and solidification of binders or other melted components [15].
2. *Attraction forces between solid particles:* molecular forces such as valance forces, hydrogen bonds, and van der waals' forces as well as electrostatic and magnetic forces may adhere particles together [15].
3. *Mechanical interlocking bonds:* fibers and bulky particles can form interlocking bond [15].
4. *Adhesion and cohesion forces:* binders can adhere to solid particles and form bonds similar to solid bridges [15].
5. *Interfacial forces and capillary pressure:* Cohesion of water molecules between particles can form liquid bridges. The surface tension and capillary pressure of liquid molecules bring solid particles together resulting in bond formation [15].

The compression forces during densification operation are combination of thermal, mechanical, and atomic forces process [16]. The compression process of grinds is generally accomplished in three stages [17]. The first stage is mostly rearrangement of the particles under low pressure that removes the air blocked between particles. By increase in applying pressure, the particles are brought in together and inter-particle bonds are formed. The compression is continued to a certain point that elastic and plastic deformation is occurred, and fiber interlocking are formed. Meanwhile, lignin and glass transition components from cell wall release and flow through

particles [18]. The density of compact particles is increased close to the density of the plant cell wall [19]. The last stage is hardening that strong solid bridges are formed by cooling and solidification of the molten components [16,20].

Densified biomass is a commodity product with improved handling and flowability resulting in cheaper and more efficient transportation and storage. Pelletizing and briquetting are two types of standard densification processes with more than 130 years antiquity [18,21]. Pelletizing is the most popular densification process for biomass in which finely ground biomass is converted into a homogenous cylindrical pellet with diameter 6-8 mm, length 3.15-40mm [22] and density around 1000-1200 kg m^{-3} (bulk density >600 kg m^{-3}) [23]. Effective pelletizing depends on moisture content of the feedstock, feedstock density, particle size, fiber strength, the feedstock's lubricating characteristics and the presence of natural binders. High temperature steam might be used occasionally in pelletizing operations to activate natural binders and lubricants in biomass feedstock [24]. A binding agent might be added to improve the quality of the pellets [25].

Briquettes are another type of densified biomass with bigger size. The typical diameter of briquette is 25-85 mm with densities ranging 700-1200 kg m^{-3} depending on the material used and compressing conditions [26]. Briquettes can be made from larger particle sizes and higher moisture content, at lower specific energy consumption. However, they are prone to absorb more water during storage leading to biological degradation and also have lower mechanical strength [10].

The other type of densified biomass with a square cross section is a large size cube. The size of cube cross section is between 12.7 to 38.1 mm and its length ranging from 25 to 100 mm. Cubes are usually made of chopped biomass instead of ground biomass. Thus, less number of unit operation are required for cubing process. However, the density of cubes are rather low and ranging from 450-550 kg m^{-3} [27].

There are some other densification systems such as tabletizer and agglomerator that can be used in relevant processing industries like food and pharmacy [28]. Although the densified biomass significantly improves handling, storage and transportation of biomass but the chemical properties such as low calorific value, fibrous and hydrophilic nature, and low energy density of biomass should be still upgraded.

Binders

Several components exist in the biomass that act as a natural binder including lignin, starch, protein, fat, and water [29,30]. Preheating the biomass softens the lignin that adhere to the biomass particles and facilitate binding in densification process. Surface tension of water molecules and present capillary pressure increase interfacial forces and improve densification. However, chemical binders can still be added to reduce required energy for densification and meanwhile enhance pellet density, strength, and durability [29]. Particularly, densification of torrefied biomass is energy intensive due to weakening of solid bridges after thermal decomposition and binders could assist the efficient densification.

There are several chemical binders like gelatinized starch, lignosulfonate, saw dust, hydrated lime, bentonite, agro colloids, molasses, and crude glycerol [27,29,30]. Cost and environmental impacts are the main parameters for a binder selection [30]. The binder is usually added by 0.5 to 20% to biomass before densification process. It can make a bridge, matrix, or cause a chemical reaction that result in inter-particle bond formation [30].

Torrefaction

Torrefaction is a one of the most promising pretreatment processes to enhance the biomass properties as a drop-in biofuel. In torrefaction the biomass will be thermally treated by hot carrier gas (usually an inert gas) or indirect heating medium at a temperature between 200– 300°C under

atmospheric condition [9,31–33]. As a result, in addition to the moisture removal, biomass will be marginally decomposed. The OH functional group present in the biomass will be mainly removed resulting an increase in carbon content and calorific value of the torrefied biomass [9]. Although the thermal degradation involves loss of mass, the energy density of biomass would be enhanced.

During the torrefaction each component undergoes different reactions transforming the structure of initial biomass. Bergman et al. described the thermochemical changes of biomass during the torrefaction in the five different stages [6] :

- Regime A (50-120°C): The free bound water is evaporated, and biomass shrinks without any chemical changes. The biomass would retain its structure if rewetted.
- Regime B (120-150°C): This range of temperature is suitable for densification while the lignin content starts softening and acts similar to binder.
- Regime C (150-200°C): Reactive drying section with cleavage of hydrogen and carbon bonds and depolymerization of hemicellulose. The biomass structure deforms that cannot return to initial structure by wetting. The shortened polymers are produced and condensed within solid structures [6].
- Regime D (200-250°C): This range is the starting of hemicellulose torrefaction which comprises primary devolatilization and decarbonylation reactions. The inter- and intramolecular hydrogen breaks down and volatile components formed by C-C and C-O bonds [9]. Also, the NMR analysis of beech (hardwood) has shown that syringyl demethoxylation of lignin and changes in cellulose crystallinity start above 200 °C and 230 °C, respectively [34].
- Regime E (250-300°C): In this high temperature regime, the biomass structure is thoroughly transformed. The hemicellulose decomposition into volatiles and solids

products are intensified. Also, a limited depolymerization, guaiacyl demethoxylation, and monomer degradation of lignin as well as marginal degradation of cellulose take place [34]. The biomass transformed to brittle and non-fibrous structure.

The results of torrefaction can be summarized as follow:

- Torrefaction will lead to produce more uniform biomass [35].
- The moisture content of biomass will be significantly reduced. This would lead to decrease the transportation costs as well as prevention of biomass decomposition [9].
- The biomass grindability will be enhanced [36]. This will expand the biomass usage in pulverized co-firing systems [37].
- The increase in C/O ratio will increase calorific value [9,31–33].
- The energy density of torrefied biomass will be improved [9,31–33].
- The biomass nature changes from hydrophilic to hydrophobic after torrefaction due to removal of polar hydroxyl, carbonyl groups which benefits to reduce the microbial degradation and storage costs.
- Apart from abovementioned advantages, the bulk density of the torrefied biomass will be generally reduced. The loss of material during the torrefaction conduct to more porous material with lower bulk density [9]. This would intensify the necessity of integration of torrefaction with some densification processes to decrease transportation costs and enhance the handling and flow-ability of materials.
- As a result of torrefaction, the bounding forces between particles would be weakened. Therefore, high die temperature, more compressive pressure, or binding agent is necessary for densification of torrefied biomass [38–40].

Temperature, residence time, and particle size are the most important parameters in biomass torrefaction [41]. The effects of torrefaction temperature and residence time have been studied by severity factor for certain particle size [42–44]. The torrefaction degree can be divided into light (200–235 °C), mild (235–275°C), and severe torrefaction (275–300°C) [8]. A holding time of 30-60 min was ascertained to be common for torrefaction based on previous studies [9]. The higher torrefaction temperature causes more thermal decomposition of the biomass that leads to produce higher energy density bio-coal but with less mass yield. On the other hand, greater amounts of volatile organic species would be released with potential of more heat generation by oxidizing.

Integrated torrefaction with proper densification process like pelletizing offers a synergistic pathway in biomass processing that yields a high value torrefied biomass with an inherent ease of handling, storage, and transportation of the densified pellets. The torrefied pellet with improved energy density, higher heating value, enhanced grindability and less degradation has similar characteristics to coal [9,31–33]. Therefore, it can be used as biocoal in all relevant processes such as power generation plants, industrial heating services, and domestic usages.

Table 2-1 listed the properties of torrefied pellets especially within post torrefaction pathway.

Table 2-1. Examples of properties of torrefied pellet from TOP and TAP pathways

	Temperature	Residence time	Mass loss%	H/C	HHV (MJ/kg)	Pellet density (kg/m^3)	Bulk density (kg/m^3)	Volumetric energy density GJ/m^3	MC%	Durability	Hardness (Meyer hardness) (N/mm^2)	Water uptake%	Ref.
Douglas-fir TOP	260	15 min	15.1	0.11	20.8	1207.3			7.7	98.60%			[45]
Douglas-fir TAP	260	15 min	14.9	0.12	22.0	1031.2			2.9	97%			
Oil palm fiber	275	30 min	35	0.42	20.3								[46]
White commercial	280-290	30 min	30		22.7	930	530	12.0			12	9	[47]
Brown commercial	280-290	30 min	30		23.1	970	540	12.5			12	8	
Control-pellet	280-290	30 min	30		22.5	700	380	8.5			3	9	
SPF-TOP	280-290	30 min	30		22.5	1250	700	15.9			11	11	
Scot pine pellet-TAP	270	1 h	41.9 (w.b)		24.3					89%	CS*: 0.35 J/g.pellet		[48]
TOP	280	1 h			22.65					89.91			[49]
TOP					20-24		750-850	15-18.7	1-5				[9]
Sawdust-TOP	280	15	30	0.11		1050					4.5	13.6	[50]
ISO-TOP					21.0		>650-700			>95%			[22]

*CS: Compression strength

Torrefaction products

Torrefaction products divide into solid biocoal and an off-gas stream called torgas [51]. The torgas composed of non-condensable gas like CO_2 and CO as well as condensable gasses primarily of steam from evaporated moisture, and organic molecules such as methanol, acetic acid, and formaldehyde [52]. The limitations of gas emission and potential additional value of torgas prevent the venting gas to the atmosphere in industrial scale [52]. The volatiles from torrefaction process can be either combusted using thermal oxidizer or catalytic oxidizer [53] to destroy VOCs and generate heat energy for auto-thermal torrefaction. The other option is condensation of volatiles and utilize the liquid condensate in relevant applications like wood vinegars, wood protection, additive agent in coating of pellets, or production of green chemicals [54,55].

The volatile stream from torrefaction of biomass can be separated into condensable and non-condensable gas. The presence and quantity of different compositions significantly depend on feedstock type and torrefaction temperature [55,56].

Non-condensable components

The non-condensable fraction of torrefaction gas consists mainly carbon dioxide, carbon monoxide and a trace of hydrogen and methane [6,41,57] that can be neglected as potential side streams [55]. The carbon dioxide is produced by primary decarboxylation reaction of acid carboxyl groups in the hemicellulose while carbon monoxide is presumably formed in the secondary reaction of carbon dioxide and steam with porous char [41,58]. By increase in torrefaction temperature and decomposition of lignin and cellulose, the carbon monoxide can be further generated by decarbonylation of simple carbonyl compounds [9,57]. Therefore the ratio of CO to CO_2 increased with torrefaction temperature [9,57,58]. The carbon monoxide is the primary source

of the heat value of the non-condensable gas product [4,9]. By oxidation, the toxic effect of carbon monoxide is alleviated, and energy is produced as well.

Condensable components

The condensable portion of volatile stream primarily consists of (i) Water, (ii) Organics: acids, ketones, alcohols, furans, aldehyde, and (iii) lipids such as phenols, fatty acids, waxes, etc. [51,55]. The main component of the condensable fraction is water which is either from initial moisture content (free water), the bound water, and water produced from chemical dehydration and decomposition reactions.

A typical concentration of torgas from torrefaction of willow at a temperature of 300°C [41] which were derived by [59] is shown in Table 2-2.

Table 2-2. The concentration of torgas component from torrefaction of Willow at 300°C [41,59]

Components	%wt
Acid acetic	15.30%
Water	38.85%
Formic acid	5.92%
Methanol	10.95%
Lactic acid	9.22%
Furfural	0.75%
Hydroxyacetone	3.22%
Carbon dioxide	12.13%
Carbon monoxide	3.65%
Total Volatile	100 %

Volatile stream utilization

As it is mentioned above, the concentration of different components in the torrefied gas is varied according to the type of the biomass and torrefaction temperature [55,56]. However, It has been proved that in the temperature range of torrefaction (200°C to 300°C) which is the mild

pyrolysis, thermal decomposition of hemicellulose is the major source of produced volatiles [9]. For instance, acetic acid as one of the key components in torgas originates from acetoxy- and methoxy- groups of sides chains in xylose units [9]. At higher torrefaction temperature, a few phenolic compounds can be produced by the decomposition of lignin and cellulose. So, the volatile stream from biomass torrefaction mainly comprises distillates rather than tar constituents. Therefore, it has generally been used as a mixture instead of being separated into the compounds.

Thus far, the volatile stream has normally been combusted with an additional fuel (natural gas or biomass) in a combustor to provide the required energy of drying and torrefaction. The other potential usage of the volatile stream that has been investigated by several studies [56,60,61] is to be condensed and utilized as wood vinegars or pyroligneous acid [56]. Additionally, the achievements in upgrading the bio-oil from fast pyrolysis can be exploited in producing value added products by torrefaction condensate. The general composition of pyrolysis bio-oil is shown in

Table 2-3. Bio-oil and torrefaction condensate have a common group of components with different quantities. One of the most abundant common components are the carboxylic acids. Removal or deoxygenation of carboxylic acids is an important step to provide bio-oil stability since the high acidity renders further reactions and corrosion problems [62]. It has been shown that the catalytic hydrodeoxygenation (HDO) of carboxylic acids is the efficient method to remove oxygen [63–65]. The produced hydrocarbon compounds by HDO reaction would upgrade the properties of the bio-oil or condensate as a fuel.

Table 2-3. A typical composition of bio-oil fast pyrolysis [62]

Components	%wt
water	20-30
carboxylic acids	10-15
aldehydes	10-20
furfurals	1-4
alcohols	2-5
ketones	1-5
carbohydrates	5-10
phenols	2-5
lignin fragments	15-30

By and large, the volatile products of torrefaction can be utilized in following categories:

1. Torrefied gas from torrefaction can be oxidized or combusted in thermal or catalytic oxidizer and produce energy [66].
2. The condensable fraction of torgas which is a mixture of different components can be condensed and used as wood vinegars or pyroligneous acid in relevant applications [56]
3. The main valuable components in condensate such as acetic acid, methanol, and furfural can be separated and used as a precursor to produce other value-added chemicals [55].
4. The components in condensate can be upgraded to produce bio-oil that can be used in boilers, engines, and turbines [67].

Torrefaction kinetics

Comprehensive and detailed understanding of torrefaction mechanism and reaction kinetics is indispensable to establish the thermochemical conversion processes and design of the corresponding equipment [2]. Reaction kinetics, which imply the rate of chemical reactions,

encompass the amount of reactant conversion, loss of materials, and the speed of the reactions assisting to determine the mass and energy balance and the design parameters of the process equipment. The various kinetics of torrefaction have been vigorously challenged in recent years by a number of writers that are mainly derived based on biomass pyrolysis processes [2,4,68].

As it is mentioned earlier, the biomass weight loss and its component decomposition typically follow the main regimes of dehydration, hemicellulose decomposition and limited degradation of cellulose and lignin [6,9,34]. It was believed that the reaction of biomass constituents take place independently with no combination effect and the total mass loss of biomass can be estimated effectively by summation of each component mass loss [35,68]. Thus, numerous studies have been carried out on individual decomposition rate of hemicellulose, cellulose, and lignin. Nevertheless, there are several other studies to investigate the reaction kinetics of a biomass as lumped [68–70]. Table 2-4 shows examples of reported kinetics for biomass components, hardwood, and softwood.

One-step kinetics

The one-step kinetic model is the simplest kinetic model for torrefaction of wood and its components [2,8,68]. The overall rate of reaction of a sample with nth order can be written as [35,68]:

$$Biomass \xrightarrow{k} volatiles + chars \tag{2-1}$$

$$\frac{dX}{dt} = k(1 - X)^n$$

Where X is the conversion of the sample. *Table 2-4* shows examples of derived kinetic models for decomposition of hemicellulose, cellulose, lignin, pine(softwood), and birch(hardwood). Peng et al. [68] reported that the one-step kinetic model could predict the torrefaction reaction reasonably well over the long residence time; however, it could not validate the low weight loss over the short residence time torrefaction.

Multi-step kinetics

One of the famous two-step kinetic model was proposed by Blasi and Lanzetta [71], which is applied by a number of researchers. Prins et al [31] used the suggested two-step model for decomposition of willow, which could model the formation of volatiles within parallel reactions (Eq. 2-2).

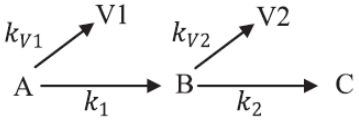

(2-2)

$$Biomass \xrightarrow{k1} Intermedites \xrightarrow{k2} Chars$$
$$\downarrow k_{v1} \qquad \downarrow k_{v2}$$
$$Volatiles \qquad Volatiles$$

They further showed that for wood pyrolysis below 300°C, the reactions were the rate-limiting step for particles smaller than 2 mm where the impact of inter-particle heat and mass transfer becomes insignificant [31]. Bates et al. [59,72] continued studies on willow torrefaction and modeled the volatiles compositions and mass yield during the temperature range of 230-300°C.

Branca and Blasi [70] proposed a three-step kinetic model for wood pyrolysis based on three reactions at different temperature ranges: depolymerization (255–320 °C), devolatilization (255–435 °C), and charring (330–435 °C).

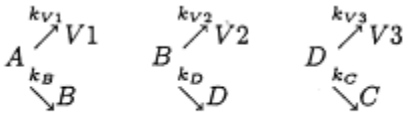

$$k_1 = k_{V1} + k_B, \quad k_2 = k_{V2} + k_D, \quad k_3 = k_{V3} + k_C \tag{2-3}$$

The first reaction zone was related to degradation of extractives and the most reactive fractions of hemicellulose. The second reaction described the degradation of cellulose and part of

lignin and hemicellulose and the third was for lignin and small fractions of cellulose and hemicellulose [70].

Multi-components kinetics

The multi-components kinetics models were proposed by assuming that the weight loss of the biomass is contributed from the decomposition of three major biomass components, hemicellulose, cellulose, and lignin corresponding organic pseudo -components in temperature ranges.

Roberts [73] assumed that the reaction time of hemicelluloses in wood pyrolysis was only a few seconds. Therefore, he (1971) proposed a two-component model based on the pyrolysis of cellulose and lignin for wood pyrolysis:

$$wood_{Cellulose} \rightarrow volatiles + chars \quad (2\text{-}4)$$
$$wood_{Lignin} \rightarrow volatiles + chars$$

Peng et al. [68] developed the two component model for torrefaction of BC softwood (Eq.5) and evaluated the model for torrefaction within short residence time of commercial interest (i.e. a weight loss lower than 35% with a residence time shorter than 1 hour).

$$wood_{Fast\ reaction\ group} \overset{k1}{\rightarrow} volatiles + chars \quad (2\text{-}5)$$
$$wood_{Medium\ reaction\ group} \overset{k2}{\rightarrow} volatiles + chars$$

The residual weight fraction W_{TGA} of wood samples considering the first order reaction for both components was stated by following formula:

$$W_{TGA} = (1 - C_1 - C_2) + C_1\, exp(-k_1 t) + C_2\, exp(-k_2 t) \quad (2\text{-}6)$$
$$k = A \cdot e^{-\frac{E_a}{RT}}$$

Where C_1 may be set as the hemicelluloses content of BC softwood, and C_2 represents the combined cellulose and lignin contents.

According to Shafizadeh [74] the major decomposition rate of hemicellulose occurs in the range of 225-325°C, for cellulose is 305-375°C, and lignin is varied between 250-500°C.

Table 2-4. Examples of reported kinetic models for biomass constituents, softwood, and hardwood

Material	Temperature (°C)	order of reaction (n)	Activation energy, Ea (kJmol-1)	Pre-exponential factor, A (s^{-1})	Ref.
Hemicellulose	200-300	3	187.06	6.88×10^{14}	[35]
Cellulose	200-300	1	124.42	4.77×10^{7}	[35]
Lignin	200-300	1	37.58	0.11	[35]
Pine	200-300	1	131	2.94×10^{8}	[68]
Pine	150-500	1	88	5.0×10^{8}	[75]
Pine (two-component model), Eq. 2-6	200-300 C1: 0.263	1 1	115.6 225.4	1.15×10^{8} 4.48×10^{16}	[68]
Birch (two-component model)	230-280	1 1	551.13 163.26	106.6 2.8×10^{10}	[76]
Willow (multi-step)	230-300	1 (k_1) 1 (k_{v1}) 1 (k_2) 0 (k_{v2})	75.976 114.214 151.711 -	2.48×10^{4} 3.23×10^{7} 1.10×10^{10} 1.45	[31]

Particle size effects

Particle size affects the torrefaction reaction rate because of the diffusion of generated vapors through internal pores of biomass particles. In other words, the rate of heat transfer to and within the particle should be faster than reaction rate to ensure the minimum residence time corresponding that the overall controlling factor is the intrinsic kinetics (absence of heat transfer limitation)[31].

Two general criteria were proposed by Prins et al. [31]; Biot number, which expresses the ratio between heat convection and conduction rates of the particle, and external Pyrolysis number, which is the ratio of heat convection rate and reaction rate.

$$Bi = \frac{\alpha \cdot L_c}{\lambda} \quad (2\text{-}7)$$

$$P_y' = \frac{\alpha}{k \cdot \rho \cdot c_p \cdot L_c} \quad (2\text{-}8)$$

α : external heat transfer coefficient in $Wm^{-2}\ K^{-1}$

L_c: is the ratio of the particle volume to surface area in m

λ: thermal conductivity in $Wm^{-1}\ K^{-1}$

k: global reaction rate s^{-1}

c_p: the thermal conductivity in $Wm^{-1}\ K^{-1}$

The desired kinetic control is achieved when: (a) Biot number is much smaller than unity, so that heat conduction within the particle is much faster than heat convection to the particle and (b) external Pyrolysis number is much larger than unity, which indicates that heat convection to the particle is much faster than the chemical reactions taking place [31].

Prins et al. [31] showed that for pyrolysis of wood below 300 °C, the reaction was the rate-limiting step for particles smaller than 2mm where the impact of intra-particle heat and mass transfer became insignificant.

Peng et al. [77] fitted a series of TGA and fixed bed experimental data from different particle seizes 0.23, 0.67, and 0.81 mm, to the hard core (non-shrinkage) particle model with a first order

torrefaction reaction and found that the global reaction rate was inversely proportional to the particle size to a power of 0.24. The process is controlled by the intrinsic reaction kinetics, if the global reaction rate is independent of the particle size.

Detailed mathematical model is required to study the heat transfer within the particles during the torrefaction reaction and weight loss of the biomass particle. Bates et al. [78] developed the model to study mass and energy changes of the different biomass particle size and shape and compared it with experimental data. They observed that the temperature difference between centerline of the particle and reactor increase by particle sizes from 2.38 to 12.75 mm. According to earlier studies of Van der Stelte [79], the maximum temperature difference between the centerline and the surface of the particle changes proportionally to the square of the particle radius (r in m^2). Bates et al. [78] showed that the length of heat-up time from initial temperature to 200°C, which is the temperature that torrefaction starts, was about 45 s and 16.5 min for 2.38 mm and 12.75 mm particle size, respectively. The heating time correlates to heat transfer rate and depending on external heat transfer limitation or internal heat transfer limitation, it can change linearly ($\rho \cdot c_p \cdot L_c/\alpha$) or quadratically $\rho \cdot c_p \cdot L_c^2/\lambda$ with particle size, respectively. Interestingly their model as well as experimental data showed that there is no difference between mass and energy yield of different particle size when the temperature was 250°C [78]. This might prove that the different particle size affects the heating time which probably influence the reactor size.

Oxidative torrefaction

Oxidative torrefaction is the heating treatment of biomass in an environment containing oxygen at the temperature range of 200–300°C. The non-oxidative torrefaction occurs in an inert condition that incurs additional operating costs to supply an inert gas and heat requirement. Therefore, the oxidative torrefaction can potentially reduce the cost since there is no need to

separation processes to extract nitrogen or purify the flue gas. The oxidative torrefaction mechanisms include devolatilization, thermal degradation of biomass and oxidative reactions [8,80–82]. The presence of oxidative reactions resulting exothermic reactions that reduces the heating demand for biomass torrefaction. Moreover, increase in O2 concentration intensify the rate of thermal decomposition which shorten the residence time [81,83–85].

Wang et al. [81] investigated the oxidative torrefaction of sawdust with a carrier gas containing 3–6% O_2 and densification of torrefied sawdust to pellets. The properties of torrefied sawdust and its pellets, including density, energy consumption for pelletization, higher heating value, and energy yield in oxidative environments were similar to those of the biomass torrefied in inert atmospheres. Chen and co-workers [86] determined the reaction characteristics of two fibrous biomass materials (oil palm fiber and coconut fiber) and two ligneous ones (eucalyptus and Cryptomeria japonica) at 300°C for 1 h torrefaction in inert and oxidative atmospheres (5-21% O_2) at various superficial velocities. They studied the structure of biomass by Scanning electron microscope (SEM). The results indicate that the fibrous biomass is more sensitive to O_2 concentration than the ligneous biomass. The increase in O_2 concentration decreases the solid yield. As a whole, the performance of non-oxidative torrefaction was better than that of oxidative torrefaction. They observed that ligneous biomass can be torrefied in oxidative environments at lower O_2 concentrations, whereas fibrous biomass is more suitable for non-oxidative torrefaction.

Lu et al. [87] investigated the torrefaction of eucalyptus and oil palm fiber in an inert condition and air (21% O_2) at temperatures of 250–350°C for 1 h. They observed the optimum operation for eucalyptus in air and N_2 atmospheres at temperatures of 275°C and 325 °C, respectively; but it was inappropriate to torrefy oil palm fiber in air, resulting from low solid and energy yields. Rousset et al. [88] studied the property variation of Eucalyptus grandis in oxidative

torrefaction (2, 6, 10, and 21% O_2) at two temperatures of 240 and 280 °C for 1 h. They observed that the O_2 concentration did not significantly affect the solid yield and composition of the biomass torrefied at 240°C, but it was very significant at the O_2 concentration of 21 vol% at 280°C.

Wet torrefaction

Wet torrefaction or hydrothermal carbonization is thermal treatment of biomass in liquid water or aqueous phase instead of gas phase at temperature range of 180–260°C corresponding to pressure range 200-700 psi (1.4 -4.8 MPa) [8]. The reaction time of wet torrefaction is in the range of 5–240 min, resulting in the formation of hydrophobic solid fuel, aqueous compounds, and gases [89]. The energy density of biomass is intensified with its heating value being increased by 3–47% [90].

Yan et al. [91] showed that wet torrefaction of loblolly pine by hot compressed water at 200–260°C for 5 min was more successful than dry torrefaction in inert condition at 250–300°C in terms of energy yield and energy densification under similar mass yield. In another study [92], they observed the decrease in the solid mass by increasing temperature of we torrefaction, while the heat value of the solid and amount of gas release increased, similar to dry torrefaction. Lynam et al. [90] carried out the wet torrefaction of loblolly pine in acetic acid and/or lithium chloride solutions at 230°C for 5 min and observed the increased energy density of solid product. According to Chen et al. [93] wet torrefaction can be performed at temperatures about 100°C lower than of dry torrefaction with the same improvement in calorific value. They claimed that Although the wet torrefaction treatment is a promising method to upgrade biomass feedstock due to its low temperature operation even though it requires high pressure.

Steam torrefaction

Steam torrefaction is treatment of biomass using saturated steam or superheated steam, so-called steam explosion treatment [8], which has been widely applied for the production of lignocellulosic bioethanol [94]. Steam explosion is usually carried out at temperatures 200–260°C under pressure 1-35 MPa for 5–10 min followed by rapid decompression [95,96]. As a result, the fibrous structure of the biomass is ruptured. It would advance the enzymatic hydrolysis and fermentation due to increase in availability of the defibrillated cellulose [96]. It has been shown that hydrolysis rate of hemicellulose in steam explosion treatment can be improved by use of acidic gases or dilute acid (e.g. SO_2, H_2SO_4) [97–99]. Biomass lignin releases during steam explosion and deposits on the surface of biomass particles. This would lead to higher strength of densified biomass [96].

After steam explosion, low molecular weight volatiles are removed and the calorific value and carbon content of biomass being increased [8]. Liam et al. observed that similar to conventional dry torrefaction, the biomass bulk density, mean particle size and equilibrium moisture content decreased after steam torrefaction [100]. Their treated pellets showed no defect with high durability. Steam explosion is able to increase the calorific value, hydrophobicity and carbon content at much lower temperatures and shorter residence time. The significant implication of steam explosion treatment is the higher mechanical strength and elasticity of treated pellets compared to other torrefaction methods [100–102]. Table 2-5 listed some of the differences between various types of torrefaction.

Table 2-5. Different type of torrefaction and their properties.

	Dry Torrefaction [9]	Oxidative Torrefaction [8,80–82]	Steam Torrefaction (Steam Explosion) [8,95]	Wet Torrefaction (Hydrothermal Carbonization) [8,89,90]
Temperature	200-300°C	200-300°C	200-260°C	180-260°C
Media	Inert gas (N_2)	Inert gas (N_2) +O_2	Superheated steam	Hot Compressed water
Pressure	atmospheric	atmospheric	200-700 psi	200-700 psi
Residence time	30-60 min	30-80 min	5-10 min	5-240 min
Comparative advantages	• Lower pressure • Lower cost	• Lower pressure • Lower cost	• Lower residence time • Lower temperature • Higher mechanical strength	• Lower residence time • Lower temperature • Higher energy density • Higher heat value • Lower ash content
Comparative disadvantages	• Lower mechanical strength • Higher ash content	• Lower energy yield • Higher ash content	• Higher pressure • Higher cost • Higher ash content	• Higher pressure • Lower yield • Waste water production • Higher cost

Torrefaction reactor

Several torrefaction reactors have been developed by technology suppliers mainly by upgrading from drying or pyrolysis. However, the proper reactor type with optimum efficiency, high flexibility to various type of feedstock with different specification, and proven scalability is still under investigation. The torrefaction reactors technologies can be classified into two major categories: Directly heated and Indirectly heated reactors [103]. In directly heated reactors the heating media is in contact with the biomass requiring free oxygen content of hot gas. Although the heat transfer distribution is more uniform in direct heated reactor, there is a risk of spontaneous combustion during torrefaction [104]. In indirectly heated reactor, the hot gas or hot media does not contact the biomass, the risk of combustion is minimized but the heat transfer distribution is not that uniform [103,104]. In addition to the type of heat contact, the movement of biomass and the nature of working media are also important [105]. Moreover, it is worth noting that only a few reactor types can handle a wider range of particle sizes [37]. Koppejan et al. [106]and Dhungana et al. [103] have reviewed different type of torrefaction reactors and their properties. The typical properties of existing types of torrefaction reactor are listed in Table 2-6. Some of the pioneer developers and their reactor technologies are ECN: moving bed, UmU: rotating drum, Topell: fluidized bed and CENER: indirectly in- and externally heated rotating shaft [37]. Table 2-7 shows some of known developers for torrefaction.

Fixed-bed torrefaction reactor

The fixed bed reactor is the simplest batch type of the reactor that is usually used in lab scale or pilot scale [107]. The specified amount of biomass is heated up by heat conduction from electrical heater (lab scale) or hot gas from biomass combustion. The main drawback of fixed bed reactor is temperature gradient due to non-uniform heat distribution [107]. The typical mass loss

of 20-30% and energy yield of 90% has been reported for this type of the reactor. Energy research Center of the Netherlands (ECN) designed a pilot scale with capacity of 20 liters in 2005s Jaap Kiel. a commercial scale fixed bed reactor was established by Integrofuels company in 2010s with capacity of 48,000 tons/year [107].

Fluidized bed torrefaction reactor

Fluidized bed reactors have been used in laboratory, pilot and commercial scales [107]. There are different types of fluidized bed torrefaction reactor including Bubbling bed reactor and Torbed reactor [37]. The main concept is fluidizing the biomass by entering hot inert gas flow that providing a uniform heat transfer distribution within the biomass bed [107]. The Bubbling bed reactors is the simple type of fluidizing bed reactor where biomass heated gently by hot gas.

In a Torbed reactor the hot gas is blown through the angled blades with rather high velocity (50-80 m/s) that moves the biomass in a vertical and horizontal directions. As a result, the biomass particles are heat up very fast and torrefied in a short residence time (about 80 sec) leading to small reactor sizes. Although higher torrefaction temperature can be controlled in this reactor, it is sensitive to the particle size of the feedstock [37]. Moreover, there is a possibility of fines formation [105]. Topell energy designed a Torbed reactor with capacity of 60,000 tons/year in 2010s. They tested the torrefaction in temperature range of 280-320°C and 90 sec residence time [108].

Moving bed torrefaction reactor

In a moving bed torrefaction reactor the biomass continuously moves vertically or horizontally through the reactor using mechanical mechanisms. In a Moving Compact Bed reactor, the biomass enters from the top and is heated directly by the carrier gas entering from the bottom. The reactor volume and hence the residence time is relatively low resulting the rather low cost of

investment [6]. The main drawback of the moving compact bed reactor is the risk of channeling resulting the non-uniform heat transfer distribution, which has not been reported for 100 kg/h scale. The other disadvantage is pressure drop over the bed for small biomass particles [37].

Rotary drum reactor

A rotary drum reactor is a continuous reactor that can be heated directly or indirectly. In an indirectly heated rotating drum reactor the heat is transferred from the drum wall to the biomass particles while the drum rotates causing the particles mixed and exchange heat. Similar to all indirect heating reactors, the heating medium does not have to be oxygen free and released volatiles can be combusted to provide required heating in the reactor[37,103,107]. The high capacity of 600,000 tons/year has been reported for rotary drums [37]. Other available capacities are related to Bio Energy Development North AB (SWE) which is established in 2011s with 25,000-30,000 tons/year capacity and Atmosclear in 2010s with capacity of 50,000 ton/years [107].

Screw type reactors

A screw type reactor is a continuous reactor that can be vertical, horizontal or inclined [103] and the heating transfer can be directly or indirectly [37]. However, the usual type is heated indirectly and the biomass is moved by one or multiple auger screws. There is a limitation for well mixing of the biomass and also a possibility of hot zones and char formation [37]. The commercial scale of screw torrefaction reactor is developed by BioLake B.V. in 2010s with production capacity of 5,000-10,000 tons/year, and FoxCoal B. V. in 2012 with production capacity of 35,000 tons/year [107].

Table 2-6: Different type of torrefaction reactors and their properties, modified from [51,103,105,109]

Reactor type	Advantages	Limitations	Heating
Rotary drum	• Relatively simple equipment • Low pressure drop • Uniform heat transfer • Large size variation of biomass • Various methods to control torrefaction process • Proven technology for biomass drying	• Low heat transfer (specially in indirect heating) • Difficult to measure and control temperature • Less plug flow compared with other reactors • Bigger system size (Large footprint and cost) • Necessary proper drum sealing • Scalability unproven	direct/ indirect
Moving bed	• Relatively simple and low cost reactor • High heat transfer • High bed density • High capacity of the reactor able to support large biomass throughput • Feed stock flexibility (Process low density biomass without large disadvantages)	• Significant pressure drop • Difficult to control temperature (risk for hotspots) • Possibility for channel formation between biomass particles causing unequal torrefaction • Non-uniform temperature distribution, especially with indirect heating • Selective to biomass size and structure, due to pressure drop • Scalability unproven	direct/ indirect
Screw type	• Good biomass flow (close to plug flow) • Proven technology for torrefaction • Large size variation of biomass • Relatively cheap reactor	• Higher possibility of hot spots • Low heat transfer rate • Require feedstock with very low moisture content • Non-homogenous product • Require shaft sealing • Scalability unproven	Indirect

Reactor type	Advantages	Limitations	Heating
Fluidized bed	• Excellent heat transfer rate • Proven scalability	• Sensitive to particle size • Necessary to have additional gas equipment to supply fluidizing fluids • Possibility of attrition (fines formation) • Difficult to get plug flow • Slow temperature response	direct
Torbed	• Low residence time (<100 s) • Large throughput due to fast heat transfer • No moving parts (low maintenance) • Ability to precisely control product • Small foot print • Scalable technology (to 25 t/h) • Efficient reaction kinetics	• Low flexibility to particle size • • High utility fuel demand (but low energy consumption) • Volumetric reactor capacity is limited • High temperature leads to a greater loss of volatiles • Risk of tar formation due to relative higher loss of volatiles	direct
Multiple heart furnace	• Proven equipment design • Higher possibility of scale up • Close to plug flow • Good temperature and residence time control • Possibility of adding fines • Good heat transfer • Large size variation of biomass • Proven scalability	• Lower heat transfer rate compared with other direct reactors • Limited volumetric capacity • Relatively larger reactors • Require shaft sealing • Low efficient combustion of the flue gas	direct
Belt conveyor	• Good temperature control • Large size variation of biomass • Relatively low investment costs • Easy control of residence time through the speed of the belt	• Possibility of clogging the holes in the belt with tar and dust, causing unequal torrefaction • Limited upscaling potential since capacity is dependent on the surface area of the belt (other systems are volume dependent) • Limited temperature control	direct

Reactor type	Advantages	Limitations	Heating
	• Proven technology from biomass drying industry	• System has too many mechanical parts, which increases maintenance costs	
Microwave	• Radiation based heat transfer instead of convection and conduction • High heat transfer and fast torrefaction • less dependent on the size of the biomass particle • Good temperature control	• Unproven technology for drying or torrefaction of biomass - effects of rapid heating of biomass not known • Electric energy needed for process • Heating of biomass interior is not uniform • Requires integration with other conventional heaters to achieve uniform heating	direct

Table 2-7. Different Torrefaction developers and technology, [37,51]

Reactor type	Developer	Reactor technology	Capacity	Location
Rotary drum	Torr-coal (NL)	Torr-Tech	35 kt/yr	Dilsen-Stokkem (BE)
	Andritz (AT)	ACB/ECN	10 kt/yr	Frohnleiten (AT)
	Atmosclear (UK)/Airless (CH)	CDS (UK)	50 kt/yr	--
	ETPC-Umea University (SWE)	BioEndev	25-35 kt/yr	--
	Torkapparater (S)	--	100 kt/yr	--
	Teal Sales Inc (US)	--	15 kton/yr	White Castle (US/LA)
	BIO3D (FR)	--	--	--
	Stramproy (BE)	--	--	--
	Earth care products (US)	--	20 kton/yr	Independence (US/KS)
	TSI (US)	--	--	--
	CENER (SP)	--	--	Aoiz (SP)
Moving bed	ECN (NL)	ECN:BO2	5 ton/h	--
	Thermya (FR)	Torspyd	20 kt/yr	--
	Buhler (GER)	--	--	--
	Torrec (FI)	--	10 kton/yr	Mikkeli (FI)
	LMK Energy (FR)	--	20 kton/yr	Mazingarbe (FR)
	Grupo Lantec (SP)	--	20 kton/yr	Urnieta (SP)
	Andritz (DK) / ECN (NL)	--	10 kton/yr	Stenderup (DK)
Screw type	BioLake BV/ATO (NL)	ECN:BO2	5-10 kt/yr	--
	BTG (NL)	BTG	5 ton/h	--
	Foxocoal (NL)	--	35 kt/yr	--
	Solvay (FR) / New Biomass	--	80 kt/yr	Quitman (US/MS)
	Energy (US)		80 kt/yr	
	Arigna Fuels (IR)	--	--	County Roscommon (IR)
	Agri-Tech Producers LLC (US/SC)	--	13 kton/yr	Allendale (US/SC)
	BioEndev (SWE)	--	16 kton/yr	Holmsund, Umea (SWE)

Reactor type	Developer	Reactor technology	Capacity	Location
Fluidized bed	River Basin Energy (US)	--	6 t/h	Laramie (US/WY)
	Bio Energy Development & Production (CAN)	--	--	Nova Scotia (CAN/NS)
Torbed	Topell (NL)	Torbed	60 kt/yr	Duiven (NL)
Multiple heart furnace	CMI-NESA (BE)	NESA	--	Seraing (BE)
	Integro Earth Fuels LLC (US)	--	11 kton/yr	Greenville (US/SC)
	CEA (FR)	--	--	Paris (FR)
	Wyssmont (USA)	Wyssmont	50 kt/yr	Fort Lee (US/NJ)
	Terra Green Energy (US)	--	--	McKean County (USA/PA)
Belt conveyor	Agri-Tech producers LLC/RTF (US)	Torr-Tech	5 ton/h	United States
	4 EnergyInveste (NL)	Stramproy	5.5 ton/h	Netherland
	New Earth Eco Technology (US)	Eco-Pyrovac	2 ton/h	United States
	Stramproy Green Investment (NL)	Stramproy	45 kt/yr	Netherland
	Horizon Bioenergy (NL)	Oscillating belt conveyor	45 kt/yr	Steenwijk (NL)
Microwave	CanBiocoal (UK)	Rotawave	110 kt/yr	Chester (UK)

Multiple hearth furnace

The multiple hearth reactor is a kind of moving bed reactor that biomass is fed from the upper side of the reactor to the first hearth and then swept to the next hearth sequentially. The temperature increases gradually from 220°C to 300°C passing each layer. The heating media is applied directly on each layer. This reactor is efficient in terms of well mixing and compatible for large scales. However, the residence time is about 30 minutes resulting to a high specific reactor volume [37].

Belt conveyor torrefaction reactor

A Belt conveyor concept has been used for drying of the biomass and its technology was proven for a plug flow torrefaction reactor. The biomass moves via multiple porous belt or a vibrating grate and is heated directly by hot gas medium. The belt speed or vibration frequency is controlled to define a residence time. The main disadvantage of this reactor is possible clogging of the belt or grates. Also, the specific volume of the reactor limited the usage of low bulk density materials [37]. Agritech Producer Columbia constructed a commercial scale (50,000 tons/year) of this type of reactor, namely Torre -Tech ® 5.0 in 2010s. Its operating temperature was in range of 300-400°C, and residence time was 30 min [107].

Microwave torrefaction reactor

Microwave torrefaction reactor is a lab scale reactor that provide the uniform heating via frequency electromagnetic waves, within short residence time, for a different particle size of feedstock. However, the electricity requirement hinders larger scale torrefaction at reasonable costs [37,107]. Nevertheless, Rotawave Ltd. developed a commercial scale of microwave torrefaction reactor in 2011s with production capacity of 110,000 tons/year [107].

System description and energy consumption

A typical flow diagram for a conventional integrated torrefaction and pelletizing (TOP process [66]) is shown in Figure 2-1.a. The process configuration of different plants might vary based on the type of biomass feedstock, initial moisture content, particle size, process temperature, residence time, torrefaction technology, heat integration method, and production capacity [51,52,110,111].

Moisture content of the initial biomass is about 60 wt.% which is naturally dried in the field to 30-40 wt.% and hauled to plant facilities [52,110,111]. The biomass logs or large size feedstocks are usually chipped by chipping unit and screened through proper sieves. According to CEN TC/335 P45 specifications, 80% of wood chips would be within the range of 3.15–45mm and 20% oversized are recycled [111]. According to Westbrook et al. [112] the diesel fuel consumption for chipping of the southern pine is 1.5-3 L/ton of feedstock which is compatible with 1.18-1.92 L/m^3 of solid wood reported by [113]. The screening of initial wood chips is usually performed to reduce the ash content of the biomass and providing more consistent feedstock [51,114].

The chipped biomass is sent to the dryer to reduce the moisture content. In pelletizing plants, a low moisture content in range of 6-15% is favored for the initial biomass [38,110,115]. Water reduces the friction as a lubricant and acts as a binder during pelletizing that improves the pellet durability. Moreover, pellets with very low moisture content are prone to absorb more water and elongate during storage time which is not desired [110]. Similarly, in torrefaction plants, the biomass moisture content should be reduced to less than 15 wt.% before torrefaction [37]. The main reasons for drying the biomass before torrefaction are: (1) variable moisture content of the initial biomass and its latent heat requirement governs the heat balance of the system and changes the control parameters, (2) higher moisture content of the torgas (torrefaction gas), lowers the adiabatic flame temperature. So, the energy of the torgas would not be sufficient for thermal

treatment [37]. Rotary dryers are normally employed for this concept [110]. The required energy for drying section (evaporating the water) depends on the feedstock capacity and initial moisture content which is usually provided by combustion of the torgas assisted by a part of biomass as a fuel or any other auxiliary fuel [6]. The required energy for drying can be calculated basically from the latent heat of the water content as well as water and biomass sensible heat from inlet temperature to the drying temperature [1].

The dried biomass is sent to torrefaction section. Temperature, residence time and particle size are the most important parameters in biomass torrefaction [41]. The effects of torrefaction temperature and residence time have been studied by severity factor for certain particle size [42–44]. The torrefaction degree can be divided into three levels: light (200–235 °C), mild (235–275°C), and severe torrefaction (275–300°C) [8]. A holding time of 30-60 min was ascertained to be common for torrefaction based on previous studies [9]. A higher torrefaction temperature causes more thermal decomposition of the biomass producing higher energy density bio-coal but with less mass yield. On the other hand, greater amounts of volatile organic species would be released with potential of more heat generation by oxidizing. The properly designed and operated torrefaction system, is said to be running at the point of " auto-thermal operation", which means that the thermal energy required for the drying and torrefaction process can be delivered by combustion of torrefaction gas [66]. In the sever torrefaction temperature, the energy of the torgas combustion might be higher than the thermal requirement (above the auto-thermal operation) [51]. It is therefore important to utilize that energy in an adjacent heat exchanger or boiler to optimize the overall thermal efficiency. Several types of reactor with different technologies have been developed for biomass torrefaction such as compact moving bed, fluidized bed, belt dryer, rotary drum, screw conveyer, and microwave. Most of these reactors are upgraded from previous

technologies for drying or pyrolysis purposes with related advantages and disadvantages [51]. In section 2.4.7 Torrefaction reactor, different type of reactors with their advantages and disadvantages are briefly described.

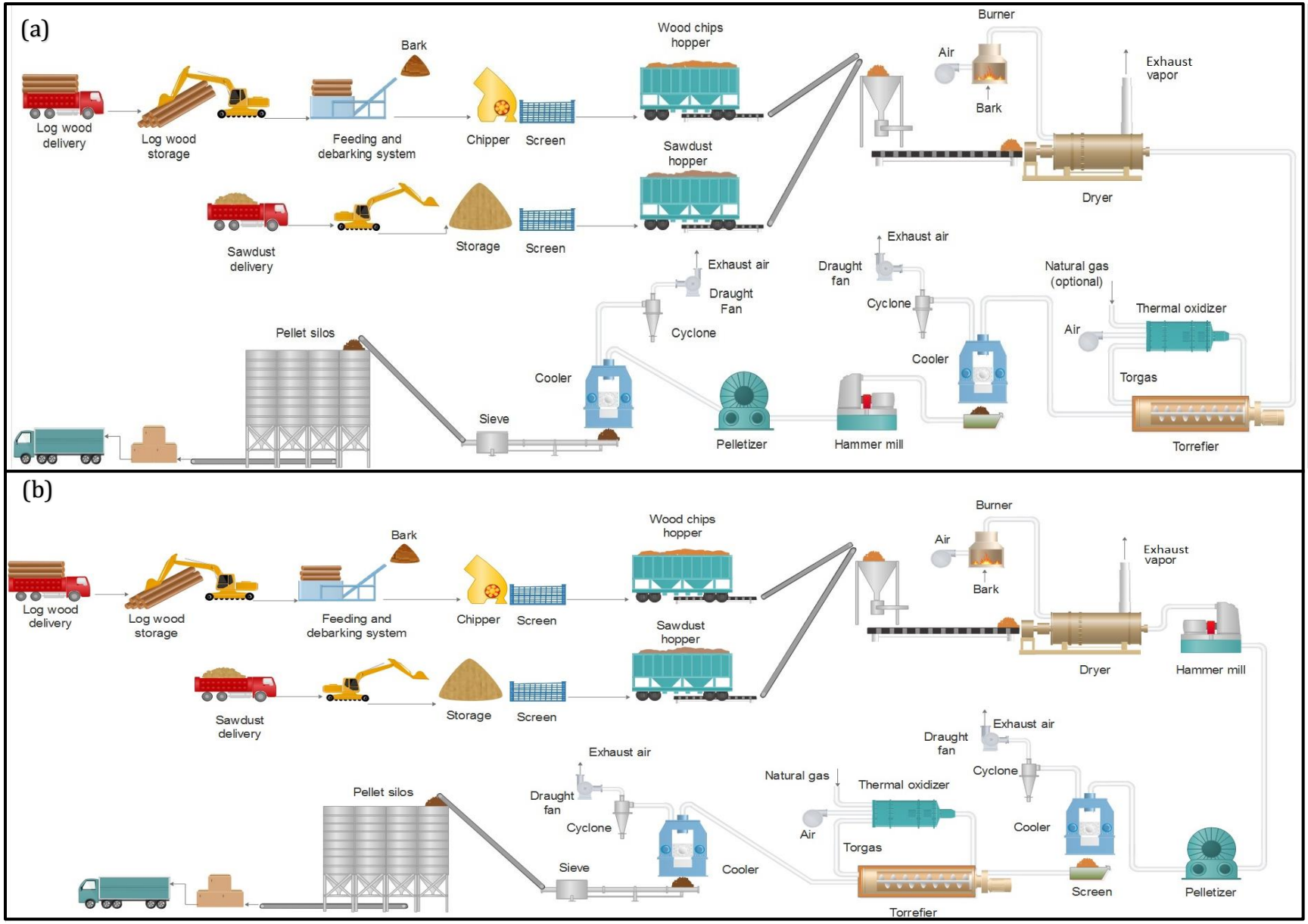

Figure 2-1. (a) Conventional pathway for integrated torrefaction and pelletizing (TOP). (b). Torrefaction of biomass pellet (TAP)

A detailed mass and energy balance is required for the specific capacity of production and for each type of biomass based on the selected torrefaction technology. The torrefaction reaction and in other words the biomass degradation starts from 200°C and is mildly exothermic in temperature range of 250-300°C [31]. Therefore, only little energy is required to compensate the heat loss from the reactor that can be estimated by the biomass sensible heat at torrefaction temperature [1,116].

After torrefaction, the torrefied biomass is cooled to below self-ignition temperature by water or air cooling to prevent possible combustion of torrefied biomass in the atmospheric oxygen [51,106,111]. Then, the biomass is sent to a hammer mill to be ground to a proper size for pelletizing. Torrefaction significantly enhances the grindability of biomass. The required power consumption for grinding torrefied biomass is 80-90% lower than raw biomass [36,66]. Also, the capacity of milling increases by 7.5 to 15 times depending on the different torrefaction conditions [66]. It is shown that the specific grinding energy consumption decreased linearly with the increase in torrefaction temperature [36]. The recommended particle size for high quality pellets is 0.6-0.8 mm [30]. The energy consumptions for grinding the raw and torrefied wood chips for some woody material are shown in

Table 2-8.

Densification is an energy intensive process for torrefied material that is in contrast to grinding. It has been discerned by several researchers that torrefaction can hinder densification process by weakening the bonding between particles; hence, the high die temperature, more compressive pressure, or binding agent is necessary for densification step [8,36,38–40]. The required energy for pelletizing of torrefied biomass is reported in range of 80-323 kWh/t [45,117,118]; However, Topell Energy claimed to achieve the energy consumption of 45 kWh/t

by adding appropriate binder [106]. The energy consumptions for pelletizing of the raw and torrefied samples are listed in Table 2-9.

The produced pellets should be cool down again to reduce the risk of ignition [110]. Then the pellets are screened to check the quality and sent to the storage facilities. The unshaped pellets and fines are recycled to the mill [110].

A typical flow diagram of a TAP plant (Torrefaction after pelletizing) is depicted in Figure 2-1-b. Similar to the conventional procedure for producing torrefied pellets, there can be various equipment configuration for post-torrefaction of biomass pellets. Apart from different characteristics of torrefied pellets from these two pathways, the main differences between equipment configuration and energy consumptions of conventional plants (TOP) and post-torrefaction plants (TAP) are relevant to grinding and pelletizing sections. In TAP pathway the specific energy for grinding is pretty high compared to conventional pathway (

Table 2-8) while the pelletizing can be done easier without binder requirement (Table 2-9). The other possible item that might be affected by these two pathways is the reactor type and its geometry. In post-torrefaction pathway the higher bulk density of biomass pellets requires smaller reactors which can reduce the capital cost of the reactors. Moreover, it provides a wide range of flexibility for different feedstocks as well as more operational comfort [37]. However, detailed studies are required to identify the associated control parameters.

According to new challenges, the thermal treatment can be done as a preprocessing plant in depot as well as a pretreatment section at bio-refinery plant. In bio-refinery scenarios, the heating requirement for drying might be provided with available hot gas [52]. Thus, the torrefaction gas can be condensed and utilized in relevant applications like wood vinegars, wood protection,

additive agent in coating of pellets, or production of green chemicals [54,55]. On the other hand, the excess heat production in severe torrefaction might be used in boiler or other exchangers [52].

Table 2-8. Specific energy consumption for grinding raw and torrefied wood chips

Material	Initial particle size (mm)	Final size (mm)	Eg[a] (kWh/t)	Ref.
Pine chips	20.94-70.59 × 1.88-4.94 × 15.08-39.07	d_{50}[b]=0.71	237.7	[36]
Pine 275°C chips		d_{50}=0.27	52	
Logging residue		d_{50}=0.74	236.7	
Logging residue 275		d_{50}=0.46	78	
Beech chips	2-4 mm	d_{50}=0.227	850	[119]
Beech 280°C chips		d_{50}=0.14	90	
Spruce chips		d_{50}=0.197	750	
Spruce 280 chips		d_{50}=0.093	150	
Birch chips	10 and 40 mm	-	171.9	[120]
Birch 225°C chips		d_{50}=0.2-0.4	85.1	
Birch 275°C chips		d_{50}=<0.18	20.5	
Spruce chips		-	161.4	
Spruce 225°C chips		d_{50}=0.2-0.4	96.5	
Spruce 275°C chips		d_{50}=<0.18	22.7	
Pine chips	30×30×5	d_{50}=3.2	124	[121]
Pine chips	d_{50}=9.2	d_{95}[c]=1	113.2-119.1	[122]
Pine bark	d_{50}=8.25	d_{95}=1	18.1-23.6	
Poplar	d_{50}=8	d_{95}=1	82-89	
Pine chips	d_{50}=4.93	d_{gs}[d]=2-8	31.5-199.2	[123]
Spruce Chips	d_{50}=7.38	d_{gs}=2-8	17.3-251.9	
Beech chips	d_{50}=5.83	d_{gs}=2-8	28.3-307	
Qak chips	d_{50}=4.98	d_{gs}=2-8	24.6-170.2	
Douglas fir wood chips	38-51	<1.5	74	[45]
Douglas fir 260°C			10	

a Eg: Specific energy consumption for grinding

b The particle diameter obtained from the cumulative distribution data at 50%.

c The particle diameter obtained from the cumulative distribution data at 95%.

d The size of grinding sieve

Table 2-9. Specific energy consumption for pelletizing raw and torrefied wood samples

Material	pelletizing (kWh/t)	Ref.
Douglas fir	210	[45]
Douglas fir 260 (without binder)	323	
Douglas fir 260 (with binder)	128	
Wood	50-60	[117]
Torrefied wood	150	
Corn stover (MC:15%)	101	[124]
Miscanthus (MC:15%)	324	
Pine sawdust (Mc:11%)	166	[125]
Torrefied pine (235-255 °C)	70-80	[118]
Torrefied logging residue (240-250°C)	90	
Hardwood	144	[126]
Chinese fir (MC:15%)	5.7	Single pellet [127]
Camphor (MC:15%)	5.2	
Rice straw (MC:15%)	3.7	
Pine	7.6	Single pellet [128]
Pine 280°C (MC:0.2-0.8%) (die temperature 170-230°C)	8.5-8.76	
Fir	8.7	
Fir 280°C (MC:0.2-0.8%) (die temperature 170-230°C)	9.2-9.5	
Spruce	8.1	
Spruce 280°C (MC:0.2-0.8%) (die temperature 170-230°C)	8.5-8.7	

Mass and energy yield

As the torrefaction temperature increases, the calorific value of the torrefied biomass is enhanced while the solid mass yield and energy yield decrease. A suitable trade off should be considered to maintain the optimal overall thermal efficiency of the plant. The thermal efficiency can be calculated by dividing the thermal output (heating value multiply by mass flow) by the thermal input. The higher thermal efficiency improves the process economics [51]. The typical mass yield over 70% for temperature range of 200-300°C and residence time of 30-60 min have been reported from several studies [66,128]. The typical mass and energy balances for different

pilot test plants in SECTOR project (Production of Solid Sustainable Energy Carriers from Biomass by Means of TORrefaction) for pine torrefaction are in range of 79-81.3% db for mass yield, 87.6-90.5% db for energy yield, and 83.6-92.4% for net thermal efficiency [37]. Prins et al. studied the torrefaction of beech and willow at 250°C and 300°C temperature in residence time of 30 min and 10 min, respectively. The mass yield was in range of 67-87% db and energy yield was 80-97% [129]. Batidzirai et al. modelled the mass and energy balance for torrefaction of eucalyptus and straw (particle size 20-30 mm) based on the confidential information from a pilot torrefaction plant. For torrefaction at 275 °C temperature for 60 min, the mass yield of 48% and 65%, and thermal efficiency of 94% and 96% were reported for eucalyptus and straw, respectively [51]. Mcnamee et al. examined the torrefaction of North American pine chips (size range 5-30 mm) in the temperature range of 250-290 °C for 30 min. The mass yield of 72.2-90.7% db and energy yield of 84-91.3% db were obtained from their experiments [130]. The torrefaction of SPF (a mixture of spruce, pine, and fir) in different temperatures and 60 min residence time was performed by Peng et al. showed the mass yield in range of 71.5-86.7% and energy yield of 77.34-90.89%[39]. The more complete review of older torrefaction results from several studies including mass yield, energy yield and higher heating value of various types of biomass has been gathered by Chen et al. [8]. After determining the mass and energy balance and thermal efficiency of the plant, the optimum process condition can be obtained, thereby the equipment properties are specified and economic evaluation can be performed.

Life cycle assessment (LCA)

Life cycle assessment of conventional pathway for torrefied pellet production has been performed in some studies and the results have been compared with wood pellet production [111,126,130–133]. The difference in torrefaction temperature and heat integration system

influence the GHG emission results. Mcnamee et al. [130] showed that GHG emissions for torrefied pellet production ranging from 25.4 - 46.7 gCO_2 eq./MJ and for wood pellets was 35.6-47.8 gCO_2 eq./MJ depending on different torrefaction temperature and usage of torgas, wood chips or natural gas for heat provide). Adams et al. [111] compared torrefied and conventional wood pellets for UK consumption, finding GHG emissions considering drying requirement and fuel source ranging from 17 to 40 gCO_2eq./MJ for torrefied pellets and 27–40 gCO_2eq./MJ for conventional pellets. Agar et al. [132] indicated that emissions from production of torrefied pellets are 45 gCO_2 eq./MJ versus 43 gCO_2 eq./MJ for conventional wood pellets.

The GHG emissions for wood pellets and torrefied pellets supply chains were investigated in G. Gardbro et al. study [131]. Different scenarios including short transportation distance (Sweden to Denmark) and long transportation distance (The USA to Netherland) were explored. The GHG emissions from the wood pellets and torrefied pellets were calculated to be 16.7 and 15 $kgCO_2$eq/MWh (about 4.58 and 4.16 gCO_2 eq./MJ) for the first scenario and for the second scenario it was 21.1 and 20.8 $kgCO_2$eq./MWh (about 5.86 and 5.77 gCO_2 eq./MJ), respectively. The higher GHG emissions in the second scenario were due to the longer transportation distance, especially the ocean shipping influence. Thereby, they inferred that a shorter length of the supply chain is preferred from a GHG perspective [131].

McKechnie et al. [126] studied the emissions associated with steam-treated pellet production. They showed the close GHG emissions of 5.3 $kgCO_2$eq./ GJ and 5.5 $kgCO_2$eq./GJ for steam-treated pellet and conventional production, respectively. Mass loss during the steam treatment process (requiring greater biomass input than conventional pellets) and the lower electricity requirement were the major factors of different emissions. Although different assumptions were used in above mentioned studies, the results have not shown a significant

reduction in GHG emissions from torrefied pellets compared to conventional pellets. However, the improved properties of torrefied pellets increase the rate of co-firing resulting further reduction in GHG emissions [132].

Economic analysis

The economic evaluation for conventional torrefaction and pelletizing has been performed by several studies for different production capacities. The primary step for economic analysis is estimating the capital cost of each equipment. The costs of some of the major items in a combined torrefaction and pelletizing plant are listed in Table 2-10. The capital cost of a torrefaction reactor depends significantly on the technology of torrefaction [1,6]. Bergman et al. studied three different types of reactors including indirectly heated screw reactor, directly heated rotating drum, and directly heated moving bed reactors with the base year of 2004. The capital investment of these reactors for production of 227 kt/year torrefied biomass were €13.4, €5.6, and €2.2 million (about $14.74, $6.16, and $2.42 million, exchange rate at 2004: 1 Euro=1.24 Dollar), respectively [6]. According to their results, the moving bed reactor showed the most attractive residence time characteristics despite the lowest capital investment. Using these data and applying the scaling factor of 0.8, Peng et al. estimated the investment costs of these three reactors for production of 138 kt/year torrefied biomass in 2010. The obtained capital costs were as follows: screw reactor: $28.74 million, rotating drum: $12.54 million, and moving bed: $4.65 million [128]. Nevertheless, the information regarding to energy consumption and capital cost of different torrefaction reactor is scarce. Figure 2-2 shows the capital cost of some type of torrefaction reactor in M$ versus different capacities based on literature.

Table 2-10. Capital cost of equipment for torrefaction and pelletizing plant

Plant equipment	Scale factor	Base capacity (t/h)	Capital cost-base cost ($)	Life time years	Year cost based	Ref.
Primary grinder	0.99	6	650000		2010	[134]
Chipper	0.6-0.7	5	70000		2013	[51]
Chipping cost			4.37 $/ton		2011	[135]
Rotary drum dryer	0.6	6	430000	15		[134]
	0.6	8	300000		2007	[136]
	0.65	6	440000		2013	[51]
	0.6	1 t water/h	820194	15	2014	[110]
	0.6	6	350000	15	2004	[137]
Solid fuel burner	0.6	6	143000	10	2004	[137]
	0.7	1 MW	95483	10	2014	[110]
Hammer mill	0.6	6	150000	10	2010	[134]
	0.7	5	70000		2013	[51]
	0.6	6	60000	10	2004	[137]
		8	36200		2007	[136]
		1	55404	10	2014	[110]
Feeder	0.57	6	44700	15	2010	[134]
	0.57	1	17367	15	2014	[110]
Pellet mill	0.85	6	350000	10	2010	[134]
	0.61	5	13000		2013	[51]
	0.6	6	315000	10	2004	[137]
		8	232000		2007	[136]
		1	84805	10	2014	[110]
Pellet cooler	0.58	6	170000	15	2010	[134]
	0.6	6	32000	15	2004	[137]
		8	34900		2007	[136]
	0.58	1	27713	15	2014	[110]
Screener/shaker	0.6	6	18300		2007	[134,136]
	0.6	6	24000	20	2004	[137]
	0.6	1	8756	10	2014	[110]
Bagging system	0.63	6	450000		2007	[134,136]
Conveyor	0.75	1	32409	10	2014	[110]
Torrefaction reactor (moving bed reactor)	0.72	5	4400000-6250000		2013	[51]
	0.6	1	673283	15	2014	[110]
Packaging unit	0.6	6	80000	10	2004	[137]
Storage bin	0.6	6	24000	20	2004	[137]

Plant equipment	Scale factor	Base capacity (t/h)	Capital cost-base cost ($)	Life time years	Year cost based	Ref.
Miscellaneous equipment	0.6		168000	10	2004	[137]
Conveyors, tank, other fixed equipment	0.75	4	1130000		2007	[134,136]
Front end loader	0.6		100000	10	2004	[137]
Loader/lifter		1	24372	10	2014	[110]
Fork lifter	0.6		82000	10	2004	[137]
Dump truck	0.6		100000	15	2004	[137]
Office building	0.6		72000	20	2004	[137]
Land use	0.6		40000	25	2004	[137]
pellets storage silo	0.85	1 tonne	490	20	2014	[110]
Storage lots	0.85	1 tonne	89	20	2014	[110]

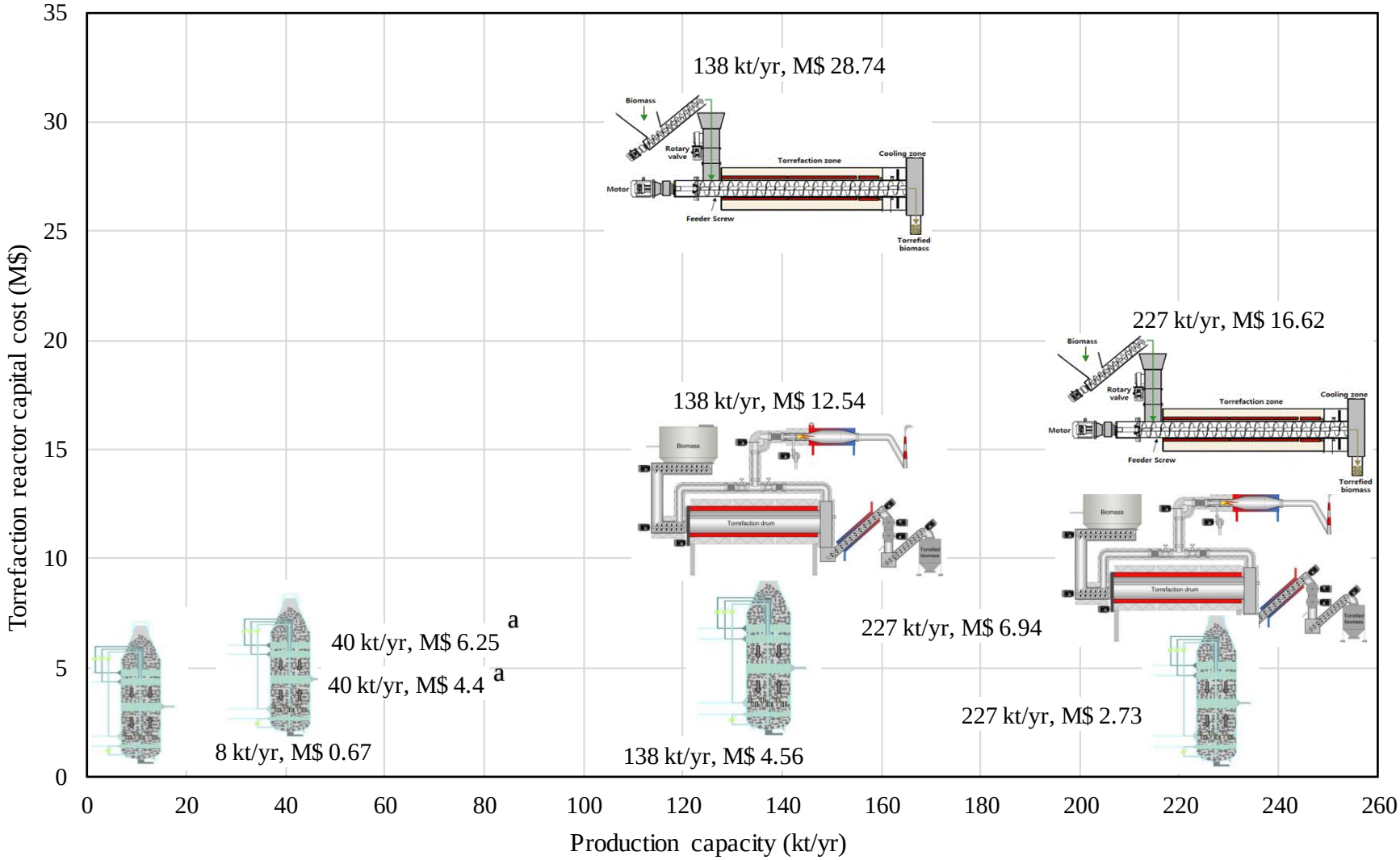

a The cost is higher than other reported data for moving bed reactors since it includes moving bed reactors, gas burners, gas b lowers and heat exchangers.

Figure 2-2. Capital cost of some different technology of torrefaction reactor from literature review. [6,51,110,128]

Berman et al. carried out the primary evaluation of TOP process with ECN Technology (Energy research Centre of the Netherlands). Based on the calorific value of produced pellet, the market price of torrefied pellet was determined about €150 and €185 per ton ($198 and $238 Mg^{-1}) for co-firing market and domestic market, respectively compared to conventional wood pellet with price of €120 and €150 per ton ($159 and $198 Mg^{-1}). The profitability analysis for 10 years' lifetime project showed the internal rate of return (IRR) of 30% for torrefied pellet and 13% for conventional wood pellet. A more detailed economic evaluation was performed by Topell Energy later and showed a significant higher investment cost rather Bergman et al. [106]. Their cost estimation includes turnkey costs and outside battery limits along with actual built torrefaction plants.

Table 2-11 and Table 2-12 show the total capital cost reported by some technology developers. The specific investment cost in is calculated approximately based on interest rate of 8%, lifetime of 15 years and calorific value HHV=21 MJ kg^{-1}.

Topell energy estimated the approximate extra costs of $35 Mg^{-1} ($1.9 GJ^{-1}) for regular wood pellet at the power generation plant [13]. Their analysis showed the total capital investment of $29 million for 100,000 Mg^{-1} annual production TOP pellet and $19.5 million for 124,000 Mg yr^{-1} production of wood pellets [13]. Peng et al. reported a total capital investment in range of 22.1 to $31.0 million for a torrefied pellet plant (TOP) with 126,000 Mg^{-1} annual production capacity and $18.1 million for a 180,000 Mg yr^{-1}production of wood pellet [19]. These values were in the range of $23.4 million to $117.5 million for 50,000 to 500,000 Mg^{-1} production reported by Batidzirai et al. [14].

The calculated production costs by Pirraglia et al. was $199 Mg^{-1} for torrefied pellet production in a plant with 100,000 Mg^{-1} annual production capacity [43]. Peng et al. compared the

economics of wood pellet production and torrefied pellet production from different feedstocks. They reported the production costs of 65 to \$132 Mg^{-1} for conventional wood pellets and \$82 to \$152 Mg^{-1} for torrefied wood pellets [19]. Topell energy reported the cost of \$7.4 and \$6.8 GJ^{-1} (\$161 and \$118 Mg^{-1}) for torrefied pellet and conventional wood pellet production, respectively [13].

Apart from the technical alterations in processing, the major differences between final characteristics of wood pellets and torrefied pellets are moisture content, bulk density, calorific value and volumetric energy density. The first two items causing significant changes in transportation and storage cost. By lower moisture content and hydrophobic nature of torrefied pellets, loss of material due to biodegradation is reduced [9], and outdoor storage could be realized [13]. On the other side, the denser product would occupy less area and improve storage and transportation economics [135].

In Bergman et al. study the cost of sea transportation was considered about €35 $ton^{-1}$for conventional and €28 ton^{-1} for torrefied pellet and cost of road transportation was considered about €4.4 ton^{-1} for both conventional and torrefied pellet. Thus lower production volume of torrefied pellets (higher energy density) resulting lower cost of transportation [66]. The same assumptions for sea transportation and road transportation were used in other reports [106,128,138]. Srivastava et al. in their study for biomass supply logistics in Michigan U.S estimated the cost of road transportation for wood pellets and torrefied pellets at the fixed cost of \$3.72 ton^{-1} (~\$4.1 Mg^{-1}) and variable cost of \$0.074 per ton-mile [135].

Table 2-11. Capacity and investment cost of some torrefaction developers [51]

Developer	Reactor Technology	Capacity	Investment cost	
		kt/yr	M$	$/GJ
Ebes	Rotary drum	10	5.1	2.84
Thermya	Moving bed	20	5.2	1.45
4Energyinvest	Belt conveyor	42	16.9	2.24
Topell/RWE	Torbed	60	19.5	1.81
Torr-coal group	Rotary drum	70	22.8	1.81
UMEA University	Rotary drum	30	14.3	3.58

Table 2-12. Examples of economic evaluation of torrefied and conventional pellets

Feedstock, Ref	Base year cost	Pellet type	Production rate Annual thousand Mg	Total capital investment M$	Total capital investment M$ 2017	Total production cost $ Mg^{-1}	Total production cost $ Mg^{-1} 2017	Pellet price $ Mg^{-1}	Pellet price $ Mg^{-1} 2017	Calorific value LHV MJ kg^{-1}
Green Wood, [66]	2004	Torrefied	56	9	12	67	86	202-252	258-323	20.40
		Raw	80	7	9	62	79	164-205	209-261	16.50
Wood, [106]	2011	Torrefied	100	29	28	161	156			
		Raw	124	20	19	118	115			
Wood, [138]	2004	Torrefied	64	8	10	118	151	165	211	18.28
		Raw	80	5	7	109	140	143	183	15.80
Straw, [134]	2008	Raw	70-150			171-122	167-121			
Eucalyptus-straw, [51]	2012	Torrefied	50-500	24-118	23-114	98-52	96			
Mill wood residue, [128]	2012	Torrefied	138	22	21	77	75			HHV:22.65
		Raw	180	18	18	65	63			HHV:18.55
MPB infested trees, [128]	2012	Torrefied	138	22	21	151	147			HHV:22.65
		Raw	180	18	18	132	128			HHV:18.55
Straw, [139]	2012	Torrefied	56-59	23	22	178	173			19.20
Beech, [139]	2012	Torrefied	56-59	18	17	182	176			19.20

Simulation

Simulation is a useful technique to facilitate performing the mass and energy balance of the system in different operating conditions to obtain the design parameter information and equipment specifications. This would be beneficial to scale-up the process and estimating the cost of the investment. Aspen Plus software is a powerful tool with good database, which is usually used for simulating the process plants.

So far, some researchers attempted to run the simulation, specifically to calculate the required thermal energy of the process by simplifying the complex kinetic of torrefaction reaction and composition of volatile products. Aspen Plus software has been widely used for simulation of a torrefaction system [52,140–144]. Aspen Plus has a good database for solids, electrolytes, and polymers in addition to the conventional chemicals, and comprises diverse unit operations. The intermediate chemical makeup of the biomass, complex chemistry of torrefaction, and complicated thermodynamic equations of solid phase in equilibrium with gas and liquid phases are some of the main challenges of the biomass torrefaction simulation. No work has yet been published capable of predicting the compositions of torrefaction products at specified operating conditions. A preliminary experimental data is required to specify the torrefaction kinetics of a defined biomass feedstock and probable torrefaction products composition.

In most of the previous studies, the drying has been defined as a simple conversion in an stoichiometric (RStoic) reactor [52,141,143,145]. This approach estimates the approximate heat requirement for evaporation of water content, but it does not necessarily represent the mass and heat transfer in a real dryer. In an RStioc dryer, the operating conditions of heating media (hot air or hot gas) including temperature and moisture content, and temperature profile of solid and gas streams in the dryer cannot be predicted. Moreover, the exhaust gas composition would not be

explored. Recently, Bach et al. [144] simulated the drying process in a solid dryer (and not a reactor) in the Aspen Plus and they used hot air as a heating media. However, they did not scrutinize the details about the type of the dryer, kinetics of drying, moisture content in the outlet air, or variation of the inside temperature [144].

For the reaction section, the regression models have been derived from the known compositions of the input biomass, torrefied biomass, and volatile gas product versus temperature and time, and then the results being implemented to the model in a stoichiometric reactor (RStoic) [140] or conversion reactor (RYield) [52,141,145], or in a combination of both [142,146]. Bach et al. [144], asserted that none of the pre-defined reactors in Aspen Plus could model the complicated torrefaction process. Hence, they proposed a user defined hierarchy reactor to estimate the compositions of torrefied material and weight fraction of known components in the gas stream at different reaction temperature and duration. They implemented a FORTRAN code, which combined the kinetics data of willow torrefaction and the composition of gas product proposed by Prins et al. [31], and calculated the mass yield, energy yield, product composition, and higher heating value of the torrefaction of Norway birch within a temperature range of 240 to 300°C [144]. Cherry et al. investigated different cases of wood torrefaction at 180, 230 and 270°C, and the integration with biorefinery. For the dried feedstock cases and torrefaction temperature of 270°C, the process were above the auto-thermal operation point, where the excess energy could be used in an adjacent heat exchanger or a boiler [52]. Arteaga-Perez et al. simulated the torrefaction of Pinus radiata and Eucalyptus globulus at temperature of 250°C and 280 °C Arteaga-Pérez et al. carried out process simulation of Pinus radiate and Eucalyptus globules torrefaction with Aspen one software [143]. They investigated the torrefaction simulation between 250°C – 280°C based on the work of Kiel et al. [66]. The highest efficiency (96%) was reported for

Eucalyptus at 250 °C when moisture in the feedstock was ≤20%. They considered the definite components (Water, acetic acid ($C_2H_4O_2$), formic acid (CH_2O_2), methanol (CH_3OH), furfural ($C5H_4O_2$), carbon dioxide, and carbon monoxide) as the most abundant components in the volatile product based on several studies [41,59,147]. Syu and Chiueh [148] modeled a torrefaction system of rice straw by Aspen Plus software. They used the same components of [41] for volatile components for the torrefaction at 250°C for 30 min. The highest energy efficiency was for feedstock with lower 12 wt% moisture content [148].

The biomass feedstock and capacity, moisture content, torrefaction temperature, torgas energy management, and the system configuration might affect the total external energy requirement [6,52,148]. The detailed simulation of a dryer resembling the real industrial conditions was not explored in previous studies. The compositional changes of the biomass and torgas based on the kinetics of reactions and in a temperature range of torrefaction have been rarely addressed [144]. Moreover, reviewing the literature, the alteration of biomass proximate analysis within the torrefaction and its effects on the enthalpy variation were not explored in detail.

Key technical standards for solid biofuels

The original physical and chemical properties of the biomass pose several problems in handling, transportation, and storage. The pre-treatment processes are applied to improve solid biofuel properties; however, technical standards are still required to be developed and implemented to maintain the quality of the of biofuels and mitigate their potential hazards.

Solid biofuels' potential hazards

The common issues regarding biofuels safety are self-heating, off-gassing, dust and gas formation, biological health hazards, and operational injuries [149,150].

Self-heating is a well-known phenomenon for many types of materials. Chemical oxidation, water up taking, and microbial degradation might result in exothermal reactions that increase temperature of a biofuel and start spontaneous combustion. The more volume of material can generate more heat that increase the peril of combustion in a large scale storage. On the other hand, the cooling process depends on the open surface area of the material. Thus, the ratio of volume/surface is an important parameter to control the biofuel self-heating. Temperature of biofuel storage should be measured and monitored regularly as well [149].

Biomass off-gassing might occur through its supply chain and is caused by releasing volatile organic compounds due to auto-oxidation, thermal reactions, or biodegradation. These emissions include condensable and non-condensable gases such as aldehydes, ketones, CO, CO_2, and CH_4 that contribute to health hazard, self-heating, or ignition processes [149]. There is a possibility of oxygen depletion in the storage due to the reaction of the torrefied pellet with oxygen and production of CO. Therefore; the closed storage should frequently be ventilated, especially before entrance [150]. The high CO concentration in the biofuel storage can be counted as a sign of "any activity" in the bulk and should be measured regularly [149].

In addition to self-heating and off-gassing, the impacts, compression, and abrasion forces during operation, handling, and transportation of solid biofuels might lead to formation of fines and dust. Dust productions not only pose respiratory and health issues, but also create a potential source of ignition and explosion [150].

In case of torrefied material, self-heating and off-gassing are moderated. Removal of polar hydroxyl group reduces the propensity for oxidation reactions and the hydrophobic nature of torrefied biomass result in less water absorption and biological reactions. Moreover, off-gassing is decreased due to lower amount of volatiles [9]. However, torrefied material are brittle and more

prone to dust formation. The higher accessibility of dust surface to air increase the reactivity of the material and therefore increase the possibility of explosion [150]. It has been shown that reactivity of the torrefied biomass is rather high and comparable with coal [4,151]. The explosion severity of the torrefied dust was tested by Wilen et al. [152], compared with raw wood and different types of coal, and expressed in terms of Kmax value (Table 2-13). The Limiting Oxygen Concentration is the maximum allowable concentration of oxygen in the mixture of dust and air before explosion happening. The torrefied wood dust was classified as St1 in their report. The Kmax or Kst value is the parameter of explosion severity test indicating the maximum rate of pressure rise (bar. m/s) in accordance with EN 14034-1 and 14034-2; ASTM E 1226. The explosion classes are listed in Table 2-14.

Table 2-13. Explosion parameter of different biofuels' dusts [152]

	Explosion pressure Pmax (barg)	Rate of pressure rise Kmax (m.bar/s)	Limiting Oxygen Concentration LOC (%)
Torrefied wood dust	9.0	150	11
Wood dust	9.1-10.0	57-100	10-12
Peat dust	9.1-11.9	120-157	13.5
Lignite dust	9.4-11.0	90-176	13-15
Coal dust	8.9-10.0	37-86	14

Table 2-14. Explosion classes

Explosion class	Kmax value (m.bar/s)	
St0	0	Non-explosive
St1	≤200	Weak, normal
St2	201-300	strong
St3	> 300	violent

In addition to health and reactivity issues, the spread of dusts over other equipment and electrical devices and possible ignition from mechanical sparks, electrostatic discharge, or electrical equipment would initiate dust explosion [149].

Technical standards and risk mitigation procedures

The most important key technical standards related to the solid biofuels include fuel specification and classes, quality assurance, solid biofuel production, and safe handling, storage, and transportation. The EN 15234-1:2011 Fuel quality assurance -Part 1 covers all relevant information regarding quality assurance of biofuel in the whole supply chain from raw biomass to distribution to the final customer. The ISO has started to develop international standards for solid biofuels (SO/TC 238) since 2007 (http://www.iso.org). In the United States, American Society of Agricultural & Biological Engineers (ASABE) is responsible for gathering data and establishing the relevant standards. On the other hand, the Committee for European Standardization (CEN) has been developing the standards of solid biomass (CEN/TC 335) in Europe from 2000. By the advancement of solid fuel trading, overall quality assurance systems should be developed to guarantee a certain fuel quality. The written standards are generally about the physical and mechanical test methods, chemical test methods, sampling, fuel specifications, safe handling and storage, and quality assurance [153]. The draft ISO/DIS 17225-8:2015 Fuel specification and classes-part 8 (Graded thermally treated and densified biomass fuels) is being established to provide a preliminary specification of graded torrefied pellets (Appendix A).

Currently, practical experiences on torrefied biofuels are limited. The existing safety procedures for handling woody materials and pellets might be applied for torrefied biomass and pellets. For loading and transportation, general precautions are valid for torrefied biofuels as well. In long distance transportation, the wood pellets are transported in bulk carriers via ocean shipping

as the most cost efficient method [154]. However, according to International Maritime Organization (IMO), the torrefied biomass with similar characteristics of coal are not permitted to be transported in bulk without special permission [37].

In general, three following major aspects should be in the specified ranges of established standards: First, the influential chemical and physical properties of torrefied pellets such as dimension, moisture content, ash content, bulk density, and calorific value; Second, the quality of pellets in terms of the stability of the pellets to compression (hardness), impacts and abrasion (durability), and water during handling, storage, and transportation [21]; Third, the safe handling and storage of the torrefied pellets.

There are some guidelines developed for solid biofuels to mitigate the health and safety hazards during the handling, storage, and transportation like Danish Technological Institute practice [150] and IEA Bioenergy Task 32 report [149]. Detailed regulations should be classified to prevent dust formation and minimize the risk of self-heating and ignition, preserving the operator's health and safety. The acceptable standards like the new ISO standard, which is under development, are required to classify the torrefied pellet as a commodity [37].

Summary of literature review

Lignocellulosic biomass has been proven as a promising feedstock for solid drop-in biofuels. The proper preprocessing and pretreatment methods should be performed based on availability and properties of the specific biomass to improve the efficient and economic application of biomass in bioenergy applications. For instance, forest residue and energy crops are two major sources of biomass in the united states along with deforestation and food production concerns.

Densification processes, specifically pelletizing plants have been widely commercialized around the world. The United States is one of the largest producers and exporters of the wood pellet with about 9 million tons annual production [39]. However, torrefaction process design is still in its early phase.

Several studies have been conducted on the kinetic analysis of the torrefaction process, effective parameters such as temperature, residence time, and particle size, and also different types of the reactor. Nevertheless, most of the proposed reactors are in pilot scale or have not fully developed yet for industrial scale. The integration of torrefaction and pelletization were mostly investigated over the conventional TOP configuration and a few recent studies focused on the torrefaction of densified biomass (TAP). The torgas product from torrefaction has been generally combusted to compensate the energy requirement in the integrated system corresponding to an auto-thermal operation. The lack of sufficient data on the detailed design parameters, energy consumption, or scaling up factors of the reactors resulted in unclear performance assessment and energy management of the torrefaction systems.

One of the main research gaps is the absence of a robust biomass process simulation to modeling the preprocessing and pretreatment based on the small scale operating data and scaling up to the industrial levels. The chemical makeup of the biomass, complex chemistry of torrefaction, and complicated thermodynamic equations of solid phase, especially in equilibrium with gas and liquid phases are some of the main challenges of the biomass process simulation. Such vague technical data together, resulted in few reliable techno-economic analysis reports on torrefaction system and integrated torrefaction and pelletization.

In this dissertation we aimed to filling the existing gaps between academia and industry by:

- Developing a detailed process simulation of the integrated torrefaction and pelletization to address all the design parameters, energy consumption, mass and energy efficiencies, and system optimizations.
- Investigation of the other possible configuration of torrefied pellet production, which is torrefaction after pelletization (TAP), through experiment and simulation.
- Conducting a techno-economic analysis of production of torrefied pellets at two configurations of TOP and TAP and determining the most feasible plant parameters to achieve the comparable delivered cost with coal at the power generation plants.

References

[1] Basu P. Biomass gasification, pyrolysis and torrefaction: practical design and theory. Academic press; 2013.

[2] Chew JJ, Doshi V. Recent advances in biomass pretreatment–Torrefaction fundamentals and technology. Renew Sustain Energy Rev 2011;15:4212–22.

[3] Haghighi Mood S, Hossein Golfeshan A, Tabatabaei M, Salehi Jouzani G, Najafi GH, Gholami M, et al. Lignocellulosic biomass to bioethanol, a comprehensive review with a focus on pretreatment. Renew Sustain Energy Rev 2013;27:77–93. doi:10.1016/j.rser.2013.06.033.

[4] van der Stelt MJC, Gerhauser H, Kiel JHA, Ptasinski KJ. Biomass upgrading by torrefaction for the production of biofuels: A review. Biomass and Bioenergy 2011;35:3748–62. doi:10.1016/j.biombioe.2011.06.023.

[5] Lee D, Owen VN, Boe A, Jeranyama P. Composition of Herbaceous Biomass Feedstocks. 2007.

[6] Bergman PCA, Boersma AR, Zwart RWR, Kiel JHA. Torrefaction for biomass co-firing in existing coal-fired power stations. Energy Cent Netherlands, Rep No ECN-C-05-013, Petten, Netherlands 2005.

[7] Demirbaş A. Estimating of Structural Composition of Wood and Non-Wood Biomass Samples. Energy Sources 2005;27:761–7. doi:10.1080/00908310490450971.

[8] Chen WH, Peng J, Bi XT. A state-of-the-art review of biomass torrefaction, densification, and applications. Renew Sustain Energy Rev 2015;44:847–66. doi:10.1016/j.rser.2014.12.039.

[9] Tumuluru JS, Sokhansanj S, Hess JR, Wright CT, Boardman RD. A review on biomass

torrefaction process and product properties for energy applications. Ind Biotechnol 2011;5. doi:10.1089/ind.2011.0014.

[10] Tumuluru JS, Hess JR, Boardman RD, Wright CT, Westover TL. Formulation, pretreatment, and densification options to improve biomass specifications for co-firing high percentages with coal. Ind Biotechnol 2012;8:113–32. doi:10.1089/ind.2012.0004.

[11] Dai J, Sokhansanj S, Grace JR, Bi X, Lim CJ, Melin S. Overview and some issues related to co-firing biomass and coal. Can J Chem Eng 2008;86:367–86. doi:10.1002/cjce.20052.

[12] Luque R, Speight J. Gasification for Synthetic Fuel Production: Fundamentals, Processes and Applications. Elsevier; 2014.

[13] Svanberg M, Halldórsson Á. Supply chain configuration for biomass-to-energy: the case of torrefaction. Int J Energy Sect Manag 2013;7:65–83. doi:http://dx.doi.org/10.1108/17506221311316489.

[14] Rumpf H, Knepper W (Ed. . The strength of granules and agglomerates. Int Symp Agglom 1962:379–418.

[15] Kaliyan N. Densification of biomass. ProQuest; 2008.

[16] Tabil L, Adapa P, Kashaninejad M. Biomass Feedstock Pre-Processing – Part 2: Pre-Treatment. Biofuel's Eng Process Technol 2011. doi:10.5772/18495.

[17] Holman LE. The compaction behaviour of particulate materials. An elucidation based on percolation theory. Powder Technol 1991;66:265–80.

[18] Stelte W, Sanadi AR, Shang L, Holm JK, Ahrenfeldt J, Henriksen UB. Recent developments in biomass pelletization - a review. BioResources 2012;7:4451–90.

[19] Stelte W, Holm JK, Sanadi AR, Barsberg S, Ahrenfeldt J, Henriksen UB. Fuel pellets from biomass: The importance of the pelletizing pressure and its dependency on the

processing conditions. Fuel 2011;90:3285–90. doi:10.1016/j.fuel.2011.05.011.

[20] Mani S, Tabil LG, Sokhansanj S. An overview of compaction of biomass grinds. Powder Handl Process 2003;15:160–8.

[21] Karunanithy C, Wang Y, Muthukumarappan K, Pugalendhi S. Physiochemical characterization of briquettes made from different feedstocks. Biotechnol Res Int 2012;2012:165202. doi:10.1155/2012/165202.

[22] ISO. ISO/TS 17225-8 Solid biofuels - Fuel specifications and classes; Part 8: Graded thermally treated and densified biomass fuels. Swedish Stand Institute, ISO/TC 238 N638, Stock Sweden 2016.

[23] García-Maraver A, Popov V, Zamorano M. A review of European standards for pellet quality. Renew Energy 2011;36:3537–40. doi:10.1016/j.renene.2011.05.013.

[24] Jannasch R, Quan Y, Samson R. A Process and Energy Analysis of Pelletizing Switchgrass. Final Report [online].[Dostęp 09.11. 2012]. Quebec Canada: 2001.

[25] Chen S. Life cycle assessment of wood pellet. Chalmers university of technology, Goteberg, Sweden, 2009.

[26] Araujjo S, Boas MAV, Neiva DM, de Cassia Carneiro A, Vital B, Breguez M, et al. Effect of a mild torrefaction for production of eucalypt wood briquettes under different compression pressures. Biomass and Bioenergy 2016;90:181–6. doi:10.1016/j.biombioe.2016.04.007.

[27] Sokhansanj S, Turhollow a. F. Biomass Densification - Cubing Operations and Costs for Corn Stover. Appl Eng Agric 2004;20:495–9.

[28] Tumuluru JS, Wright CT, Hess JR, Kenney KL. A review of biomass densification systems to develop uniform feedstock commodities for bioenergy application. Biofuels,

Bioprod Biorefining 2011;5:683–707. doi:10.1002/bbb.324.

[29] Peng J, Bi XT, Lim CJ, Peng H, Kim CS, Jia D, et al. Sawdust as an effective binder for making torrefied pellets. Appl Energy 2015;157:491–8. doi:10.1016/j.apenergy.2015.06.024.

[30] Kaliyan N, Morey RV. Factors affecting strength and durability of densified biomass products. Biomass and Bioenergy 2009;33:337–59.

[31] Prins MJ, Ptasinski KJ, Janssen FJJG. Torrefaction of wood: Part 1. Weight loss kinetics. J Anal Appl Pyrolysis 2006;77:28–34.

[32] Chen D, Zhou J, Zhang Q. Effects of torrefaction on the pyrolysis behavior and bio-oil properties of rice husk by using TG-FTIR and Py-GC/MS. Energy & Fuels 2014:140824102646000. doi:10.1021/ef501189p.

[33] Peng JH, Bi XT, Sokhansanj S, Lim CJ. Torrefaction and densification of different species of softwood residues. Fuel 2013;111:411–21. doi:10.1016/j.fuel.2013.04.048.

[34] Melkior T, Jacob S, Gerbaud G, Hediger S, Le Pape L, Bonnefois L, et al. NMR analysis of the transformation of wood constituents by torrefaction 2012. doi:10.1016/j.fuel.2011.06.042.

[35] Chen WH, Kuo PC. Isothermal torrefaction kinetics of hemicellulose, cellulose, lignin and xylan using thermogravimetric analysis. Energy 2011;36:6451–60. doi:10.1016/j.energy.2011.09.022.

[36] Phanphanich M, Mani S. Impact of torrefaction on the grindability and fuel characteristics of forest biomass. Bioresour Technol 2011;102:1246–53. doi:10.1016/j.biortech.2010.08.028.

[37] Koppejan J, Sokhansanj S, Melin S, Madrali S. Status overview of torrefaction

technologies, a review of the commercialisation status of biomass torrefaction. IEA Energy Technol Network, IEA Bioenergy Task 32 2015.

[38] Mani S, Tabil LG, Sokhansanj S. Effects of compressive force, particle size and moisture content on mechanical properties of biomass pellets from grasses. Biomass and Bioenergy 2006;30:648–54. doi:10.1016/j.biombioe.2005.01.004.

[39] Peng JH, Bi HT, Lim CJ, Sokhansanj S. Study on density, hardness, and moisture uptake of torrefied wood pellets. Energy & Fuels 2013;27:967–74. doi:10.1021/ef301928q.

[40] Stelte W, Nielsen NPK, Hansen HO, Dahl J, Shang L, Sanadi AR. Pelletizing properties of torrefied wheat straw. Biomass and Bioenergy 2013;49:214–21.

[41] Prins MJ, Ptasinski KJ, Janssen FJJG. Torrefaction of wood: Part 2. Analysis of products. J Anal Appl Pyrolysis 2006;77:35–40.

[42] Guo S, Dong X, Wu T, Zhu C. Influence of reaction conditions and feedstock on hydrochar properties. Energy Convers Manag 2016;123:95–103. doi:10.1016/j.enconman.2016.06.029.

[43] Li MF, Chen LX, Li X, Chen CZ, Lai YC, Xiao X, et al. Evaluation of the structure and fuel properties of lignocelluloses through carbon dioxide torrefaction. Energy Convers Manag 2016;119:463–72. doi:10.1016/j.enconman.2016.04.064.

[44] Iroba KL, Tabil LG, Sokhansanj S, Dumonceaux T. Pretreatment and fractionation of barley straw using steam explosion at low severity factor. Biomass and Bioenergy 2014;66:286–300. doi:10.1016/j.biombioe.2014.02.002.

[45] Ghiasi B, Kumar L, Furubayashi T, Lim CJ, Bi X, Kim CS, et al. Densified biocoal from woodchips: Is it better to do torrefaction before or after densification? Appl Energy 2014;134:133–42. doi:10.1016/j.apenergy.2014.07.076.

[46] Chen W-HH, Zhuang Y-QQ, Liu S-HH, Juang T-TT, Tsai C-MM. Product characteristics from the torrefaction of oil palm fiber pellets in inert and oxidative atmospheres. Bioresour Technol 2016;199:367–74. doi:10.1016/j.biortech.2015.08.066.

[47] Peng J, Wang J, Bi XT, Lim CJ, Sokhansanj S, Peng H, et al. Effects of thermal treatment on energy density and hardness of torrefied wood pellets. Fuel Process Technol 2015;129:168–73.

[48] Shang L, Nielsen NPK, Dahl J, Stelte W, Ahrenfeldt J, Holm JK, et al. Quality effects caused by torrefaction of pellets made from Scots pine. Fuel Process Technol 2012;101:23–8. doi:10.1016/j.fuproc.2012.03.013.

[49] Shang L, Nielsen NPK, Stelte W, Dahl J, Ahrenfeldt J, Holm JK, et al. Lab and Bench-Scale Pelletization of Torrefied Wood Chips-Process Optimization and Pellet Quality. Bioenergy Res 2014;7:87–94. doi:10.1007/s12155-013-9354-z.

[50] Li H, Liu X, Legros R, Bi XT, Jim Lim C, Sokhansanj S. Pelletization of torrefied sawdust and properties of torrefied pellets. Appl Energy 2012;93:680–5. doi:10.1016/j.apenergy.2012.01.002.

[51] Batidzirai B, Mignot a. PR, Schakel WB, Junginger HM, Faaij APC. Biomass torrefaction technology: Techno-economic status and future prospects. Energy 2013;62:196–214. doi:10.1016/j.energy.2013.09.035.

[52] Cherry RS, Wood R a, Westover TL. Analysis of the Production Cost for Various Grades of Biomass Thermal Treatment. US Dep Energy, Idaho Natl Lab INL/EXT-13-30348, Idaho Falls, Idaho 2013.

[53] Leonhardt MA. Torrefaction systems and methods including catalytic oxidation and/or reuse of combustion gases directly in a torrefaction reactor, cooler, and/or dryer/preheater.

US Pat Trademark Off US8203024B2, Washington, DC 2012.

[54] Thrän D, Witt J, Schaubach K, Kiel J, Carbo M, Maier J, et al. Moving torrefaction towards market introduction – Technical improvements and economic-environmental assessment along the overall torrefaction supply chain through the SECTOR project. Biomass and Bioenergy 2016;89:184–200. doi:10.1016/j.biombioe.2016.03.004.

[55] Stelte W. Torrefaction of unutilized biomass resources and characterization of torrefaction gasses. Danish Technol Institute, Energy Clim Cent Renew Energy Transp Sect Biomass, Denmark 2012.

[56] Fagernas L, Kuoppala E, Arpiainen V. Composition, utilization and economic assessment of torrefaction condensates. Energy and Fuels 2015;29:3134–42. doi:10.1021/acs.energyfuels.5b00004.

[57] Chang S, Zhao Z, Zheng A, He F, Huang Z, Li H. Characterization of products from torrefaction of sprucewood and bagasse in an auger reactor. Energy and Fuels 2012;26:7009–17. doi:10.1021/ef301048a.

[58] Shen DK, Gu S, Bridgwater A V. The thermal performance of the polysaccharides extracted from hardwood: Cellulose and hemicellulose. Carbohydr Polym 2010;82:39–45. doi:10.1016/j.carbpol.2010.04.018.

[59] Bates RB, Ghoniem AF. Biomass torrefaction: Modeling of volatile and solid product evolution kinetics. Bioresour Technol 2012;124:460–9. doi:10.1016/j.biortech.2012.07.018.

[60] Hagner M, Kuoppala E, Fagerns L, Tiilikkala K, Setala H. Using the copse snail Arianta arbustorum (Linnaeus) to detect repellent compounds and the quality of wood vinegar. Int J Environ Res 2015;9:53–60.

[61] Baimark Y, Niamsa N. Study on wood vinegars for use as coagulating and antifungal agents on the production of natural rubber sheets. Biomass and Bioenergy 2009;33:994–8. doi:10.1016/j.biombioe.2009.04.001.

[62] He Z, Wang X. Hydrocarbon production from carboxylic acids via catalytic deoxygenation: Required catalytic properties. ACS Symp Ser 2013;1132:301–29. doi:10.1021/bk-2013-1132.ch014.

[63] Rachmady W, Vannice M. Acetic acid hydrogenation over supported platinum catalysts. J Catal 2000;192:322–34. doi:10.1006/jcat.2000.2863.

[64] Joshi N, Lawal A. Hydrodeoxygenation of acetic acid in a microreactor. Chem Eng Sci 2012;84:761–71. doi:10.1016/j.ces.2012.09.018.

[65] Pham TN, Shi D, Resasco DE. Kinetics and Mechanism of Ketonization of Acetic Acid on Ru/TiO2 Catalyst. Top Catal 2013;57:706–14. doi:10.1007/s11244-013-0227-7.

[66] Bergman PCA. Combined torrefaction and pelletisation the TOP process. Energy Cent Netherlands, Rep No ECN-C-05-073, ECN, Petten, Netherlands 2005.

[67] Czernik S, Bridgwater A V. Overview of applications of biomass fast pyrolysis oil. Energy and Fuels 2004;18:590–8. doi:10.1021/ef034067u.

[68] Peng J, Bi XT, Lim J, Sokhansanj S. Development of torrefaction kinetics for British Columbia softwoods. Int J Chem React Eng 2012;10.

[69] Shafizadeh F, Chin PPS. Thermal deterioration of wood. ACS Symp. Ser. Am. Chem. Soc., 1977.

[70] Di Blasi C, Branca C. Kinetics of primary product formation from wood pyrolysis. Ind Eng Chem Res 2001;40:5547–56.

[71] Di Blasi C, Lanzetta M. Intrinsic kinetics of isothermal xylan degradation in inert

atmosphere. J Anal Appl Pyrolysis 1997;40:287–303. doi:10.1016/S0165-2370(97)00028-4.

[72] Bates RB, Ghoniem AF. Biomass torrefaction: Modeling of reaction thermochemistry. Bioresour Technol 2013;134:331–40. doi:10.1016/j.biortech.2013.01.158.

[73] Roberts AF. The heat of reaction during the pyrolysis of wood. Combust Flame 1971;17:79–86. doi:10.1016/S0010-2180(71)80141-4.

[74] Shafizadeh F. Pyrolytic reactions and products of biomass. Fundam. Thermochem. biomass Convers., Springer; 1985, p. 183–217.

[75] Grųnli MG, Sųrensen LH, Hustad JE. Thermogravimetric analysis of four Scandinavian wood species under nonisothermal conditions. Nord. Semin. biomass Combust. NTH, 1992.

[76] Bach QV, Khalil R a., Tran KQ, Skreiberg O. Torrefaction kinetics of norwegian biomass fuels. Chem Eng Trans 2014;37:49–54. doi:10.3303/CET1437009.

[77] Peng JH, Bi HT, Sokhansanj S, Lim JC. A Study of particle size effect on biomass torrefaction and densification. Energy & Fuels 2012;26:3826–39. doi:10.1021/ef3004027.

[78] Bates RB, Ghoniem AF. Modeling kinetics-transport interactions during biomass torrefaction: The effects of temperature, particle size, and moisture content. Fuel 2014;137:216–29. doi:10.1016/j.fuel.2014.07.047.

[79] Stelt MJC Van Der. Chemistry and reaction kinetics of biowaste torrefaction. 2010. doi:978-90-386-2435-8.

[80] Chen W-H, Lu K-M, Liu S-H, Tsai C-M, Lee W-J, Lin T-C. Biomass torrefaction characteristics in inert and oxidative atmospheres at various superficial velocities. Bioresour Technol 2013;146:152–60. doi:10.1016/j.biortech.2013.07.064.

[81] Wang C, Peng J, Li H, Bi XT, Legros R, Lim CJ, et al. Oxidative torrefaction of biomass residues and densification of torrefied sawdust to pellets. Bioresour Technol 2013;127:318–25. doi:10.1016/j.biortech.2012.09.092.

[82] Broström M, Nordin A, Pommer L, Branca C, Di Blasi C. Influence of torrefaction on the devolatilization and oxidation kinetics of wood. J Anal Appl Pyrolysis 2012;96:100–9. doi:10.1016/j.jaap.2012.03.011.

[83] Calvo LF, Otero M, Jenkins BM, Morán A, García AI. Heating process characteristics and kinetics of rice straw in different atmospheres. Fuel Process Technol 2004;85:279–91. doi:10.1016/S0378-3820(03)00202-9.

[84] Chiang W-F, Fang H-Y, Wu C-H, Chang C-Y, Chang Y-M, Shie J-L. Pyrolysis Kinetics of Rice Husk in Different Oxygen Concentrations. J Environ Eng 2008;134:316–25. doi:10.1061/(ASCE)0733-9372(2008)134:4(316).

[85] Fang MX, Shen DK, Li YX, Yu CJ, Luo ZY, Cen KF. Kinetic study on pyrolysis and combustion of wood under different oxygen concentrations by using TG-FTIR analysis. J Anal Appl Pyrolysis 2006;77:22–7. doi:10.1016/j.jaap.2005.12.010.

[86] Chen WH, Lu KM, Lee WJ, Liu SH, Lin TC. Non-oxidative and oxidative torrefaction characterization and SEM observations of fibrous and ligneous biomass. Appl Energy 2014;114:104–13. doi:10.1016/j.apenergy.2013.09.045.

[87] Lu K-M, Lee W-J, Chen W-H, Liu S-H, Lin T-C. Torrefaction and low temperature carbonization of oil palm fiber and eucalyptus in nitrogen and air atmospheres. Bioresour Technol 2012;123:98–105. doi:10.1016/j.biortech.2012.07.096.

[88] Rousset P, Macedo L, Commandré J-M, Moreira A. Biomass torrefaction under different oxygen concentrations and its effect on the composition of the solid by-product. J Anal

Appl Pyrolysis 2012;96:86–91. doi:10.1016/j.jaap.2012.03.009.

[89] Eseyin AE, Steele PH, Pittman Jr. CU. Current Trends in the Production and Applications of Torrefied Wood/Biomass - A Review. BioResources 2015;10:8812–58. doi:10.15376/biores.10.4.8812-8858.

[90] Lynam JG, Coronella CJ, Yan W, Reza MT, Vasquez VR. Acetic acid and lithium chloride effects on hydrothermal carbonization of lignocellulosic biomass. Bioresour Technol 2011;102:6192–9. doi:10.1016/j.biortech.2011.02.035.

[91] Yan W, Acharjee TC, Coronella CJ, Vásquez VR. Thermal pretreatment of lignocellulosic biomass. Environ Prog Sustain Energy 2009;28:435–40. doi:10.1002/ep.10385.

[92] Yan W, Hastings JT, Acharjee TC, Coronella CJ, Vásquez VR. Mass and Energy Balance of Wet Torrefaction of Lignocellulosic Biomass† n.d. doi:10.1021/EF901273N@PROOFING.

[93] Chen WH, Ye SC, Sheen HK. Hydrothermal carbonization of sugarcane bagasse via wet torrefaction in association with microwave heating. Bioresour Technol 2012;118:195–203. doi:10.1016/j.biortech.2012.04.101.

[94] Balat M, Balat H, Öz C. Progress in bioethanol processing. Prog Energy Combust Sci 2008;34:551–73. doi:10.1016/j.pecs.2007.11.001.

[95] Biswas AK, Yang W, Blasiak W. Steam pretreatment of Salix to upgrade biomass fuel for wood pellet production. Fuel Process Technol 2011;92:1711–7. doi:10.1016/j.fuproc.2011.04.017.

[96] Stelte W. Steam explosion for biomass pre-treatment. Danish Technol Inst 2013:1–15.

[97] Bura R, Mansfield SD, Saddler JN, Bothast RJ. SO2-Catalyzed Steam Explosion of Corn Fiber for Ethanol Production. Appl Biochem Biotechnol 2002;98–100:59–72.

doi:10.1385/ABAB:98-100:1-9:59.

[98] Boussaid AL, Esteghlalian AR, Gregg DJ, Lee KH, Saddler JN. Steam pretreatment of Douglas-fir wood chips. Can conditions for optimum hemicellulose recovery still provide adequate access for efficient enzymatic hydrolysis? Appl Biochem Biotechnol 2000;84–86:693–705.

[99] SHEVCHENKO SM, CHANG K, DICK DG, GREGG DJ, SADDLER JN. Structure and properties of lignin in softwoods after SO2-catalyzed steam explosion and enzymatic hydrolysis. Cellul Chem Technol 2001;35:487–502.

[100] Lam PS, Sokhansanj S, Bi XT, Lim CJ, Larsson SH. Drying characteristics and equilibrium moisture content of steam-treated Douglas fir (Pseudotsuga menziesii L.). Bioresour Technol 2012;116:396–402. doi:10.1016/j.biortech.2012.03.093.

[101] Z. Tooyserkani, S. Sokhansanj, X. Bi, C. J. Lim, J. Saddler, A. Lau, et al. Effect of Steam Treatment on Pellet Strength and the Energy Input in Pelleting of Softwood Particles. Trans ASABE 2012;55:2265–72. doi:10.13031/2013.42484.

[102] Chang J, Cheng W, Yin Q, Zuo R, Song A, Zheng Q, et al. Effect of steam explosion and microbial fermentation on cellulose and lignin degradation of corn stover. Bioresour Technol 2012;104:587–92. doi:10.1016/j.biortech.2011.10.070.

[103] Dhungana A, Basu P, Dutta A. Effects of Reactor Design on the Torrefaction of Biomass. J Energy Resour Technol 2012;134:041801. doi:10.1115/1.4007484.

[104] Nhuchhen DR. Studies on advanced means of biomass torrefaction. Dalhousie University, Halifax, Nova Scotia, 2016. doi:10.1007/s13398-014-0173-7.2.

[105] Nhuchhen D, Basu P, Acharya B. A Comprehensive Review on Biomass Torrefaction. Int J Renew Energy Biofuels 2014;2014:1–56. doi:10.5171/2014.506376.

[106] Koppejan J, Sokhansanj S, Melin S, Madrali S. Status overview of torrefaction technologies. 2012.

[107] Junsatien W, Soponpongpipat N, Phetsong S. Torrefaction reactors. J Sci Technol MSU 2013;32.

[108] Jaya Shankar Tumuluru, Sokhansanj S, Wright CT, Boardman RD. Biomass Torrefaction Process Review and Moving Bed Torrefaction System Model Development. 2010.

[109] Eriksson A-M. Torrefaction and gasification of biomass. The potential of torrefaction combined with entrained-flow gasification for production of synthesis gas 2012.

[110] Chai L, Saffron CM. Comparing pelletization and torrefaction depots: Optimization of depot capacity and biomass moisture to determine the minimum production cost. Appl Energy 2016;163:387–95. doi:10.1016/j.apenergy.2015.11.018.

[111] Adams PWR, Shirley JEJ, McManus MC. Comparative cradle-to-gate life cycle assessment of wood pellet production with torrefaction. Appl Energy 2015;138:367–80. doi:10.1016/j.apenergy.2014.11.002.

[112] Westbrook MD, Greene WD, Izlar RL. Harvesting Forest Biomass by Adding a Small Chipper to a Ground-Based Tree-Length Southern Pine Operation * n.d.

[113] Webster P. Large chippers, Internal project information note 19/06 2007.

[114] Schorr C, Muinonen M, Nurminen F, Nordin A. Torrefaction of biomass. vol. 117. Finland: 2012. doi:10.1017/CBO9781107415324.004.

[115] Samuelsson R, Larsson SH, Thyrel M, Lestander TA. Moisture content and storage time influence the binding mechanisms in biofuel wood pellets. Appl Energy 2012;99:109–15. doi:10.1016/j.apenergy.2012.05.004.

[116] Xu F, Linnebur K, Wang D. Torrefaction of Conservation Reserve Program biomass: A

techno-economic evaluation. Ind Crops Prod 2014;61:382–7. doi:10.1016/j.indcrop.2014.07.030.

[117] Stelte W, Dahl J, Nielsen N peter k., Hansen H ove. Densification concepts for torrefied biomass. Denmark: 2012.

[118] Järvinen T, Agar D. Experimentally determined storage and handling properties of fuel pellets made from torrefied whole-tree pine chips, logging residues and beech stem wood. Fuel 2014;129:330–9. doi:10.1016/j.fuel.2014.03.057.

[119] Repellin V, Govin A, Rolland M, Guyonnet R, Vincent R, Alexandre G, et al. Energy requirement for fine grinding of torrefied wood. Biomass and Bioenergy 2010;34:923–30. doi:10.1016/j.biombioe.2010.01.039.

[120] Tapasvi D, Khalil R, Skreiberg Ø, Tran KQ, Grønli M. Torrefaction of Norwegian birch and spruce: An experimental study using macro-TGA. Energy and Fuels, vol. 26, 2012, p. 5232–40. doi:10.1021/ef300993q.

[121] Rezaei H, Lim CJ, Lau A, Sokhansanj S. Size, shape and flow characterization of ground wood chip and ground wood pellet particles. Powder Technol 2016;301:737–46. doi:10.1016/j.powtec.2016.07.016.

[122] Esteban LS, Carrasco JE. Evaluation of different strategies for pulverization of forest biomasses. Powder Technol 2006;166:139–51. doi:10.1016/j.powtec.2006.05.018.

[123] Temmerman M, Jensen PD, Herbert J. Von Rittinger theory adapted to wood chip and pellet milling, in a laboratory scale hammermill. Biomass and Bioenergy 2013;56:70–81. doi:10.1016/j.biombioe.2013.04.020.

[124] Jackson J, Turner A, Mark T, Montross M. Densification of biomass using a pilot scale flat ring roller pellet mill. Fuel Process Technol 2016;148:43–9.

doi:10.1016/j.fuproc.2016.02.024.

[125] Mediavilla I, Fernández MJ, Esteban LS. Optimization of pelletisation and combustion in a boiler of 17.5 kWth for vine shoots and industrial cork residue. Fuel Process Technol 2009;90:621–8. doi:10.1016/j.fuproc.2008.12.009.

[126] McKechnie J, Saville B, MacLean HL. Steam-treated wood pellets: Environmental and financial implications relative to fossil fuels and conventional pellets for electricity generation. Appl Energy 2016;180:637–49. doi:10.1016/j.apenergy.2016.08.024.

[127] Jiang L, Yuan X, Xiao Z, Liang J, Li H, Cao L, et al. A comparative study of biomass pellet and biomass-sludge mixed pellet: Energy input and pellet properties. Energy Convers Manag 2016;126:509–15. doi:10.1016/j.enconman.2016.08.035.

[128] Peng JH. A study of softwood torrefaction and densification for the production of high quality wood pellets. Univeristy of British Columbia, Vancouver, Canada, 2012.

[129] Prins MJ, Ptasinski KJ, Janssen FJJG. More efficient biomass gasification via torrefaction. Energy 2006;31:3458–70. doi:10.1016/j.energy.2006.03.008.

[130] Mcnamee P, Adams PWR, Mcmanus MC, Dooley B, Darvell LI, Williams A, et al. An assessment of the torrefaction of North American pine and life cycle greenhouse gas emissions. Energy Convers Manag 2016;113:177–88. doi:10.1016/j.enconman.2016.01.006.

[131] Gardbro G. Techno-economic modeling of the supply chain for torrefied biomass. Umeå University, Sweden, 2014.

[132] Agar D, Gil J, Sanchez D, Echeverria I, Wihersaari M. Torrefied versus conventional pellet production – A comparative study on energy and emission balance based on pilot-plant data and EU sustainability criteria. Appl Energy 2015;138:621–30.

doi:10.1016/j.apenergy.2014.08.017.

[133] Rentizelas AA, Li J. Techno-economic and carbon emissions analysis of biomass torrefaction downstream in international bioenergy supply chains for co-firing. Energy 2016;114:129–42. doi:10.1016/j.energy.2016.07.159.

[134] Sultana A, Kumar A, Harfield D. Development of agri-pellet production cost and optimum size. Bioresour Technol 2010;101:5609–21. doi:10.1016/j.biortech.2010.02.011.

[135] Srivastava A, Abbas D, Saffron C, Pan F. Economic analysis of woody biomass supply chain logistics for biofuel production in Michigan. East Lansing, MI.: 2011.

[136] Campbell K. A feasibility study guide for an agricultural biomass pellet company. Agric Util Res Institute, St Paul, Minnesota 2007.

[137] Mani S, Sokhansanj S, Bi X, Turhollow A. Economics of producing fuel pellets from biomass. Appl Eng Agric 2006;22:421–6. doi:10.13031/2013.20447.

[138] David Agar. The Feasibility of Torrefaction for the Co-Firing of Wood in Pulverised-Fuel Boilers. Åbo Akademi University, 2015.

[139] Arpianen V, Wilen C. Report on optimization opportunities by integrating torrefaction into existing industries-SECTOR. 2012.

[140] Dudgeon R. An Aspen Plus Model of Biomass Torrefaction. Electr Power Res Inst … 2009:12.

[141] Haryadi, Hardianto T, Pasek AD, Suwono A, Azhari R, Ardiansyah W. The Aspen TM Software Simulation of a Peat Torrefaction System Using RYield and SSplit Block as Reactor Model. Proc Int Symp Sustain Energy Environ Prot 2009:23–6.

[142] Nikolopoulos N, Isemin R, Atsonios K, Kourkoumpas D, Kuzmin S, Mikhalev A, et al. Modeling of wheat straw torrefaction as a preliminary tool for process design. Waste and

Biomass Valorization 2013;4:409–20. doi:10.1007/s12649-013-9198-y.

[143] Arteaga-Perez LE, Segura C, Espinoza D, Radovic LR, Jimenez R. Torrefaction of Pinus radiata and Eucalyptus globulus: A combined experimental and modeling approach to process synthesis. Energy Sustain Dev 2015;29:13–23. doi:10.1016/j.esd.2015.08.004.

[144] Bach QV, Skreiberg Ø, Lee CJ. Process modeling and optimization for torrefaction of forest residues. Energy 2017;138:348–54. doi:10.1016/j.energy.2017.07.040.

[145] Visconti A, Miccio M, Juchelkova D. Equilibrium-based simulation of lignocellulosic biomass pyrolysis via Aspen Plus. Recent Adv Appl Math Model Simul 2015:242–51.

[146] Arteaga-Pérez LE, Segura C, Espinoza D, Radovic LR, Jiménez R. Torrefaction of Pinus radiata and Eucalyptus globulus: A combined experimental and modeling approach to process synthesis. Energy Sustain Dev 2015;29:13–23. doi:10.1016/j.esd.2015.08.004.

[147] Park C, Zahid U, Lee S, Han C. Effect of process operating conditions in the biomass torrefaction: A simulation study using one-dimensional reactor and process model. Energy 2015;79:127–39. doi:10.1016/j.energy.2014.10.085.

[148] Syu FS, Chiueh PT. Process simulation of rice straw torrefaction. Sustain Environ Res 2012;22:177–83.

[149] Koppejan J, Lönnermark A, Baxter D. Health and Safety Aspects of Solid Biomass Storage, Transportation and Feeding Health and Safety Aspects of Solid Biomass Storage, Transportation and Feeding Report prepared by 2013.

[150] Stelte W. Best Practice Guideline - Storage and Handling of torrefied biomass. Danish Technol Institute, Denmark 2015.

[151] Arias B, Pevida C, Fermoso J, Plaza MG, Rubiera F, Pis JJ. Influence of torrefaction on the grindability and reactivity of woody biomass. Fuel Process Technol 2008;89:169–75.

doi:10.1016/j.fuproc.2007.09.002.

[152] Wilén C, Jukola P, Järvinen T, Sipilä K, Verhoeff F, Kiel J. Wood torrefaction–pilot tests and utilisation prospects. vol. 122. 2013.

[153] VTT & NEN. Solid Standards; Enhancing the implementation of quality and sustainability standards and certification schemes for solid biofuels (EIE/11/218). n.d.

[154] Stelte W. Logistics and storage of torrefied biomass : Safety aspects 2013;93:1–214. doi:10.1016/0016-2361(86)90163-8.

CHAPTER 3

TORREFACTION AFTER PELLETIZATION (TAP): ANALYSIS OF TORREFIED PELLET QUALITY AND CO-PRODUCTS[1]

[1] Manouchehrinejad M and Mani S. Submitted to Biomass and Bioenergy, (2018).

Abstract

Torrefaction is a thermal pretreatment method to increase the energy density and decrease the grinding energy of biomass. In this study, torrefaction of two types of commercially available wood pellets was carried out in the temperature range of 230 to 290°C for 30 min residence time. Torrefaction produces both the solid fuel and the volatile stream known as torgas. The torgas generated during torrefaction was separated into condensable liquids (tor-liquid) and non-condensable gases. The changes in physical and fuel properties Solid and volatile products yields and changes in physical and fuel properties of the torrefied pellets and the torgas compositions were also determined as well as the yields of solid and volatile products. The torgas generated during torrefaction was separated into condensable liquids (tor-liquid) and non-condensable gases. The increase in torrefaction temperature reduced the pellet mass yield from 89 to 52%, while it increased the condensable liquid yield from 5 to 23%. The heating value (24 MJ kg^{-1}) and the volumetric energy density (12.5 GJ m^{-3}) of pellets torrefied in the range of 275 to 280°C were comparable to that of coal. The hydrophobicity (resistance to water uptake) of the torrefied pellets was improved, but the pellets' density, hardness, and durability were adversely reduced with an increase in torrefaction temperature. The non-condensable fraction of torgas was mainly composed of carbon dioxide, carbon monoxide and traces of methane. The condensable liquid was rich in organic acids, ketones, furfural, and levoglucosan, which could be potentially transformed into high-value chemicals and other commercially viable products.

Keywords: Torrefied pellets, Torgas, hardness, durability, water uptake.

Nomenclature

C	Carbon
CP	Commercial wood pellet
D	Diameter (m)
E	Energy yield (%)
E_a	Activation energy (kJ mol^{-1})
H	Hydrogen
$HHVd$	Higher heating value-bone dry (MJ kg^{-1})
HHV_{raw}	Higher heating value of raw biomass (MJ kg^{-1})
HHV_{tor}	Higher heating value of torrefied biomass (MJ kg^{-1})
k_T	Degradation rate at any temperature (min-1)
k_{T_s}	Degradation rate at the setup temperature (min^{-1})
L	Length (m)
N	Nitrogen
O	Oxygen
R	Universal gas constant: 8.31×10^{-3} kJ $(mol\ C)^{-1}$
SF	Severity factor
T_E	Temperature value (°C)
T_R	Reference temperature: 100 (°C)
T_S	Setup (torrefaction) temperature (°C)
t_T	Time of heating-up phase (min)
t_{T_s}	Converted isothermal time (min)
TAP	Torrefaction After Pelletization
TOP	Torrefaction Before Pelletization

Introduction

The United States (US) is the largest manufacturer of wood pellets in the world with a total annual production of 6.3 million Mg in 2016. It is also the largest exporter of wood pellets to the United Kingdom and European Countries for designated district heating and power generation applications [1]. The domestic utilization of wood pellets has so far been limited to animal bedding, and residential heating applications. The capacity of wood pellets usage for power generation is still an under-developed asset in the US. Power generation contributes the largest fraction of total GHG emissions in the US (29%). Coal and natural gas power plants contributed 67% of this fraction [2]. Co-firing of wood pellets with coal is an alternative that could potentially reduce GHG emissions. Wood pellets are generally produced from sawmill residues, barks and wood chips [3]. The typical pellet production process can be found in scientific literature [4]. The US has more than 90 operating pellet mills with an overall production capacity of 11.9 million Mg $year^{-1}$[5]. Although wood pellets have a high bulk density (500-650 kg m^{-3}) and low moisture content (7-10% wb), the pellet energy density (7.8-10.5 GJ m^{-3}) is relatively low due to high oxygen content compared to the coal (1.75-1.86 times higher) for co-firing applications [6]. In addition, wood pellets are highly fibrous, hydrophilic, and difficult to grind compared to that of coal [6]. To overcome the above challenges, pellets can be thermally pretreated in the absence of oxygen to produce a brittle and high energy density solid fuel as a potential replacement for coal.

The thermal pretreatment process, called torrefaction, is a low temperature pyrolysis process where biomass is heated to a temperature between 200-300°C in an inert environment under atmospheric pressure [7]. The high energy content and low grindability of torrefied biomass increase the wood's potential for direct use in pulverized co-firing systems [8]. After torrefaction, the bulk density of the torrefied biomass is decreased, thus densification methods such as

pelletization and briquetting are recommended. The integration of both the torrefaction and densification technologies is critical to produce a drop-in replacement for coal, while reducing the costs associated with the handling, transporting and storing of biomass for power generation applications. Furthermore, torrefied biomass is as an excellent feedstock for other thermal conversion technologies such as gasification and pyrolysis to produce chemicals and biofuels [9,10].

The Energy Research Center of the Netherlands (ECN) was the has first research center to developed an integrated torrefaction and pelletization technology (TOP process) to produce solid biofuels as similar to coal [6]. In the TOP process, biomass is first torrefied, then reduced in size and densified into solid pellets. However, the pelletizing of torrefied biomass is a major challenge due to the weakening of bonding forces between biomass particles and the loss of natural binding characteristics of lignin in the biomass after torrefaction. Hence, the addition of binding agents or higher die temperatures, and/or higher compression pressures are required to produce high-quality solid pellets [11–13]. The aforementioned problems along with maintenance and safety issues due to dust-making and abrasive nature of torrefied biomass [14,15] and related costs have hampered the production of torrefied pellets as an upgraded biofuel commodity. Nevertheless, the other potential pathway for producing torrefied pellets is **t**orrefaction **a**fter **p**elletization (TAP), which might be the key to accelerating the commercialization of torrefied pellet production. The uniform shape and size of torrefied biomass pellets with high bulk density could facilitate efficient handling, feeding, and safe torrefaction operation [14].

Torrefaction produces both the solid fuel and the volatile stream known as torgas. Torgas is composed of non-condensable gases such as CO_2 and CO as well as condensable volatile organic compounds (VOCs) such acetic acid, acetone, formaldehyde, and water [16]. Torgas can be

combusted in a thermal or a catalytic oxidizer [17] to destroy VOCs and generate heat energy for auto-thermal torrefaction. In addition, the condensates from these volatiles can be utilizated relevant applications such as wood vinegar, wood protection products, additive agents in the coating of pellets, and the production of green chemicals [18,19]. The composition of torgas is highly dependent on the feedstock type and torrefaction temperature [19,20].

When torrefaction is integrated after the pelletization, the existing pelletizing plants have an opportunity to produce both raw pellets and torrefied pellets. In addition, no significant interruption in the regular operation of wood pellet production is required. The use of densified feedstock such as wood pellets potentially reduces the equipment size and thus cost, and thus facilitating es the heat distribution during torrefaction [14].

Earlier studies on torrefaction of biomass pellets mostly focused on the elemental analysis and energy density of the final solid product [21–25]. The physical properties of individual torrefied pellets were investigated in terms of hardness [23], durability [22,25], and water resistance [22,24] for specific materials. However, the composition of torrefaction co-products has received little attention within previous studies. Chen et al. investigated the overall calorific value and water content of the condensable co-products from torrefaction of oil palm fiber pellets [21]. They showed that the calorific value of the condensed liquid would be increased after dewatering [21]. Ghiasi et al. compared the mass and energy balance of torrefied douglas-fir wood pellets that were produced via two pathways, of TOP and TAP. which The TAP pathway reached yielded higher energy efficiency for TAP pellets [22]. Doassans-Carrère et al. suggested that the TAP pathway might be more appropriate for the lower bulk density biomass materials [24].

A review of the relevant literature shows that the optimum conditions for torrefaction of the biomass pellets and the consequent fuel and physical properties of the solid product was not

fully elucidated. Although various biomass types have the potential to be used as a feedstock, commercial wood pellets are the most promising to augment the production process of torrefied pellets. Moreover, the torgas composition has previously not been explored in fine detail.

The main objectives of this study were to experimentally investigate the torrefaction of wood pellets at various temperatures, to comprehensively evaluate the changes in the physical quality and fuel properties of torrefied pellets, and to determine the compositions of the torgas stream (condensed liquid and non-condensable gases) to assess their alternative useage as co-products.

Materials and methods

Materials

Wood pellets were acquired from two commercial manufacturers in the Southeastern US and designated as CP1 and CP2. The CP1 wood pellets were produced from small round wood logs of southern yellow pine, and the CP2 wood pellets were produced from a mix of sawmill residues from softwood and hardwood species. The samples were sealed in plastic containers and stored at 4°C. The sub-samples were collected, oven dried, sealed and stored at room temperature for all of the experimental studies.

Torrefaction experiment

A laboratory scale batch torrefaction reactor was used in this study as reported in [26]. A steel batch reactor with a volume of 0.0135 m^3 was used to hold a known amount of wood pellets and was placed inside a heated electric furnace (Thermolyne Furnace, Type 30400, Dubuque, Iowa). The reactor was sealed with a steel gasket to maintain anoxic condition during torrefaction. The sample temperature inside the reactor was monitored and controlled with a thermocouple to a pre-determined torrefaction temperature. The air inside the reactor was purged and displaced with

nitrogen gas before heating. During heating, nitrogen gas was continuously supplied through the reactor with a flux rate of 2 L min^{-1} to prevent air entering in the torrefaction reactor. The volatile gases evolved from the decomposition of biomass during torrefaction are collectively termed "torgas." The torgas was sent through a series of condensers (metal vessels) housed in an ice-bath to collect the condensable liquids. The non-condensable fraction of the torgas was bubbled through a water bath and vented into the atmosphere. Samples of the non-condensable gas were taken using gas collection bags for compositional analysis.

About 1000 g of wood pellets were charged into the reactor at room temperature and was heated at a rate of 3°C min^{-1} under inert condition to the pre-determined torrefaction temperature. Both CP1 and CP2 pellets were torrefied at four different temperatures (230, 250, 275, and 290°C) for 30 min. The holding time of 30 min was ascertained to be a common control for torrefaction based on previous studies [7]. After torrefaction, the reactor was cooled with fans until the sample reached the room temperature. The nitrogen gas flow was continued until the reactor temperature dropped below 50 °C. The torrefied pellets after each run were weighed, sealed in an airtight plastic bags and stored at room temperature for further analysis. The condensed fraction of torgas was collected from the series of condensers, weighed and sealed in glass vials and refrigerated for further analysis. The mass yields of the products were obtained by dividing the weight of the torrefied solid and condensed liquid by the weight of the initial solid feedstock and were reported in percentage (Eq. 1). An estimation of the mass yield of non-condensable gas was given by the difference of the total of solid and liquid yields from 100. The energy yield of the torrefaction system was calculated by multiplying the solid mass yield by the ratio of the dry higher heating value of the torrefied biomass and raw biomass (Eq. 2).

$$Mass\ yield(\%) = \frac{Mass\ of\ dry\ basis\ torrefied\ solid\ or\ Mass\ of\ tor_{liquid}}{Mass\ of\ dry\ basis\ feedstock} \times 100 \quad (1)$$

$$Energy\ yield(\%) = Massyield \times \frac{HHV_{tor}}{HHV_{raw}} \quad (2)$$

The severity factor was used to estimate the effect of torrefaction temperature and residence time [27]. Nevertheless, the effect of the reaction temperature on torrefaction severity was more significant than residence time in most of the previous studies [28,29]. The equation used for severity factor in this study is defined as Eq. 3 and Eq. 4 [30]. The residence time was modified in the severity factor equation by incorporating the heating time within the equations Eq. 5 and Eq. 6 [31]:

$$SF = log[t.exp(T - T_R/T_E)] \quad (3)$$

$$\frac{R \cdot T_R \cdot T}{E_a} \approx T_E \quad (4)$$

$$t = t_{T_s} = \sum_{T=30}^{T_s} t_T \cdot \frac{k_T}{k_{T_s}} \quad (5)$$

$$k_T = k_{T_s} \cdot exp\left(\frac{-E_a}{R} \cdot \left(\frac{1}{T} - \frac{1}{T_s}\right)\right) \quad (6)$$

Where SF is the severity factor, E_a is the activation energy of pine treatment 160 (kJ mol^{-1}) [32]; R is the universal gas constant 8.31×10^{-3} kJ (mol C)$^{-1}$; T (°C) is any temperature during the preheating, T_E is the temperature value (°C), T_S (°C) is the setup (torrefaction) temperature, T_R is the reference temperature of 100°C, t_{T_s} (min) and k_{T_s} (min^{-1}) are the converted isothermal time and the degradation rate, respectively, at the setup temperature, and t_T(min) and k_T(min^{-1}) are the time and the degradation rate, respectively, at any temperature during the heating up phase [31].

Analytical Methods

Analysis of solid fuels

The wood pellet samples were characterized before and after torrefaction. The moisture content of both raw and torrefied pellets was determined based on ASABE standard S358.3 MAY 2012 [33]. A known amount of sample was dried for 24 h in a convective oven at 103°C. The moisture content of the samples was then calculated in triplicate according to the gravimetric method. The bulk density of wood pellets was measured based on the standard method for determining the tapped bulk density, which is also called bulk volume of granular or fibrous materials [34]. The sample was poured freely into a suitable cylinder. The filled cylinder was then tapped gently on a hard surface five times. The bulk density was calculated by dividing the weight of the sample by its net volume in the cylinder and presented as mass per unit volume. Bulk density measurements were repeated five times. The pellet density of raw and torrefied pellets was also measured by dividing the mass of each pellet by its volume. At least fifteen pellets were used to determine the average pellet density of each sample.

A portion of raw pellets and torrefied pellets was ground separately through a lab- scale heavy-duty knife mill (Rotor 1690 rpm and 60 Hz, Power 1.5 kW, Retsch SM 2000, Germany) with a sieve size of 0.25 mm to determine fuel properties. Proximate analysis (Ash, volatiles, fixed carbon and moisture content) was performed in a micro thermo-gravimetric analyzer (TGA701, LECO Corporation, St. Joseph, MI) according to ASTM D 7582 procedure for coal and coke [35]. The amounts of ash, volatiles, and fixed carbon were reported in dry basis. The ultimate analysis was carried out with an elemental analyzer (LECO CHNS 932, LECO Corporation, St. Joseph, MI) based on ASTM D3176 protocol [36]. The C, H, N, S weight percentage was measured directly by the analyzer and oxygen content was estimated by difference. The higher heating value (HHV)

of the sample was determined in an adiabatic oxygen bomb calorimeter (IKAC 2000, IKA Works, Inc., NC) using the standard test method ASTM D5865 [37]. The high heating value of bone-dry biomass (HHV_d) was calculated based on the moisture content of the sample. The proximate analysis of all samples, ultimate analysis, and heat value experiments were performed in triplicate.

The compressive resistance or hardness of pellets was analyzed by the MTS peak load compression system (MTS System Corporation, MTS Insight™30 Material Testing Systems, Eden Prairie, MN). A single pellet with a diameter in the range of 5.7 to 6.5 mm and length of 15.7 to 16.1 mm (L/D is shown in Table 2) was replaced on the lower plate of the compression system in the radial direction, and the upper plate was lowered at a rate (10 mm/min) until the impact force reached the peak point at a point of failure of pellets. The force versus displacement data was recorded and stored in the computer. The peak force recorded for each compression test was reported as pellet hardness. For each sample, at least ten pellets were compressed to measure pellet hardness.

Pellet durability is defined as the stability of the pellet under impact, compression, and abrasion during handling and transport [38]. In this study, durability of raw and torrefied pellets was measured by applying the tumbler testing unit according to ASAE S269.4 [39]. A 500 g sample of pellets was placed in the tumbling box device and tested for 10 min at 50 rpm. After tumbling, the sample was sieved (5.7 mm), and the ratios of mass before and after tumbling were reported as the durability index based on Eq. 7:

$$Durability = \frac{Mass\ of\ pellets\ after\ trumbling}{Mass\ of\ pellets\ before\ trumbling} \quad (7)$$

The water uptake rate of the raw and torrefied pellets was studied by immersing them (at least five) in water for a specific time (30 min to one week) at room temperature. A solid to water

ratio of 1:20 was used for each immersion test in a glass beaker (50 ml). Each pellet was removed, gently wiped with a dry cloth and weighted for each pre-defined time intervals (0.5, 1, 2, 5, 12, 24, 48, 72, and 168 hrs.). The differences in weight before and after immersion were determined as the amount of water uptake. In addition, the dimension of each pellet after a one-week immersion in water was measured and stated as the increase in axial and radial dimensions. Afterward, the pellets were oven dried overnight and the variations in dry weight compared to the initial dry weight prior to immersion was expressed as leaching percent.

Analysis of torgas

The torgas consists of both condensable and non-condensable gases. The non-condensable gas samples were collected using gas collection bags at three time intervals (0, 15, and30 min) during the entire torrefaction holding time (30 min). The analysis of gas composition was carried out using a Gas Chromatography Thermal Conductivity Detection system (GC-TCD) equipped with a Carboxen 1000 and 60/80 SS Packed Column (15 ft (4.572 m) × 1/8 in (3.175 mm)). The temperature of the programmed method initialized at 35°C, was held for 5 min, and increased to 200°C at a rate of 20°C min^{-1} and held for 3.75 min. 50 µL of the sample was injected. The weight percent of each component was also estimated from standard curves.

The composition analysis of condensable liquid samples was performed by Gas Chromatography/Mass Spectrometry (GC/MS) and High-Performance liquid chromatography (HPLC). The GC/MS was used to verify the presence of individual components using the NIST Mass Spectral Library while the water-soluble components (Glucose, Fructose, Xylose, arabinose, Sorbitol, Levoglucosan, Formate, Acetate, Hydroxyacetone, Acetone, 5-HMf, and Furfural) were quantified by the HPLC analysis using the external standard method. The GC/MS experiment was carried out in an Agilent GC-MSD (Hewlett-Packard 5973 and 6890) fitted with an HP-5MS

Capillary Column (30 m × 0.25 µm × 0.25 µm) and a CIS-4 inlet (Gerstal). The sample separation was done by raising the temperature from 40°C to 275°C at 15 °C min^{-1} rate; A constant inlet temperature of 260°C and a helium flow rate of 0.8 mL min^{-1}were held while the 1µL liquid sample was injected. HPLC was performed on a Shimadzu LC-20 AT with a Coragel 64-H transgenomic analytical column (7.8 mm × 300 mm) and a RID-10A refractive index detector. The 5 µL sample was automatically injected, and the HPLC ran for 55 min at a rate of 0.6 mL min^{-1}. During this process, the pressure was kept below 9 MPa, and sulfuric acid 4 mN was used in the mobile phase.

The water content of the liquid samples was measured using a Mettler Toledo DL31 Karl Fischer Titrator. The moisture content on a weight percentage basis was determined by analyzing samples suspended in Hydranal, titrated with CombiTitrant 5 Keto. The test was repeated three times for each sample.

Results and discussion

Torrefaction yields and pellet compositions

The wood pellets were successfully torrefied at different temperatures of 230, 250, 270, and 290°C (Fig. 1). Both CP1 and CP2 commercial pellets retained their initial shape and integrity after torrefaction. The mass yield and energy yield at various torrefaction temperatures are shown in Fig.2. Although the decreasing trend over increase in torrefaction temperature in mass and energy yields were similar for both CP1 and CP2 pellets, slightly greater reductions were observed for the CP2 pellets, persumably due to differences in initial feedstock compositions. The decomposition rate in CP1 wood pellets (softwood source) was lower than that of CP2 wood pellets (mixed of softwood and hardwood). Similar results were reported by previous studies on torrefaction of hardwood and softwood biomass materials [40–42]. Nanou et al. [41] investigated the torrefaction of different biomass types in a pilot scale. The mass yield of softwood material (spruce) from torrefaction at 260°C was about 79% compared to that of ash (73%) and willow (77%) as hardwood materials [43]. Hemicellulose is the major contributor to the dry mass loss during the biomass torrefaction [40]. The higher content and different type of hemicellulose in hardwood samples resulted in the higher degradation rate compared to the softwood biomass [40,41].

Figure 3-1. Control and torrefied pellets at different torrefaction temperature; (a) CP1 pellets, (b) CP2 pellets. T#: Torrefied at #°C. e.g., T230: torrefied at 230°C.

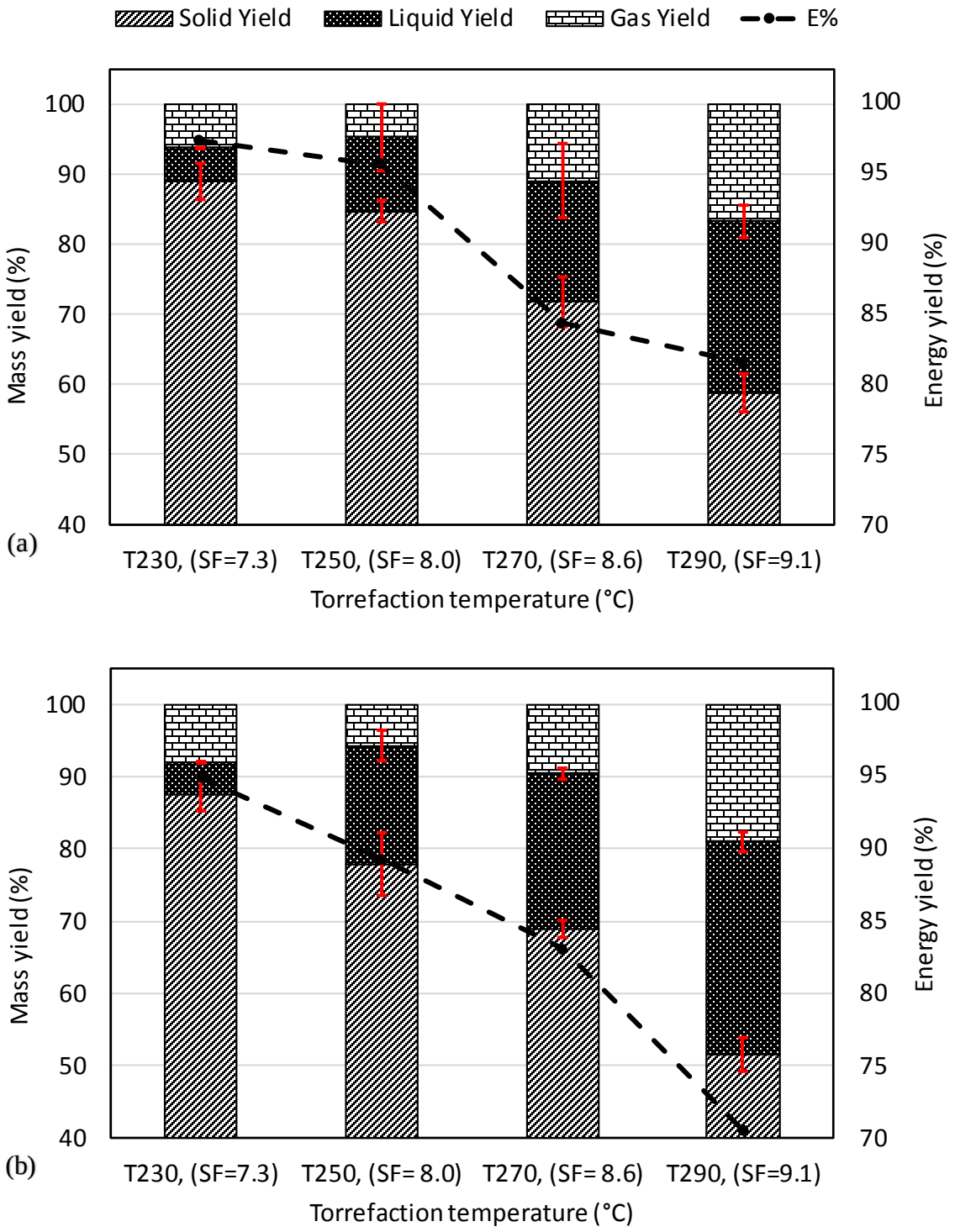

Figure 3-2. The mass yield and energy yield of (a) CP1 pellet, and (b) CP2 pellet from torrefaction at different temperatures. SF: Severity factor, E%: Energy yield. The error bars represent the standard deviations of double experiments.

In this study, the difference between mass yields of CP1 and CP2 pellets appeared substantial at 290°C. As the degree of torrefaction increased to 290°C (corresponds to 9.1 severity factor), the solid yield decreased to about 60% for CP1 and 52% for CP2 pellet samples indicating faster devolatilization rate of solids in CP1 samples with increased torgas yield (both tor-liquid and non-condensable gases). The torrefaction experiments were repeated two times to ensure repeatability. The standard deviations were in the range of 1.2 to 4.3% for solid mass yields and 0.1 to 4.7% for the tor-liquid yield. The mass balance was closed by calculating the gas yield by subtracting the tor-liquid and solid mass yields from 100. The exact mass balance in literature has been reported in the range of 93 to 104 % [41,44,45].

The chemical compositions of both raw and torrefied wood pellets are given in Table 1. The removal of hydroxyl (OH) groups during the torrefaction decreased both O/C ratio and H/C ratio for both torrefied pellets, which increased the percentage of the fixed carbon, reduced the percentage of the volatile matter, and slightly increased the ash content as reported elsewhere [11,46]. The higher heating value of both the torrefied pellet samples increased by 26% when the torrefaction temperature was increased from 230 to 290°C (Fig. 3) and were improved by more than 37% compared to the raw pellets (Table 1). The similar increase in the higher heating values by the increase in the torrefaction temperature were reported by other researchers [11,21,29,40]. The higher heating value of the CP1 torrefied pellets satisfied the ISO/TS 17225-8, solid biofuel specifications [47] in the temperature range of 230 to 290°C, while in the case of CP2 the minimum torrefaction temperature should be about 245°C corresponding to a 20% dry mass loss. The resulted higher heating values at 275 and 280°C of CP1 and CP2 pellets, respectively, were comparable to that of coal (24 MJ kg^{-1}) for heat and power generation applications [48].

Although higher heating values were obtained at higher torrefaction temperatures, the

energy yields were reduced accordingly. The energy yields of CP1 and CP2 pellets were dropped to 81.5 and 70.5%, respectively, at 290°C torrefaction, which is mainly due to the loss of materials (Fig. 2). Since the energy densification is indispensable in the torrefaction process, the ideal torrefaction operating condition should be investigated for each specific biomass feedstock. The optimal operating condition for producing torrefied pellets as a replacement to coal with similar higher heating value corresponds to a solid mass yield of ~70% (30% mass loss) at a torrefaction temperature of 275°C for CP1 wood pellets (Fig. 3a) and a mass yield of 60% (40% mass loss) at a temperature of 280°C for CP2 wood pellets (Fig. 3b).

Table 3-1. Fuel properties of raw and torrefied CP1 and CP2 pellets.

	Ctrl.		T230		T250		T270		T290		ISO/TS
	CP1	CP2	CP1	CP2	CP1	CP2	CP1	CP2	CP1	CP2	[47]
C (%, db)	48.62 (0.51)	46.65 (0.42)	51.64 (0.14)	49.87 (0.02)	53.03 (0.27)	53.63 (0.15)	58.37 (0.06)	55.88 (0.21)	64.34 (0.07)	62.71 (2.91)	--
H (%, db)	6.31 (0.07)	6.10 (0.02)	6.06 (0.02)	5.84 (0.01)	5.94 (0.02)	5.65 (0.01)	5.67 (0.03)	5.49 (0.02)	5.35 (0.04)	5.08 (0.05)	--
N (%, db)	0.13 (0.00)	0.13 (0.01)	0.14 (0.00)	0.16 (0.00)	0.14 (0.00)	0.17 (0.00)	0.15 (0.01)	0.19 (0.00)	0.18 (0.00)	0.13 (0.06)	N1.0≤1.0
O (%, db)	44.25 (0.59)	45.93 (0.05)	41.46 (0.23)	42.45 (0.17)	40.34 (0.25)	38.85 (0.10)	34.9 (0.12)	36.51 (0.00)	29.03 (0.03)	31.23 (2.15)	--
Moisture (%, wb)	6.22 (0.32)	5.68 (0.02)	1.74 (0.02)	1.69 (0.35)	1.45 (0.02)	1.52 (0.05)	1.52 (0.03)	1.55 (0.03)	1.27 (0.02)	1.41 (0.06)	A5.0≤5.0
Ash (%, db)	0.70 (0.02)	1.44 (0.04)	0.82 (0.05)	1.67 (0.14)	0.83 (0.05)	1.70 (0.06)	0.90 (0.05)	1.82 (0.01)	1.1 (0.05)	2.33 (0.11)	--
Volatile (%, db)	80.26 (0.11)	80.82 (0.14)	78.94 (0.18)	75.14 (5.51)	77.37 (0.1)	72.93 (0.17)	69.63 (0.14)	68.47 (0.18)	59.56 (0.25)	56.22 (0.16)	--
Fixed carbon (%, db)	19.05 (0.09)	17.73 (0.13)	20.23 (0.2)	23.19 (5.37)	21.82 (0.09)	25.37 (0.22)	29.47 (0.16)	29.68 (0.14)	39.34 (0.2)	41.45 (0.28)	--
HHV_d (MJ kg^{-1})	19.57 (0.41)	18.67 (0.52)	21.38 (0.83)	20.18 (0.73)	22.05 (0.08)	21.36 (0.13)	22.97 (0.85)	22.48 (0.44)	27.10 (0.56)	25.54 (0.83)	21

Number enclosed in the parenthesis are standard deviations with n =3

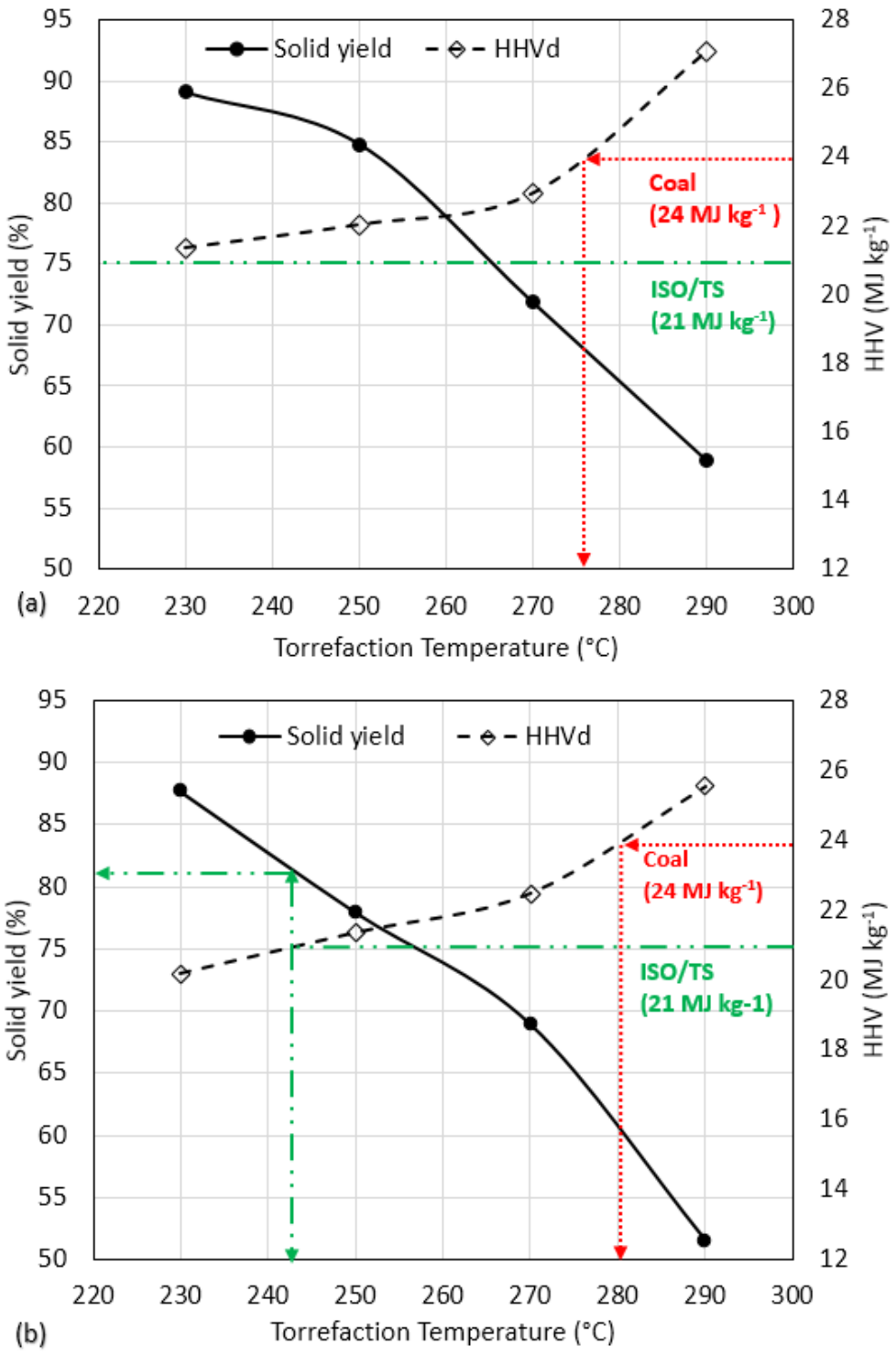

Figure 3-3. The solid mass yield and HHV of (a) torrefied CP1 pellet and (b) torrefied CP2 pellet at different temperatures.

Properties of torrefied pellets

The physical properties of both raw and torrefied wood pellets produced at various torrefaction temperatures are given in Table 2. As the temperature of torrefaction increased, the rate of biomass degradation (mainly hemicellulose) increased and the inter-particle hydrogen bondings weakened. The combination of these two effects led to the formation of more voids between particles in the pellet and thus decreased pellet density and hardness [13,46,49,50]. However, the pellet shape and integrity was maintained after torrefaction, even at high temperatures (270 and 290°C). Stelte et al. investigated the pellet properties of torrefied spruce [49] and torrefied wheat straw [13]. Pellets formed from wheat straw at 300°C barely maintained physical integrity and pellets could not be formed from torrefied spruce. The wheat and spruce torrefied pellets at lower temperature around 275°C were also defective [13,49]. The cross-linking and polycondensation of lignin in the voids formed by thermal decomposition [51] might be a reason for higher integrity of torrefied pellets produced with the TAP method.

Hardness of the torrefied pellets decreased drastically at higher torrefaction temperatures, similar to what was observed by Stelte et al. [13,49]. The lower the hardness of torrefied pellets, the lower will be the energy required for grinding or pulverization, if the pellets are used for co-firing with coal in a conventional pulverizer. However, a reasonable hardness value (higher than 100 N) of the torrefied pellet is required to prevent the formation of dust and fines during handling and transport, which could be maintained at or below the torrefaction temperature of 270°C [13].

The increased in torrefaction temperature decreased the durability of wood pellets. For the CP1 pellets, the durability of the torrefied pellet gradually reduced from 98% (raw

pellets), to 86% at 270 °C and further dropped to 74% at of 290°C. Although the downward trend in pellet durability was similar for CP2 pellets, the drop was even sharper and plummeted to the lowest index value of 37% at the torrefaction temperature of 290°C. The softwood biomass contains more lignin compared to the hardwood [41] and lignin has greater decomposition resistance during the torrefaction process. Therefore, the lignin content of CP1 pellet samples was likely higher than that of CP2 pellets, which were a mixture of softwood and hardwood. This could explain a higher durability of torrefied CP1 pellets. No binder percentage was reported in the initial compositions of raw pellets. Nevertheless, according to the ISO/TS 17225-8, solid biofuel specifications [47] and the North American pellet fuel standard [52], the pellet durability index should be higher than 95%. Thus, all of the torrefied pellets produced in this study are vulnerable to dust formation during handling, transport, and shipping, unless the torrefied pellets are used within or closer to the production facility. Alternatively, the overall quality of torrefied pellets could be improved by appropriately incorporating binders either before or after torrefaction. When economical, the wood pellets could be transported to the user site or near to the power plant, where the pellet could be torrefied and used onsite for power generation.

The bulk density of torrefied pellets also decreased with the increase in torrefaction temperature (Table 2.). However, it did not substantially change the volumetric energy density of the torrefied pellets. The volumetric energy density was constant until 270°C but dropped drastically at 290°C due to the severe decomposition of pellets, caused the breakage

Table 3-2. Physical properties of raw and torrefied CP1 and CP2 pellets.

	Ctrl.		T230		T250		T270		T290		ISO/TS
	CP1	CP2	CP1	CP2	CP1	CP2	CP1	CP2	CP1	CP2	[47]
Pellet density ($kg\ m^{-3}$)[a]	1231.60 (86.45)	1077.50 (106.75)	1185.18 (70.85)	1003.99 (72.64)	1132.38 (72.68)	902.26 (65.44)	991.88 (89.04)	912.86 (62.94)	862.39 (109.64)	733.31 (78.4)	--
Bulk density ($kg\ m^{-3}$)[b]	669.14 (18.36)	651.75 (13.68)	644.63 (7.67)	634.81 (8.7)	634.85 (5.71)	586.03 (1.48)	554.93 (2.78)	547.8 (5.84)	361.70 (1.1)	316.23 (0.83)	BD550≥ 550
Pellet moisture (%, wb)[c]	4.98 (0.00)	6.73 (0.01)	0.82 (0.00)	0.62 (0.00)	0.59 (0.00)	0.62 (0.00)	0.55 (0.00)	0.5 (0.00)	0.31 (0.00)	0.47 (0.00)	--
Average L/D[a]	2.48 (0.90)	1.51 (0.63)	2.56 (0.92)	1.5 (0.52)	2.91 (1.04)	1.72 (0.6)	2.71 (0.99)	1.88 (0.65)	2.75 (0.95)	1.59 (0.36)	0.13-6.67
Volumetric energy density ($GJ\ m^{-3}$)[d]	12.28	11.48	13.52	12.59	13.80	12.33	12.55	12.12	9.68	7.96	--
Hardness (N)[b]	477.10	409.13	400.56	279.64	238.73	231.16	177.74	167.17	103.27	46.07	--
Durability index (%)	98.00	96.20	92.00	91.10	86.90	83.70	85.70	76.00	74.30	37.30	DU95.0 ≥ 95,0

a Number enclosed in the parenthesis are standard deviations with n =15.
b Number enclosed in the parenthesis are standard deviations with n =5.
c Number enclosed in the parenthesis are standard deviations with n =3.
d Volumetric energy density was calculated by the product of bulk density and net calorific value of pellets.

of the inter-particle bonding and higher void space between particles within the pellet. Nevertheless, the overall quality and energy density of torrefied pellets could be maintained at the optimal torrefaction temperature range of 275-280°C for both CP1 and CP2 commercial wood pellets. Hygroscopicity or the water uptake rate by pellets can be inferred as the stability of pellets under rainy or humid conditions. It was observed that the raw pellets immersed in water disintegrated immediately while the torrefied pellets remained intact even after one week (Fig. S1.). The water immersion test for torrefied pellets has been studied by other researchers at various durations; for instance: 2 hours [22], 15 hours [6], and 17 days (for torrefied briquettes) [53] and reported the similar conclusion. Ghiasi et al. investigated the water uptake behaviors of torrefied pellets from both pathways (TOP and TAP) and observed that the TAP torrefied pellets had lower water uptake rate [22]. Pellet moisture contents over the immersion period for both samples are illustrated in Fig. 4. Moisture absorption of torrefied biomass was lower at higher temperatures, but all samples eventually reached the saturation point as observed in other similar studies elsewhere [22,28,53]. The maximum moisture content of torrefied pellets between the torrefaction temperature range of 250 - 290°C was about 21% (Fig. 4). In general, the water uptake behaviors of both torrefied pellets at 230°C and 250°C were similar. As the torrefaction temperature increased to 270°C, the CP1 torrefied pellets showed slightly higher resistance to water uptake compared to the CP2 torrefied pellets. The moisture content of immersed CP1 torrefied pellets at 270°C reached to about 11% after 72 hours, while the CP2 torrefied pellets passed the same moisture content in the first 12 hours. The same trend was observed for the torrefied samples at 290°C. The overall drop in water uptake of torrefied pellets explained the increase in the hydrophobicity of wood pellets by torrefaction. The change in the hydrophobic behavior of torrefied pellets could be due to the removal of hydroxyl (-OH) groups from pellets, particle

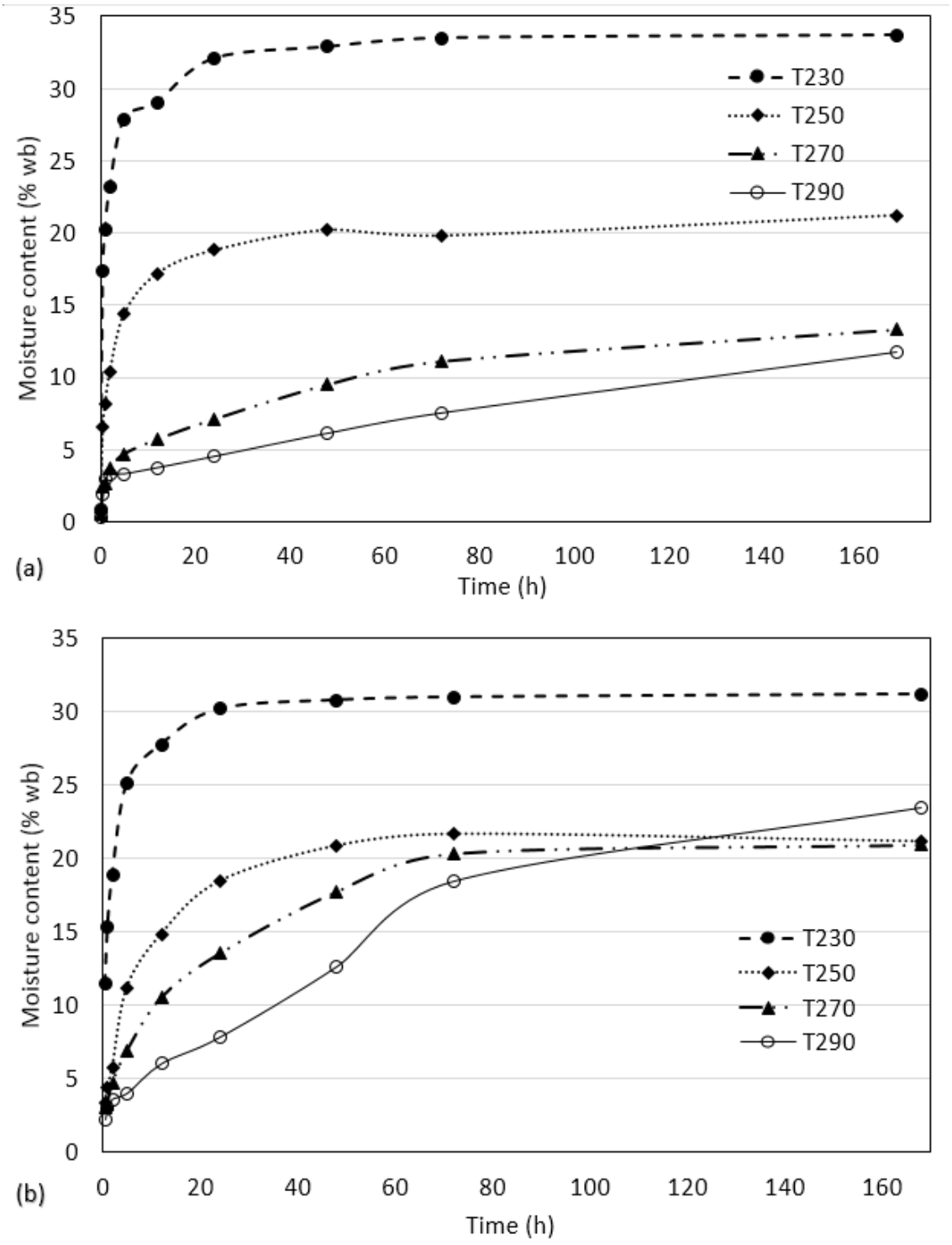

Figure 3-4. Moisture content of pellets after immersing in water for different duration (a) CP1 torrefied pellets, and (b) CP2 torrefied pellets.

coverage by lignin layer, and the increase in hydrophobic carbon content [46,54]. The lignin content of softwood biomass is higher than hardwood [41]. Lignin is the least hydrophilic

constituent of the biomass [55]. During thermal treatment in the torrefaction process, lignin is the least decomposed component, however, the lignin softening and polycondensation in the more porous structure of the treated biomass [51] would most likely result in the blockage of remained hydroxyl groups and increase of the hydrophobicity. Although CP2 pellet samples showed more mass loss during the torrefaction and probably more removal of hydroxyl groups, the lower lignin content of CP2 pellets resulted in higher water uptake. The water uptake study further suggested that torrefaction could provide a way in dealing with moisture absorption problems associated with biomass during storage [28].

The axial and radial expansion of pellets after one-week immersion were measured and are included in the Supporting Information document. Although no uniform trend in the dimensional expansion was observed, the density of the torrefied pellets was reduced in general after immersion. The further assessment showed that the torrefied pellets at lower temperatures had higher solid leaching potential. The change of color of the water (Fig. S1) could indicate the increased dissolved organic carbon (DOC) content and chemical oxygen demand (COD) of water due to the dissolution of the pellets [56]. Nevertheless, in this study, we did not conduct the analysis of the water after immersion. The leaching test is usually carried out to evaluate the environmental impacts of torrefied pellet storage in outdoor storage areas. Therefore, if the pellets are stored under a roof (which is most often the case), there is no need for testing the leaching behavior [56].

Non-condensable gas compositions

The compositions of non-condensable gas products consisted of carbon dioxide (CO_2), carbon monoxide (CO) and a trace of methane (CH_4) are shown in Fig.5, which were similar to other reported studies [42,45,57]. The CO concentrations variations were corresponding to 0.9 to 5.9% yield (considering the gas yield and gas composition) for CP1 torrefied pellets and 1.2 to 6.6

% for CP2 torrefied pellets. The obtained CO_2 yield ranged from 5.3 to 10.7% and 6.7 to 12.2% for CP1 and CP2 pellets, respectively. For the CP1 pellets, the concentration of CH4 was less than 0.1 and 0.2% at 270 and 290°C (Fig. 5), respectively, equal to 0.1% yield. CP2 pellets torrefied at 290°C resulted in a 0.2% CH4 yield. Prins et al. reported the CO yield in range of 0.2 to 1.2% for torrefaction of willow, and 0.05 to 0.9% for torrefaction of larch in temperature range of 230 to 290°C [42]. The mass yield of CO_2 for willow torrefaction was 1.9 to 4.1 % and for larch torrefaction was 0.3 to 2% [42], which were lower than CO_2 yields from CP1 and CP2 pellets in this study. Bergman et al. reported the relative composition (without considering the carrier gas) of 12% for CO and 80% for CO_2 from torrefaction of wood at 280°C and 17.5 min [57]. In this study, the relative composition of CO and CO_2 for both CP1 and CP2 pellets varied from about 15 to 35% and from 85 to 64%, respectively. CO_2 was formed primarily by decarboxylation reaction of acid carboxyl groups in hemicellulose, while CO was presumably formed in the secondary reaction of carbon dioxide and steam with porous char [9,58]. When the torrefaction temperature and decomposition rate of lignin and cellulose increased, the CO was possibly further generated by decarbonylation of simple carbonyl compounds [7,45]. Therefore, the ratio of CO to CO_2 increased with torrefaction temperature, similar to that reported by [58]. The CO is the primary source for the heating value of the non-condensable gas product, and it should be flared or burned

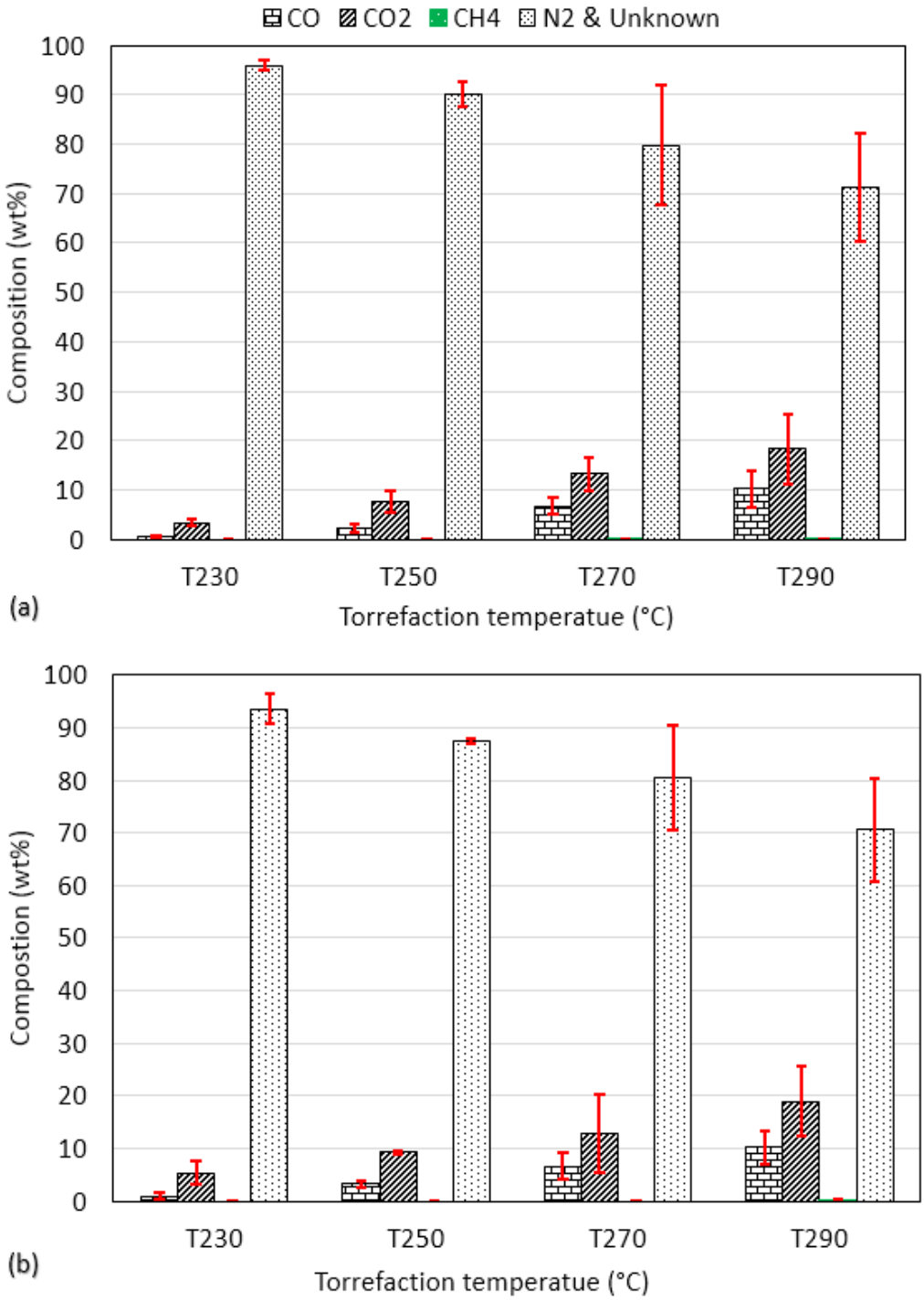

Figure 3-5. The composition of gas products from torrefaction of (a) CP1 pellets, and (b) CP2 pellets at different temperature. The error bars represent the standard deviations of three samples.

out for safety [7,9]. In this study, nitrogen gas was used as an inert carrier gas, which could be replaced by the flue gas produced from the combustion of non-condensable fraction of torgas in the industrial scale torrefaction system [59].

Tor-liquid compositions

The tor-liquid product included a multicomponent mixture of water, acids, ketones, alcohols, furans, aldehyde, phenols, etc. Table S2 gives the area percentage of the most abundant components in tor-liquid products as a result of GC/MS analysis. The water-soluble components were quantified through HPLC and depicted in Table 3 for different torrefaction temperatures. The main components in the tor-liquid included acetate and formate, hereafter presumed as acetic acid and formic acid, respectively, levoglucosan, hydroxyacetone, furfural, acetone, 5-HMF, and 2-methoxyphenol. Similar composition of volatile products have been reported in literature from torrefaction of biomass materials [41,42,45,57,60]. Methanol, also known as wood alcohol, is a common product of removing methoxyl groups from hemicellulose structure [61] and it has been reported as a main component in volatile stream of torrefaction process in several reports. However, it was not observed from torrefaction of CP1 and CP2 pellets, which might be due to earlier emission of alcoholic compounds, mainly methanol, and simple aldehydes during storage and drying of biomass feedstock in pelletization process [62]. In general, the overall concentrations of the organic compounds increased as the torrefaction temperature increased, indicating a higher degree of severity of torrefaction.

Table 3-3. The composition of tor-liquid from CP1 and CP2 wood pellets.

Compositions (g L^{-1})	T230		T250		T270		T290	
	CP1	CP2	CP1	CP2	CP1	CP2	CP1	CP2
HPLC results								
Acetic acid	46.7	67.7	42.8	124.1	163.4	141.1	93.8	136.4
Formic acid	20.9	0.0	23.2	19.1	52.7	20.4	38.1	3.9
Furfural	8.7	21.2	8.6	11.9	16.7	10.5	10.1	9.7
Hydroxyacetone	5.7	7.2	7.3	8.4	41.2	14.7	29.5	21.7
Acetone	4.0	10.2	0.6	1.6	0.8	2.0	2.2	3.5
5-HMF	0.8	2.1	1.2	0.7	1.7	0.9	4.5	1.7
Glucose	0.0	0.2	0.0	0.0	0.0	0.0	0.4	0.5
Fructose	0.0	0.0	0.2	0.0	1.3	0.0	0.0	0.1
Xylose	0.1	0.1	0.1	0.1	0.1	0.1	0.1	0.2
Arabinose	0.5	0.1	0.5	0.0	0.1	0.0	0.0	0.1
Sorbitol	0.1	0.0	0.2	0.0	0.0	0.1	0.0	0.0
Levoglucosan	4.4	17.0	4.9	5.4	30.4	12.4	47.3	36.7
2-Methoxyphenol	0.3	0.6	0.4	1.1	0.9	1.3	1.9	1.9
Karl Fischer Titrator								
Water	766.0	685.1	738.8	638.0	665.6	588.9	548.7	479.5

The organic acids (acetic acid and formic acid) were the primary constituents in the tor-liquid, which in turn are the main products of decomposition from hemicellulose [41,42,45]. The maximum concentration of acetic acid in tor-liquid was 163 g L^{-1} and 141 g L^{-1} from torrefaction of CP1 and CP2 pellets, respectively, at the temperature of 270°C. The higher acetic acid concentration in CP2 tor-liquid might be related to the higher concentration of acetyl groups in the hemicellulose structure of CP1 biomass [45]. Levoglucosan is the main product of the cellulose

decomposition [45]. The levoglucosan concentration increased from 4.4 to 47 g L^{-1} for the CP1 torrefied pellet, and from 17 to 37 g L^{-1} for the CP2 torrefied pellets in a torrefaction temperature range of 230 to 290°C. The other possible products of thermal decomposition of wood were ketones. Acetone, the simplest ketone, and hydroxyacetone (acetol, hydroxyl ketone) were formed by the degradation of hemicellulose and cellulose in the biomass. The highest concentration of hydroxyacetone was measured to about 41 g L^{-1} in CP1 samples at 270°C, and it decreased to 29.5 g L^{-1} at 290°C, while it was about 15 g L^{-1} for CP2 samples at 270°C and increased to 22 g L^{-1} at 290°C. The average concentration of furfural, the possible aldehyde product from dehydration of hemicellulose fraction, was 10 g L^{-1} from 230°C to 290°C for both torrefied pellets. The small amount of 5-HMF (hydroxymethyl furfural) also appeared at a higher torrefaction temperature. Also, the concentrations of 2-Methoxyphenol, representative of phenolic compounds, increased at higher torrefaction temperature (290 °C), which is derived from the decomposition of lignin at higher temperatures [63].

The combined evaporation of initial moisture within the pellet and the dehydration of biomass particle due to thermal disruption of hydroxyl group, led to the formation of water as the major component in the tor-liquid [44]. The water percentage in tor-liquid products of torrefaction of both CP1 and CP2 pellets decreased from 77 to 48% when the torrefaction temperature increased from 230 to 290°C, due to an increased proportion of volatile organic molecules in the torgas as reported elsewhere [29,44]. The downward trend of moisture content might be the result of greater decomposition of biomass at higher temperatures [44] and higher number of reactions of water with volatile matter and char [29].

Application of torgas

The constitution of torgas varies largely by biomass compositions and the torrefaction temperature [19,20]. The non-condensable gas fraction is generally comprised of carbon dioxide and carbon monoxide, and the condensable liquid fraction comprised of water, organic acids, and other volatile organic compounds. The normalized compositions of torgas at different torrefaction temperatures for CP1 and CP2 pellets are shown in Table 4. So far, research related to methods for utilizing torgas has been focused on the torgas has been either flaring, or burning it along with other combustion aids (usually, natural gas) in a combustor to produce heat energy. Although the conventional thermal oxidation of volatile organic compounds with natural gas is an efficient method to remove the VOCs and to produce energy, it is an expensive process [64]. To date, in addition, a number of studies have been focused on the catalytic destruction of VOCs in fixed bed adiabatic reactors [65]. Catalytic oxidation can be effectively implemented for moderate flow rates and low concentration of VOCs (i.e., similar to a torrefaction volatile stream or torgas) at the temperature range of 250-500°C in the presence of appropriate catalysts to minimize environmental emissions [65].

Another method is the condensation of the torgas into a liquid co-product stream, which can be used as a solvent or precursor to produce value-added chemicals or products. The non-condensable fraction (mostly CO and CO_2) can be combusted or returned to the torrefaction system as an inert gas media. For example, if the torrefaction process is integrated into a typical wood pellet plant with an annual production capacity of 140,000 Mg (dry basis), the condensable liquid yield could reach up to 24,220 Mg of tor-liquid at 270°C torrefaction temperature. This is equivalent to approxiametly 4000 Mg of acetic acid or 400 Mg of furfural (Fig. 6.).

Table 3-4. Torgas compositions of CP1 and CP2 pellets torrefaction at different temperature based on the experimental data from GC/TCD (for non-condensable products) and HPLC (for condensable products).

	T230		T250		T270		T290	
Composition (wt %)	CP1	CP2	CP1	CP2	CP1	CP2	CP1	CP2
Water	3.65	2.98	7.76	10.47	11.52	12.66	13.42	14.11
Acetic acid	0.57	0.73	1.31	4.28	3.06	6.12	4.54	9.66
Formic acid	0.25	0.00	0.71	0.66	0.99	0.89	1.85	0.27
Furfural	0.11	0.23	0.26	0.41	0.31	0.46	0.49	0.69
Hydroxyacetone	0.07	0.08	0.22	0.29	0.77	0.64	1.43	1.53
Acetone	0.05	0.11	0.02	0.06	0.02	0.09	0.10	0.25
5-HMF	0.01	0.02	0.04	0.02	0.03	0.04	0.22	0.12
Levoglucosan	0.06	0.08	0.18	0.38	0.60	0.91	2.32	3.22
2-methoxyphenol	0.00	0.00	0.01	0.03	0.02	0.03	0.09	0.13
CO	0.93	1.24	1.06	1.49	3.66	3.25	5.92	6.63
CO_2	5.30	6.75	3.64	4.18	7.17	6.33	10.66	12.23
CH_4	0.00	0.00	0.00	0.00	0.05	0.00	0.12	0.16
Total Volatile	10.99	12.34	15.21	22.08	28.19	31.07	41.15	48.45
Solid yield	89.01	87.66	84.79	77.92	71.81	68.93	58.85	51.55

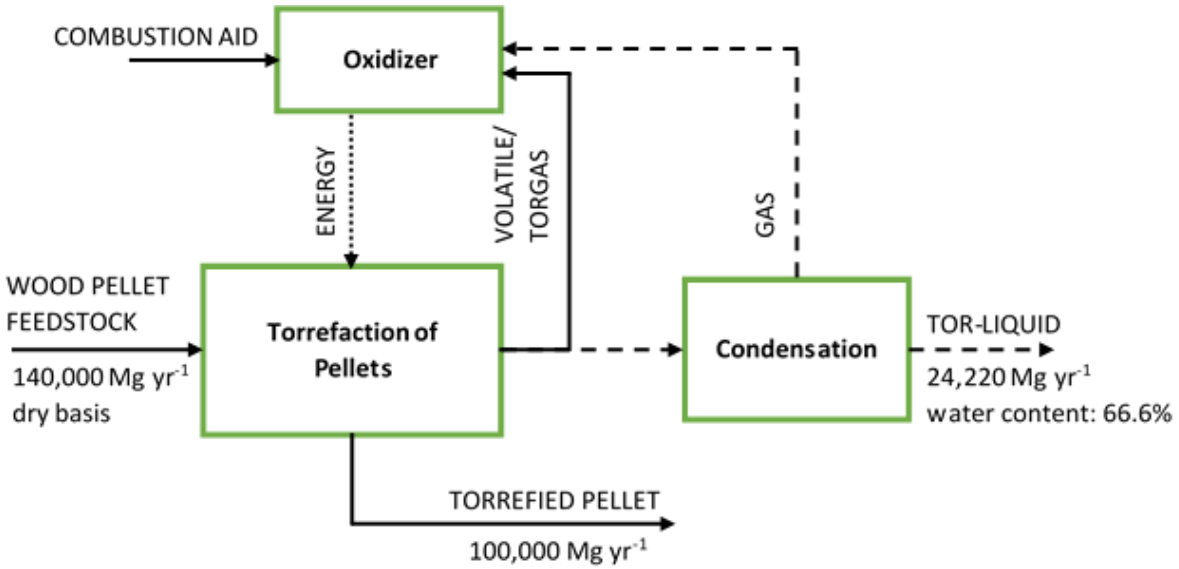

Figure 3-6. Products distribution for torrefaction of CP1 pellets at 270°C.

Nevertheless, the tor-liquids should be economically separated and purified in order to sell the products as industrial chemicals. Alternative uses for the entire liquid mixtures should be further investigated. It has been asserted that the volatile liquid stream can be utilized as a wood vinegar or pyro-ligneous acid [20,66,67]. Fagernas et al. explored the application of tor-liquids from torrefaction of spruce and bamboo gathered at three different liquid streams from three temperature ranges: Stream 1 between 20 and 105°C; Stream 2 between 105 and 240°C; and Stream 3 between 240 and 300°C [20]. Since the composition of the condensates changes with temperature, their applications vary widely. The first stream mainly consisted of water. The second stream consisted of tar free acetic acid and furfural mixtures, which can be used as a "pesticide, herbicide, fungicide, insecticide, and bug repellent.". The third stream mainly consisted of phenolic compounds, which could be used as wood preservatives or wood protection agents [20]. Generally, wood vinegar can be utilized as a growth-promoting agent [68,69], as a fungicide for natural rubber production (as an acetic acid replacement) [67], as a repellent [70], as an additive agent in pelletization [19], and as a wood protection agent [20]. Fagernas et al. evaluated the

economic aspects of different torrefaction liquid streams. They concluded that the recovery and selling of the valuable co-products in liquid streams could considerably reduce the production costs of torrefied pellets [20]. The alternative option for utilizing tor-liquid is similar to aqueous processing methods such as hydrodeoxygenation (HDO) and dehydration/hydrogenation used to upgrade the aqueous phase of pyrolysis bio-oil [71]. Further research is required to investigate the potential application of tor-liquid to produce high-value chemicals.

Conclusions

The torrefaction of wood pellets (TAP process) is a potential pathway to produce energy-dense pellets as a tradable solid biofuel to replace coal. The increase in torrefaction temperature from 230 to 290°C improved the heating value (up to 38%) and hydrophobicity of the torrefied wood pellets compared to the raw wood pellets. However, the mass and energy yields were decreased. The similar higher heating value to that of coal was obtained for the torrefied CP1 and CP2 pellets at 275 to 280°C. Although the torrefied wood pellets were produced at high torrefaction temperatures without a binder (with preservation of initial shape and integrity) the hardness and durability of the torrefied pellets needs to be improved to prevent dust formation. This is of particular importance when, long distance transportation is required. The torgas could be either burned to produce energy or condensed into liquids to produce valuable chemicals such as acetic acid and furfural as co-products.

Acknowledgments

This research was fully supported by the Consortium for Advanced Wood-to-Energy Solutions (CAWES) with funding provided by USDA Forest Products Laboratory and U.S. Endowment for Forestry and Communities. The authors thank Ms. Joby Miller for the assistance in conducting the GC/MS and HPLC analyses. The Herty Advanced Materials Development Center, Georgia Southern University, Savannah, GA is also acknowledged for performing the durability test.

References

[1] D. Thrän, D. Peetz, K. Schaubach, Global Wood Pellet Industry and Trade Study 2017, IEA Bioenergy. Task 40 (2017) 222. http://task40.ieabioenergy.com/wp-content/uploads/2013/09/IEA-Wood-Pellet-Study_final-2017-06.pdf (accessed November 28, 2017).

[2] U.S. Energy Information Administration, Monthly Energy Review (MER), August 2016 Table A5, U.S. Dep. Energy, Washington, DC. DOE/EIA-00 (2016) 239. doi:0035(2016/8).

[3] W. McDow, Y. Qian, W. McDow, The Wood Pellet Value Chain, US Endow. For. Communities. (2013) 59. http://www.usendowment.org/images/The_Wood_Pellet_Value_Chain_Revised_Final.pdf (accessed August 7, 2017).

[4] S. Mani, S. Sokhansanj, X. Bi, A. Turhollow, Economics of producing fuel pellets from biomass, Appl. Eng. Agric. 22 (2006) 421–426. doi:10.13031/2013.20447.

[5] EIA Energy Information Administration- Independent Statistics and Analysis, Densified biomass fuel manufacturing facilities in the United States by state, region, and capacity, U.S. Dep. Energy, Washington, DC. (2017). https://www.eia.gov/biofuels/biomass/#about (accessed November 28, 2017).

[6] P.C.A. Bergman, Combined torrefaction and pelletisation the TOP process, Energy Cent. Netherlands, Rep. No. ECN-C-05-073, ECN, Petten, Netherlands. (2005). http://www.ecn.nl/publications.

[7] J.S. Tumuluru, S. Sokhansanj, J.R. Hess, C.T. Wright, R.D. Boardman, A review on

biomass torrefaction process and product properties for energy applications, Ind. Biotechnol. 5 (2011). doi:10.1089/ind.2011.0014.

[8] J. Koppejan, S. Sokhansanj, S. Melin, S. Madrali, Status overview of torrefaction technologies, a review of the commercialisation status of biomass torrefaction, IEA Energy Technol. Network, IEA Bioenergy Task 32. (2015).

[9] M.J. Prins, K.J. Ptasinski, F.J.J.G. Janssen, More efficient biomass gasification via torrefaction, Energy. 31 (2006) 3458–3470. doi:10.1016/j.energy.2006.03.008.

[10] A.A. Boateng, C.A. Mullen, Fast pyrolysis of biomass thermally pretreated by torrefaction, J. Anal. Appl. Pyrolysis. 100 (2013) 95–102. doi:10.1016/j.jaap.2012.12.002.

[11] J.H. Peng, X.T. Bi, S. Sokhansanj, C.J. Lim, Torrefaction and densification of different species of softwood residues, Fuel. 111 (2013) 411–421. doi:10.1016/j.fuel.2013.04.048.

[12] J. Peng, X.T. Bi, C.J. Lim, H. Peng, C.S. Kim, D. Jia, H. Zuo, Sawdust as an effective binder for making torrefied pellets, Appl. Energy. 157 (2015) 491–498. doi:10.1016/j.apenergy.2015.06.024.

[13] W. Stelte, N.P.K. Nielsen, H.O. Hansen, J. Dahl, L. Shang, A.R. Sanadi, Reprint of: Pelletizing properties of torrefied wheat straw, Biomass and Bioenergy. 53 (2013) 105–112. doi:10.1016/j.biombioe.2013.03.012.

[14] L. Kumar, A.A. Koukoulas, S. Mani, J. Satyavolu, Integrating torrefaction in the wood pellet industry: A critical review, Energy and Fuels. 31 (2017) 37–54. doi:10.1021/acs.energyfuels.6b02803.

[15] C. Wilén, P. Jukola, T. Järvinen, K. Sipilä, F. Verhoeff, J. Kiel, Wood torrefaction–pilot

tests and utilisation prospects, 2013.

[16] R.S. Cherry, R. a Wood, T.L. Westover, Analysis of the Production Cost for Various Grades of Biomass Thermal Treatment, U.S. Dep. Energy, Idaho Natl. Lab. INL/EXT-13-30348, Idaho Falls, Idaho. (2013).

[17] M.A. Leonhardt, Torrefaction systems and methods including catalytic oxidation and/or reuse of combustion gases directly in a torrefaction reactor, cooler, and/or dryer/preheater, U.S. Pat. Trademark Off. US8203024B2, Washington, DC. (2012).

[18] D. Thrän, J. Witt, K. Schaubach, J. Kiel, M. Carbo, J. Maier, C. Ndibe, J. Koppejan, E. Alakangas, S. Majer, F. Schipfer, Moving torrefaction towards market introduction – Technical improvements and economic-environmental assessment along the overall torrefaction supply chain through the SECTOR project, Biomass and Bioenergy. 89 (2016) 184–200. doi:10.1016/J.BIOMBIOE.2016.03.004.

[19] W. Stelte, Torrefaction of unutilized biomass resources and characterization of torrefaction gasses, Danish Technol. Institute, Energy Clim. Cent. Renew. Energy Transp. Sect. Biomass, Denmark. (2012).

[20] L. Fagernas, E. Kuoppala, V. Arpiainen, Composition, utilization and economic assessment of torrefaction condensates, Energy and Fuels. 29 (2015) 3134–3142. doi:10.1021/acs.energyfuels.5b00004.

[21] W.-H.H. Chen, Y.-Q.Q. Zhuang, S.-H.H. Liu, T.-T.T. Juang, C.-M.M. Tsai, Product characteristics from the torrefaction of oil palm fiber pellets in inert and oxidative atmospheres, Bioresour. Technol. 199 (2016) 367–374. doi:10.1016/j.biortech.2015.08.066.

[22] B. Ghiasi, L. Kumar, T. Furubayashi, C.J. Lim, X. Bi, C.S. Kim, S. Sokhansanj, Densified biocoal from woodchips: Is it better to do torrefaction before or after densification?, Appl. Energy. 134 (2014) 133–142. doi:10.1016/j.apenergy.2014.07.076.

[23] J. Peng, J. Wang, X.T. Bi, C.J. Lim, S. Sokhansanj, H. Peng, D. Jia, Effects of thermal treatment on energy density and hardness of torrefied wood pellets, Fuel Process. Technol. 129 (2015) 168–173.

[24] N. Doassans-Carrère, S. Muller, M. Mitzkat, REVE: Versatile Continuous Pre/Post-Torrefaction Unit for Pellets Production, (2015) 14386. doi:10.1007/978-3-658-04355-1.

[25] L. Shang, N.P.K. Nielsen, J. Dahl, W. Stelte, J. Ahrenfeldt, J.K. Holm, T. Thomsen, U.B. Henriksen, Quality effects caused by torrefaction of pellets made from Scots pine, Fuel Process. Technol. 101 (2012) 23–28. doi:10.1016/j.fuproc.2012.03.013.

[26] M. Phanphanich, S. Mani, Impact of torrefaction on the grindability and fuel characteristics of forest biomass, Bioresour. Technol. 102 (2011) 1246–1253. doi:10.1016/j.biortech.2010.08.028.

[27] R.P. Overend, E. Chornet, Fractionation of lignocellulosics by steam-aqueous pretreatments, Philos. Trans. R. Soc. A Math. Phys. Eng. Sci. 321 (1987) 523–536. doi:10.1098/rsta.1987.0029.

[28] A. Pimchuai, A. Dutta, P. Basu, Torrefaction of agriculture residue to enhance combustible properties, Energy and Fuels. 24 (2010) 4638–4645. doi:10.1021/ef901168f.

[29] W.H. Chen, S.H. Liu, T.T. Juang, C.M. Tsai, Y.Q. Zhuang, Characterization of solid and liquid products from bamboo torrefaction, Appl. Energy. 160 (2015) 829–835. doi:10.1016/j.apenergy.2015.03.022.

[30] P.R. Stuart, M.M. El-Halwagi, Eds, Integrated biorefineries: design, analysis, and optimization, CRC Press. (2012).

[31] M. Borrega, K. Nieminen, H. Sixta, Degradation kinetics of the main carbohydrates in birch wood during hot water extraction in a batch reactor at elevated temperatures, Bioresour. Technol. 102 (2011) 10724–10732. doi:10.1016/j.biortech.2011.09.027.

[32] M.R. Pelaez-Samaniego, V. Yadama, M. Garcia-Perez, E. Lowell, Abundance and characteristics of lignin liquid intermediates in wood (Pinus ponderosa Dougl. ex Laws.) during hot water extraction, Biomass and Bioenergy. 81 (2015) 117–128. doi:10.1016/j.biombioe.2015.06.012.

[33] ANSI/ASAE, ANSI/ASAE S358.3 MAY2012 Moisture measurement-forages, Am. Soc. Agric. Biol. Eng. (Approved June 2012 as an Am. Natl. Stand.). (2012) 3–5.

[34] ASTM E873-82, Standard test method for bulk density of densified particulate biomass fuels, Annu. B. ASTM Stand. 82 (2006) American Society for Testing and Materials, West C. doi:10.1520/E0873-82R06.

[35] ASTM, ASTM D7582-15 Standard Test Methods for Proximate Analysis of Coal and Coke by Macro, Annu. B. ASTM Stand. (2015) American Society for Testing and Materials, West C. doi:10.1520/D7582.

[36] ASTM, ASTM D3176-15 Standard Practice for Ultimate Analysis of Coal and Coke, Annu. B. ASTM Stand. (2015) American Society for Testing and Materials, West C. doi:10.1520/D3176-15.2.

[37] ASTM, ASTM D5865-13 Standard Test Method for Gross Calorific Value of Coal and Coke, Annu. B. ASTM Stand. (2013) American Society for Testing and Materials, West

C. doi:10.1520/D5865-13.2.

[38] C. Karunanithy, Y. Wang, K. Muthukumarappan, S. Pugalendhi, Physiochemical characterization of briquettes made from different feedstocks, Biotechnol. Res. Int. 2012 (2012) 165202. doi:10.1155/2012/165202.

[39] ASAE, ASAE S269.4 Pellets, and crumbles-definitions and methods for determining density, durability, and moisture content, Am. Soc. Agric. Eng. DEC96. (1998) St. Joseph, MI.

[40] M.F. Li, L.X. Chen, X. Li, C.Z. Chen, Y.C. Lai, X. Xiao, Y.Y. Wu, Evaluation of the structure and fuel properties of lignocelluloses through carbon dioxide torrefaction, Energy Convers. Manag. 119 (2016) 463–472. doi:10.1016/j.enconman.2016.04.064.

[41] P. Nanou, M.C. Carbo, J.H.A. Kiel, Detailed mapping of the mass and energy balance of a continuous biomass torrefaction plant, Biomass and Bioenergy. 89 (2016) 67–77. doi:10.1016/j.biombioe.2016.02.012.

[42] M.J. Prins, K.J. Ptasinski, F.J.J.G. Janssen, Torrefaction of wood: Part 2. Analysis of products, J. Anal. Appl. Pyrolysis. 77 (2006) 35–40.

[43] P. Nanou, M.C. Carbo, J.H. a. Kiel, Biomass Torrefaction on Pilot Scale, Energy Res. Cent. Netherlands. (2015).

[44] A. Zheng, Z. Zhao, S. Chang, Z. Huang, F. He, H. Li, Effect of torrefaction temperature on product distribution from two-staged pyrolysis of biomass, Energy and Fuels. 26 (2012) 2968–2974. doi:10.1021/ef201872y.

[45] S. Chang, Z. Zhao, A. Zheng, F. He, Z. Huang, H. Li, Characterization of products from

torrefaction of sprucewood and bagasse in an auger reactor, Energy and Fuels. 26 (2012) 7009–7017. doi:10.1021/ef301048a.

[46] J.H. Peng, H.T. Bi, C.J. Lim, S. Sokhansanj, Study on density, hardness, and moisture uptake of torrefied wood pellets, Energy & Fuels. 27 (2013) 967–974. doi:10.1021/ef301928q.

[47] ISO, ISO/TS 17225-8 Solid biofuels - Fuel specifications and classes; Part 8: Graded thermally treated and densified biomass fuels, Swedish Stand. Institute, ISO/TC 238 N638, Stock. Sweden. (2016).

[48] GREET Life Cycle Model, GREET Transportation Fuel Cycle Analysis Model, GREET 1.8b, Argonne Natl. Lab. Copyr. 2012 UChicago Argonne, LLC. September (2008). http://greet.es.anl.gov/.

[49] W. Stelte, C. Clemons, J.K. Holm, A.R. Sanadi, J. Ahrenfeldt, L. Shang, U.B. Henriksen, Pelletizing properties of torrefied spruce, Biomass and Bioenergy. 35 (2011) 4690–4698. doi:10.1016/j.biombioe.2011.09.025.

[50] H. Li, X. Liu, R. Legros, X.T. Bi, C. Jim Lim, S. Sokhansanj, Pelletization of torrefied sawdust and properties of torrefied pellets, Appl. Energy. 93 (2012) 680–685. doi:10.1016/j.apenergy.2012.01.002.

[51] M.J. Boonstra, J. Van Acker, B.F. Tjeerdsma, E. V Kegel, Strength properties of thermally modified softwoods and its relation to polymeric structural wood constituents, Ann. For. Sci. 64 (2007) 679–690. doi:10.1051/forest:2007048.

[52] PFI Standards Committee, Pellet fuel institute (PFI) standard specification for residential/commercial densified fuel, June (2011).

http://www.weedcenter.org/cig/docs/PFI-Standard-Specification-November-2011.pdf.

[53] F.F. Felfli, C.A. Luengo, J.A. Suárez, P.A. Beatón, Wood briquette torrefaction, Energy Sustain. Dev. 9 (2005) 19–22. doi:10.1016/S0973-0826(08)60519-0.

[54] N. Kaliyan, R.V. Morey, Natural binders and solid bridge type binding mechanisms in briquettes and pellets made from corn stover and switchgrass, Bioresour. Technol. 101 (2010) 1082–1090. doi:10.1016/j.biortech.2009.08.064.

[55] C. Piao, J.E. Winandy, T.F. Shupe, From hydrophilicity to hydrophobicity: A critical review: Part I. Wettability and surface behavior, Wood Fiber Sci. 42 (2010) 490–510.

[56] C. Göbl, U. Wolfesberger-Schwabl, Production of solid sustainable energy carriers from biomass by means of torrefaction, Deliverable No. D8.5: Report on test methods and properties of torrefied biomass, 2012. http://rapsodee.mines-albi.fr/IWBTE/co/Accueil.html (accessed November 2, 2016).

[57] P.C.A. Bergman, A.R. Boersma, R.W.R. Zwart, J.H.A. Kiel, Torrefaction for biomass co-firing in existing coal-fired power stations, Energy Cent. Netherlands, Rep. No. ECN-C-05-013, Petten, Netherlands. (2005).

[58] S. Li, J. Lyons-Hart, J. Banyasz, K. Shafer, Real-time evolved gas analysis by FTIR method: An experimental study of cellulose pyrolysis, Fuel. 80 (2001) 1809–1817. doi:10.1016/S0016-2361(01)00064-3.

[59] T. Westover, T. Westover, Tests to Reduce TorreCat TM Technology to Practice Technology to Practice, 2016. doi:INL/EXT-16-38088.

[60] S. Ren, H. Lei, L. Wang, Q. Bu, Y. Wei, J. Liang, Y. Liu, J. Julson, S. Chen, J. Wu, R.

Ruan, Microwave torrefaction of douglas fir sawdust pellets, Energy and Fuels. 26 (2012) 5936–5943. doi:10.1021/ef300633c.

[61] D.K. Shen, S. Gu, A. V. Bridgwater, The thermal performance of the polysaccharides extracted from hardwood: Cellulose and hemicellulose, Carbohydr. Polym. 82 (2010) 39–45. doi:10.1016/j.carbpol.2010.04.018.

[62] L.P. Otwell, M.E. Hittmeier, U. Hooda, H. Yan, W. Su, S. Banerjee, HAPs release from wood drying, Environ. Sci. Technol. 34 (2000) 2280–2283. doi:10.1021/es991083q.

[63] L.E. Arteaga-Pérez, C. Segura, V. Bustamante-García, O. Gómez Cápiro, R. Jiménez, Torrefaction of wood and bark from Eucalyptus globulus and Eucalyptus nitens: Focus on volatile evolution vs feasible temperatures, Energy. 93 (2015) 1731–1741. doi:10.1016/j.energy.2015.10.007.

[64] P. Lestinsky, V. Brummer, D. Jecha, P. Skryja, P. Stehlik, Design of an catalytic oxidation unit for elimination of volatile organic compound and carbon monoxide, Ind. Eng. Chem. Res. 53 (2014) 732–737. doi:10.1021/ie402158c.

[65] M.S. Kamal, S.A. Razzak, M.M. Hossain, Catalytic oxidation of volatile organic compounds (VOCs) – A review, Atmos. Environ. 140 (2016) 117–134. doi:10.1016/j.atmosenv.2016.05.031.

[66] M. Hagner, E. Kuoppala, L. Fagerns, K. Tiilikkala, H. Setala, Using the copse snail Arianta arbustorum (Linnaeus) to detect repellent compounds and the quality of wood vinegar, Int. J. Environ. Res. 9 (2015) 53–60.

[67] Y. Baimark, N. Niamsa, Study on wood vinegars for use as coagulating and antifungal agents on the production of natural rubber sheets, Biomass and Bioenergy. 33 (2009) 994–

998. doi:10.1016/j.biombioe.2009.04.001.

[68] K. Tiilikkala, L. Fagernäs, J. Tiilikkala, History and Use of Wood Pyrolysis Liquids as Biocide and Plant Protection Product, Open Agric. J. 4 (2010) 111–118.

[69] J. Mu, Z. Yu, W. Wu, Q. Wu, Preliminary study of application effect of bamboo vinegar on vegetable growth, For. Stud. China. 8 (2006) 43–47.

[70] K. Orihashi, Y. Kojima, M. Terazawa, Deterrent effect of rosin and wood tar against barking by the gray-sided vole (Clethrionomys rufocanus bedfordiae), J. For. Res. 6 (2001) 191–196.

[71] T.P. Vispute, G.W. Huber, Production of hydrogen, alkanes, and polyols by aqueous phase processing of wood-derived pyrolysis oils, Green Chem. 11 (2009) 1433. doi:10.1039/b912522c.

CHAPTER 4

GRINDABILITY OF TORREFIED WOOD CHIPS AND WOOD PELLETS[1]

[1] Manouchehrinejad M, Giesen I Van, Mani S. Submitted to Fuel Processing Technology, (2018).

Abstract

Torrefaction process improves the grindability of raw biomass by transforming its fibrous structure to more brittle and friable, coal-like material. Torrefied biomass are more desirable feedstock for co-firing applications, especially in existing coal-fired power plants. Therefore, measuring the grindability and the specific energy consumption are critical for understanding the comminution behavior of torrefied biomass, designing, and selecting appropriate milling equipment. In this study, the effect of torrefaction temperature on the specific grinding energy consumption and the grindability of torrefied wood pellets and wood chips was investigated and compared with coal. The applicability of three well-known grinding equations (Kick, Rittinger and Bond) was studied for the torrefied biomass using a knife mill. The specific grinding energy of both torrefied wood chips and pellets was linearly decreased with increased torrefaction temperature over a range of 250-290°C. The Rittinger's model was the best-fitted for both wood chips (R^2=0.72-0.90) and wood pellets (R^2=0.67-0.76). When the intercepts were considered, the Rittinger's and Bond's equations were well fitted with the experimental data (R^2=0.79-0.99) for all torrefied biomass. The grindability of torrefied biomass was measured using the Hardgrove Grindability Index (HGI) and the International Organization for Standardization (ISO) grindability index. The relationship between the Bond Work Index (BWI), based on the Bond's theory and HGI was developed for wood chips and wood pellets. The BWI decreased with an increase in torrefaction temperature contrary to HGI index. The developed grindability parameters for torrefied biomass can be used for modeling and selecting suitable milling equipment.

Keywords: Grindability, Specific energy consumption, Torrefied biomass pellet, HGI, BWI.

Introduction

Lignocellulosic biomass is one of the most promising renewable energy resources with a potential to reduce GHG emissions, especially NO_X and SO_X emissions [1]. Biomass can be utilized directly as a solid biofuel for heat and power generation [2] or as a precursor to produce a variety of liquid and gaseous biofuels, biochemicals, and bioproducts [3]. One of the most common uses of biomass is combustion and co-firing with coal to produce heat and power. However, the biomass fuel properties are one of the major hindrances to co-firing with coal for power generation. Despite its low cost and the potential to reduce GHG emissions, the structural heterogeneity and low energy density of biomass over coal will not only reduce the output thermal energy and but also require additional equipment to preprocess biomass in the existing coal power plants [4–6]. The low bulk density and hygroscopicity of raw biomass poses additional challenges during handling, transport and storage operations.

Thermal pretreatment by torrefaction has improved the thermal and physical properties of biomass with reduced moisture content, increased calorific value, improved hydrophobicity and grindability [7–12]. Torrefaction is a process of thermal treatment of biomass in the temperature range of 200-300°C under an inert condition at the atmospheric pressure. Biomass mainly consisted of cellulose, hemicellulose, lignin and inorganic ash. During torrefaction, biomass (mainly hemicellulose fraction) is thermally decomposed; the fibrous structure of the biomass is broken to some extent, to produce a brittle and coal like solid fuel. Nevertheless, the treated biomass still needs to be densified due to its low bulk density for improved handling, transport and storage [8,13–15]. Torrefied biomass pellets with properties similar to coal can be used as fuels in several heating systems, smaller boilers, or industrial boilers, but they can also be best suited for co-firing with coal [16]. The torrefied biomass could also be used as a feedstock for other

conversion processes such as gasification [17], pyrolysis [18] enzymatic reaction, and bioethanol production [19]. The improved properties of torrefied pellets increase the rate of co-firing compared to that of raw pellets with a higher reduction in GHG emissions [20]. If torrefied biomass can be used in the existing coal boilers, the grindability of torrefied biomass needs to be determined.

Grindability of a material relates to the rate of energy required for grinding from an initial size to a specific particle size distribution. It may also be referred to as the resistance of a material to grinding to a certain size [21]. Comminution of biomass plays a crucial role in all biomass conversion processes. The biomass particle shape and size are modified through size reduction while increasing the bulk density and energy density (with respect to volume) of the biomass [22]. The increased surface area of the particles minimizes mass and heat transfer limitations and improves the efficiency of conversions [23–25]. A proper particle size distribution significantly affects the combustion function by increasing the flame stability and biomass burnout as well as reducing the CO emissions [26]. In addition, various particle size or particle size distribution are required for different processes [22]. For instance, biomass particle size smaller than 2 mm is appropriate for fast pyrolysis [27] and fluidized bed reactors [28], while circulating fluidized bed reactors work with up to 6 mm particles [28]. The industrial standard cut-size for pulverized coal in power generation plants is in the range of 75 μm [29], and this number for biomass has been proposed to be below 1000 μm [30], which provides the similar residence time to pulverized coal during complete combustion [31].

The general relation for energy consumption of grinding a specific material and the product size has been proposed by Walker et al. 1937 [32], and other relationships proposed by Rittinger [33], Kick [34], and Bond [35,36], which are collectively known as comminution laws. In general,

the comminution laws were developed for hard, brittle and friable material like coal, and were widely applied by mineral and food industries [37,38]. The grinding theories have been extensively used for defining a grindability index, which is commonly used for designing the grinding equipment [39].

Grinding of raw biomass has been investigated in several studies [22,25,40,41]. Also, the grinding of torrefied biomass at various torrefaction temperatures have been explored [8,42–46]. It has been proven that the energy required for grinding of biomass depends on its moisture content, structural compositions, initial and final particle sizes, the feed rate, and the grinder parameters [40]. Although biomass can be utilized directly after the initial size reduction, it is usually densified and transported to a biorefinery or bioenergy plants. Raw biomass is usually pre-ground to particles smaller than 2 mm size for densification (e.g., pelletizing). Hence, the grinding energy of compressed pre-ground particles in the wood pellets and torrefied wood pellets could be lower than that of uncompressed biomass. However, in order to estimate the energy consumption and to design the milling devices, more operating data and specific grindability parameters are required. The existing milling facilities in power generation plants are adapted with coal and with a certain range of grindability. Some of the standard tests for grindability measurement of coal include Hardgrove Grindability Index (HGI) test [29] and Bond Work Index (BWI) test [36], but, no standard grindability test has been fully developed yet for biomass or torrefied biomass. The essential difference between the fibrous and anisotropic nature of biomass and friable and the brittle nature of coal casts doubts on using the similar grindability indices for both materials. Some of the grindability indices proposed for biomass through specific methods include Modified Hardgrove Grindability Index (HGI) [39], Resistance to Impact Milling (RIM) [47], Hybrid Work Index [48], ISO grindability [49], and Specific Grinding Energy (SGE) [50]. The first three tests

were proposed in accordance with grindability methods for brittle materials, mainly for uncompressed biomass, and based on the pre-crushing requirements. The ISO grindability has been specifically developed for analyzing the grindability characteristics of uncompressed biomass materials which simply relates to the specific energy required for size reducing the biomass from a defined initial size (< 8 mm) to the final size (<2 mm) [49]. The latter procedure (SGE), was proposed to obtain the required specific energy for grinding the biomass pellet (densified material) with a top particle size of 1 mm (1000 μm) as a single parameter, which was investigated within three different mill types (impact mill, cutting mill, and hammer mill) [50].

The grinding behavior of wood pellets and torrefied wood pellets is required for defining and differentiating the characteristics of torrefied biomass [41,50,51]. Williams et al. investigated the applicability of BWI and HGI for raw and torrefied wood chips and wood pellets [51,52]. They also studied the particle size and shape and energy consumption of grinding different biomass pellets through different milling equipment including planetary ball mill, Bond ball mill, knife mill, and Ring-roller mill [53]. While a number of studies have been carried out on the grindability of different types of treated and non-treated biomass with various industrial mills [8,39,41,48,50,51], few studies in the literature investigated the applicability of comminution laws (Kick's, Rittinger's, and Bond's equations) for raw biomass materials [22,41]. Since the torrefaction process transforms the fibrous biomass to more brittle structure, comminution equations for brittle material might also describe the grinding behavior of treated biomass and consequently, the grindability indices as similar to coal. The torrefaction parameters, specifically torrefaction temperature, would also impact the grinding energy and applicability of existing grindability indices. The grindability properties of raw or thermally treated biomass is critical for not only knowing the grinding energy consumption but also determining the design parameters

required for selecting or designing milling equipment. They can also be used for modeling the grinding operations in the process simulation platform such as Aspen Plus.

The objectives of this study were: 1) to determine the effect of torrefaction temperature on the specific grinding energy of wood chips and wood pellets, 2) to investigate the applicability of comminution equations for grinding of treated (torrefied) and un-treated wood chips and wood pellets, 3) to develop the grindability indices of torrefied material based on the Hardgrove (HGI) and Bond (BWI) methods, and compare with ISO grindability analysis.

Materials and methods

Materials

The wood chips and wood pellets produced from southern yellow pine were acquired from the commercial pelleting plant in the Southeastern U.S. The moisture content of wood chips and pellets as received were 7.9%±0.02 and 6.2%±0.32, respectively, measured in accordance with the ASABE standard S358.3 MAY 2012 [54]. The samples were packed in the airtight container and stored at room temperature. Torrefaction experiment was carried out using a lab scale batch torrefaction reactor with a reactor capacity of 1.5 kg of feedstock. Nitrogen gas was used as the inert gas with a flow rate of 2 L min^{-1} at atmospheric pressure. The reactor was heated at 3°C min^{-1} to the torrefaction temperature and then kept for 30 min residence time. Three temperatures (250, 270, and 290°C) for wood chips and four temperatures (230, 250, 270, and 290°C) for wood pellets were tested in this study. Preliminary tests showed that no or minor difference on the fuel properties was observed between raw wood chips and 230°C torrefied wood chips. So, experiments performed only in the more favored torrefaction temperature range (i.e., 250 to 290°C) for wood chips. On the other hand, the low temperature torrefaction (i.e., 230°C) for wood pellets was investigated to check the possible impact of ground particles present in the pellets on grindability.

After each run, the torrefied materials were sealed and stored at room temperature for further analysis.

The bulk density of the raw and torrefied materials was measured based on the standard method [55]. The proximate analysis (ash, volatiles, fixed carbon and moisture content) was conducted according to the ASTM D 7582 procedure using a micro thermo-gravimetric analyzer (TGA701, LECO Corporation, St. Joseph, MI) [56]. The dry basis amounts of ash and volatile matters were measured whereas the fixed carbon was calculated by subtraction. The higher heating value of the raw and torrefied materials was measured using an oxygen bomb calorimeter (IKAC 2000, IKA Works, Inc., NC) based on the standard test method ASTM D5865 [57].

The dimensions of at least fifteen pellets were used to define the average pellet diameter. For defining the average diameter of wood chips, a batch of wood chips was separated into four groups of chunks, bigger chips, smaller chips, and shreds. The total weight and dimension (length, width, and thickness) of wood chips from each group were measured. The average characteristic size was calculated based on the summation of the average cubic root of each group times the weight fraction.

Grinding experiment

The wood chips and pellets were ground using a laboratory heavy-duty knife mill (Retsch SM 2000, Germany). The knife mill used in this study consisted of a cutting blade rotor (1690 rpm, 60 Hz), which was powered by a 1.5 kW electric motor. The instantaneous power consumption (W) during the grinding experiment was recorded every two seconds using a data logger and transferred through a multi-function transducer (CR Manetics Inc., MO) attached with a computer. Three different screen sizes 0.5, 1, and 2 mm were used in the knife mill to classify the ground materials for each sample studied.

Preliminary tests were conducted to specify the amount of biomass samples required for each run in order to consistently operate the grinder. The relevant time of grinding and the efficiency of grinding was estimated by measuring the throughput rate. Once the proper amount of biomass sample for grinding was determined, the grinding experiment with each screen size was performed in triplicate. The grinder motor was equipped with a circuit breaker to avoid motor overloading. The net specific energy for grinding of each sample was calculated by integrating the power-time curve divided by the mass of the output material and reported in kWh Mg^{-1}. Careful attention was paid to subtracting the base power from the instantaneous power consumption data before the integration. Prior to each trial, the mill was let to cool down and return to the room temperature. The throughput of the knife mill ranged from 3 to 10 kg h^{-1} for raw materials and 4 to 32 kg h^{-1} for torrefied materials.

Particle size distribution

Particle size distribution of the ground biomass was determined by sieving the material in accordance with ANSI/ASAE standard S319.3 [58]. One hundred grams of each ground sample was placed in a stack of sieves arranged from the largest to the smallest opening. The sieve sizes were 1250 (only for 2 mm runs), 800 (for 1 and 2 mm runs), 500 (for 1 and 2 mm runs), 315, 250, 200, 160, 125, 100, and 63 µm. Sieving experiment was conducted on a vibratory sieve shaker (Retsch AS200, Germany). A 10-minute sieve shaking time at 60 Hz was sufficient for the samples. The particle size distribution experiment was repeated three times for each ground sample. After sieving, the mass retained on each sieve was weighed, and the particle size distribution, geometric mean diameter (dgw), geometric standard deviation (Sgw) of particle diameter, and 80% passing size of the product (P80) were determined.

Size reduction parameter in accordance with comminution theories

The relationship between the energy consumption for grinding and the product particle size was generally proposed by Walker et al. [32] who assumed that the net specific energy for size reduction E, is the function of the characteristic dimension (x) of the product, the exponent n, and a constant K related to the material:

$$dE = -K\ {}^{dx}/_{x^n} \quad (1)$$

This general equation was further developed, and three famous size reduction theories of Rittinger, Kick, and Bond were established based on different exponent values (Eq. 1 to 3) [34,35].

Kick's Theory: $E = K_K . Ln\left({}^{xf}/_{xp}\right)$ n=1, x > 50 mm (2)

Rittinger's Theory: $E = K_R . \left({}^{1}/_{xp} - {}^{1}/_{xf}\right)$ n=2, x < 0.05 mm (3)

Bond's Theory: $E = K_B . ({}^{1}/_{\sqrt{xp}} - {}^{1}/_{\sqrt{xf}})$ n=1.5 0.05<x<50 mm (4)

In this study, the specific energy of grinding (kWh Mg^{-1}) for each sample was plotted versus $Ln(xf/xp)$, $(1/xp - 1/xf)$, and $(1/\sqrt{xp} - 1/\sqrt{xf})$ to investigate the applicability of Kick's, Rittinger's, and Bond's theory, respectively. The xf (μm) and xp (μm) refer to the average size of the feed particles and the product particle size in, respectively. In the Bond's theory xp refers to the infinite size that 80% of particles pass through it (P80).

Grindability indices

Volumetric Hardgrove Grindability Index (HGI)

The Hardgrove Grindability Index (HGI) test [29] to define the grindability of the specific mass of brittle materials like coal, was developed based on Rittinger's theory [59]. However, it has been shown that milling is a volumetric process; hence the constant mass which implies the smaller volume for denser fuels fails to represent the direct comparison between fuels [39]. Thus, the

volumetric Hardgrove Grindability Index (HGI) test was introduced by Bridgeman et al. [39] for bulkier material like biomass.

Primarily, the calibration curve was obtained according to the modified volumetric HGI test[39]. Four types of standard reference ground coals were purchased from Preiser Scientific, U.S. with known HGI (38, 56, 88, and 101) and sieved using 1.18 mm and 600 μm size sieves. The 50 cm^3 of each sample between the two sieve sizes was measured by a cylinder with an accuracy of $\pm 0.1\ cm^3$ and weighted as Wv with an accuracy of $\pm 0.01g$. The sample then was placed into a stainless steel grinding bowl in a Hardgrove Grindability Index Tester (Preiser Scientific Z90-9300-01, U.S.) and eight balls were put on the sample evenly and covered by the upper grinding cap. The bowl was placed into the machine and sample was ground for 60 revolutions under a known force (29 kg). After grinding, the sample was removed and sieved using a 75 μm sieve size for 5 minutes. The two parts after sieving were weighted. The mass of oversize was designated as Wo and the passing fraction as Wp. If the loss of sample (Wv –Wo –Wp) was greater than 0.5g, the test was abandoned [4]. The m% was calculated using Eq. 5:

$$\mathrm{m\%} = \frac{W_v - W_0}{W_v} \tag{5}$$

Each test was repeated three times for every standard reference coal sample, and the m% values were plotted versus the HGI value for the calibration curve (Figure 4-1).

After obtaining the calibration curve, the HGI value of the biomass was evaluated. The samples need to be pre-crushed for HGI test [29]. In this experiment, the ground sample from 2 mm knife mill screen was used for HGI test and sieved with 1.18 mm and 600 μm sieve sizes. The grinding process for the HGI test was carried out following the same procedure applied for calibration and repeated three times for each sample. The HGI value for the biomass samples was derived from the calibration curve.

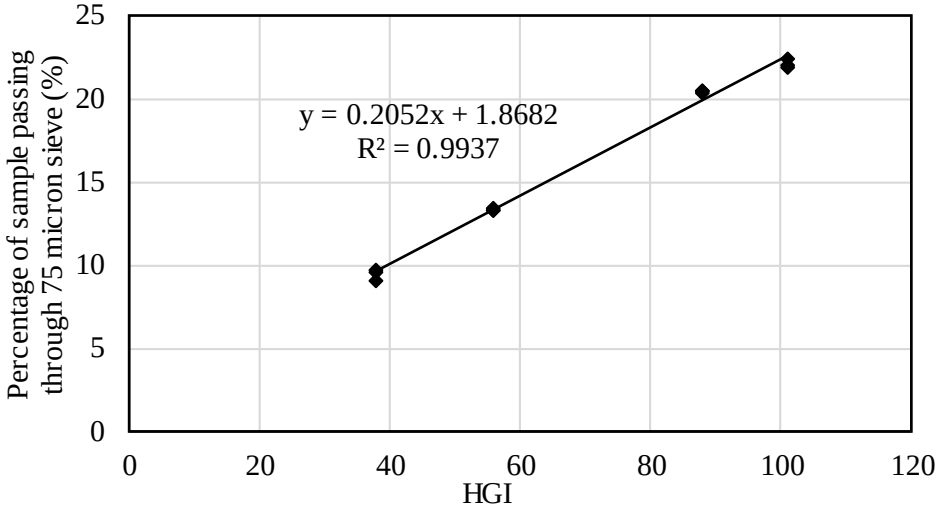

Figure 4-1. HGI calibration curve

Bond work index (BWI)

The other well-known grindability index which has been extensively applied in the mineral industry and is valid for coal is Bond Work Index (BWI). The BWI is defined as the specific energy (kWh Mg^{-1}) required for grinding the material from the infinite size to that 80% of particles passing 100 μm sieve [60]. Bond redefined his theory to rather be an empirical relationship, which is commonly written as Eq.6:

$$W = 10.BWI.(1/\sqrt{P_{80}} - 1/\sqrt{F_{80}}) \quad (6)$$

Where W (kWh Mg^{-1}) is specific required energy for grinding, F_{80} and P_{80} are the 80% passing size of the feed and product (μm), respectively, and BWI (kWh Mg^{-1}) is the Bond Work Index that is the specific characteristics of material representing its resistance to the grinding. The BWI index test has been standardized through a rotary ball mill and widely used for brittle materials [36]. In the original procedure, a horizontal axis rotating ball mill was used, and the number of revolutions counted to determine the specific input energy and the relevant equation was proposed to calculate

the BWI (kWh Mg $^{-1}$). However, limited studies have been reported for grinding fibrous biomass with other types of mills such as planetary ball mill [48] and hammer mill [41].

In this study, the Bond Work Index (kWh Mg $^{-1}$) was measured based on the energy data obtained through grinding of each type of biomass with knife mill at different screen sizes. The average feed wood chips and wood pellet size was used as F80.

ISO grindability index

The grindability of biomass for uncompressed biomass was defined in accordance with Rittinger's theory[49]:

$$\gamma = ESP/(1/xp - 1/xf) \quad (7)$$

Where γ is a grindability index (mm kWh Mg $^{-1}$), and ESP is the specific energy for grinding (kWh Mg $^{-1}$). For ISO grindability, the average feed wood chips and wood pellet size was used as xf (mm) and the median value of the final particle size dgw (mm) used for xp.

Statistical analysis

The effects of torrefaction temperature and knife mill screen size for wood chips and wood pellets on the specific energy consumption and the particle size were analyzed using R Studio statistical software package version 3.2.2. A two-way factorial analysis of variance (ANOVA) test was performed on specific grinding energy, geometric mean diameter (dgw), geometric standard deviation (Sgw) of particle diameter, 80% passing size of the product (P80), and ISO grindability indices of all combination of torrefaction temperature and screen size samples. If the change in torrefaction temperature or screen size was significant ($P<0.05$), we conducted the Duncan multiple comparison method to determine the exact effective layer on the means.

Result and discussion

The physical and fuel properties of the raw and torrefied wood chips and wood pellets are shown in Table 4-1. As the torrefaction temperature increases, the fixed carbon increased, and volatile matters values decreased, approaching to the values of coal samples. The moisture content and ash content of the torrefied biomass was considerably lower than that of coal samples. Torrefaction reduces the bulk density of both wood chips and wood pellets while increasing the energy content. Therefore, torrefied wood chips need to be densified to increase the volumetric energy density and to improve efficient transport and storage. However, the volumetric energy density for torrefied wood pellets was comparable with that of coal. Figure 4-2 shows the initial and ground samples from different knife mill screen sizes. The specific energy consumption for grinding and particle sizes of torrefied wood chips and wood pellets are given in Table 4-2. A significant reduction in grinding energy was observed for the torrefied biomass compared to that of raw biomass (control) for both the wood pellets and wood chips as reported elsewhere [42,44–46]. The ANOVA results given in Table 4-3 indicated that the torrefaction temperature and the screen size significantly changed the specific grinding energy and the ground particle size. In this study, the required grinding energy for torrefied wood chips at 250°C was reduced by 90% compared to that of the untreated wood chips. Further increase in the torrefaction temperature decreased the energy consumption for both torrefied pellets and chips.

There was no significant difference between the specific grinding energy of the torrefied wood chips at 270°C and 290°C. The specific grinding energy of the torrefied pellets at 230°C was 60% lower than that of the untreated pellets, and it dropped by more than 80% for torrefied pellets at 250°C. The energy consumptions of grinding of torrefied pellets at 270°C and 290°C were only slightly lower than that of 250°C torrefied pellets and were not statistically different ($P<0.05$).

Table 4-1 Fuel properties of treated (torrefied) and un-treated of both densified (pellet) and un-densified pine wood biomass and two coal samples.

	Proximate analysis (%db) [a]			Moisture [a]	Calorific value HHV [a]	Bulk density [c]	Volumetric energy density [d]
	Ash	Volatile	Fixed carbon	(%wb)	(MJ kg^{-1})	(kg m^{-3})	(GJ m^{-3})
Wood chips							
Ctrl. (un-treated)	0.68 (0.02)	81.01 (0.11)	18.31 (0.08)	7.91 (0.02)	20.42 (0.46)	238.06 (5.28)	4.86
T250	0.77 (0.02)	75.29 (0.22)	23.94 (0.2)	1.34 (0.09)	21.83 (0.10)	221.04 (2.21)	4.83
T270	0.82 (0.14)	72.75 (0.27)	26.43 (0.3)	1.23 (0.18)	23.20 (0.39)	201.26 (2.70)	4.67
T290	0.82 (0.03)	63.57 (0.09)	35.62 (0.1)	1.44 (0.06)	26.41 (0.13)	182.3 (5.40)	4.81
Wood pellets							
Ctrl. (un-treated)	0.70 (0.02)	80.26 (0.11)	19.05 (0.09)	6.22 (0.32)	19.57 (0.41)	669.14 (18.36)	13.10
T230 [b]	0.82 (0.05)	78.94 (0.18)	20.23 (0.2)	1.74 (0.02)	21.38 (0.83)	644.63 (7.67)	13.78
T250	0.83 (0.05)	77.37 (0.1)	21.82 (0.09)	1.45 (0.02)	22.05 (0.08)	634.85 (5.71)	14.00
T270	0.90 (0.05)	69.63 (0.14)	29.47 (0.16)	1.52 (0.03)	22.97 (0.85)	554.93 (2.78)	12.75
T290	1.1 (0.05)	59.56 (0.25)	39.34 (0.2)	1.27 (0.02)	27.10 (0.56)	361.70 (1.1)	9.80
Bituminous coal Illinois#6, DECS-24[e]	11.60	35.40	39.70	28.20	28.20	590-676[g]	16.6-22
Subbituminous PRB [f]	5.19	30.72	34.94	29.15	17.00	-	-

a Number enclosed in the parenthesis are standard deviations with n =3.
b T#: Torrefied at #°C. e.g., T230: torrefied at 230°C.
c Number enclosed in the parenthesis are standard deviations with n =5.
d Volumetric energy density was calculated by the product of bulk density and calorific value of biomass.
e [61] Derived from Penn-State Coal Bank.
f [5]
g [62]

Figure 4-2. Wood chips, wood pellets and ground samples of wood pellets through screens sizes of 2 mm, 1 mm, and 0.5 mm, a) untreated, (b) T230, (c1) T250, d) T270, e) T290. The torrefied wood chips at 230 were not provided.

Table 4-2 Specific grinding energy and particle size distribution data of ground samples.

		Initial average size (mm)[ii]	Screen size (mm)	Specific grinding energy (kWh Mg^{-1})		iii, iv, v, vi dgw (mm)		Sgw (mm)		P80 (mm)	
Wood chips	Ctrl	9	2	353.53 (23.36)	aA	0.60 (0.01)	aA	0.50 (0.01)	aA	1.34 (0.01)	aA
			1	405.78 (1.96)	aB	0.53 (0.01)	aB	0.42 (0.01)	aB	0.99 (0.00)	aB
			0.5	1073.75 (82.07)	aC	0.26 (0.01)	aC	0.17 (0.02)	aC	0.61 (0.01)	aC
	T250 [i]	8.52	2	32.08 (4.16)	bA	0.33 (0.01)	bA	0.39 (0.01)	bA	1.02 (0.02)	bA
			1	45.17 (6.26)	bB	0.27 (0.00)	bB	0.31 (0.00)	bB	0.82 (0.01)	bB
			0.5	116.39 (14.51)	bC	0.17 (0.05)	bC	0.15 (0.02)	bC	0.41 (0.01)	bC
	T270	8.22	2	16.32 (2.40)	cA	0.26 (0.01)	cA	0.36 (0.01)	cA	0.96 (0.01)	cA
			1	28.79 (2.42)	cB	0.20 (0.00)	cB	0.26 (0.00)	cB	0.74 (0.01)	cB
			0.5	60.94 (4.03)	cC	0.12 (0.00)	cC	0.10 (0.00)	cC	0.31 (0.01)	cC
	T290	7.85	2	12.85 (3.14)	cA	0.23 (0.00)	dA	0.34 (0.01)	dA	0.95 (0.01)	dA
			1	20.39 (2.58)	cB	0.17 (0.00)	dB	0.23 (0.00)	dB	0.71 (0.01)	dB
			0.5	43.02 (5.23)	cC	0.09 (0.00)	dC	0.09 (0.00)	dC	0.22 (0.00)	dC
Wood pellets	Ctrl	6.51 (0.18)	2	72.53 (1.56)	aA	0.50 (0.03)	aA	0.40 (0.02)	aA	1.14 (0.03)	aA
			1	67.04 (6.05)	aB	0.43 (0.02)	aB	0.36 (0.03)	aB	0.95 (0.06)	aB
			0.5	327.22 (10.48)	aC	0.23 (0.03)	aC	0.17 (0.02)	aC	0.45 (0.00)	aC
	T230	6.22 (0.06)	2	20.47 (2.90)	bA	0.44 (0.01)	bA	0.39 (0.02)	aA	1.05 (0.05)	bA
			1	30.82 (2.81)	bB	0.39 (0.01)	bB	0.34 (0.00)	aB	0.91 (0.01)	bB
			0.5	146.10 (12.77)	bC	0.22 (0.03)	bC	0.17 (0.01)	aC	0.44 (0.00)	bC
	T250	6.16 (0.07)	2	9.06 (0.58)	cA	0.37 (0.03)	cA	0.36 (0.04)	bA	1.00 (0.00)	cA
			1	14.84 (1.47)	cB	0.31 (0.01)	cB	0.29 (0.01)	bB	0.81 (0.01)	cB
			0.5	62.20 (0.95)	cC	0.17 (0.00)	cC	0.14 (0.00)	bC	0.41 (0.00)	cC
	T270	5.95 (0.70)	2	7.71 (0.91)	cA	0.38 (0.01)	cA	0.36 (0.00)	bcA	0.95 (0.00)	dA
			1	15.5 (2.52)	cB	0.31 (0.01)	cB	0.27 (0.02)	bcB	0.77 (0.03)	dB
			0.5	50.76 (5.63)	cC	0.17 (0.00)	cC	0.14 (0.00)	bcC	0.40 (0.00)	dC
	T290	5.68 (0.16)	2	4.24 (1.08)	dA	0.36 (0.01)	cA	0.33 (0.00)	cA	0.88 (0.01)	dA
			1	10.84 (2.15)	dB	0.31 (0.01)	cB	0.27 (0.01)	cB	0.78 (0.02)	dB
			0.5	34.00 (4.90)	dC	0.16 (0.02)	cC	0.14 (0.00)	cC	0.41 (0.01)	dC

i) T#: Torrefied at #°C. e.g., T250: torrefied at 250°C.

ii) This value was used as F80. Number enclosed in the parenthesis are standard deviations with n =15 for pellets. The average size of wood chips (section 2.1) was used as the initial average diameter.

iii) Number enclosed in the parenthesis are standard deviations with n =3.

iv) Geometric mean diameter (dgw), geometric standard deviation (Sgw), and 80% passing size (P80).

v) a-d: For wood chips or wood pellets, the same alphabets (a-d) are not significantly different (α=0.05) for comparing different torrefaction temperatures.

vi) A-C: For woodchips or wood pellets, the same alphabets (A-C) are not significantly different (α=0.05) for comparing knife mill screen sizes.

Table 4-3 ANOVA results table for specific grinding energy, dgw, Sgw, P80, ISO grindability indices of wood chips and wood pellets.

		Specific grinding energy				dgw				Sgw				P80				ISO grindability			
		Df	Mean Sq	Pr(>F)		Mean Sq	Pr(>F)			Mean Sq	Pr(>F)			Mean Sq	Pr(>F)			Mean Sq	Pr(>F)		
Wood chips	T	3	7.32E+05	2.20E-16	***	1.64E-01	2.20E-16	***		3.63E-02	2.20E-16	***		1.61E-01	2.20E-16	***		1.34E+05	2.20E-16	***	
	SC	2	1.76E+05	2.20E-16	***	1.19E-01	2.20E-16	***		2.29E-01	2.20E-16	***		1.61E+00	2.20E-16	***		9.95E+02	3.55E-04	***	
	(T×SC)	6	1.05E+05	2.20E-16	***	9.45E-03	1.44E-11	***		2.36E-03	2.41E-09	***		1.11E-02	2.20E-16	***		5.76E+02	3.49E-04	***	
	Res.	24	6.35E+02			2.25E-04				9.10E-05				9.00E-05				8.80E+01			
Wood pellets	T	4	2.99E+04	2.20E-16	***	2.16E-02	4.53E-15	***		7.74E-03	1.27E-09	***		3.99E-02	6.65E-15	***		3.37E+03	2.20E-16	***	
	SC	2	4.89E+04	2.20E-16	***	1.91E-01	2.20E-16	***		1.85E-01	2.20E-16	***		1.36E+00	2.20E-16	***		1.34E+03	2.92E-16	***	
	(T×SC)	8	9.22E+03	2.20E-16	***	7.47E-04	3.00E-02	*		7.42E-04	2.65E-02	*		6.13E-03	4.41E-07	***		3.31E+02	2.08E-13	***	
	Res.	30	2.70E+01			2.93E-04				2.83E-04				5.60E-04				9.10E+00			

T: temperature, SC: Screen size, T x SC: Temperature and Screen interaction. Res: Residuals.

Significant codes: Pr (>F) '***' 0.001 '**' 0.01 '*' 0.05 '.' 0.1

A similar reduction in grinding energy after torrefaction of biomass has been reported in the literature [8,63]. Lower energy consumption could reduce the size reduction expenses by improving the milling capacity by 7.5 to 15 times depending on the different torrefaction conditions [63]. Thermal decomposition of hemicellulose during biomass torrefaction and softening of lignin caused the weakening of the viscoelasticity of woody cell wall that influences the grindability of biomass [64].

The relationship of specific grinding energy consumption and torrefaction temperature within the range of torrefaction (250-290°C) is depicted for both torrefied chips and pellets in Figure 4-3. The reduction in grinding energy for wood chips with increasing torrefaction temperature was almost linear for all the screen sizes. Phanphanich and Mani [8] found a linear relationship between specific energy consumption for grinding torrefied wood chips using a hammer mill (1.5 mm) and torrefaction temperature 230 to 290°C ($R^2 > 0.9$). In case of torrefied wood pellets, despite a strong linearity of the specific grinding energy versus torrefaction temperature for torrefied pellets with the smallest screen size (0.5 mm), no considerable change in energy consumption was found between different torrefaction temperatures versus screen sizes of 1 mm and 2 mm (Figure 4-3). This behaviour could be due to the fact that pellets were made from ground wood chips with a particle size range of 0.6 to 0.8 mm [65]. Consequently, the grinding energy consumption of wood chips was much higher than wood pellets. For torrefaction temperature range of 250 to 290°C, the specific grinding energy of torrefied pellets was in the range of 4 to 62 kWh Mg^{-1}, and 13 to 116 kWh Mg^{-1} for torrefied wood chips. Nevertheless, the grinding energy for pellets through the 0.5 mm screen size was only slightly lower than that of wood chips. In general, the smaller the screen size, the higher was the specific grinding energy consumption. Besides Phanphanich and Mani [8], Repellin et al. [42] investigated the trend of changes in the grinding energy consumption of biomass with

anhydrous weight loss (AWL) through torrefaction at different temperatures (160 to 300°C) and duration (5, 20, 40, and 60 min). They observed that the grinding energy for spruce and beech wood chips decreased rapidly when AWL increased from 0% to 8% [42]. Shang et al. reported the exponential relationship between specific energy requirement of grinding scot pine pellets and total weight loss due to torrefaction (230 to 270°C) [13].

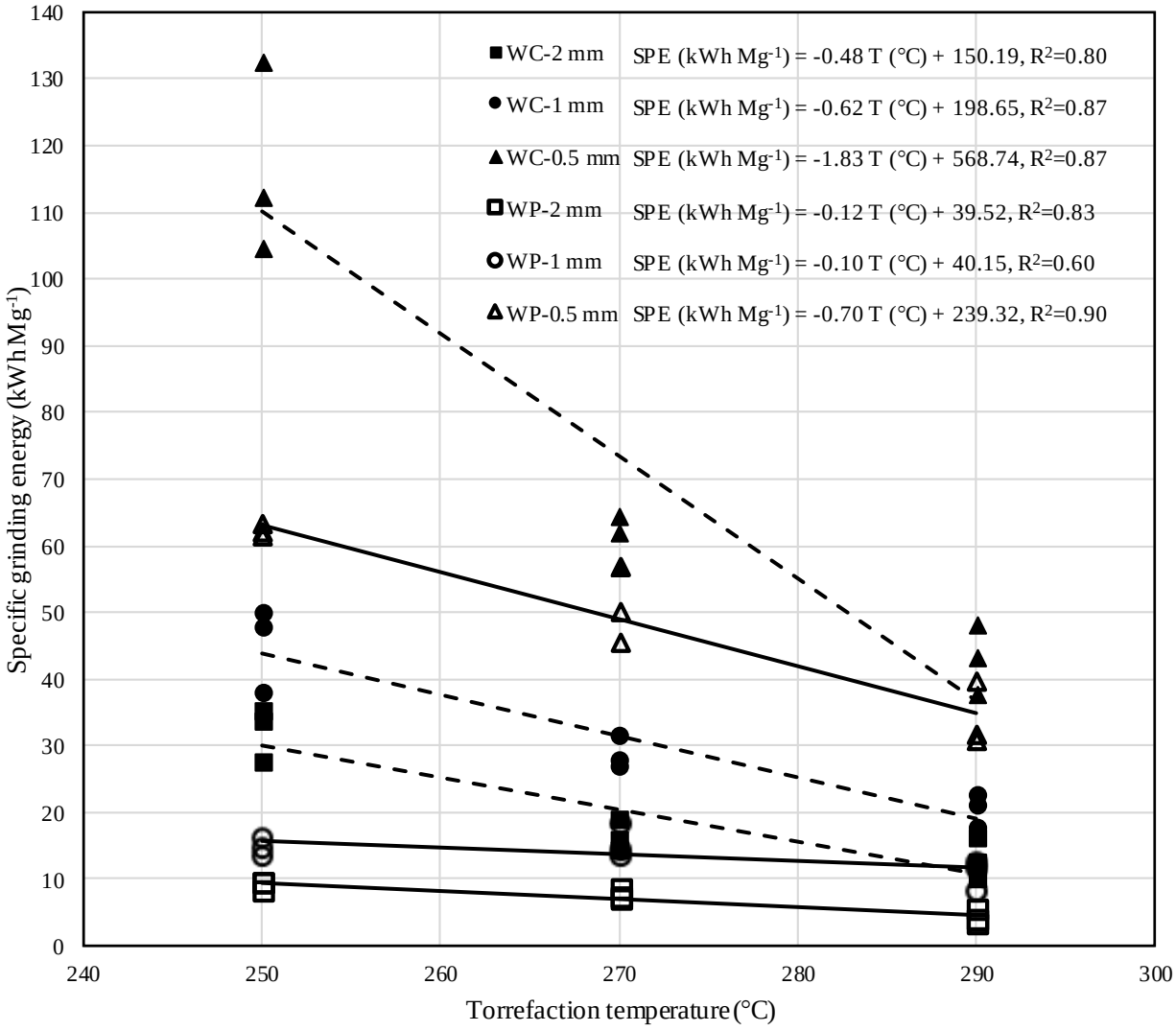

Figure 4-3. Specific energy consumption of grinding biomass through different knife mill screen sizes (2, 1, and 0.5 mm) versus torrefaction temperature (250-290°C), SPE: Specific grinding energy, WC: wood chips, WP: wood pellets.

The variation in the mean particle size of ground biomass at different torrefaction temperature is shown in Figure 4-4 and Table 4-2. Overall, the average particle size of ground biomass decreased significantly with torrefaction temperature for both wood chips and wood pellets (Table 4-3). In case of the raw (untreated) samples, the particle size of ground wood pellets was smaller than that of ground wood chips, which is consistent with the study by Rezaei et al. [66]. However, the mean particle sizes of ground torrefied wood pellets were larger than that of the ground torrefied wood chips. According to Rezaei et al. the ground wood pellets are more round and spherical shape than ground wood chips. It is likely that rounder particles of ground wood pellets preserved its structure during thermal treatment. The rectangular shape of ground wood chips becomes more brittle during thermal decomposition and break easily to smaller particle sizes.

For wood chips, the mean particle size was almost halved at 250°C torrefaction temperature, and it continued to decrease significantly ($P<0.05$) as the torrefaction temperature increased (Figure 4-4a and Table 4-2). The similar trend was observed for uncompressed torrefied materials in the previous studies [8,42,44,46]. The average particle size of torrefied wood pellets was slightly reduced by torrefaction at 230°C compared with control, and then it almost plateaued with increasing torrefaction temperature. Thus, the higher torrefaction temperature (above 250°C) did not show a significant impact on the size of pre-ground particles for wood pellets (Figure 4-4b).

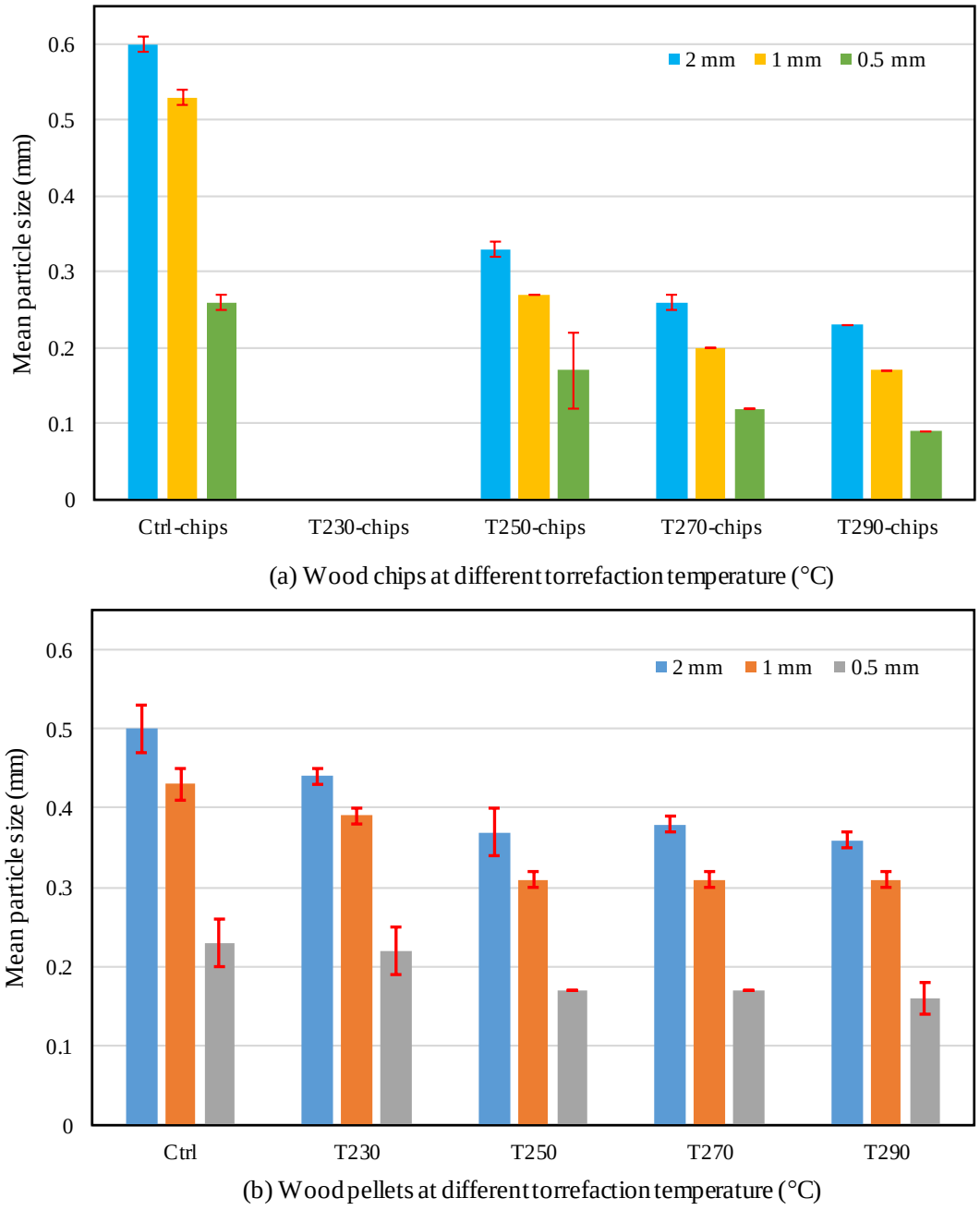

Figure 4-4. Mean particle size of ground samples versus torrefaction temperature, a) wood chips, b) wood pellets. No measurement for T230 wood chips. The error bars represent the standard deviations of mean particle size from three samples.

The particle size distribution and cumulative passing percentage of ground samples through 2 mm screen are depicted in Figure 4-5. The particle size distribution of ground wood pellets was narrower than ground wood chips. The particle size distribution of all wood pellet samples was almost uniform as pellets were made from the same initial particle sizes. However, torrefaction skewed the trend to smaller sizes. The cumulative passing percentage curves for ground wood pellets and ground wood chips with 2 mm screen size, show the wide distribution of particle sizes. The P_{80} for ground torrefied wood pellets through 2 mm screen was slightly smaller than that of torrefied wood chips (Figure 4-5b and Table 4-2).

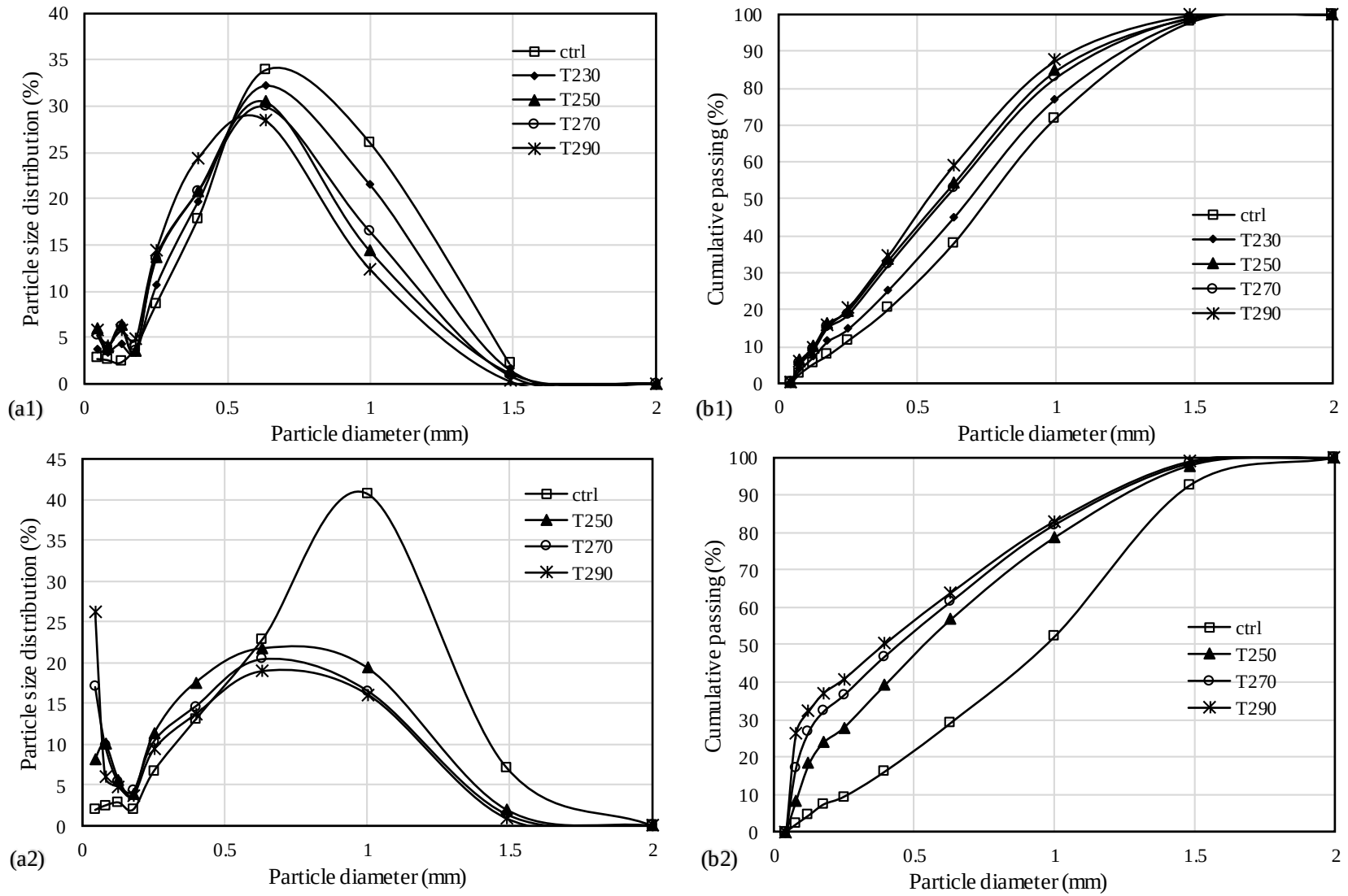

Figure 4-5. Particle size distributions and cumulative passing percentage graphs at various torrefaction-temperature and knife mill screen size of 2mm. (a1) and (b1) ground wood pellet and (a2) and (b2) ground wood chips.

The grinding parameters for each comminution equation for torrefied pellets and torrefied wood chips are given in Table 4-4. In order to test the applicability of each comminution equation, two straight lines were fitted to the grinding data with and without an interception. In case of wood chips fitted exactly with comminution equations (without interceptions), the Kick's theory poorly fitted with the experimental data, while Rittinger's and Bond's equations showed better fitting with the R-square changed from 0.72-0.90 and 0.67-0.90, respectively. The data fitting with considering intercepts showed a higher R-square value for all three equations (Table 4-3). Overall, Rittinger's equation showed a higher fitting accuracy for wood chips, which were in agreement with the finding by Naimi et al. study [22]. Naimi et al. investigated the size reduction of chopped douglas-fir and hybrid willow through knife mill with different screen sizes 2, 4, and 6 mm. They explored the applicability of Kick's, Rittinger's, and Bond's theory and found that none of the theories with the original equation fitted to the experimental data. However when the intercept was considered, Rittinger's equation had the best fit with R^2=0.78 for willow and R^2=0.97 for douglas-fir [22]. The results were very similar for wood pellets as well. Both Rittinger's and Bond's curves showed high R-square value (>0.92) for wood pellets. Among three comminution equations, the Rittinger's equation was best fitted with experimental data for wood pellets. This result further justified the applicability of ISO grindability index for torrefied wood pellets.

Table 4-4 Size reduction parameters for grinding theories [i, ii, iii]

		Kick			Rittinger			Bond	
		Eq. 2	Eq.2 + C [iv]		Eq.3	Eq.3 + C [iv]		Eq. 4	Eq.4 + C [iv]
Wood chips									
Ctrl	K_K	488.09	1969.50	K_R	266657.00	306072.00	K_B	26053.00	38479.00
	C	-	-1976.30	C	-	-110.84	C	-	-344.01
	R^2	0.41	0.95	R^2	0.90	0.92	R^2	0.85	0.96
T250	K_K	48.08	259.76	K_R	16498.00	22716.00	K_B	2673.50	4613.90
	C	-	-298.71	C	-	-28.86	C	-	-55.04
	R^2	0.28	0.84	R^2	0.72	0.79	R^2	0.76	0.94
T270	K_K	24.43	129.23	K_R	6720.60	9454.90	K_B	1284.90	1753.10
	C	-	-159.36	C	-	-17.09	C	-	-15.40
	R^2	0.33	0.97	R^2	0.88	0.97	R^2	0.90	0.98
T290	K_K	14.79	81.26	K_R	3748.50	4948.80	K_B	723.15	855.74
	C	-	-114.29	C	-	-9.41	C	-	-5.54
	R^2	0.29	0.88	R^2	0.84	0.90	R^2	0.90	0.93
Wood pellets									
Ctrl	K_K	133.63	804.36	K_R	63991.00	112690.00	K_B	7320.70	15422.00
	C	-	-848.47	C	-	-152.00	C	-	-214.88
	R^2	0.27	0.91	R^2	0.72	0.92	R^2	0.67	0.97
T230	K_K	56.07	425.31	K_R	25812.00	54617.00	K_B	3099.80	7678.00
	C	-	-472.66	C	-	-95.65	C	-	-122.54
	R^2	0.23	0.98	R^2	0.67	0.98	R^2	0.60	0.99
T250	K_K	22.76	164.44	K_R	8865.20	17646.00	K_B	1262.30	3083.10
	C	-	-193.96	C	-	-36.87	C	-	-51.50
	R^2	0.24	0.96	R^2	0.71	0.98	R^2	0.62	0.99
T270	K_K	19.70	122.13	K_R	7357.60	12822.00	K_B	1046.20	2496.90
	C	-	-139.25	C	-	-23.72	C	-	-41.58
	R^2	0.28	0.97	R^2	0.76	0.98	R^2	0.62	0.98
T290	K_K	13.12	82.58	K_R	4708.40	7953.20	K_B	697.10	1813.50
	C	-	-93.93	C	-	-14.55	C	-	-31.51
	R^2	0.26	0.90	R^2	0.70	0.87	R^2	0.56	0.94

i) The average feed wood chips and wood pellet size was used as xf.

ii) For Kick's and Rittinger's equations, mean particle size (dgw) was used as xp. For Bond's P80 was used as xp.

iii) The K and C coefficients are in kWh Mg^{-1}, and xf and xp are in μm.

iv) Columns refer to the results of fitting data using comminution theories (Kick's, Rittinger's, and Bond's equation) with considering interception (C value).

The ISO grindability, HGI, and BWI indices for raw and treated wood chips and wood pellets are summarized in Table 4-5. The higher ISO index corresponds to higher specific energy requirement for grinding, and it also depended on the initial and final particle size of the sample. The ISO index has been specifically introduced for grinding of uncompressed materials such as wood chips, and it can be applicable to densified materials like wood pellets. The ISO index for both wood chips and wood pellets were decreased with torrefaction temperature of up to 250°C, but it did not significantly change with a further increase in temperature. Also, there was no statistical difference between screen sizes of 1 and 2 mm (Table 4-3). The higher the ISO index, the lower will be the grindability of the material.

The HGI index for wood chips and wood pellets were increased with the increase in the torrefaction temperature. The HGI index for the torrefied wood pellet was similar to one of the coal samples used in the calibration process. The HGI index is a positive value based on the mass of ground material passing the 75 μm sieve. Unfortunately, no meaningful HGI index was achieved for the control and slightly treated biomass (T230), due to their fibrous nature (Table 4-4). The higher the HGI index, the easier to grind the material or the lesser energy required for grinding [52].

The higher value of BWI represents the higher resistant for grinding, as similar to the ISO index. There was an uncertainty about the F80 of the pellet, where the average pellet diameter was used as F80 in accordance with Williams et al. [47] study. The BWI of the raw wood chips (2605 kWh Mg^{-1}) was almost four times higher than that of the raw pellets (732 kWh Mg^{-1}). For the torrefied biomass at 250°C, the ratio of raw wood chips BWI over the torrefied wood chips BWI decreased by two times. Further increase in torrefaction temperature (beyond 270°C) did not change a major reduction in BWI for both torrefied pellets torrefied wood chips. Therefore, the

torrefaction of biomass at the higher temperature (270 °C) generates a uniform brittle material that eliminates the initial particle size effect and represents true grinding behavior of torrefied biomass (Table 4-5).

While the HGI index is usually used in the coal industry, the bond index is also a more common index used by all mineral industries. Therefore, the correlation between HGI and BWI has been proposed in several studies [67,68]. Williams et al. [52] reported a correlation between HGI and BWI for biomass pellets. Since torrefied biomass has the similar characteristic as coal, the correlation between BWI and HGI might be very useful. In this study, despite the limited data points for torrefied wood chips and wood pellets, the following correlations were derived for torrefied wood chips and pellets:

Torrefied wood chips (250 to 290°C): $BWI = 1585.78/HGI^{0.98}$, $R^2 = 0.99$ (8)

Torrefied wood pellets (250 to 290°C): $BWI = 390.84/HGI^{0.48}$, $R^2 = 0.99$ (9)

Although BWI showed a decreasing trend with the increase in HGI, additional experimental data are required to develop a reliable correlation. The HGI and BWI indices, which represents the grindability of different material independent of the initial or final particle sizes may be more applicable to simulate the grinding unit operation than that of the ISO index.

Table 4-5 Grindability indices of torrefied wood pellets and wood chips

	Knife mill screen size (mm)	ISO grindability (mm. kWh Mg^{-1}) [i, ii, iii]		HGI	BWI (kWh Mg^{-1})
Wood chips					
Ctrl	2	233.91 (10.38)	aA	n.a	2605.30
	1	236.16 (3.50)	aA		
	0.5	289.67 (46.73)	aB		
T250	2	11.20 (1.25)	bA	6.3	267.35
	1	12.57 (1.64)	bA		
	0.5	20.36 (4.59)	bB		
T270	2	4.51 (0.68)	bcA	12.5	128.49
	1	6.03 (0.46)	bcA		
	0.5	7.35 (0.66)	bcB		
T290	2	3.07 (0.79)	cA	24	72.32
	1	3.63 (0.48)	cA		
	0.5	4.13 (0.63)	cB		
Wood pellets					
Ctrl	2	39.28 (2.46)	aA	n.a	732.07
	1	30.47 (1.10)	aA		
	0.5	79.84 (10.9)	aB		
T230	2	9.75 (1.34)	bA	n.a	309.98
	1	12.91 (1.57)	bA		
	0.5	33.45 (0.88)	bB		
T250	2	3.61 (0.55)	cA	10.91	126.23
	1	4.91 (0.55)	cA		
	0.5	11.15 (0.14)	cB		
T270	2	3.18 (0.43)	cA	14.43	104.62
	1	5.02 (0.66)	cA		
	0.5	8.74 (0.92)	cB		
T290	2	1.62 (0.43)	cA	36.13	69.71
	1	3.57 (0.72)	cA		
	0.5	5.76 (1.34)	cB		

i) Number enclosed in the parenthesis were standard deviations with n =3.

ii) a-d: For wood chips or wood pellets, the same alphabets (a-d) are not significantly different (α=0.05) for comparing different torrefaction temperatures.

iii) A-C: For woodchips or wood pellets, the same alphabets (A-C) are not significantly different (α=0.05) for comparing knife mill screen sizes.

Conclusion

The grindability of both torrefied wood pellets and wood chips was investigated using a knife mill at different torrefaction temperatures with different screen sizes (2, 1, and 0.5 mm). In general, the specific grinding energy and the mean particle size decreased with an increase in torrefaction temperature (230 to 290°C). The variation of specific grinding energy versus torrefaction temperature (250 to 290°C) followed a rather linear trend for both torrefied wood chips and wood pellets. Rittinger's comminution theory showed the best conformity for both torrefied wood pellets and torrefied wood chips. The calculated Bond Work Index (BWI) for raw wood chips and raw wood pellets were 2605 and 732 kWh Mg^{-1} and were dropped by 90 and 83%, respectively after torrefaction at 250°C. The bond work index of both torrefied pellets and wood chips reached to the same value (about 70 kWh Mg^{-1}) at 290°C. The volumetric Hardgrove Grindability Index (HGI) was applicable only for the torrefied material above 250°C. The relationship between BWI and HGI could be used to simulate the grinding behavior of torrefied biomass.

Acknowledgments

The authors acknowledge and thank the Consortium for advanced Wood-to-Energy Solutions (CAWES) with funding provided by the USDA Forest Service (www.fs.fed.us), the U.S. Endowment for Forestry and Communities (www. usendowment.org), and consortia members. CAWES is a public/private partnership initially formed by the USDA Forest Service, the U.S. Endowment for Forestry and Communities, and a number of innovative private companies and university partners committed to advancing sustainable, scalable, distributed wood-to-energy solutions that stimulate forest restoration and rural economic development.

References

[1] J.S. Tumuluru, J.R. Hess, R.D. Boardman, C.T. Wright, T.L. Westover, Formulation, pretreatment, and densification options to improve biomass specifications for co-firing high percentages with coal, Ind. Biotechnol. 8 (2012) 113–132. doi:10.1089/ind.2012.0004.

[2] U.S. Department of Energy, Combined Heat and Power (CHP) Technical Potential in the United States, (2016) 219. https://www.energy.gov/sites/prod/files/2016/04/f30/CHP Technical Potential Study 3-31-2016 Final.pdf (accessed July 18, 2017).

[3] Sanjay P Mande, Thermochemical conversion of biomass, Renew. Energy Eng. Technol. Princ. Pract. (2009) 705–728. doi:10.1016/S0038-092X(98)00109-1.

[4] D.A. Tillman, E. Hughes, B.A. Gold, Cofiring of biofuels in coal fired boilers: Results of case study analysis, Natl. Renew. Energy Lab., Golden, CO (United States). 1 (1994).

[5] D.A. Tillman, Biomass cofiring: The technology, the experience, the combustion consequences, Biomass and Bioenergy. 19 (2000) 365–384. doi:10.1016/S0961-9534(00)00049-0.

[6] L. Baxter, Biomass-coal co-combustion: Opportunity for affordable renewable energy, Fuel. 84 (2005) 1295–1302. doi:10.1016/j.fuel.2004.09.023.

[7] W.H. Chen, P.C. Kuo, Isothermal torrefaction kinetics of hemicellulose, cellulose, lignin and xylan using thermogravimetric analysis, Energy. 36 (2011) 6451–6460. doi:10.1016/j.energy.2011.09.022.

[8] M. Phanphanich, S. Mani, Impact of torrefaction on the grindability and fuel characteristics of forest biomass, Bioresour. Technol. 102 (2011) 1246–1253. doi:10.1016/j.biortech.2010.08.028.

[9] M.J. Prins, K.J. Ptasinski, F.J.J.G. Janssen, Torrefaction of wood: Part 1. Weight loss kinetics, J. Anal. Appl. Pyrolysis. 77 (2006) 28–34.

[10] D. Chen, J. Zhou, Q. Zhang, Effects of torrefaction on the pyrolysis behavior and bio-oil properties of rice husk by using TG-FTIR and Py-GC/MS, Energy & Fuels. (2014) 140824102646000. doi:10.1021/ef501189p.

[11] J.H. Peng, X.T. Bi, S. Sokhansanj, C.J. Lim, Torrefaction and densification of different species of softwood residues, Fuel. 111 (2013) 411–421. doi:10.1016/j.fuel.2013.04.048.

[12] J.S. Tumuluru, S. Sokhansanj, J.R. Hess, C.T. Wright, R.D. Boardman, A review on biomass torrefaction process and product properties for energy applications, Ind. Biotechnol. 5 (2011). doi:10.1089/ind.2011.0014.

[13] L. Shang, N.P.K. Nielsen, J. Dahl, W. Stelte, J. Ahrenfeldt, J.K. Holm, T. Thomsen, U.B. Henriksen, Quality effects caused by torrefaction of pellets made from Scots pine, Fuel Process. Technol. 101 (2012) 23–28. doi:10.1016/j.fuproc.2012.03.013.

[14] S.H. Larsson, M. Rudolfsson, M. Nordwaeger, I. Olofsson, R. Samuelsson, Effects of moisture content, torrefaction temperature, and die temperature in pilot scale pelletizing of torrefied Norway spruce, Appl. Energy. 102 (2013) 827–832. doi:10.1016/j.apenergy.2012.08.046.

[15] P. Basu, S. Rao, B. Acharya, A. Dhungana, Effect of torrefaction on the density and volume changes of coarse biomass particles, Can. J. Chem. Eng. 91 (2013) 1040–1044. doi:10.1002/cjce.21817.

[16] A. Goetzl, Developments in the global trade of wood pellets, Work. Pap. Ind. No. ID-039, US Int. Trade Comm. Washington, DC. (2015).

[17] C. Couhert, S. Salvador, J.-M. Commandré, Impact of torrefaction on syngas production

from wood, Fuel. 88 (2009) 2286–2290. doi:10.1016/j.fuel.2009.05.003.

[18] A.A. Boateng, C.A. Mullen, Fast pyrolysis of biomass thermally pretreated by torrefaction, J. Anal. Appl. Pyrolysis. 100 (2013) 95–102. doi:10.1016/j.jaap.2012.12.002.

[19] M.M.I. Sheikh, C.-H. Kim, H.-J. Park, S.-H. Kim, G.-C. Kim, J.-Y. Lee, S.-W. Sim, J.W. Kim, Effect of torrefaction for the pretreatment of rice straw for ethanol production, J. Sci. Food Agric. 93 (2013) 3198–3204. doi:10.1002/jsfa.6155.

[20] D. Agar, J. Gil, D. Sanchez, I. Echeverria, M. Wihersaari, Torrefied versus conventional pellet production – A comparative study on energy and emission balance based on pilot-plant data and EU sustainability criteria, Appl. Energy. 138 (2015) 621–630. doi:10.1016/j.apenergy.2014.08.017.

[21] K. Shah Ariffin, Prediction of energy consumption of geologically different marble deposits in ground calcium carbonate (GCC) production, Geol. Soc. Malaysia Bull. 46 (2003) 255–262. http://www.gsm.org.my/products/702001-100650-PDF.pdf (accessed July 11, 2018).

[22] L.J. Naimi, S. Sokhansanj, X. Bi, C.J. Lim, A.R. Womac, A.K. Lau, S. Melin, Development of size reduction equations for calculating energy input for grinding lignocellulosic particles, Appl. Eng. Agric. 29 (2013) 93–100. doi:10.13031/2013.42523.

[23] J.R. Hess, C.T. Wright, K.L. Kenney, E.M. Searcy, Uniform-Format Solid Feedstock Supply System: A Commodity-Scale Design to Produce an Infrastructure-Compatible Bulk Solid from Lignocellulosic Biomass--Executive Summary, Idaho National Laboratory (INL), 2009.

[24] P. Kumar, D.M. Barrett, M.J. Delwiche, P. Stroeve, Methods for pretreatment of lignocellulosic biomass for efficient hydrolysis and biofuel production, Ind. Eng. Chem.

Res. 48 (2009) 3713–3729. doi:10.1021/ie801542g.

[25] J.S. Tumuluru, L.G. Tabil, Y. Song, K.L. Iroba, V. Meda, Grinding energy and physical properties of chopped and hammer-milled barley, wheat, oat, and canola straws, Biomass and Bioenergy. 60 (2014) 58–67. doi:10.1016/j.biombioe.2013.10.011.

[26] S. Paulrud, Upgraded Biofuels -Effects of Quality on Processing, Handling Characteristics, Combustion and Ash melting, (2004). https://pub.epsilon.slu.se/533/1/Agraria449.pdf (accessed November 8, 2017).

[27] S.R.A. Kersten, X. Wang, W. Prins, W.P.M. van Swaaij, Biomass Pyrolysis in a Fluidized Bed Reactor. Part 1: Literature Review and Model Simulations, Ind. Eng. Chem. Res. 44 (2005) 8773–8785. doi:10.1021/ie0504856.

[28] A. V Bridgwater, Principles and practice of biomass fast pyrolysis processes for liquids, J. Anal. Appl. Pyrolysis. 51 (1999) 3–22. https://ac.els-cdn.com/S0165237099000054/1-s2.0-S0165237099000054-main.pdf?_tid=9ddcd65e-c4cf-11e7-b8d5-00000aab0f6b&acdnat=1510178344_022c5c1c569a37fe0ef3bdfbaf44b459 (accessed November 8, 2017).

[29] ASTM, ASTMD409/D409M-12 Standard Test Method for Grindability of Coal by the Hardgrove-Machine Method, Annu. B. ASTM Stand. (2016) 1–15. doi:10.1520/D0409.

[30] S. Kastberg, C. Nilsson, Combustion optimisation study of biomass powder, Proc. from 1 St World Conf. Biomass Energy Ind. (2000) 890–892.

[31] L.S. Esteban, J.E. Carrasco, Evaluation of different strategies for pulverization of forest biomasses, Powder Technol. 166 (2006) 139–151. doi:10.1016/j.powtec.2006.05.018.

[32] W.H. Walker, W.K. Lewis, W.H. McAdams, E.R. Gilliland, Principles of chemical engineering, (1937).

[33] P. Von Rittinger, Lehrbuch der Aufbereitungs Kunde, Ernst Korn. (1867).

[34] F. Kick, D. Gasetzder, proportionalen widerstande Und Science anwendung, Felix, Leipzig. (1885).

[35] F.C. Bond, The 3rd theory of comminution, Trans. Am. Inst. Min. Metall. Eng. 193 (1952) 484–494.

[36] F.C. Bond, Crushing and grinding calculations, Part I, Br. Chem. Eng. 6 (1961) 378–385.

[37] T.B. Reed, A survey of biomass gasification, Sol. Energy Res. Inst. 3 (1979).

[38] R.L. Earle, Unit operations in food processing, Elsevier, 2013.

[39] T.G. Bridgeman, J.M. Jones, A. Williams, D.J. Waldron, An investigation of the grindability of two torrefied energy crops, Fuel. 89 (2010) 3911–3918. doi:10.1016/j.fuel.2010.06.043.

[40] S. Mani, L.G. Tabil, S. Sokhansanj, Grinding performance and physical properties of wheat and barley straws, corn stover and switchgrass, Biomass and Bioenergy. 27 (2004) 339–352. doi:10.1016/j.biombioe.2004.03.007.

[41] M. Temmerman, P.D. Jensen, J. Herbert, Von Rittinger theory adapted to wood chip and pellet milling, in a laboratory scale hammermill, Biomass and Bioenergy. 56 (2013) 70–81. doi:10.1016/j.biombioe.2013.04.020.

[42] V. Repellin, A. Govin, M. Rolland, R. Guyonnet, R. Vincent, G. Alexandre, R. Mathieu, G. René, V. Repellin, A. Govin, M. Rolland, R. Guyonnet, Energy requirement for fine grinding of torrefied wood, Biomass and Bioenergy. 34 (2010) 923–930. doi:10.1016/j.biombioe.2010.01.039.

[43] L. Wang, E. Barta-Rajnai, T. Skreiberg, R. Khalil, Z. Czégény, E. Jakab, Z. Barta, M. Grønli, Effect of torrefaction on physiochemical characteristics and grindability of stem

wood, stump and bark, Appl. Energy. (2017). doi:10.1016/j.apenergy.2017.07.024.

[44] L. Wang, E. Barta-Rajnai, Ø. Skreiberg, R. Khalil, Z. Czégény, E. Jakab, Z. Barta, M. Grønli, Impact of Torrefaction on Woody Biomass Properties, Energy Procedia. 105 (2017) 1149–1154. doi:10.1016/j.egypro.2017.03.486.

[45] J. Deng, G. jun Wang, J. hong Kuang, Y. liang Zhang, Y. hao Luo, Pretreatment of agricultural residues for co-gasification via torrefaction, J. Anal. Appl. Pyrolysis. 86 (2009) 331–337. doi:10.1016/j.jaap.2009.08.006.

[46] P. Bergman, A. Boersma, J. Kiel, M.J. Prins, K. Ptasinski, F.J. Janssen, Torrefaction for entrained-flow gasification of biomass, 2nd World Conf. Technol. Exhib. Biomass Energy, Ind. Clim. Prot. a (2005) 78–82. https://www.ecn.nl/docs/library/report/2005/c05067.pdf (accessed November 14, 2017).

[47] C. Brischke, C.R. Welzbacher, A.O. Rapp, Detection of fungal decay by high-energy multiple impact (HEMI) testing, Holzforschung. 60 (2006) 217–222. doi:10.1515/HF.2006.036.

[48] D.T. Van Essendelft, X. Zhou, B.S.-J.S.-J. Kang, D.T. Van Essendelft, X. Zhou, B.S.-J.S.-J. Kang, Grindability determination of torrefied biomass materials using the Hybrid Work Index, Fuel. 105 (2013) 103–111. doi:10.1016/j.fuel.2012.06.008.

[49] ISO/AWI 21596-1, Solid Biofuels - Grindability Determination--Part 1: Grindability determination of uncompressed fuels, (2014).

[50] J.H.A. Khalsa, D. Leistner, N. Weller, L.I. Darvell, B. Dooley, Torrefied biomass pellets - Comparing grindability in different laboratory mills, Energies. 9 (2016) 794. doi:10.3390/en9100794.

[51] A.N. Rollinson, O. Williams, Experiments on torrefied wood pellet: study by gasification

and characterization for waste biomass to energy applications, R. Soc. Open Sci. 3 (2016) 150578. doi:10.1098/rsos.150578.

[52] O. Williams, C. Eastwick, S. Kingman, D. Giddings, S. Lormor, E. Lester, Investigation into the applicability of Bond Work Index (BWI) and Hardgrove Grindability Index (HGI) tests for several biomasses compared to Colombian la Loma coal, Fuel. 158 (2015) 379–387. doi:10.1016/j.fuel.2015.05.027.

[53] O. Williams, G. Newbolt, C. Eastwick, S. Kingman, D. Giddings, S. Lormor, E. Lester, Influence of mill type on densified biomass comminution, Appl. Energy. 182 (2016) 219–231. doi:10.1016/j.apenergy.2016.08.111.

[54] ANSI/ASAE, ANSI/ASAE S358.3 MAY2012 Moisture measurement-forages, Am. Soc. Agric. Biol. Eng. (Approved June 2012 as an Am. Natl. Stand.). (2012) 3–5.

[55] ASTM E873-82, Standard test method for bulk density of densified particulate biomass fuels, Annu. B. ASTM Stand. 82 (2006) American Society for Testing and Materials, West C. doi:10.1520/E0873-82R06.

[56] ASTM, ASTM D7582-15 Standard Test Methods for Proximate Analysis of Coal and Coke by Macro, Annu. B. ASTM Stand. (2015) American Society for Testing and Materials, West C. doi:10.1520/D7582.

[57] ASTM, ASTM D5865-13 Standard Test Method for Gross Calorific Value of Coal and Coke, Annu. B. ASTM Stand. (2013) American Society for Testing and Materials, West C. doi:10.1520/D5865-13.2.

[58] ANSI/ASAE, ANSI/ASAE S319.4 FEB2008 (R2012) Method of Determining and Expressing Fineness of Feed Materials by Sieving, Am. Soc. Agric. Eng. Stand. Februrary (2013) 447–550. doi:https://doi.org/10.13031/2013.24485.

[59] P.T.R. John F. Unsworth, David J. Barratt, Coal quality and combustion performance: an international perspective, Elsevier, 1991.

[60] F.C. Bond, Testing and calculations, SME Miner. Process. Handb. (1985) 16–27.

[61] E. Rokni, A. Panahi, X. Ren, Y.A. Levendis, Curtailing the generation of sulfur dioxide and nitrogen oxide emissions by blending and oxy-combustion of coals, Fuel. 181 (2016) 772–784. doi:10.1016/J.FUEL.2016.05.023.

[62] H.W. Jackman, R.J. Helfinstine, Drying and Preheating Coals Before Coking, Part 1. Individual coals, Illinois State Geol. Surv. Urbana. 423 (1968). http://library.isgs.illinois.edu/Pubs/pdfs/circulars/c423.pdf (accessed July 10, 2018).

[63] P.C.A. Bergman, Combined torrefaction and pelletisation the TOP process, Energy Cent. Netherlands, Rep. No. ECN-C-05-073, ECN, Petten, Netherlands. (2005). http://www.ecn.nl/publications.

[64] M.J. Prins, K.J. Ptasinski, F.J.J.G. Janssen, More efficient biomass gasification via torrefaction, Energy. 31 (2006) 3458–3470. doi:10.1016/j.energy.2006.03.008.

[65] N. Kaliyan, R.V. Morey, Factors affecting strength and durability of densified biomass products, Biomass and Bioenergy. 33 (2009) 337–359.

[66] H. Rezaei, C.J. Lim, A. Lau, S. Sokhansanj, Size, shape and flow characterization of ground wood chip and ground wood pellet particles, Powder Technol. 301 (2016) 737–746. doi:10.1016/j.powtec.2016.07.016.

[67] C. Rattanakawin, W. Tara, Characteristics of Mae Moh lignite: Hardgrove grindability index and approximate work index, Songklanakarin J. Sci. Technol. 34 (n.d.) 103–107. http://rdo.psu.ac.th/sjstweb/journal/34-1/0125-3395-34-1-103-107.pdf (accessed April 13, 2017).

[68] F. Tichánek, Contribution To Determination of Coal Grindability Using Hardgrove Method Příspěvek Ke Stanovení Melitelnosti Uhlí Metodou, LIV (2008) 27–32. http://gse.vsb.cz/2008/LIV-2008-1-27-32.pdf (accessed April 13, 2017).

CHAPTER 5

PROCESS SIMULATION OF INTEGRATED BIOMASS TORREFACTION AND PELLETIZATION (IBTP) PLANT [1]

[1] Manouchehrinejad M and Mani S. To be submitted to Applied Energy, (2018).

Abstract

A comprehensive process simulation model was developed for the integrated biomass torrefaction and pelletization (iBTP) system using Aspen Plus V9 software. The main unit operations including drying, torrefaction, grinding, pelletization, and cooling were simulated in details to represent the thermodynamic conditions on an industrial scale. A detailed solid convective dryer and a rotary kiln torrefaction reactor including the kinetics were modeled to study the thermal decomposition of biomass at different temperatures. The model was used to estimate the mass yield, energy yield, thermal and electrical energy requirement, product specifications, and emissions for production of torrefied wood pellets from pine wood feedstock in various scenarios. The total energy consumptions for production of torrefied pellets were 6.7 to 15.3 MJ kg^{-1} for torrefaction temperature range of 250 to 290°C, where the torgas products provided 45 to 88% of the total thermal energy requirement. The usage of natural gas and biomass bark as the auxiliary fuel in burner was studied for evaluation of exhaust gas compositions.

Keywords: Biomass, Torrefied pellet, Process simulation, Mass balance, Energy balance, ASPEN Plus

Introduction

Integrated torrefaction and pelletization, known as the TOP process, was initially developed by Energy Research Centre of the Netherlands (ECN) to provide a proper coal-like feedstock from biomass resource for power generation plants [1]. Torrefaction is a thermal conversion process in an inert environment within the temperature range of 200-300°C [2]. The torrefaction products are solid torrefied biomass and a volatile stream (called torgas) contained volatile compounds from the initial biomass. As a result of removing the polar hydroxyl and carbonyl groups during the torrefaction process, the biomass C/O ratio will be increased, improving its calorific value and hydrophobicity [3,4]. Moreover, the inter-particles bondings are weakened through thermal degradation that significantly improves the biomass grindability, promoting the use of biomass in pulverized co-firing systems [5,6].

Torrefaction process was primarily proposed for pretreatment of the biomass and producing bio-coal for power generation applications and direct combustion. However, there are also a number of studies that have demonstrated the benefits of the torrefaction process prior to the other thermal conversion methods such as pyrolysis [7] and gasification [8] to produce bioenergy. Despite the great advantages of torrefaction on improving the energy content, hydrophobicity, and grindability of biomass, the density of the torrefied biomass would be reduced as the result of mass loss [9]. Torrefaction of lignocellulosic biomass around 290°C reduced the bulk density by 25% [10]. Therefore, densification of torrefied materials is necessary to increase the energy density of the final product that would further facilitate handling and flowability, and decrease transportation and storage costs [3,11]. Currently, wood pelletizing plants are extensively designed and commercialized all over the world, but the industrialization of torrefaction plants is

in its early phase. Accordingly, the integrated biomass torrefaction and pelletization process (iBTP) has not been fully developed yet.

Several studies have been conducted on the torrefaction kinetics and mechanism determination for different biomass types as well as the reactor technological development to improve the system efficiency of torrefaction [12,13]. However, the performance assessment of the proposed kinetics and technologies for torrefaction process or a combined torrefaction and the pelletizing system is challenging even for certified models due to lack of operating data. One of the critical issues is the energy management for a combined torrefaction and pelletization system. Despite a certain activation energy requirement for heating-up the biomass to the torrefaction set-point, most of the biomass torrefaction reactions are exothermic beyond the 250°C. Moreover, the produced volatile stream contains valuable energy, which can be captured and utilized in the system again. The "auto-thermal operation" concept asserted by Bergman et al. 2005 implied that the thermal energy required for the drying and torrefaction processes can be totally supplied by combustion of the torrefaction gas products [1,2]. On the other hand, scaling up the system to the pilot and industrial level would change the energy integration in the process along with the certain impacts on the equipment size and system parameters. The energy management and scale-up, together with the complex mass and energy balance calculations and optimizations necessitate the developing of process simulation for such a system. A robust process simulation model incorporated with mathematical models and relevant kinetics is a useful tool to verify the systems at different scales, evaluating the mass and energy requirement and various operating conditions impacts, and determination of unit operation design parameters, especially in the design phase. A process simulation is beneficial to estimate the efficiency of the system, enabling process optimization with minimum energy consumption and consequent cost expenses. Having the operating

conditions of different equipment in the system and compositional analysis of the exhaust streams, the hazard and operability study (HAZOP) of the system and conducting the process safety analysis would be facilitated.

Often, in literature, the Aspen Plus software has been used for simulation of a torrefaction system [14–19]. Aspen Plus has a good database for solids, electrolytes, and polymers in addition to the conventional chemicals, and comprises diverse unit operations. The intermediate chemical makeup of the biomass, complex chemistry of torrefaction, and complicated thermodynamic equations of the solid phase in equilibrium with gas and liquid phases are some of the main challenges of the biomass torrefaction simulation. No work has yet been published capable of predicting the compositions of torrefaction products at specified operating conditions. A preliminary experimental data is required to specify the torrefaction kinetics of a defined biomass feedstock and probable torrefaction products composition. Recently, in a study on the pyrolysis of biomass (which is a heat treatment process at temperature above 500°C), a database of 149 possible reactions of the elemental constituents of biomass including cellulose, hemicellulose, and lignin and subsequent secondary reactions were implemented in the Aspen Plus software, which enabled the simulation to roughly estimate the pyrolysis products of any lignocellulosic biomass at different temperatures. The gas and char yields were modified later by the ash alkali metal content of the initial biomass [20].

In most of the previous studies, the drying has been defined as a simple conversion in a stoichiometric (RStoic) reactor [15,17,19,21]. This approach estimates the approximate heat requirement for evaporation of water content but it does not necessarily represent the mass and heat transfer in a real dryer. In an RStioc dryer, the operating conditions of heating media (hot air or hot gas) including temperature and moisture content, and temperature profile of solid and gas

streams in the dryer cannot be predicted. Moreover, the exhaust gas composition would not be explored. Recently, Bach et al. [18] simulated the drying process in a solid dryer (and not a reactor) in the Aspen Plus and they used hot air as a heating media. However, they did not scrutinize the details about the type of the dryer, kinetics of drying, moisture content in the outlet air, or variation of the inside temperature [18]. For the reaction section, the regression models have been derived from the known compositions of the input biomass, torrefied biomass, and volatile gas product versus temperature and time, and then the results being implemented to the model in a stoichiometric reactor (RStoic) [14] or conversion reactor (RYield) [15,19,21], or in a combination of both [16,22]. Bach et al. [18], asserted that none of the pre-defined reactors in Aspen Plus could model the complicated torrefaction process. Hence, they proposed a user-defined hierarchy reactor to estimate the compositions of torrefied material and weight fraction of known components in the gas stream at different reaction temperature and duration. They implemented a FORTRAN code, which combined the kinetics data of willow torrefaction and the composition of gas product proposed by Prins et al. [4], and calculated the mass yield, energy yield, product composition, and higher heating value of the torrefaction of Norway birch within a temperature range of 240 to 300°C [18]. The Bergman et al. [2] and Cherry et al. [19] investigated the mass and energy balance of torrefaction of a hardwood (willow) and a softwood (pine), respectively at various temperature and different scenarios. According to the Bergman et al. none of the drying and torrefaction scenarios of wood with initial moisture content of 50%, within the temperature range of 250-300°C and residence time of 7.5 to 30 min were auto-thermal, which meant auxiliary fuels were needed along with the torgas to combust in a burner and to provide the required energy for the system [2]. Cherry et al. investigated different cases of wood torrefaction at 180, 230 and 270°C, and the integration with biorefinery. For the dried feedstock cases and torrefaction temperature of 270°C,

the process was above the auto-thermal operation point, where the excess energy could be used in an adjacent heat exchanger or a boiler [19]. The biomass feedstock and capacity, moisture content, torrefaction temperature, torgas energy management, and the system configuration might affect the total external energy requirement [2,19,23]. The detailed simulation of a dryer resembling the real industrial conditions was not explored in previous studies. The compositional changes of the biomass and torgas based on the kinetics of reactions and in a temperature range of torrefaction have been rarely addressed [18]. Moreover, reviewing the literature, the alteration of biomass proximate analysis within the torrefaction and its effects on the enthalpy variation were not explored in details.

The goal of this study was to provide a process simulation framework for the integrated lignocellulosic biomass torrefaction and pelletization (iBTP) with the Aspen Plus software. Unlike the previous works, the dryer section was simulated through a solid convective dryer to study the real condition of the outlet solid and off gas. The kinetics of torrefaction reactions were applied directly into the model within the pre-defined reactors in Aspen Plus, which can be changed based on the specific feedstock. The relevant calculation blocks were incorporated into the reaction section to apply the torgas composition in the torrefaction results and modifying the torrefied solid ultimate and proximate analysis. The grinding, pelletizing, cooling, and screening unit operations were also simulated based on the available data in literature or common practices for the lignocellulosic material. The simulation was validated for the southern pine wood biomass using different sets of available experimental and industrial data. Last but not least, the model was used to simulate the production of torrefied pellets at the specific production capacity (100,000 Mg yr^{-1} of torrefied pellets) and to investigate the energy efficiency and auto-thermal condition in the

system. The design parameters of unit operation could be obtained from the model, which are used to predict the feasibility and cost of the industrial plant.

Model development

Process description

A typical flow diagram of a conventional iBTP plant is illustrated in Figure 5-1. The process configuration of different plants might vary based on the type of biomass feedstock, initial moisture content, particle size, process temperature, residence time, torrefaction technology, heat integration method, and production capacity [19,24–26].

The initial raw biomass with a specified particle size distribution and moisture content in the range of 30-50 wt.% [26] is sent to a dryer. The most common type of a biomass dryer is a rotary dryer, which can be classified as direct and indirect heated types [27]. Biomass goes through a rotating drum equipped with a number of longitudinal flights and a hot air of flue gas passes in parallel flow, co-current or countercurrent. Within rotation of the drum, the materials are showered by the drum flights through the hot gas, improving the heat and mass transfer. As a result of heat and mass transfer in the dryer, the water in the biomass is evaporated and transferred to the gas phase. The off-gas, with increased humidity and reduced temperature, passes through a cyclone to separate any entrained fine particles and then vents to the atmosphere. The temperature of outlet gas is in the range of 71-110°C. It is necessary to keep the temperature of off-gas above the acid gas temperature to prevent precipitation and corrosion problems in the stack. In pelletizing plants, a definite amount of moisture content in the range of 6-15% is favored for the inlet biomass to the pellet mills [25,28,29]. Water reduces the friction as a lubricant and acts as a binder during pelletizing, improving the pellet durability. Moreover, pellets with very low moisture content are

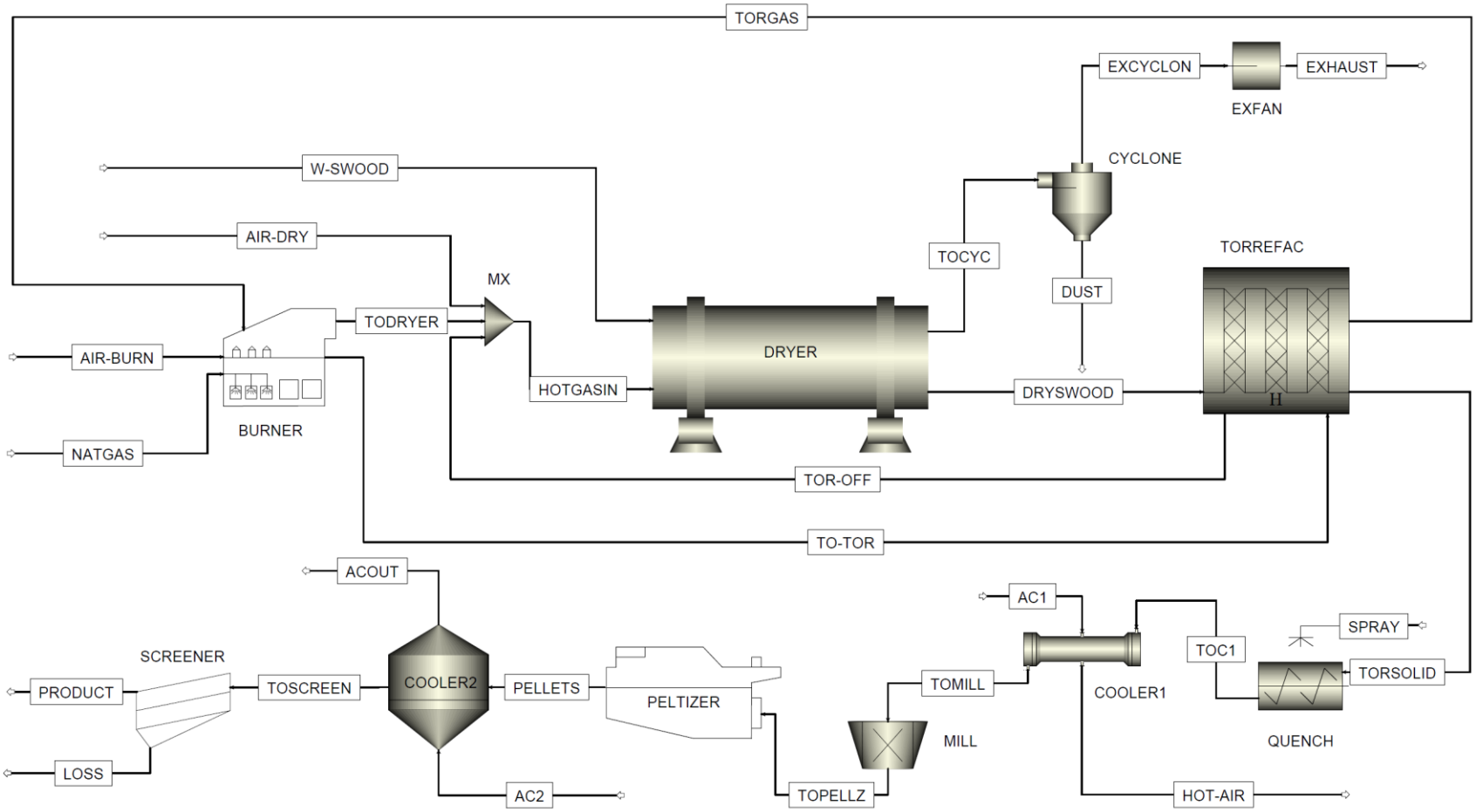

Figure 5-1. Flow diagram of the integrated torrefaction and palletization model.

prone to absorb more water and elongate during storage time, which is not desired [25]. Similarly, in torrefaction plants, the biomass moisture content should be reduced to less than 15 wt.% before torrefaction [5]. The main reasons for drying of biomass before torrefaction are: (1) variable moisture content of the initial biomass and its latent heat requirement governs the heat balance of the system and changes the control parameters, and (2) the higher moisture content of torgas (torrefaction gas), lowers the adiabatic flame temperature in the burner. So, the energy of the torgas would not be sufficient for thermal treatment [5]. The required energy for drying section (evaporating the water) depends on the feedstock capacity and initial moisture content and is usually provided by combustion of the torgas assisted by a part of biomass as a fuel or any other auxiliary fuel [2]. The dried biomass is then sent to the torrefaction section. For a specific feedstock; temperature, residence time, and particle size are the most important parameters in biomass torrefaction [30]. The effects of torrefaction temperature and residence time have been studied by severity factor for certain particle size [31–33]. The torrefaction degree can be divided into three levels: light (200–235 °C), mild (235–275°C), and severe torrefaction (275–300°C) [13]. A holding time of 10-60 min is common for torrefaction based on previous studies [3,4,13]. A higher torrefaction temperature causes more thermal decomposition of biomass, producing higher energy density bio-coal but with less mass yield. On the other hand, greater amounts of volatile organic species would be released with the potential of more heat generation by oxidizing. In the sever torrefaction temperature, the energy of the torgas combustion might be higher than the thermal energy requirement of the system (above the auto-thermal operation) [24]. Therefore, it is important to utilize that energy in an adjacent heat exchanger or a boiler to optimize the overall thermal efficiency. A trade-off between mass yield and solid properties and energy of torgas is required to determine the appropriate temperature and residence time of the torrefaction. The

biomass degradation in torrefaction reaction starts at 200°C and is mildly exothermic in the temperature range of 250-300°C [4]. Several types of the reactor with different technologies have been developed for biomass torrefaction such as a compact moving bed, fluidized bed, belt dryer, rotary drum, screw conveyor, and microwave. Most of these reactors are upgraded from previous technologies for drying or pyrolysis purposes with related advantages and disadvantages [24].

After torrefaction, the torrefied biomass is cooled to below self-ignition temperature by water quenching or air cooling, or a combination of both to prevent possible combustion of torrefied biomass in the atmospheric oxygen [24,26,34]. The biomass is then sent to a hammer mill to be ground to a proper size for pelletization. Torrefaction improves the grindability of biomass to a great extent. The required power consumption for grinding torrefied biomass is 80-90% lower than raw biomass [1,6]. On the other hand, densification is an energy-intensive process for torrefied materials contrary to the grinding process. It has been discerned by several researchers that torrefaction can hinder densification process by weakening the bonding between particles; Hence, the high die temperature, more compressive pressure, or binding agent is necessary for densification step [6,13,28,35,36]. The produced pellets should be cool down again to reduce the risk of ignition [25]. Finally, the pellets are screened to check the quality and sent to the storage facilities. The unshaped pellets and fines are recycled to the mill [25]. The dry material loss during handling and operations can be minimized by usage of fabric filters or baghouses, electrical precipitators, scrubbers, and cyclones and recycling to the system. Nevertheless, the total amount of 2 to 3% dry weight loss was considered in this study, which is in the range of previous studies [37,38].

General assumptions

The main unit operations in the model were drying, torrefaction, an integrated combustion unit, grinding, pelletization, and cooling (tor-coolers and pellet coolers). The general assumptions for this simulation model in Aspen Plus V9 software were as follows:

- The biomass feedstock was defined as a non-conventional solid with definite ultimate and proximate analysis. The solid property models of HCOALGEN and DCOALIGT, which are adapted for the coal, were used for enthalpy and density calculation of lignocellulosic biomass with a reasonable approximation. A detailed description is provided in supporting information.
- The particle size distribution affects the heat transfer within the dryer and the rotary kiln reactor and it changes after the pelletization process. Therefore, the stream class used in the model was MCINCPSD, which needs particle size distribution for non-conventional and conventional solids.
- The PR-BM (Pen-Robinson equation with Boston-Mathias modifications) property model was used to estimate the properties of available conventional components in liquid and gas phases.
- The system operates at atmospheric pressure; however, blowers were considered elsewhere to compensate for the possible pressure reduction in a real industrial case and to estimate the relevant electricity requirement.
- The ambient air temperature was 25°C with a relative humidity of 50%.
- Aspen Plus is a thermodynamically based simulator, so the mechanical aspects of equipment or physical arrangement were not necessarily incorporated into the model.

Dryer

A directly heated single-pass rotary dryer was simulated via a solid convective dryer in Aspen plus. A biomass feedstock with high moisture content (W-SWOOD) and a hot gas (HOTGASIN) flowed co-currently through the dryer (Figure 5-1). The HOTGASIN mainly consisted of the hot flue gas from the torrefier section, which might be compensated with the direct flue gas from the burner. The final inlet hot gas was diluted with air to modify the inlet temperature, which can vary from 232-1093°C [39] based on the moisture content and mass flow rate of the biomass feedstock and hot gas. Though, the high temperature hot gases are avoided due to the risk of fire in a dryer and preventing the burning of the biomass surface at the initial hot temperature [40]. The hot gas flowrate was adjusted to obtain a 10% (wb) moisture content in the biomass at the dryer outlet. The moisture mass balance for the solid phase and gas phase was calculated simultaneously with heat transfer between solid and gas phase along the length of the dryer. The evaporation rate from biomass particles was taken into account by considering the kinetics of drying, mass transfer coefficient between the surface of the particles and gas, and the difference between the saturated moisture content and local moisture content of the gas.

Assumptions for dryer simulation:

- A co-current convective solid dryer was considered in this study.
- Solid particles were considered to be uniform in respect to moisture content and temperature.
- Plug flow behavior was assumed for both solid and gas flow in the dryer.
- Drying kinetics, and heat and mass transfer diffusion were taken into account for intra-particle resistances for drying.

A proper dryer dimension, drying curve shape factor (based on the kinetics parameters of biomass drying), and a mass transfer coefficient was defined in the input section. The heat transfer coefficient in Aspen Plus is estimated by the Lewis number as the ratio of the thermal diffusivity to mass diffusivity. The kinetic data for drying of pine wood chips was taken from [41]. The heat loss through the dryer body was also estimated considering the body temperature of 80°C, surrounding temperature of 25°C, and convection heat coefficient of air over the cylindrical surface area of the dryer and was input to the system. Detailed calculations of drying curve shape factor and the mass transfer coefficient are explained in supporting information.

The main output of the dryer unit operation is the required energy for drying, which is the summation of the water latent heat (the difference amount between the inlet and outlet moisture content of the biomass) and the water and biomass sensible heats from inlet temperature to the outlet temperatures. The drying energy was calculated by the difference in the energy content of the hot gas (HOTGASIN) at the inlet temperature reaching to the outlet temperature (temperature of TOCYC) (Figure 5-1). The average solids residence time in the Aspen plus is simply calculated through Eq. (1) and Eq. (2):

$$V_S = V_d.(1-\varepsilon).\psi \tag{1}$$

$$\tau = \frac{V_S}{\dot{M}_S/\rho_S} \tag{2}$$

No rotational speed is considered in this calculation, therefore the residence time is higher than the real industrial scale rotary dryer, which is usually equipped with flights and have some rotational movement. A calculation block was considered to evaluate the residence time of the dryer with rotational speed based on the equation Eq. (3) [42]:

$$\tau = \frac{0.23.L}{D.\omega^{0.9}.\tan(\alpha)} \tag{3}$$

Where $\tau(min)$ is the average residence time, $\alpha\ (rad)$ is the slope of the rotary dryer (3-5°), D (m) is diameter of dryer, L (m) is length of the dryer, and $\omega(rpm)$ is the rotational speed. The value of 0.23 is a flight parameter that refers to six to eight number of flights [42].

Different terms have been used in literature for the efficiency of the drying process including drying efficiency, energy efficiency, and thermal efficiency [43]. In this study, drying efficiency was calculated by the ratio of the required energy for drying divided by the total energy input including thermal, electrical and loss energies (Eq. (4)). The thermal efficiency of drying was the ratio of energy used for the moisture evaporation divided by the total thermal energy input for drying (Eq. (5)). Drying energy efficiency was the amount of energy used for the moisture evaporation divided by the total energy input (Eq. (6)).

$$Drying\ Efficiency = \frac{Required\ energy\ for\ drying}{E_{th} + E_e} \tag{4}$$

$$Drying\ Energy\ Efficiency = \frac{evaporated\ water\ \times \lambda}{E_{th} + E_e} \tag{5}$$

$$Drying\ Thermal\ Efficiency = \frac{evaporated\ water\ \times \lambda}{E_{th}} \tag{6}$$

Torrefier

The torrefaction process is shown within the torrefier hierarchy in the Figure 5-2. The torrefaction was considered to take place in an indirect heating rotary kiln reactor, which was simulated through a series of unit operations. In the first step, the in-bond water in the biomass was converted to the conventional water in an RStoic reactor (TOREVAP). The moisture in the inlet biomass, with a molecular weight of one g/gmole (which is assumed for non-conventional solids in Aspen plus), reacts to form 1/18 ($\cong$ 0.0555556) mole of the conventional water. The mixture of biomass and moisture then entered to the series of RPlug reactors.

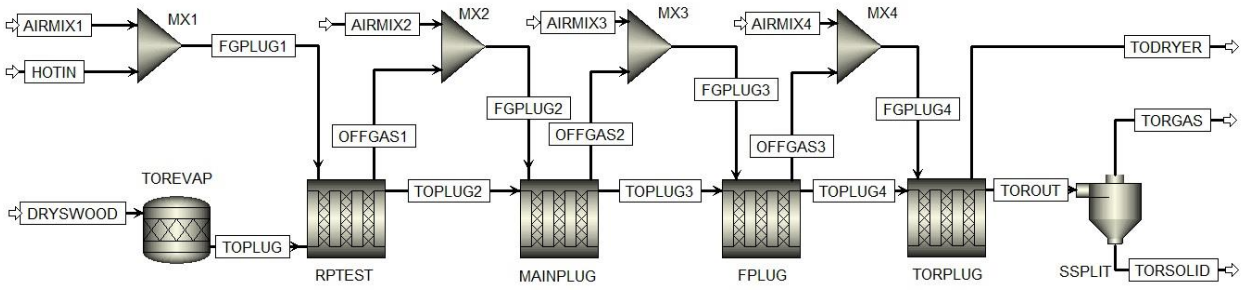

Figure 5-2. Process flow diagram of the torrefaction reactor.

The materials heated initially by the external hot flue gas to the torrefaction temperature in the first main part of the reactor (RPTEST), where the moisture content of the biomass was evaporated as well. The inlet hot flue gas temperature was adjusted to around 950°C to expedite the heating rate, minimizing the reactor length. The heating rate of 50 to 100°C min^{-1} was assumed to increase the input biomass temperature to the torrefaction set-point. Torrefaction reactions are mostly exothermic, especially at a temperature above 250 °C. Thus, control of the reaction temperature within a constant range for a specified retention time is crucial within the reactor to gain the torrefied biomass with specific properties. Therefore, the air flow injection was considered at different sections to control the temperature of the reactor at the torrefaction set point. The multiple zone profile heating champers have been extensively applied in mineral processing [44].

Torrefaction reactor assumptions:

- A co-current indirect heat rotary kiln reactor was simulated through a series of RStoich and RPlug reactors.
- Mass and heat transfer inside the solid particles and within the solid bed was faster than the torrefaction reaction rate. Therefore, the temperature and concentration in the solid bed were assumed to be uniformly distributed.
    - The Biot number ($Bi = h.L_c/k_t$) describes the ratio of the convection heat transfer coefficient around the particles over the conduction heat transfer inside the particles. Having the particle size of the initial solid biomass, the Biot number was small enough to assume the homogenous behaviors inside of the particles. Therefore, no internal heat transfer limitation was considered inside the particles.
    - The External pyrolysis number ($P\acute{y} = h/k.\rho.c_p.L_c$) is the ratio of the convection heat transfer rate around the particles versus the reaction rate. The pyrolysis number was quite bigger than unit, which implied no external heat transfer limitation within the solid bed.
- The solid phase and gas phase were well mixed across the sectional area and there was no radial dispersion along the reactor length [45]. Therefore, the temperature of the solid bed and gas were in equilibrium. It was a valid assumption due to low loading rate of solid in the rotary kiln reactors, especially in industrial scale [46]. The Peclet number, which is the ratio of convective flow to disperse flow in the axial direction is rather high in the rotary kiln, representing the plug flow behavior along the length of the reactor.
- Reactions were assumed to take place only in the solid bed domain.

- The particle size distribution was not changed in the torrefaction. (No shrinkage or breakage occurred.)
- No radiation heat transfer was considered for the torrefaction temperature range (200-300°C) [47].

The kinetics of reactions and heat transfer coefficient were the main inputs for simulating the RPlug reactors. The default kinetics mechanism of the torrefaction in this study was based on the two-step weight loss reactions in series, which proposed initially by Di Blasi and Lazentta [48], as shown in Table 5-1. The initial raw biomass (A) converts to the intermediate biomass (B) and volatile (V1) in the first step, representing mainly the degradation of extractives and hemicellulose [49]. The reaction continues in the second step, which stands for the small conversion of lignin and cellulose to produce the final torrefied biomass and another volatile stream [49]. A two-step kinetics torrefaction parameters under isometric conditions have been derived for several lignocellulosic biomass [4,49,50] that can be used directly in this simulation model. The mass flows of pseudo-components (A, B, C, V1, and V2) were calculated by the rate equations according to the reaction mechanism. The composition of intermediate and final biomass was obtained by having the kinetics parameters, the composition of initial biomass (A), and the composition of volatiles (V1 and V2). A FORTRAN block, using the equations in Table 5-1, was incorporated into the RPlug reactor. In order to define the fractional compositions of V1 and V2, the Bates and Ghoniem [51] approach was applied using the experimental torgas compositions at different torrefaction temperatures. It was assumed that the fractional compositions of pseudo-components of V1 and V2 are fixed within the range of torrefaction (usually between 200-300°C). The fractional composition of V1 and V2 was calculated by fitting the model results (volatile yields) and experimental data (total torgas composition) through the least square solution [51]. The same

procedure was used by Gul et al. as well [52]. The detailed approach is explained in the Supporting information.

Table 5-1. Kinetic mechanism of torrefaction and relevant parameters.

Parameter	Value/equation, unit	Ref.
Reaction pathway	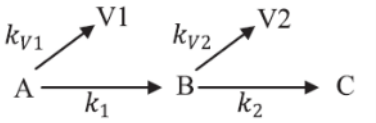	[53]
A: initial biomass, B: intermediate biomass, C: final bio-coal, V1& V2: volatile components		
$\frac{dA}{dt} = -(k1 + kv1) \times A$ $\frac{dB}{dt} = k1 \times A - (k2 + kv2) \times B$ $\frac{dC}{dt} = k2 \times B$ $\frac{dV1}{dt} = kv1 \times A$ $\frac{dV2}{dt} = kv2 \times B$	$A \rightarrow \beta B + \nu V1$ $B \rightarrow \gamma C + \xi V2$ $Y_{j,B} = \left(Y_{j,A} - \nu \times Y_{j,V1}\right)/\beta$ $Y_{j,C} = \left(Y_{j,B} - \xi \times Y_{j,V2}\right)/\gamma$ $\beta = \frac{r_{B,1}}{-r_{A,1}} = \frac{k1}{k1 + kv1}, \ \nu = \frac{r_{V1,1}}{-r_{A,1}} = \frac{kv1}{k1 + kv1}$ $\gamma = \frac{r_{C,2}}{-r_{B,2}} = \frac{k2}{k2 + kv2}, \ \xi = \frac{r_{V2,2}}{-r_{B,2}} = \frac{kv2}{k2 + kv2}$	[51]

The stoichiometry of reactions is required as well in the default model of the torrefaction RPlug reactors. According to the Di Blasi and Lazentta mechanism, there were four reactions. The reactions of biomass to biomass ($A \overset{K1}{\rightarrow} B, B \overset{K2}{\rightarrow} C$) were simply defined by stoichthe iometric coefficient of one (±1) for non-conventional biomasses A, B, and C. For the reactions of biomass to volatile ($A \overset{K_{V1}}{\longrightarrow} V1, B \overset{K_{V2}}{\longrightarrow} V2$), the stoichiometric coefficient of conventional components in V1 and V2, were calculated by dividing the fractional composition by the molecular weight of each component and implemented in the model.

Apart from the elemental composition of biomass, which was exported to the ultimate analysis of each component, the proximate analysis of the intermediate and final biomass was also needed to be modified. The elemental compositions are the basis for the calculation of density, the heat of combustion, and standard heat of formation of the biomass as a non-conventional component in the Aspen Plus. Also, the proximate analysis was required for obtaining the heat capacity based on the Kirov correlation [54]. In this study, the proximate analysis was estimated using the higher heating value correlation of the torrefied materials as a function of proximate analysis fitted with experimental data. The same approach was used by Nuchhen and Afzal [55]. Once the elemental composition obtained by kinetic parameters and volatile compositions, the higher heating value can be calculated using Boie HHV correlation [56]. The HHV value was then equalized to the amount of the higher heating value from the proximate analysis (fixed carbon, volatile material) correlation. The ash content was defined in the elemental composition calculation. The fixed carbon, volatile material, and ash percentage were constrained to sum to one.

The overall heat transfer coefficient inside the rotary kiln was calculated based on the Li et al. study [46] and incorporated via a FORTRAN block into the model for each section. The main two pathways of the inside heat transfer are i) heat transfer from wall to the bulk of the solid (conduction), and ii) heat transfer from wall to the freeboard gas (torgas) and from gas to the bulk of the solid (convection). The thermal resistance of the kiln wall thickness and heat transfer through radiation mechanism was neglected. The heat loss through the reactor body was calculated in the same way as the dryer. The detailed calculations are given in the supporting information.

In a pre-defined RPlug reactor in Aspen Plus, reactor volume is a representative of the residence time of reaction. However, Aspen Plus does not incorporate the filling grade (loading factor) of

biomass or the drum rotational speed in the RPlug. The effects of filling grade and the rotational speed of kiln were considered in the overall heat transfer coefficient calculation to modify the reactor section area. Nevertheless, the input length of the reactor did not represent the real length in a kiln rotary drum and it only determined the required residence time for kinetics conversions. The modified length of the reactor was estimated considering the solid volume flow and design parameters of the rotary kiln (i.e., rotation speed and filling grade). Detailed information is given in the supporting information. The mass yield of the torrefaction process was calculated based on the Eq. (7):

$$Y_M(\%) = \frac{M_{tor}}{M_{raw}} \times 100 \tag{7}$$

M_{tor} is the dry basis mass of the torrefied solid after the torrefaction reactor and M_{raw} is the dry basis mass of the raw feedstock.

The energy yield of the torrefaction, which represents the amount of energy stored in the solid material after the torrefaction process is calculated by Eq. (8):

$$Y_E(\%) = Y_M \times \frac{HHV_{tor}}{HHV_{raw}} \tag{8}$$

Mass and energy yield and higher heating values obtained from the model were validated with the experimental data as well.

Integrated combustion unit

The required heat for drying and torrefaction of biomass was provided by combustion of torgas and an auxiliary fuel (biomass or natural gas) in a common burner. The amount of air was adjusted by controlling the mole fraction of oxygen in the flue gas below 0.03. The combustion process was simulated through an RGibbs block, assuming the Gibbs free energy minimization for specific reactants and products. In case of using bark (biomass) as a fuel, the non-conventional biomass should be converted initially to conventional components such as Carbon, Nitrogen, Oxygen, Hydrogen, etc. The RYield reactor with a calculator was used to convert the ultimate

characteristic of the non-conventional bark biomass to relevant components. The RGibbs reactor was then used to combust those components with air in a Gibbs reactor. The heat loss in a combustion chamber reduces the temperature of flue gas. The heat loss due to radiation and convection (2.5%) and heat loss through the body of the burner (4.0%) was considered separately as a total of 6.5%. The impacts of other parameters like moisture content of the fuel and air and the fuel composition on the adiabatic flame temperature were considered by software as such. The produced flue gas was distributed to the torrefaction section and to the drying, using a design spec function, which adjusted the split ratio of the flue gas corresponding to the required heat in each section. The flue gas would be diluted with air before torrefaction and drying to reach the setpoint temperatures.

Tor-cooler

After torrefaction, the torrefied biomass is cooled to below self-ignition temperature by water or air cooling jacket, or water quenching to prevent possible combustion of torrefied biomass in the atmospheric oxygen [11,24,26,34]. In this simulation, the torrefied materials were cooled down in two steps. In the first step, the temperature was reduced to 150°C by quenching water directly to the hot torrefied water. The produced steam was evacuated and discharged. In the second step, the torrefied pellets temperature cooled to 75°C using air jacket cooling.

Grinder

A crushing unit in Aspen Plus was used for grinding simulation. The main inputs are the final average geometric diameter of output particles and the generalized size reduction parameter (Bond work index (BWI) or Hardgrove grindability index (HGI)) of the feed material. The BWI and HGI indices are commonly defined as a grindability parameter of brittle materials like coal. The grinding studies of biomass have shown that Rittinger's law is the more suitable equation for

calculating the grinding energy of biomass [10,57]. However, thermal treatment processes such as torrefaction transform the fibrous biomass to a more brittle structure like coal. Therefore, the grindability indices for coal and brittle materials might approximately describe the grinding behavior of the torrefied biomass [10]. Nevertheless, the existing milling units are mostly designed based on the BWI and HGI indices. In this study, the HGI index of the biomass, as a characteristic parameter for the grinding, was entered into the model.

Pelletizer

No pre-defined unit operation is available for pelletization in Aspen Plus. The variations in particle size distribution, temperature, and moisture content of the biomass were simulated with a granulator unit operation. The inlet biomass moisture content was increased to about 7% with water spraying to follow the real condition. The temperature of 110°C was also considered as the result of steam injection and frictions in the pelletization process. The energy consumptions for pelletizing of the torrefied woodchips was considered as 150 kWh Mg^{-1} [34] in this simulation, applied via a calculation block.

Pellet cooler

The produced pellets should be cooled down again to reduce the risk of ignition [25]. Pellet cooling is a convective and evaporative cooling process, which is similar to the mass and heat transfer processes in a rotary dryer. As a result of evaporative cooling, the water transfers from the pellets, leading to reduce the moisture content of the pellets. Convective cooling happens between the cold air and hot pellets based on the difference between the temperature, pellets surface area, and the heat transfer coefficient. A counter current pellet cooler with proper dimension based on the mass flow capacity was considered to reach the outlet pellet temperature around 50°C. The pellets were then screened to check their quality and sent to the storage facilities. In the industrial

plants, the fines are brought back to the process [37]. About 2 to 3% loss of the fine biomass was considered in this simulation.

Input data inventory

The southern pine wood chips was selected as a feedstock for this process simulation. The characteristics data of the raw biomass (Table 5-2), torrefied biomass at four different temperatures, and the relevant torgas composition were obtained from [58]. The kinetics used for torrefaction reactions were taken from torrefaction of willow by Prins et al. [4] in accordance with Di Blasi and Lanzetta [53] two-step reaction mechanism. The composition of the initial biomass (A) was input according to the experimental data. The composition (ultimate analysis) of the intermediate biomass (B) and final biomass (B) was calculated within a calculation box at the temperature of the torrefaction, based on the kinetics rates and the compositions of volatile streams V1 and V2. The composition of pseudo-components of V1 and V2 obtained using the volatile yields from the kinetics and experimental data of the torrefaction of southern pine in a temperature range of 230 to 290 °C [58] through the least square solution and are listed in Table 5-3. The rest of the thermodynamic and physical properties assumed for the process simulation are given in Table 5-4.

Table 5-2. Properties of initial woodchips and pine bark.

Wood chips properties	**Unit**	**Pine woodchips** [58]	**Pine Bark** [59]
Ultimate analysis, (db)			
Carbon (C)	%wt	49.73 (0.13)	54.33 (0.46)
Hydrogen (H)	%wt	6.17 (0.08)	6.96 (0.29)
Nitrogen (N)	%wt	0.14 (0.08)	0.23 (0.02)
Sulfur (S)	%wt	-	0.31 (0.01)
Oxygen (by difference)	%wt	43.28 (0.31)	36.59 (0.73)
Proximate analysis, (db)			
Fixed carbon	%wt	18.31 (0.08)	26.34 (2.25)
Volatile	%wt	81.01 (0.11)	72.02 (2.27)
Ash	%wt	0.68 (0.02)	1.59 (0.16)
Moisture content, (wb)	%wt	50	16.62 (3.38)
Bulk density	kg m^{-3}	238.06 (5.28)	153.17 (3.52)
Geometric mean diameter	mm	14.818	-
Higher heating value, HHV	MJ kg^{-1}	20.42 (0.46)	21.48 (0.06)
Torrefied pellet HHV, 270°C	MJ kg^{-1}	22.97 (0.85)	-
Torrefied pellet HHV, 290°C	MJ kg^{-1}	27.10 (0.56)	-

Number enclosed in the parenthesis are standard deviations with n =3.

Table 5-3. Composition of pseudo components V1 and V2.

	V1 (%wt)	V2 (%wt)
Acetic acid	5.75	21.42
Water	43.89	17.74
Formic acid	3.11	6.05
Furfural	1.34	0.74
Hydroxyacetone	0.43	8.83
Acetone	0.28	0.00
5-HMF	0.06	1.00
Levoglucosan	0.00	13.84
2-methoxyphenol	0.00	0.47
CO_2	38.99	0.00
CO	6.14	29.02
CH_4	0.00	0.89

V1: $C_{0.394}H_{1.478}O_{1.287}$

V2: $C_{1.047}H_{1.993}O_{1.330}$

Table 5-4. Assumed thermodynamic and physical properties for the base case pinewood integrated torrefaction and pelletization plant with the capacity of 100,000 Mg yr^{-1}.

Parameter	Value/ Correlation	Ref.
Feedstock capacity	34.5 Mg h^{-1} wb, 50% MC	
Working hours	7440 h	
Pine wood HHV equation based on proximate analysis	$\mathrm{HHV} = 1.533 \times \mathrm{VM} + 1.878 \times \mathrm{FC} - 138.4$, $(\mathrm{MJ\ kg^{-1}})$	[58]
Solid higher heating value based on Boie equation	$\mathrm{HHV} = [351.69 \times \mathrm{Y}_C + 1162.46 \times \mathrm{Y}_H - 110.95 \times Y_O + 104.67 \times Y_S + 62.8 \times Y_N]/1000$, $(\mathrm{MJ\ kg^{-1}})$	[56]
Inlet air condition	25°C, RH: 50%	
Dry wood bulk density	238 kg m^{-3}	[10]
Particle size distribution		[10]
Wood (torrefied wood) thermal conductivity	0.12 (0.13) W m^{-1} K^{-1}	[60]
Oxygen content in flue gas	0.03 mol% (corresponding to 18% excess air)	
Drying process		
Fill grade	15%	
Bed porosity	0.8	
Dryer Dimension (ID x Length)	2.4 x 14	
Dryer rotation speed (ω)	3 rpm	
Drying kinetics:	$\frac{(X - X_e)}{(X_c - X_e)} = 0.9044.\exp(-0.024t)$ $X_e = 0.007$ db $X_c = 1$ db at T=353 °K	[41]
Hot flue gas temperature to the dryer	kept below 450°C	
Heat loss through surface area of the dryer to the surrounding environment	$h_{conv} = 1.32 \times (\frac{\Delta T}{D})^{0.25}$ $Q_{loss} = h_{conv} \times AS \times (T_{wall} - T_{amb})$ Twall= 80°C Tamb=25°C	[61]
Torrefaction		
Torrefaction temperature	Base case: 270°C	
Torrefaction residence time	30 min	
Torrefier diameter	3 m	

Parameter	Value/ Correlation		Ref.
Torrefaction kinetics	k_1	$2.48 \times 10^4 \exp(-75{,}976/RT), s^{-1}$	[4]
	k_{V1}	$3.23 \times 10^7 \exp(-114{,}214/RT), s^{-1}$	
	k_2	$1.1 \times 10^{10} \exp(-151{,}711/RT), s^{-1}$	
	k_{V2}	$1.59 \times 10^{10} \exp(-151{,}711/RT), s^{-1}$	
Torrefaction kiln rotation speed (ω)	6 rpm		
Hot flue gas (External gas) to the torrefier	950°C		
Grindability HGI	6.3, 12.5, and 24 for torrefied wood at 250, 270, 290°C, respectively.*		[10]
Final geometric mean diameter	0.5 mm		
Pelletizing energy	150 kWh Mg^{-1}		[34]

*The HGI indices for torrefied biomass at other temperatures were estimated from the fitted equation over the available data.

Simulation scenarios

The main case scenario was a simulation of the integrated torrefaction and pelletization of southern pine woodchips for the annual production of 100,000 Mg torrefied pellets with about 5% moisture content. The base case torrefaction temperature and residence time were 270°C and 30 min, respectively. The auxiliary fuel was natural gas. The variation of mass yield, energy yield, the higher heating value of the products, thermal energy requirement in dryer and torrefier, energy loss in the system, and the auxiliary energy requirement at the torrefaction temperature range of 230 to 290°C were also explored. Relevant input data are given in Table 5-4.

In order to evaluate the direct emissions from the systems, the base case scenario was rerun replacing the natural gas auxiliary fuel with bark biomass fuel. The initial bark biomass properties are given in Table 5-2. The composition of exhaust gas to the atmosphere was compared with the base case.

Results and discussion

This section presents the results obtained from the main unit operations including drying, torrefaction, and grinding. Also, the overall mass and energy balance for the base case scenario as well as the results of different torrefaction temperatures and different auxiliary fuels are discussed in detail.

Dryer results

The main outputs of the dryer for the base case scenario are given in Table 5-5. The dryer geometry was chosen for the base case capacity providing the proper output temperatures and moisture for the solid and off-gas streams. The solid and gas temperature profiles and moisture content profiles in the dyer are shown in Figure 5-3. As the moisture content in the solid phase decreased the temperature of solid increased contrary to the gas phase. The outlet solid and off-gas temperatures were 67 and 82°C, respectively. The moisture content of the solid reached to the 10 %wb (0.11 kg water kg dry solid^{-1}) and the moisture content of the gas at the dryer outlet was 0.14 kg water kg dry solid^{-1} corresponding to a relative humidity of 42%. The dryer duty was 2.7 GJ Mg^{-1} of evaporated water, which was comparable to the reported data for rotary dryers [62]. The rest of the input energy was lost through the dryer body and vent to the atmosphere. The calculated residence time for the dryer was less than 6 min, which is in the range of reported residence time for rotary dryers [39].

Table 5-5. Dryer simulation specification and results for the base case (torrefaction temperature 270°C, 100,000 Mg yr^{-1} torrefied pellets product).

Parameter	unit	Value
Geometry (D x L)	m x m	2.4 x 14
Feed mass flow rate	kg h^{-1}	34,500
Inlet moisture content	%	50
Thermal energy supply[a]	MJ h^{-1}	63,349
Drying duty	MJ h^{-1}	41,143
Electrical energy requirement	MJ h^{-1}	1,739
Dryer evaporation rate	kg h^{-1}	15,353
Residence time	min	5.7
Dryer efficiency	%	60.2
Dryer energy efficiency[b]	%	51.2
Dryer thermal efficiency[b]	%	55.2

a The thermal energy was supplied with off gas exhausted from the torrefier and a portion of flue gas from the burner.
b Efficiency of electricity generation was assumed as 35% for the total input energy.

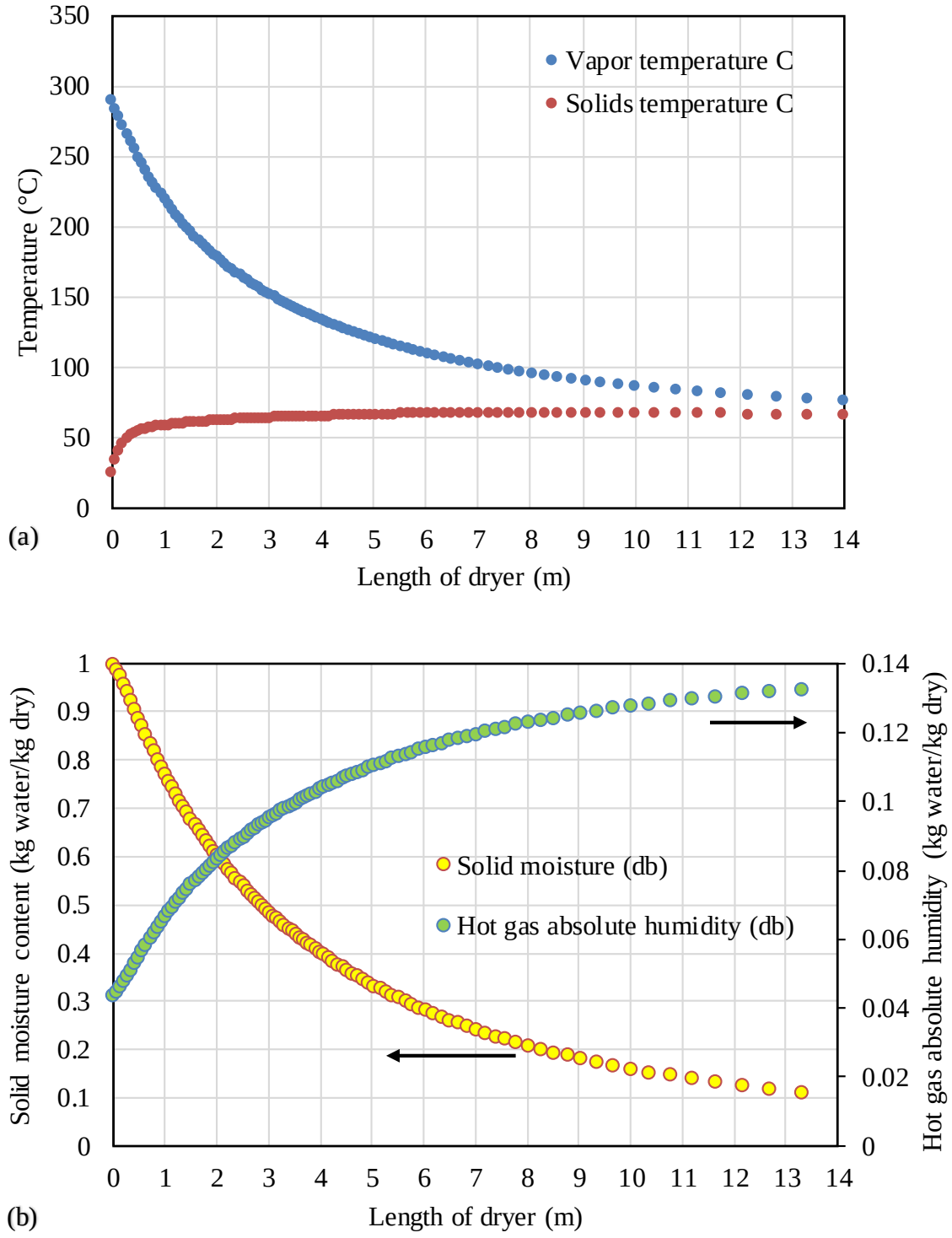

Figure 5-3. Solid and gas temperature (a) and moisture content (b) profiles in the dryer, base case scenario, 100,000 Mg yr^{-1} torrefied pellets product.

Torrefaction reactor results

Torrefaction reaction was successfully simulated through one RStoich and series of RPlug reactors. Figure 5-4 shows the results of solid mass yield, energy yield, and torsolid HHV from the simulation model within the torrefaction temperature range of 230 to 290°C and compares with the experimental data from torrefaction of pinewood material at 230, 250, 270, and 290°C and 30 min residence time [58]. The increase in torrefaction temperature resulted in further thermal decomposition of biomass, decreasing the solid mass yield. The predicted solid yields by simulation were slightly higher than the experimental data (Figure 5-4). The minor differences might be due to different biomass type in the simulation kinetics (willow) and experiments (pine) or approximate control of the reaction temperature and retention time in the lab experiments. As the result of dehydrogenation and deoxygenation in the torrefaction process, the O/C and H/C ratios in the biomass decrease, leading to the increase in the higher heating value of the remaining torsolid [63]. The higher heating values from the simulation were almost match the experimental data, which showed the accuracy of the Boie correlation, used in the simulation, for estimating the calorific value of the torrefied pine wood biomass. The energy yields calculated by Eq (8) decreased by an increase in the torrefaction temperature. Energy yield as a trade-off between the mass loss and quality gain (HHV) can be used to find the optimum torrefaction temperature.

The torgas composition from torrefaction of the pine wood within the temperature range of 230 to 290°C and 30 min residence time from the simulation results and experimental data are shown in Figure 5-5. Although the same experimental data was originally used to derive the compositions of a pseudo component of V1 and V2, this graph shows the accuracy of the stoichiometric coefficient calculated for the defined reactions in the software and also the proper implementation of the kinetics of the reaction. The acceptable conformity between the simulation

results and experimental data at the specified residence time validated the simulation parameters, which can be utilized to study of other operating conditions.

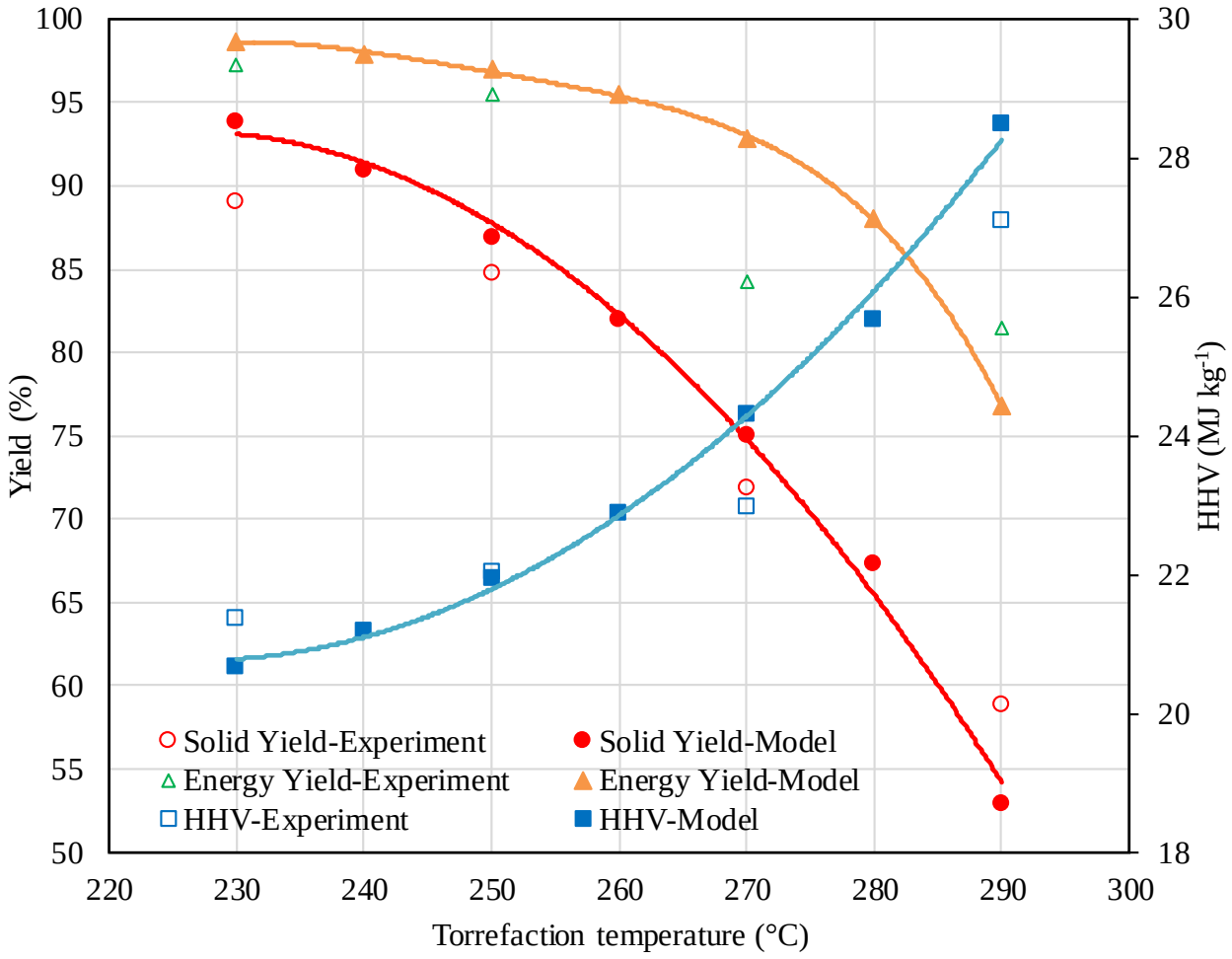

Figure 5-4. Variation of mass yield, energy yield, and higher heating value of torrefied biomass at different torrefaction temperature and 30 min residence time.

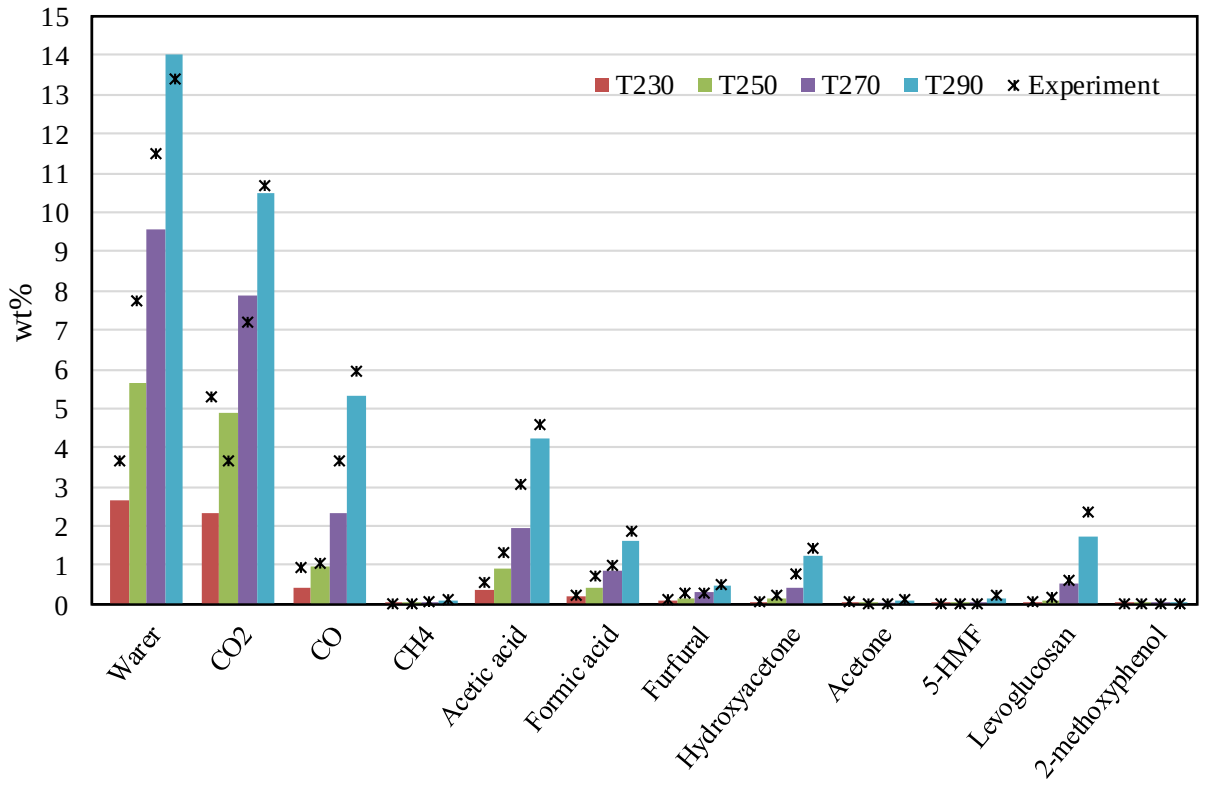

Figure 5-5. Torgas composition from pinewood torrefaction at a different temperature. T#: Torrefied at #°C. e.g., T230: torrefied at 230°C.

The general results of the torrefaction at the base case are shown in Table 5-6. The overall calculated length of the rotary kiln reactor was about 43 m, for the selected diameter (3 m) and residence time (30 min). Reaction heat strongly depends on the type of the biomass and reaction temperature. Nevertheless, the torrefaction heat of reaction at the base case was -0.12 MJ kg^{-1}, which was in the range of reported heat of torrefaction within 200 to 300°C in the literature (-0.8 to 0.7 MJ kg^{-1}) [64–66]. The biomass was heated-up to the torrefaction set point with high energy hot gas to minimize the length of the reactor and expedite the heating section. The excess energy was sent to the dryer section. Moreover, the exhaust torgas stream containing high energy value components was returned to the burner.

Table 5-6. Torrefaction reactor specification and results for the base case (torrefaction temperature 270°C, 100,000 Mg yr^{-1} torrefied pellets product).

Parameter	unit	Value
Geometry (D x L)	m x m	3 x 43
Feed mass flow rate	kg h^{-1}	19,147
Inlet moisture content	%	10
Residence time	min	30
Thermal energy supply[a]	MJ h^{-1}	71,339
Heat-up energy	MJ h^{-1}	12,298
Heat of reaction	MJ h^{-1}	-2,051
Electrical energy requirement[b]	MJ h^{-1}	2,156

a The thermal energy supplied with flue gas from the burner. The excess energy exhausted within off gas and torgas stream. The off-gas energy was sent to the dryer and torgas was returned to the burner.

b Efficiency of electricity generation was assumed as 35% for the total input energy.

Grinder results

The variation of the specific grinding energy of torrefied biomass by an increase in torrefaction temperature, which is corresponding to increase in HGI index is depicted in Figure 5-6. The specific grinding energy decreased by an increase in HGI index. The results of the Aspen Plus grinding model at torrefaction temperatures of 250, 270, and 290°C were comparable with the experimental data from a screen size of 2 mm [10].

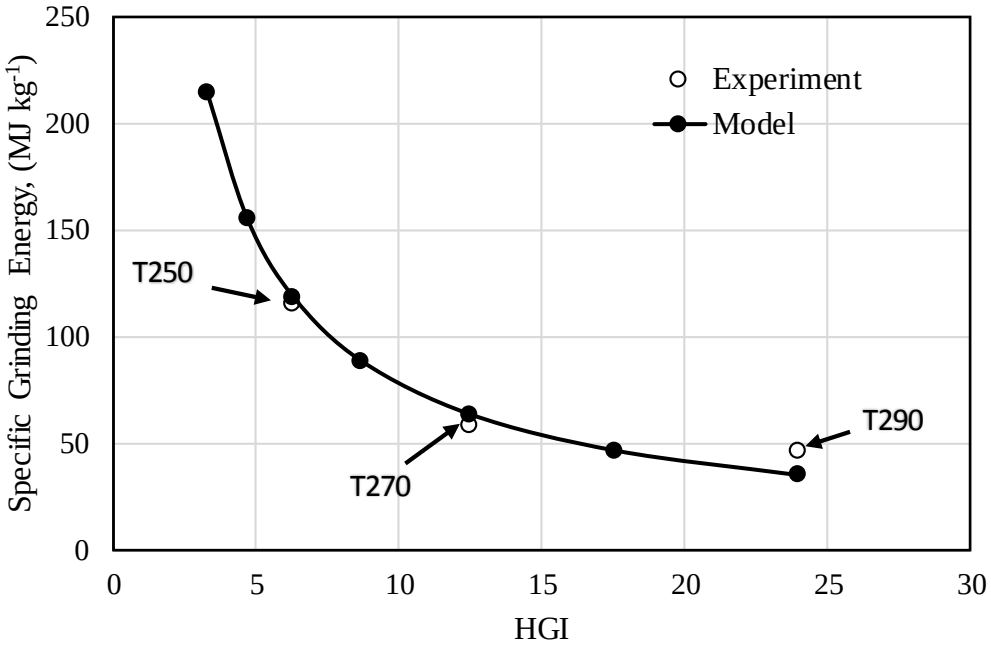

Figure 5-6. Specific grinding energy of torrefied biomass with different HGI index.

Overall plant mass and energy balance

Figure 5-7 shows the overall mass and energy balance of the torrefied pellet production for the base case scenario. Mass and energy balances were calculated assuming 100,000 Mg yr^{-1} of torrefied pellets product corresponding to 13.3 Mg h^{-1} torrefied pellet with ~ 5% moisture content. The drying step was considered to reduce the moisture content from 50 to 10%. The required energy for drying is the combination of latent heat for water evaporation and sensible heats for increasing the inlet temperatures of input biomass and water to the outlet temperatures. The input thermal energy provided the required drying duty as well as the excess energy, which is lost due to thermodynamic constraints of the heating systems. The electricity consumption in the drying section, mainly related to the exhaust fan and roller drive motor of the drum (supporting information), was about 483 kW (1739 MJ h^{-1}). The amount of the dry basis weight loss in torrefaction was about 25% at 270°C and 30 min residence time.

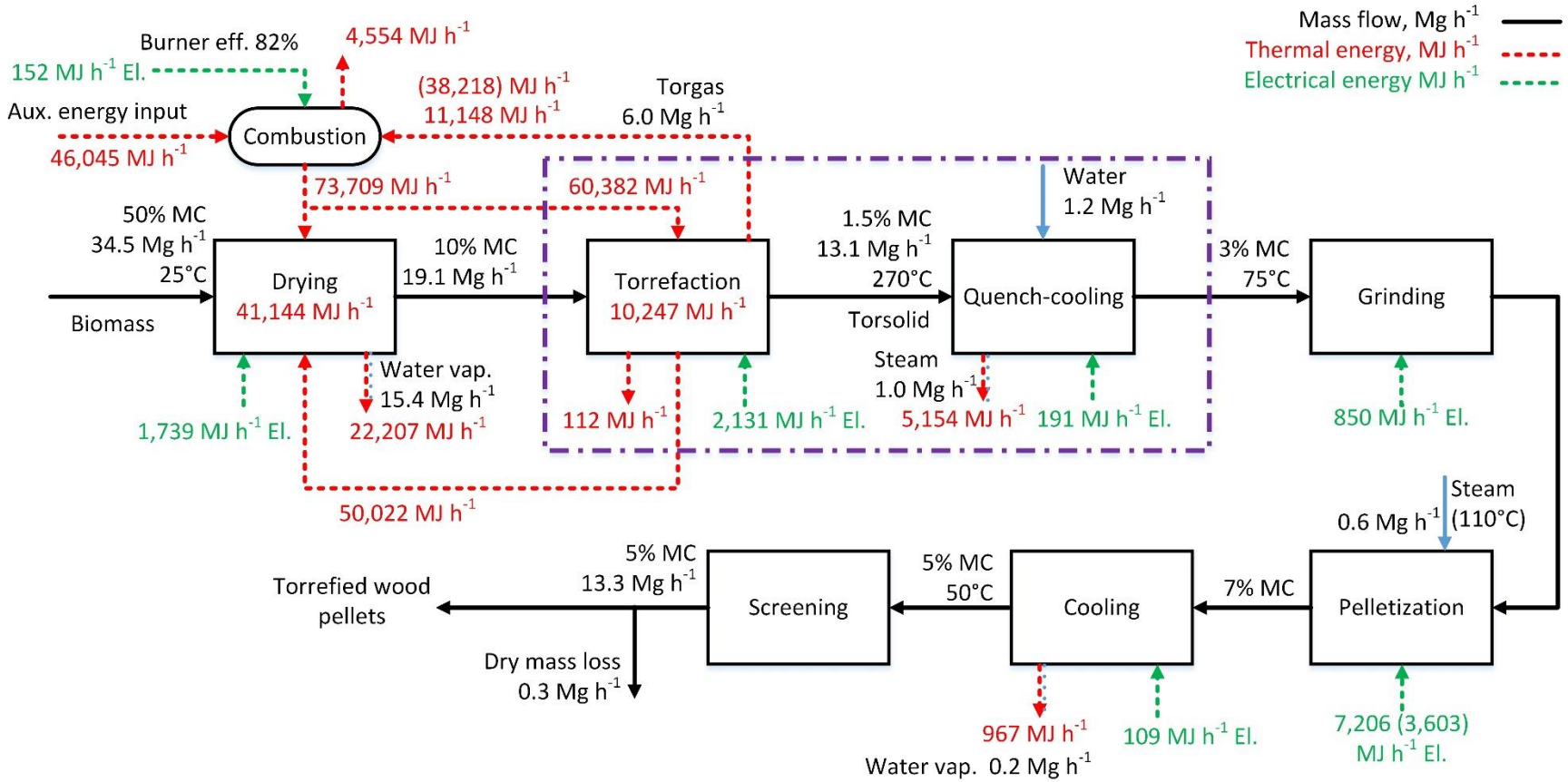

Figure 5-7. Mass and energy flows for the integrated torrefaction and pelletization system at the base case (torrefaction temperature 270°C, 100,000 Mg yr^{-1} torrefied pellets product).

The calculated energy released from torrefaction reaction at 270°C was -0.12 MJ kg^{-1} of dry feed, which was absorbed by the external media in the reactor. The electricity requirement for the torrefaction section was estimated about 592 kW (2131 MJ h^{-1}) from the relevant air and gas blowers and roller drive motor. The torgas product from torrefaction was sent to the integrated burner, where it was co-fired with the auxiliary fuel (natural gas in the base case) to provide the required heat in the torrefaction and drying sections. The overall calculated combustion efficiency was 82%, so the energy from the torgas combustion was slightly lower than its total heating value. Nevertheless, the remaining energy requirement was supplied by an increase in sensible heat after blowers. The input air for combustion was adjusted to reach less than 3% oxygen mole fraction in the flue gas. The corresponding excess air was about 18%. The hot flue gas was sent to the torrefaction reactor as the external heating media and then the excess energy was directed to the dryer, where it mixed with an extra amount of hot flue gas to dry the biomass to the specified level (10%). The auxiliary thermal energy required for the system was about 3.46 MJ kg^{-1} of product. The off-gas from the dryer was vented to the atmosphere.

The downstream unit operations mostly required electrical energy. Cooling of the torrefied biomass was simulated with the combination of direct water spraying and indirect air cooling. The amount of water was calculated in order to cool down the torrefied biomass to 150°C, which was further reduced to 75°C by the aid of air cooling. The produced steam was evacuated from the system. It was assumed that the moisture content of torrefied biomass would be increased to 3% as well. The electrical energy requirement was mainly from the air blowers. The torrefied biomass was then sent to the grinder. The obtained specific energy for grinding at the base case was 64 MJ Mg^{-1} (18 kWh Mg^{-1}), comparable with the experimental data for grinding energy of torrefied woodchips at 270°C [10]. The steam conditioning and water spraying were considered to increase

the temperature in the pelletization and to increase the moisture content of the biomass to around 7% after pelletizing. A subsequent cooling section reduced the moisture content to about 5%. Taken together, 2.5% dry mass loss apart from the loss due to torrefaction was considered in this case. Therefore, the calculated amount of feedstock was 34.5 Mg h^{-1} for the annual production of 100,000 Mg torrefied pellets at the base case. The detailed specification of main solid and gas streams depicted in Figure 5-1 are shown in Table 5-7 and 5-8.

Table 5-7. Simulation results for the gas phase streams base case (torrefaction temperature 270°C, 100,000 Mg yr^{-1} torrefied pellets product.)

	unit	NATGAS	TORGAS	AIR-BURN	HOTGASIN	TO-TOR	TOR-OFF	EXHAUST
Temperature	°C	25	277	25	25	295.2186415	1380	269
Mass Flows	kg hr^{-1}	1002	6012	25577	1	175623	29321	172352
Volume flow rate, mixture	M^3 hr^{-1}	1297	10748	22097	1	292530	141512	260594
Mass heat capacity, mixture	J $kg^{-1}K^{-1}$	2033	1660	1022	1022	1093	1538	1084
Higher heating value at 15°C	MJ kg^{-1}	51	8	0	0	0	1	0
Lower heating value at 15°C	MJ kg^{-1}	46	6	0	0	0	0	0

Table 5-8. Simulation results for the solid phase streams base case (torrefaction temperature 270°C, 100,000 Mg yr-1 torrefied pellets product.)

	unit	W-SWOOD	DRYSWOOD	TORSOLID	TOMILL	PRODUCT	LOSS
Temperature	°C	25	72	270	75	50	50
Mass Flows	kg hr^{-1}	34500	19147	13140	13343	13316	341
Volume flow rate, mixture	M^3 hr^{-1}	27	15	10	11	11	0
Mass heat capacity	J $kg^{-1}K^{-1}$	2517	2027	2299	1771	1753	1753
Moisture content	%	50	10	2	3	5	5
Higher heating value at 15°C	MJ kg^{-1}	19.66	19.66	23.44	23.44	23.44	23.44

Simulation results for different temperatures of torrefaction

The simulation model was run for different torrefaction temperatures in the range of 230 to 290°C. The variations of energy streams are displayed in Figure 5-8. The energy requirement for drying the initial biomass from 50% to 10% moisture content was almost constant. The slight increase was because of the lower mass of product at higher torrefaction temperature scenarios. The energy for heating up the biomass to the torrefaction temperature was slightly increased by the rise of the torrefaction temperature set point. On the other hand, the heat released due to the reactions was also increased. Therefore, the overall energy requirement for torrefaction was slightly decreased over the temperature. The two major energy changes were related to the miscellanies energy (other than drying and torrefaction) and lost energy, and torgas energy. The amount of energy from combustion of torgas escalated by an increase in torrefaction temperature, due to increase in torgas yield and the amount of high-value components. However, energy loss through the system and the input energy to the torrefaction raised as well. The main sources of the energy loss from the whole system were loss through the burner, exhaust gas to the atmosphere from dryer, and loss through equipment bodies. The energy loss due to convection and radiation through the burner increased slightly over the torrefaction temperature increase, while the rest of the losses were almost kept constant. On the other hand, along with the increase in torrefaction temperature, the input energy to the torrefaction increased substantially, leading to an increase in external off-gas energy and exhaust torgas energy. The rise in energy requirement at higher torrefaction temperatures was mainly compensated by the energy from the combustion of the torgas, which is resent to the burner. Therefore, the amount of supplementary energy required for the system, provided by the auxiliary fuel, decreased by an increase in temperature torrefaction. That means the process moved towards auto-thermal operation at higher torrefaction temperatures.

It is worth noting that the retention time of reaction is also important, which was kept constant in this study. Higher retention time incurs greater conversion of biomass and increases the amount of torgas yield. That might provide the auto-thermal condition at lower torrefaction temperature at the higher retention time. The proper torrefaction condition is chosen based on the trade-off between energy requirements and the final yields. The electrical energy requirement per mass of the product was almost constant over all torrefaction temperatures.

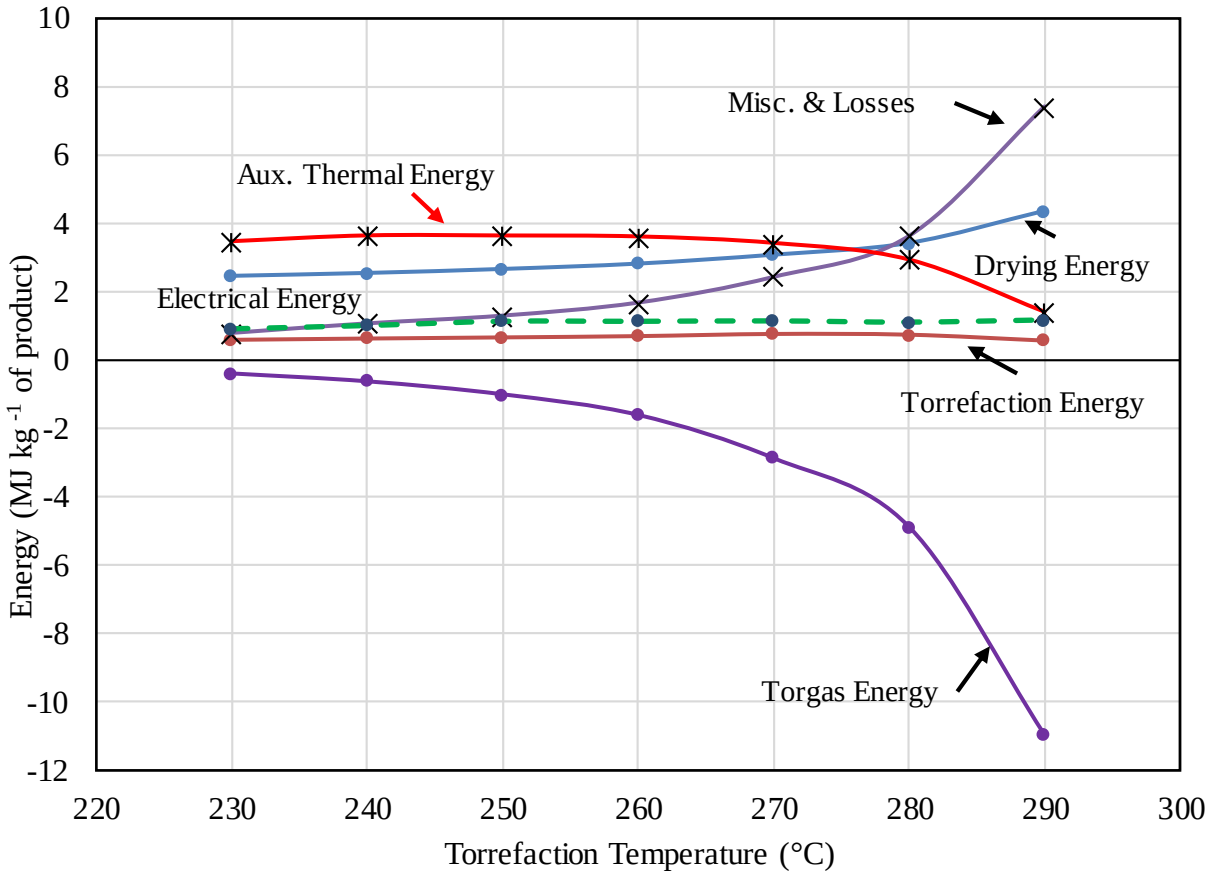

Figure 5-8. Trend of energy Flows versus torrefaction temperature.

The breakdown energy requirements for the integrated system at 250, 270, and 290°C torrefaction temperature are given in Table 5-9. The total thermal energy demand in iBTP plant related to drying, heat-up, and compensation of miscellaneous energy and losses in the system. The thermal energy demand was provided by the torgas combustion, heat of reaction, and combustion of the auxiliary fuel. Total thermal energy demand decreased by an increase in the torrefaction temperature, whereas the auxiliary energy reduced. The results from 290°C case showed the significant increase in the heat release due to the higher exothermic reaction at a higher temperature. The heat of reaction reported for torrefaction system in the literature widely ranged from -0.7 to 0.8 MJ kg^{-1} feed input to the reactor [64–66] based on temperature and type of feedstock. In this study, the heat of reaction for TAP process at a temperature range of 250 to 290°C varied from -0.06 to -0.4 MJ kg^{-1} of inlet feed to the reactor, corresponding to -0.07 to -0.83 MJ kg^{-1} of the final product. Moreover, the torgas energy content was remarkably intensified. The calculated lower heating value of torrefaction volatiles (torgas) was in the range of 3.9 to 10.4 MJ kg^{-1} at torrefaction temperatures 250 to 270°C, similar to earlier studies [66–68]. The energy released during torrefaction was slightly lower in TAP scenarios due to lower moisture content. These together resulted in a major reduction in the auxiliary energy requirement. The energy from combustion of torgas product supplied more than 88% of the total thermal energy requirement for 290°C case, whereas it supplied about 45% of the base case.

Table 5-9. Energy balance of the integrated torrefaction and pelletization plant at T250, T270, and T290.

	T250[a]	T270	T290	Ref
Feedstock flowrate, kg h^{-1}	34500	34500	34500	
Feed moisture content, %	50	50	50	
Feed HHVd, MJ kg^{-1}	19.7	19.7	19.7	
Final product, kg h^{-1}	15407	13316	9400	
Product moisture content, %	5.2	5.2	5.3	
Final Solid product HHVd, MJ kg^{-1}	22	24	29	
Torrefaction mass yield, %	87	75	53	
Feed to product ratio, wb	2.2	2.6	3.7	
Energy yield of the torrefaction, %	97	93	77	
Energy yield of the whole system, %	95	90	75	
Drying [b], MJ kg^{-1} of product	2.67	3.09	4.38	[62]
Torrefaction [c], MJ kg^{-1} of product	0.67	0.77	0.57	
Tor-cooling, MJ kg^{-1} of product	-0.36	-0.39	-0.40	
Pellet cooling, MJ kg^{-1} of product	-0.08	-0.07	-0.07	
Thermal energy requirement, MJ kg^{-1} of product	4.65	6.33	12.38	
Torgas energy, MJ kg^{-1} of product	1.00	2.87	10.97	
NG energy, MJ kg^{-1} of product	3.65	3.46	1.41	
Electrical energy required, MJ kg^{-1} of product				
Drying and burning	0.14	0.14	0.20	
Torrefaction	0.15	0.16	0.23	
Tor-cooling	0.02	0.01	0.01	
Grinding	0.12	0.06	0.04	[41,72,73]
Pelletization (with binder)	0.54 (0.27)	0.54 (0.27)	0.54 (0.27)	[69–71]
Pellet cooling	0.01	0.01	0.01	
Total energy required [d]	7.43 (6.66)	8.99 (8.21)	15.33 (14.56)	

[a] T#: Torrefied at #°C. e.g., T250: torrefied at 250°C.

[b] The energy consumed in drying.

[c] The summation of energy required for heat-up and release from the reaction.

[d] Efficiency of electricity generation was assumed as 35%.

The electrical energy requirement was increased by the torrefaction temperature as well. The pelletization energy was the major contributor to the electrical energy demand. The required energy for pelletizing of torrefied biomass has been reported in the range of 288-1163 MJ Mg^{-1} [69–71], while Topell Energy claimed to achieve the energy consumption of 162 MJ Mg^{-1} by adding appropriate binders [34]. Considering the binder addition for pelletization, the pelletizing energy could be halved, resulting in a reduction of the total electrical energy requirement up to 10%. The total energy consumption for production of the torrefied pellets, considering 35% efficiency for electricity generation varied from 7.4 to 15.3 MJ kg^{-1} (6.7 to 14.6 MJ kg^{-1} with binder) of the torrefied pellets for three torrefaction temperatures of 250, 270, and 290°C. The total energy requirement together with the mass yield and energy yield should be taken into account to choose the proper operating conditions for the system.

Simulation results for using bark as the auxiliary fuel

The required energy for the iBTP system is mainly provided by the combustion of the torgas. Below the auto-thermal points, the remaining energy requirement is compensated by the combustion of an auxiliary fuel. The direct emissions from the whole system originate from the combustion of torgas and the auxiliary fuel. In a way towards sustainability and reducing the greenhouse gas emissions, the investigation of impacts of using renewable fuels such as bark biomass instead of natural gas fuel is indispensable. The main difference between the base case scenario and the bark-fuel scenario was in the exhaust gas composition, which is shown in Table 5-10.

Table 5-10. Exhaust gas properties and emissions from iBTP with two different auxiliary fuels.

Parameter	**System exhaust gas**	
	Base case	Bark fuel
Temp (°C)	82	86

Mass flow ($kg\ h^{-1}$)	190976	151521
Volume flow ($m^3\ h^{-1}$)	197952	160119
RH (%)	36	38
Mass fraction (%)		
H_2O	0.12	0.15
N_2	0.67	0.64
O_2	0.18	0.16
CO_2	0.03	0.05
CO	1.06E-05	9.80E-06
N_2O	1.36E-08	1.43E-08
NO	2.10E-04	2.22E-04
NO_2	3.36E-07	3.99E-07
SO_2	1.41E-06	9.15E-05
H_2S	1.14E-16	2.50E-15

The notable difference was the lower amount of nitrogen compounds (NO, NO_2, and N_2O) emissions in the bark-fuel scenario. The lower airborne NOx emissions from the biomass fuels, compared to coal and natural gas, have been extensively investigated and proved in the literature [74]. The amount of CO_2 emission in bark scenario was slightly higher than the base case scenario, which is not accounted for the GHG emissions due to carbon neutrality of biomass fuels [75,76]. It is believed that in a sustainable management of biomass growth, where enough biomass pools are provided for capturing the released carbon, the neutral carbon context of biomass fuels can be largely preserved.

Discussion

In this study, the solid dryer was simulated with a good conformity to the real industrial solid dryers. The detail properties of the inlet solid and hot gas stream including the specific properties of the different component, moisture content, drying kinetics, and temperature was considered in the mass and energy calculations. The model successfully described the output limitations for the

off-gas temperature and moisture content and estimated the input energy required to perform the drying process. The drum rotation parameter and flights' surface areas are not considered in the solid convective dryer in Aspen Plus, which constraints the representation of an industrial rotary dryer to some extent. The heat transfer coefficient and residence time are affected by the excess surface area of the flights and rotation of the drum in the real industrial dryer, which can reduce the total energy requirement. Nevertheless, the model can estimate the energy input in a conservative way that covers the possible extra losses in the real systems. In this study, the modified residence time was estimated with an empirical equation for rotary drum dryers.

The torrefaction process was the main core of the system. A good agreement was observed between the mass yield, energy yield, and torgas compositions of the experimental data and simulation results. The RPlug reactor could describe the torrefaction kinetics. However, the filling grade, rotation of the kiln, and the heat transfer coefficient was implemented by the relevant FORTRAN code. The complex flash calculation between non-conventional solid and gas phase was not fully developed in the Aspen Plus V9 that limited the tracing of the reactor inside temperatures, torgas, and torsolid, separately. The other constraint was the calculated length of the reactor by the Aspen Plus model which could not represent the volume based on the non-conventional solids. In this study, the length was modified later, by having the solid properties. A more desirable reactor model could be a combination of a solid convective dryer and an RPlug that allows considering the solid properties and reactions' kinetics together.

The grinding process was simulated with a crushing unit, which has been mainly developed for size reduction of brittle materials. The general power calculation in a simple mode of crushing was based on the Bond Work Index equation, which is not a most desirable model for describing the biomass grinding. Although the calculated energy consumption with the specified HGI indices

as input was fairly comparable with the experimental data, the obtained BWI indices (from the predefined equation in Aspen Plus) were calculated for a range of soft and brittle materials. Further studies are recommended to develop a grinding unit operation in Aspen Plus for describing the biomass with the relevant grindability parameters. No unit operation has been specified in Aspen Plus to simulating a pelletization process. The variation in moisture content and particle size distribution were modeled through a combination of an RYield and a granulator model. However, the energy required for pelletizing could not be estimated from the simulation and was entered into the system via a calculation block.

The overall mass and energy balance were performed in detail. The results for the total thermal and electrical energy requirement were comparable with the literature data. Such a process simulation model with detailed information for inputs and outputs of each unit operation is a useful tool for determining the design parameters of the system and cost evaluation in a techno-economic analysis. It also benefits to trace the emission from the system and evaluate the potential environmental hazards, which is used in the life cycle assessment studies. A robust process simulation model can be used further, especially in the feasibility study phase of the project, for Hazard and Operability Studies (HAZOP) that helps to distinguish the impacts of deviating from operating conditions. A decent process simulation model, which represents the real operating conditions of the real system increase the efficiency, minimize the loss and improve the safety of the system.

Conclusion

A process simulation framework was developed for evaluation of an integrated biomass torrefaction and pelletization (iBTP) system using Aspen Plus V9 software. Several Aspen Plus unit operation blocks were combined with FORTRAN calculation blocks using kinetics data and

experimental data from the literature. A pre-defined RPlug reactor was used to simulate the torrefaction process as the main core of the system. The model was used to predict the overall mass and energy balance, efficiency, and emissions for production of torrefied pellets from pine wood feedstock. As the torrefaction temperature increased the mass yield and energy yield reduced, while the calorific value of the torrefied solid and torgas products improved. The iBTP system leaned towards auto-thermal condition at higher torrefaction temperatures, where the auxiliary energy requirement minimized. The feedstock mass and total energy input for producing 100,000 Mg yr^{-1} torrefied pellets at 270°C was 34.5 Mg h^{-1} (2.6 Mg Mg^{-1} of product) and 8.2- 9 MJ $kg^{-1}$of product, respectively. The total energy consumption, mass and energy yield, emissions' compositions, and product specifications obtained from the model can be utilized to conduct a techno-economic analysis, life cycle assessment studies, and hazard and operability studies for an industrial system.

Acknowledgments

This research was fully supported by the Consortium for Advanced Wood-to-Energy Solutions (CAWES) with funding provided by USDA Forest Products Laboratory (www.fs.fed.us) and U.S. Endowment for forestry and communities (www.usendowment.org). The authors thank the consortia members. CAWES is a public/private partnership initially formed by the USDA Forest Service, the U.S. Endowment for Forestry and Communities, and a number of innovative private companies and university partners committed to advancing sustainable, scalable, distributed wood-to-energy solutions that stimulate forest restoration and rural economic development.

References

[1] Bergman PCA. Combined torrefaction and pelletisation the TOP process. Energy Cent Netherlands, Rep No ECN-C-05-073, ECN, Petten, Netherlands 2005.

[2] Bergman PCA, Boersma AR, Zwart RWR, Kiel JHA. Torrefaction for biomass co-firing in existing coal-fired power stations. Energy Cent Netherlands, Rep No ECN-C-05-013, Petten, Netherlands 2005.

[3] Tumuluru JS, Sokhansanj S, Hess JR, Wright CT, Boardman RD. A review on biomass torrefaction process and product properties for energy applications. Ind Biotechnol 2011;5. doi:10.1089/ind.2011.0014.

[4] Prins MJ, Ptasinski KJ, Janssen FJJG. Torrefaction of wood: Part 1. Weight loss kinetics. J Anal Appl Pyrolysis 2006;77:28–34.

[5] Koppejan J, Sokhansanj S, Melin S, Madrali S. Status overview of torrefaction technologies, a review of the commercialisation status of biomass torrefaction. IEA Energy Technol Network, IEA Bioenergy Task 32 2015.

[6] Phanphanich M, Mani S. Impact of torrefaction on the grindability and fuel characteristics of forest biomass. Bioresour Technol 2011;102:1246–53. doi:10.1016/j.biortech.2010.08.028.

[7] Boateng AA, Mullen CA. Fast pyrolysis of biomass thermally pretreated by torrefaction. J Anal Appl Pyrolysis 2013;100:95–102. doi:10.1016/j.jaap.2012.12.002.

[8] Kumar A, Jones DD, Hanna MA. Thermochemical Biomass Gasification: A Review of the Current Status of the Technology. Energies 2009;2:556–81. doi:10.3390/en20300556.

[9] Basu P, Rao S, Acharya B, Dhungana A. Effect of torrefaction on the density and volume

changes of coarse biomass particles. Can J Chem Eng 2013;91:1040–4. doi:10.1002/cjce.21817.

[10] Manouchehrinejad M, Giesen I Van, Mani S. Grindability analysis of torrefied wood chips and wood pellets n.d.:1–35.

[11] Stelte W. Best Practice Guideline - Storage and Handling of torrefied biomass. Danish Technol Institute, Denmark 2015.

[12] Nhuchhen D, Basu P, Acharya B. A Comprehensive Review on Biomass Torrefaction. Int J Renew Energy Biofuels 2014;2014:1–56. doi:10.5171/2014.506376.

[13] Chen WH, Peng J, Bi XT. A state-of-the-art review of biomass torrefaction, densification, and applications. Renew Sustain Energy Rev 2015;44:847–66. doi:10.1016/j.rser.2014.12.039.

[14] Dudgeon R. An Aspen Plus Model of Biomass Torrefaction. Electr Power Res Inst … 2009:12.

[15] Haryadi, Hardianto T, Pasek AD, Suwono A, Azhari R, Ardiansyah W. The Aspen TM Software Simulation of a Peat Torrefaction System Using RYield and SSplit Block as Reactor Model. Proc Int Symp Sustain Energy Environ Prot 2009:23–6.

[16] Nikolopoulos N, Isemin R, Atsonios K, Kourkoumpas D, Kuzmin S, Mikhalev A, et al. Modeling of wheat straw torrefaction as a preliminary tool for process design. Waste and Biomass Valorization 2013;4:409–20. doi:10.1007/s12649-013-9198-y.

[17] Arteaga-Perez LE, Segura C, Espinoza D, Radovic LR, Jimenez R. Torrefaction of Pinus radiata and Eucalyptus globulus: A combined experimental and modeling approach to process synthesis. Energy Sustain Dev 2015;29:13–23. doi:10.1016/j.esd.2015.08.004.

[18] Bach QV, Skreiberg Ø, Lee CJ. Process modeling and optimization for torrefaction of

forest residues. Energy 2017;138:348–54. doi:10.1016/j.energy.2017.07.040.

[19] Cherry RS, Wood R a, Westover TL. Analysis of the Production Cost for Various Grades of Biomass Thermal Treatment. US Dep Energy, Idaho Natl Lab INL/EXT-13-30348, Idaho Falls, Idaho 2013.

[20] Peters JF, Banks SW, Bridgwater A V., Dufour J. A kinetic reaction model for biomass pyrolysis processes in Aspen Plus. Appl Energy 2017;188:595–603. doi:10.1016/j.apenergy.2016.12.030.

[21] Visconti A, Miccio M, Juchelkova D. Equilibrium-based simulation of lignocellulosic biomass pyrolysis via Aspen Plus. Recent Adv Appl Math Model Simul 2015:242–51.

[22] Arteaga-Pérez LE, Segura C, Espinoza D, Radovic LR, Jiménez R. Torrefaction of Pinus radiata and Eucalyptus globulus: A combined experimental and modeling approach to process synthesis. Energy Sustain Dev 2015;29:13–23. doi:10.1016/j.esd.2015.08.004.

[23] Syu FS, Chiueh PT. Process simulation of rice straw torrefaction. Sustain Environ Res 2012;22:177–83.

[24] Batidzirai B, Mignot a. PR, Schakel WB, Junginger HM, Faaij APC. Biomass torrefaction technology: Techno-economic status and future prospects. Energy 2013;62:196–214. doi:10.1016/j.energy.2013.09.035.

[25] Chai L, Saffron CM. Comparing pelletization and torrefaction depots: Optimization of depot capacity and biomass moisture to determine the minimum production cost. Appl Energy 2016;163:387–95. doi:10.1016/j.apenergy.2015.11.018.

[26] Adams PWR, Shirley JEJ, McManus MC. Comparative cradle-to-gate life cycle assessment of wood pellet production with torrefaction. Appl Energy 2015;138:367–80. doi:10.1016/j.apenergy.2014.11.002.

[27] Fagernäs L, Brammer J, Wilén C, Lauer M, Verhoeff F. Drying of biomass for second generation synfuel production. Biomass and Bioenergy 2010;34:1267–77. doi:10.1016/j.biombioe.2010.04.005.

[28] Mani S, Tabil LG, Sokhansanj S. Effects of compressive force, particle size and moisture content on mechanical properties of biomass pellets from grasses. Biomass and Bioenergy 2006;30:648–54. doi:10.1016/j.biombioe.2005.01.004.

[29] Samuelsson R, Larsson SH, Thyrel M, Lestander TA. Moisture content and storage time influence the binding mechanisms in biofuel wood pellets. Appl Energy 2012;99:109–15. doi:10.1016/j.apenergy.2012.05.004.

[30] Prins MJ, Ptasinski KJ, Janssen FJJG. Torrefaction of wood: Part 2. Analysis of products. J Anal Appl Pyrolysis 2006;77:35–40.

[31] Guo S, Dong X, Wu T, Zhu C. Influence of reaction conditions and feedstock on hydrochar properties. Energy Convers Manag 2016;123:95–103. doi:10.1016/j.enconman.2016.06.029.

[32] Li MF, Chen LX, Li X, Chen CZ, Lai YC, Xiao X, et al. Evaluation of the structure and fuel properties of lignocelluloses through carbon dioxide torrefaction. Energy Convers Manag 2016;119:463–72. doi:10.1016/j.enconman.2016.04.064.

[33] Iroba KL, Tabil LG, Sokhansanj S, Dumonceaux T. Pretreatment and fractionation of barley straw using steam explosion at low severity factor. Biomass and Bioenergy 2014;66:286–300. doi:10.1016/j.biombioe.2014.02.002.

[34] Koppejan J, Sokhansanj S, Melin S, Madrali S. Status overview of torrefaction technologies. 2012.

[35] Peng JH, Bi HT, Lim CJ, Sokhansanj S. Study on density, hardness, and moisture uptake

of torrefied wood pellets. Energy & Fuels 2013;27:967–74. doi:10.1021/ef301928q.

[36] Stelte W, Nielsen NPK, Hansen HO, Dahl J, Shang L, Sanadi AR. Pelletizing properties of torrefied wheat straw. Biomass and Bioenergy 2013;49:214–21.

[37] Sultana A, Kumar A, Harfield D. Development of agri-pellet production cost and optimum size. Bioresour Technol 2010;101:5609–21. doi:10.1016/j.biortech.2010.02.011.

[38] Bergman RDP, Reed DL, Taylor AM, Harper DP, Hodges DG, Bergman RDP, et al. cradle-to-gate life cycle assessment of switchgrass fuel pellets manufactured in the southeastern. Wood Fiber Sci 2015;47:1–13.

[39] Amos W a. Report on Biomass Drying Technology. Natl Renew Energy Lab 1998;106:475–485. doi:NREL/TP-570-25885.

[40] Pang S, Mujumdar AS. Drying of woody biomass for bioenergy: Drying technologies and optimization for an integrated bioenergy plant. Dry Technol 2010;28:690–701. doi:10.1080/07373931003799236.

[41] Phanphanich M, Mani S. Drying characteristics of pine forest residues. BioResources 2010;5:108–20.

[42] Perry RH, Chilton CH. Chemical engineering's handbook. McGraw-Hill Kogakusha, Ltd 1973:2–74.

[43] Vieira MGA, Estrella L, Rocha SCS. Energy Efficiency and Drying Kinetics of Recycled Paper Pulp. Dry Technol 2007;25:1639–48. doi:10.1080/07373930701590806.

[44] Boateng AA. Rotary Kilns Transport Phenomena and Transport Processes. Butterworth-Heinemann 2015.

[45] Babler MU, Phounglamcheik A, Amovic M, Ljunggren R, Engvall K. Modeling and pilot plant runs of slow biomass pyrolysis in a rotary kiln. Appl Energy 2017;207:123–33.

doi:10.1016/j.apenergy.2017.06.034.

[46] Li S-Q, Ma L-B, Wan W, Yao Q. A Mathematical Model of Heat Transfer in a Rotary Kiln Thermo-Reactor. Chem Eng Technol 2005;28:1480–9. doi:10.1002/ceat.200500241.

[47] Nhuchhen DR, Basu P, Acharya B. Investigation into overall heat transfer coefficient in indirectly heated rotary torrefier. Int J Heat Mass Transf 2016;102:64–76. doi:10.1016/j.ijheatmasstransfer.2016.06.011.

[48] Blasi C Di, Lanzetta M, Di Blasi C, Lanzetta M. Intrinsic kinetics of isothermal xylan degradation in inert atmosphere 1997;40. doi:10.1016/S0165-2370(97)00028-4.

[49] Branca C, Di Blasi C. Kinetics of the isothermal degradation of wood in the temperature range 528–708 K. J Anal Appl Pyrolysis 2003;67:207–19. doi:10.1016/S0165-2370(02)00062-1.

[50] Shang L, Ahrenfeldt J, Holm JK, Bach LS, Stelte W, Henriksen UB. Kinetic model for torrefaction of wood chips in a pilot-scale continuous reactor. J Anal Appl Pyrolysis 2014;108:109–16. doi:10.1016/j.jaap.2014.05.010.

[51] Bates RB, Ghoniem AF. Biomass torrefaction: Modeling of volatile and solid product evolution kinetics. Bioresour Technol 2012;124:460–9. doi:10.1016/j.biortech.2012.07.018.

[52] Gul S, Ramzan N, Hanif MA, Bano S. Kinetic, volatile release modeling and optimization of torrefaction. J Anal Appl Pyrolysis 2017;128:44–53. doi:10.1016/j.jaap.2017.11.001.

[53] Di Blasi C, Lanzetta M. Intrinsic kinetics of isothermal xylan degradation in inert atmosphere. J Anal Appl Pyrolysis 1997;40:287–303. doi:10.1016/S0165-2370(97)00028-4.

[54] Kirov NY. Specific heats and total heat contents of coals and related materials at elevated

temperatures. BCURA Mon Bull 1965;29:33–9.

[55] Nhuchhen D, Afzal M. HHV Predicting Correlations for Torrefied Biomass Using Proximate and Ultimate Analyses. Bioengineering 2017;4:7. doi:10.3390/bioengineering4010007.

[56] Boie W. Fuel technology calculations. Energietechnik 1953;3:309–16.

[57] Naimi LJ, Sokhansanj S, Bi X, Lim CJ, Womac AR, Lau AK, et al. Development of size reduction equations for calculating energy input for grinding lignocellulosic particles. Appl Eng Agric 2013;29:93–100. doi:10.13031/2013.42523.

[58] Manouchehrinejad M, Mani S. Torrefaction after Pelletization (TAP): Evaluation of torrefied pellet quality and co-products. Biomass and Bioenergy 2018:1–38.

[59] Shrestha R. Experimental Analysis and Modeling of Biomass Gasification using a Downdraft Gasifier. Dr Diss 2014.

[60] Mason PE, Darvell LI, Jones JM, Williams A. Comparative Study of the Thermal Conductivity of Solid Biomass Fuels. Energy Fuels 2016;30:2158–63. doi:10.1021/acs.energyfuels.5b02261.

[61] Perry's RH, Chilton CH, Kirkpatrick SD. Chemical engineers handbook. Chem Eng Handb 1999.

[62] Li H, Chen Q, Zhang X, Finney K. Evaluation of a biomass drying process using waste heat from process industries: A case study. Appl Therm Enginering 2012;35:71–80. doi:10.1016/j.applthermaleng.2011.10.009.

[63] Qu TT, Guo WJ, Shen LH, Xiao J, Zhao K. Experimental Study of Biomass Pyrolysis Based on Three Major Components: Hemicellulose, Cellulose, and Lignin. Ind Eng Chem Res 2011;50:10424–33. doi:10.1021/ie1025453.

[64] Ohliger A, Förster M, Kneer R. Torrefaction of beechwood: A parametric study including heat of reaction and grindability. Fuel 2013;104:607–13. doi:10.1016/j.fuel.2012.06.112.

[65] Stelte W, Holm JK, Sanadi AR, Barsberg S, Ahrenfeldt J, Henriksen UB. A study of bonding and failure mechanisms in fuel pellets from different biomass resources. Biomass and Bioenergy 2011;35:910–8. doi:10.1016/j.biombioe.2010.11.003.

[66] Bates RB, Ghoniem AF. Biomass torrefaction: Modeling of reaction thermochemistry. Bioresour Technol 2013;134:331–40. doi:10.1016/j.biortech.2013.01.158.

[67] Prins MJ, Ptasinski KJ, Janssen FJJG. More efficient biomass gasification via torrefaction. Energy 2006;31:3458–70. doi:10.1016/j.energy.2006.03.008.

[68] Doddapaneni TRKC, Praveenkumar R, Tolvanen H, Rintala J, Konttinen J. Techno-economic evaluation of integrating torrefaction with anaerobic digestion. Appl Energy 2018;213:272–84. doi:10.1016/j.apenergy.2018.01.045.

[69] Stelte W, Dahl J, Nielsen N peter k., Hansen H ove. Densification concepts for torrefied biomass. Denmark: 2012.

[70] Järvinen T, Agar D. Experimentally determined storage and handling properties of fuel pellets made from torrefied whole-tree pine chips, logging residues and beech stem wood. Fuel 2014;129:330–9. doi:10.1016/j.fuel.2014.03.057.

[71] Ghiasi B, Kumar L, Furubayashi T, Lim CJ, Bi X, Kim CS, et al. Densified biocoal from woodchips: Is it better to do torrefaction before or after densification? Appl Energy 2014;134:133–42. doi:10.1016/j.apenergy.2014.07.076.

[72] Repellin V, Govin A, Rolland M, Guyonnet R, Vincent R, Alexandre G, et al. Energy requirement for fine grinding of torrefied wood. Biomass and Bioenergy 2010;34:923–30. doi:10.1016/j.biombioe.2010.01.039.

[73] Tapasvi D, Khalil R, Skreiberg Ø, Tran KQ, Grønli M. Torrefaction of Norwegian birch and spruce: An experimental study using macro-TGA. Energy and Fuels, vol. 26, 2012, p. 5232–40. doi:10.1021/ef300993q.

[74] Agbor E, Zhang X, Kumar A. A review of biomass co-firing in North America. Renew Sustain Energy Rev 2014;40:930–43. doi:10.1016/j.rser.2014.07.195.

[75] Cherubini F, Peters GP, Berntsen T, Strømman AH, Hertwich E. CO2 emissions from biomass combustion for bioenergy: Atmospheric decay and contribution to global warming. GCB Bioenergy 2011;3:413–26. doi:10.1111/j.1757-1707.2011.01102.x.

[76] Schweinle J, Rödl A, Börjesson P, Neary DG, Langeveld JW a., Berndes G, et al. Assessing the environmental performance of biomass supply chains. IEA Bioenergy Task 43, Rep 2015TR01 2015:123. doi:IEA Bioenergy Task 43, Repport 2015:TR01.

CHAPTER 6

TECHNO-ECONOMIC ANALYSIS OF TORREFIED PELLET PRODUCTION THROUGH TOP AND TAP CONFIGURATIONS [1]

[1] Manouchehrinejad M and Mani S. To be submitted to Journal of Cleaner Production, (2018).

Abstract

The techno-economic analysis of an integrated torrefaction and pelletization with a new configuration of torrefaction after pelletization (TAP) was investigated in this study. The detailed operating parameters including mass and energy balances and process efficiencies, obtained from a process simulation study, were comparable with the conventional torrefied pellet production (TOP). The economic evaluation showed a 15% reduction in the total capital investment of a 100,000 Mg yr^{-1} production capacity TAP plant compared to a TOP plant. The production cost of the base case was \$6.9 GJ^{-1} and slightly lower the conventional TOP plant. The calculated minimum selling price of the TOP and TAP pellets at the plant gate was \$207 Mg^{-1} and \$197 Mg^{-1}, respectively, corresponding to \$8.5 GJ^{-1} and \$8.1 GJ^{-1}. The feasibility study of the higher production capacities showed the significant profitability of 200,000 Mg yr^{-1} plant with the similar delivered price of the regular wood pellets in the United States for the global market. The feedstock cost was the most sensitive input parameter.

Keywords: Techno-economic analysis, Torrefaction after pelletization, Torrefied pellets, Mass and energy balance, Capital investment, Minimum selling price.

Introduction

The increasing global energy demand with a projection of 28% increase from 2015 to 2040 [1], the climate change concerns, and energy security are the main drivers for shifting towards more sustainable renewable energy resources [2]. The electricity consumption, which contributes to approximately 15% of the total energy requirement, represents the largest portion of GHG emission (28%) in the United States [3]. Fossil fuels (mainly coal and natural gas) are the primary sources of the total electricity generation in the United States with 63% share [1]. The total amount of electricity generation in the United States from coal was about 1208 billion kWh in 2017 [1], corresponding to the approximate GHG emission of 1208 million Mg CO_2 eq. However, biomass co-firing has been proven to be a promising, low emission, and less expensive alternative for the electricity producers [4]. The significant portion of power generation plants with co-firing technology (10 to 100%) has been established in Europe, mainly due to stringent regulations for GHG reduction [5]. In the United States, despite the current low percentage of biomass usage (less than 2%) for the power generation, the biomass co-firing power generation plants will be prospered if high biomass availability, competitive biomass costs, low transportation costs, and lastly the influential environmental regulations get established [6].

The pretreatment processes such as torrefaction and densification have been extensively investigated to upgrade the physical and chemical properties of lignocellulosic biomass to be a suitable substitution for coal [7–10]. Torrefaction as a heat treatment process at a temperature range of 200 to 300°C and in an inert condition, decomposes the biomass structure, removes the hydrophilic hydroxyl groups, and increases the carbon content of biomass. The final dark brownish solid product with 70 to 80% mass yield has higher heating value, hydrophobic nature, and less fibrous structure, all comparable to coal, while retains 80-95% of the initial energy content [11].

Since the bulk density of torrefied biomass decreases as a result of mass loss and void formation during torrefaction, densification processes such as pelletizing and briquetting are required to increase the total energy density of the final products.

The techno-economic aspects of integrated torrefaction and pelletization process to produce torrefied pellets have been studied in several studies [12–17]. The Energy Research Centre of the Netherlands (ECN) was the first center to propose the integrated torrefaction and pelletization process, known as the TOP process [12]. In a conventional TOP process, biomass is first partially dried and then is torrefied in a torrefaction reactor. The torrefied biomass is cooled and sent to the grinder, and subsequently, it is densified in a pellet mill. The torrefied pellets are cooled, screened, and finally stored for designated usage. Bergman et al. at ECN center compared the properties of torrefied pellets from woody biomass in a moving bed torrefaction reactor with raw wood pellets [12]. The energy density of raw wood pellets was improved from 7.8-10.5 GJ m^{-3} to 14.9-18.4 GJ m^{-3} for the torrefied wood pellets. The estimated production cost and investment cost of the TOP pellets were higher than those of the wood pellets. However, considering the co-firing process and similar properties of TOP with coal, great savings in equipment, storage, and handling could be achieved at the co-firing site, resulting in the high economic potential for TOP pellets [12]. A similar analysis was performed for Topell Energy technology of production of torrefied wood pellets within a Torbed reactor [13]. The torrefied wood pellets' energy density was 17.4 GJ m^{-3} compared to 10.7 GJ $m^{-3}$of the raw wood pellets. The detailed economic estimation for a specific case showed a higher cost of the final product than ECN technology. Nevertheless, the torrefied pellet with comparable properties to coal and its application for co-firing purposes was still proposed to be beneficial considering the penalty of CO_2 emission in coal-fired plants [13]. Pirraglia et al. performed a techno-economic analysis of the conventional

torrefied wood pellets production in the United States [15]. The overall mass and energy balances were comparable with European analysis (ECN and Topell). They also investigated the use of different types of binder and the impacts on reducing capital costs [15]. Chai and Saffron compared the two types of torrefied wood pellets with conventional raw wood pellets produced from different feedstock moisture content at different depot size [16]. They concluded that the dry climates will result in more economic biomass conversion depot, and specific operating conditions of torrefaction need to be verified for humid weathers [16]. In most of the previous studies, the conventional pathway of torrefied pellet production has been investigated, which is torrefaction before pelletization (TOP method). However, the other potential pathway is the implementation of torrefaction after pelletization (TAP) in a new plant or integration of torrefaction to an existing commercial densification plant. Ghiasi et al. compared the properties of the torrefied douglas fir wood pellets from TOP and TAP pathways [18]. They stated that effective densification of the torrefied biomass was possible only with the aid of binder addition. The TAP pellets contained lower moisture content and higher heating value and showed more water stability. Moreover, the TAP pathway was more energy efficient compared to the conventional TOP pathway [18]. Kumar et al. reviewed the technical features of different pathways for production of torrefied pellets [17]. While the overall mass and energy efficiency was almost similar for both TOP and TAP approaches, the utility fuel consumption was reduced by 70% in a later case. They proposed the probable lower overall cost for the TAP case due to the higher throughput of the reactor and lower energy requirement. However, they insisted on the requirement of more detailed technical and economic information for an accurate feasibility study [17].

The goal of this study was to conduct a techno-economic analysis of torrefied wood pellets production by the TAP (torrefaction after pelletization) technology. A detailed mass and energy

balance was performed with the aid of process simulation to obtain a more accurate energy requirement and design parameter for each unit operation in the process. The technical and economic results were compared to those of torrefied wood pellets from the conventional pathway (TOP) and raw wood pellets. Sensitivity analysis was also performed to study the specific design parameters and cost factors and to investigate their impacts on the minimum selling price (MSP) of the final torrefied wood pellets.

Methods

Process description

Figure 6-1 shows the process configurations of the integrated torrefaction and pelletization in two pathways; (a) conventional torrefaction before pelletization (TOP), and (b) torrefaction after pelletization (TAP).

Wood pelletization is a common densification process, which has been broadly documented in the literature [12,19,20] and several commercial plants are working worldwide with almost the same approach. The additional unit operations required for torrefaction are shown in dashed border boxes in Figure 6-1. The initial biomass feedstock is received and stored and prepared for sending to the dryer. In case of wood logs feedstock, after debarking and chipping processes, the chipped biomass is sent to the dryer, where the moisture content reduced to 10%. The dried biomass is ground in the hammer mill to provide a proper particle size distribution and then transferred to the pellet mill. The required energy for drying section is provided by combustion of auxiliary fuel such as natural gas or biomass bark in a burner. Steam conditioning is considered to increase the temperature of biomass and facilitate the densification process [21].

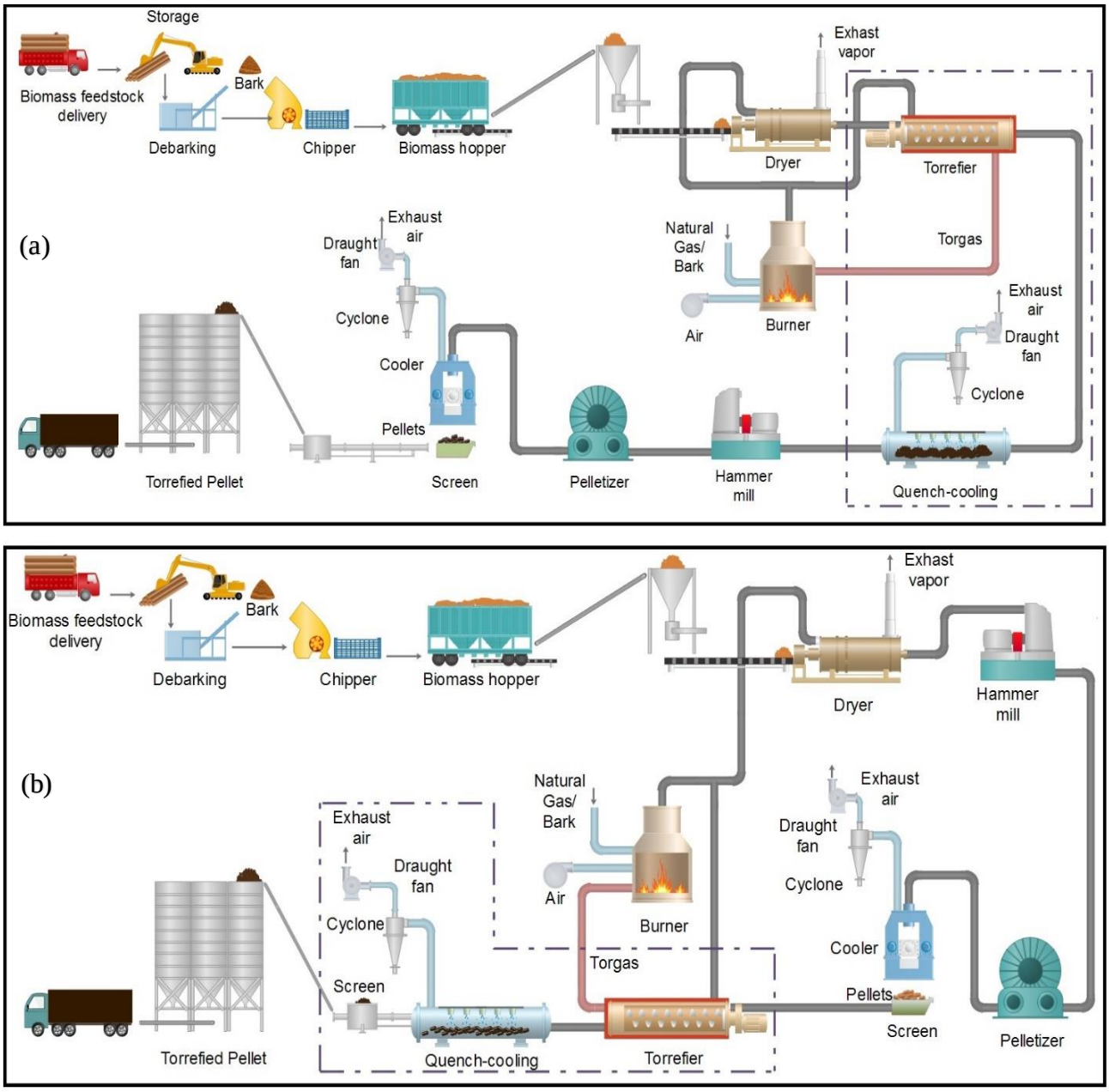

Figure 6-1. Schematic process flow diagram of an integrated torrefaction and pelletization plant (a) torrefaction before pelletization (TOP), (b) torrefaction after pelletization (TAP). The unit operations inside the dashed border boxes relate to the torrefaction process.

The prepared wood pellets are cooled in a pellet cooler and screened. Fines collected from the screener are returned to the pellet mill. In a conventional torrefied wood pellet production (TOP process) (Fig 1. a), the dried biomass is sent to the reactor, where torrefaction takes place at the specific temperature and residence time. The products of torrefaction are torrefied solid (torsolid) and volatile stream (torgas). Torrefied solid is cooled down to below self-ignition point to reduce the risk of fire and then ground in a hammer mill. A torgas stream contains volatile organic carbons and is not allowed to vent off directly to the atmosphere. In this study, torgas is returned to the burner and co-fired with an auxiliary fuel to provide the required thermal energy for drying and heat-up in torrefaction section. The ground torsoild is transferred to the pellet mill, where steam conditioning and water addition is performed to produce torrefied pellets. No binder addition was considered in the base case. The final torrefied pellets are cooled again and stored after screening. In a torrefaction after pelletization (TAP) pathway (Fig 1.b), biomass feedstock is densified with the same approach of the wood pelletization process. The cooled wood pellets are transferred to a torrefaction reactor at the same temperature and residence time of the TOP process. The produced torgas is sent to the burner. The torrefied wood pellets are cooled to around 50°C and stored after screening. The major difference between TAP and TOP process is the location of the reactor and also the reactor throughput. Since the bulk density of densified wood pellets is higher than chipped biomass, the reactor throughput is higher for the same torrefaction condition. In order to have the same amount of the pellet product, the lower reactor size is sufficient for the TAP pathway, which might be a significant cost parameter. Also, two sets of screening are required to separate the fines before torrefaction and at after the final cooling section.

Process simulation

An Aspen Plus simulation model for torrefaction and pelletization process was obtained from Manouchehrinejad and Mani [22], where the design parameters of each unit operation were described in detail. The simulation was arranged for the three processes of wood pellets production, torrefied pellets production by TOP pathway, and torrefied pellets production by TAP pathway. The auxiliary fuel was natural fuel gas. The simulation was performed to obtain the mass and energy required for each process and to identify the unit operation capacities and energy requirements that were used to carry out the techno-economic assessment of a torrefied pellet production plant. The detailed input parameters in the process simulation were obtained from Manouchehrinejad and Mani [22]. The main difference between the input parameters of TOP and TAP configurations are given in Table 6-1.

Table 6-1. Design parameter of different unit operations utilized in the Aspen plus simulation model.

Parameter	TOP	TAP	Ref.
Feedstock	34.5 Mg/h Pine wood, 50% MC		
Dryer output solid	10% MC		
Auxiliary fuel in the burner	Natural gas		
Torrefaction condition	270°C, 30 min		
Bulk density in the torrefaction	Wood chips: 238 kg m^{-3}	Wood pellets: 669 kg m^{-3}	[23,24]
Grindability HGI	T250: HGI= 6.3 T270: HGI= 12.5 T290: HGI= 24	Raw wood chips [c]	[24]
Pelletization energy consumption [a]	150 kWh Mg^{-1}	55 kWh Mg^{-1}	[13]
Tor-cooling biomass outlet temperature	75°C	50°C	
Pellet-cooling outlet temperature	50°	50°C	
Screening [b]	one	two	

a In case of considering binder, the pelletizing energy consumption was assumed to be halved in the TOP plant configuration.

b one set of screening is required for the final torrefied wood pellet products. In the TAP plant, one extra set of screening is required after initial wood pellet production.

c The HGI method is not a proper approach for specifying the grindability of raw wood chips. In this study the grinding energy of wood chips before palletization were modified by the existing data in the literature.

Economic analysis

Base case plants assumptions

The techno-economic analysis was conducted for a torrefied pellet production with both TOP and TAP configuration. The base case was the production of 100,000 Mg yr^{-1} (wet basis) torrefied pellets from pine wood logs at 270°C and 30 min residence time in a 15 years lifetime plant and 7440 operating hours. The economic evaluation of a wood pellet plant with the same production capacity was also performed and compared with the results of torrefied wood pellet production plants. The initial biomass preparation depends on the type of the feedstock. In this study, we considered the whole log wood as a base feedstock in order to produce pellets at a premium or standard PFI levels [25]. The preprocessing operations including loading, debarking, and chipping was considered and relevant capital and operating costs were incorporated into the cost evaluation.

Total capital investment

For all cases presented in Figure 6-1, the specific capacity of main unit operations were obtained from the results of process simulation mass and energy balance. The cost of the equipment was selected from previous literature and modified by Eq. (3), wherever the equipment capacity was not available. For the preprocessing operations, the equipment was scaled linearly with the rated capacity. The scale factor used for all other equipment rather than torrefaction reactor was 0.7. The torrefaction reaction is a complex process, and most of the existing reactors are in pilot scale. Therefore, the reliable data for the cost and capacity of the torrefaction reactor is scarce. The scale factor of 0.8 was used to estimate the cost of the indirect rotary kiln reactor based on ECN study [26].

$$\text{Cost } 2 = \text{Cost } 1 \times \left(\frac{\text{Capacity } 2}{\text{Capacity } 1}\right)^{Scale\,factor} \quad (1)$$

The equipment price quoted in different years were adjusted to 2017 US dollar values by Chemical Engineering Plant Cost Index (CEPCI) factors. The proper capacity and number of each unit operation were specified based on the existing maximum capacity at the commercial scale. For dryer and torrefaction reactor, single equipment was chosen to minimize the cost and facilitate the operational control of the system. The direct cost of equipment was calculated by adding 32% mechanical installation, 20% electrical installation, and 4% freight to the total purchased cost [27]. For the preprocessing stage, since the relevant lifetime of the machinery are usually lower than 15 years, two sets of equipment were considered for the whole lifetime of the plant. The relevant costs for site and site preparation, paving, receiving station, feedstock storage lot, warehouses, plant and office buildings, and administrative tools were also considered in the direct costs [27]. The indirect costs included engineering and supervision (6%), construction expenses (20%), legal expenses (4%), contractor's fee (10%), and contingency (20% [28]) as the total of 60% [29] of the total direct cost. The fixed capital cost (FCI) was referred to a summation of total direct costs and total indirect costs. The final total capital investment cost was reported for each process plant as the summation of FCI and working capital (15% to FCI for the working capital) [28].

Production costs

The operating costs consist of feedstock, fuels, utilities, as well as labor, maintenance, and overhead. The required amount of feedstock, fuels, electricity, and other consumables were obtained from the Aspen Plus simulation. The additional electricity consumption was also considered for lighting and heating (112 kW), loading/unloading and ventilation for storage (22.3 kW), and others (40 kW) [30,31] . The feedstock cost varies in a wide range based on the quality of the wood and transportation distance. For the base case analysis, the delivered wood logs cost was fixed at \$45 dry $Mg^{-1,}$ and changes were studied in sensitivity analysis. The rest of the variable

expenses included natural gas fuel ($0.12 m^{-3} [32]), binder (kraft lignin, $250 Mg^{-1}), process water ($0.78 Mg^{-1}), and electricity ($0.07 kWh^{-1}). For steam conditioning, the cost of boiler feed water (deionized water) was estimated at $2.45 Mg^{-1}. The approximate $3 Mg^{-1} of production capacity was considered for lubricants, rollers, and dies for pellet mills and the same amount was estimated for the spare parts of torrefaction and other equipment.

The manpower required to operate the plant was proposed as one plant manager, one financial manager, one marketer, one mechanic/maintenance worker, and two clerks/secretaries. Also, the required direct labors for three shifts working were structured as one supervisor, four operators, and one loader operator. The benefits and general overhead (90% of total salaries), maintenance (3% of FCI), and insurance and taxes (0.7% of FCI) were added to the operating costs [29]. The production cost was calculated by summation of operating costs and depreciation charge.

Minimum selling price and profitability

The economic performance of the integrated torrefaction and pelletization plant with a TAP method was compared to a TOP plant and a wood pellet plant through a discounted cash flow rate of return (DCFROR) analysis, and the minimum selling price (MSP) of the final product was obtained at net present value (NPV) of zero with an internal rate of return (IRR) of 10%. The plant lifetime was 15 years. The depreciation charges were calculated based on the MACRS method over the seven years [33]. For the preprocessing equipment, the depreciation charges of the second series were calculated separately after the first 7 years.

A market price for the raw and torrefied wood pellets in the base case was also proposed by considering the minimum amount of 10% return on investment (ROI). The ROI is a simple measure of performance used in economic evaluation as a ratio of the net annual income divided by the total capital investment.

Sensitivity analysis

Sensitivity analysis on the base case of the TOP and TAP plants was conducted to investigate the uncertainty of the key process inputs and cost parameters on the minimum selling price (MSP) of the torrefied pellets. The variations of mass yield of the torrefaction, natural gas fuel consumption, electrical energy consumption, feedstock cost, and torrefaction reactor cost as the process parameters, and specific changes in the internal rate of return (IRR), indirect costs, and income tax as the economic model parameters were explored. For each item, the variation range was specified based on the spread of existing information.

Scenarios

A detail analysis of different parameters on the techno-economic properties were carried out through various scenarios. The base case scenario was the production of 100,000 Mg yr^{-1} (wet basis) of wood pellets or torrefied pellets from pine wood logs at 270°C and 30 min residence time. The addition of a binder (5% of the final product) was considered in different scenarios for both TOP and TAP at the base torrefaction temperature to explore the impact of binder on the energy consumption and costs. The usage of bark biomass as an auxiliary fuel instead of natural gas was also examined. Since the main feedstock was whole wood logs, the bark from debarking system was used without extra charge for auxiliary fuel.

The effect of plant capacity on the overall project cost was evaluated by developing the simulation models for three additional product capacities: 50000, 150000, 200000 Mg yr^{-1} of TAP torrefied pellets with the same design specifications of the base case. The capacity and number of the equipment were considered accordingly. The number of labors barely changes by increase in the production capacity of the torrefied pellet plant. The ±1 person was considered in the lower or higher capacity production.

In order to evaluate the impact of torrefaction temperature on the quality of the final product and the mass and energy requirements, the simulation models were developed for two other torrefaction temperatures (250°C and 290°C) with the same assumptions of the base case.

Results and discussion

Process design and simulation

Figure 6-2 shows the mass and energy flows through different unit operations for production of the wood pellets (WP), the torrefied wood pellets in a TOP configuration, and the torrefied wood pellets in a TAP configuration at the base case, which is 100,000 Mg yr^{-1} product.

The feedstock mass flow rate in the integrated torrefaction and pelletization processes was about 26% higher than the feedstock flow rate for the wood pellet production plant mainly due to the dry mass loss in the torrefaction process. The main difference between TOP and WP plants is the integration of torrefaction and quench-cooling units between drying and grinding sections, specified in a dashed border box (Figure 6-2b). On the other hand, the TAP process is specified by adding three more steps to the conventional wood pellet production consists of torrefaction, quench-cooling, and final screening (Figure 6-2c). This configuration shows the possible combination of a standalone torrefaction system to an existing wood pellet production plant. The drying energy requirement was consistent between the three process plants, and it was about 2.7 GJ Mg^{-1} of evaporated water, similar to the reported energy requirements for rotary drum dryers [34]. Despite the usage of torgas energy in both TOP and TAP, the net energy required to be provided by an auxiliary fuel was increased by 23 to 28% in the torrefied pellet production plants compared to the WP, to provide the thermal energy requirements for drying and torrefaction processes. Nevertheless, the approximate 24% increase in the energy content of the torrefied pellets was obtained by torrefaction at 270 for both TOP and TAP cases.

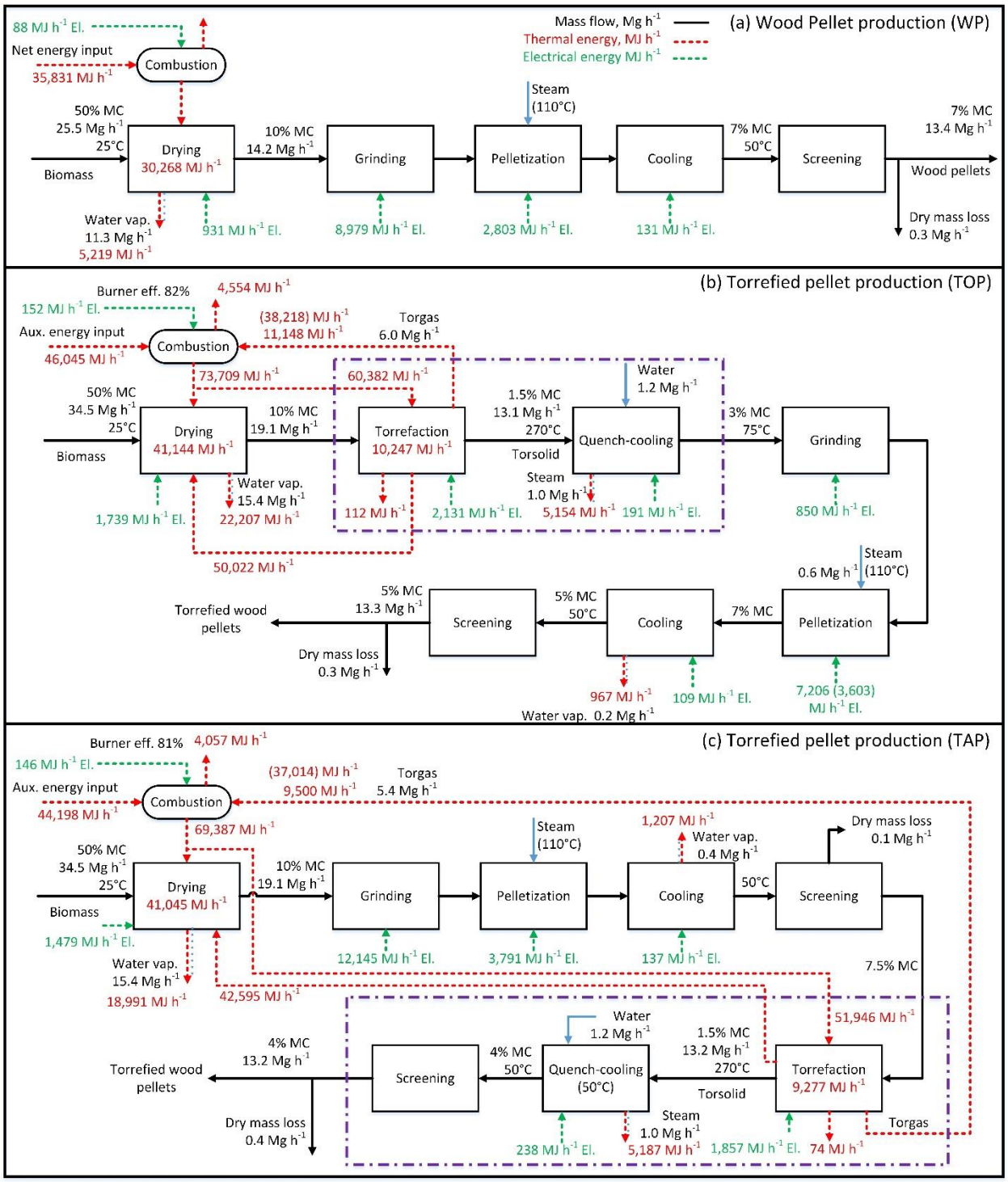

Figure 6-2. Mass and energy flow for wood pellet production plant WP (a), conventional integrated torrefaction and pelletization, TOP (b), and integrated torrefaction and pelletization TAP approach (c) at the base case production capacity 100,000 Mg^{-1} and torrefaction temperature of 270°C.

The breakdown of energy consumption per mass of the product and process parameters for TOP and TAP plants at the base case resulted from the Aspen Plus simulation are presented in Table 6-2. The final product mass flow in TOP plant was slightly higher than TAP plant due to more loss of the material through two sets of screening. However, since torrefaction process is the last step in the TAP plant, the moisture content of TAP pellets was lower than TOP pellets. The other physical differences between TOP and TAP pellets can be found elsewhere in other studies [18,23,35]. There were no considerable differences between the results of the TOP and TAP process efficiencies. The torrefaction mass and energy yield was 75% and 92%, respectively for both configurations. The torgas energy from the torrefaction of wood pellets in the TAP plant was slightly higher than the TOP plant due to lower moisture content of the input wood pellets to the reactor, resulting in the lower thermal energy requirement for the TAP plant.

For the electrical energy consumption, the specific grinding energy of the raw biomass (TAP cases) was significantly higher than torrefied biomass (TOP cases) [36], while the energy of densification was almost doubled in TOP scenarios compared to TAP cases. The grinding energy was obtained based on the power of hammer mill for grinding wood chips to a proper size for wood pellets. While a hammer mill with power of 224 kW is appropriate for grinding of 8 Mg hr^{-1} wood chips, the lower power around 55 kW is more than sufficient for the same amount of the torrefied wood chips [24,27,37].

Table 6-2. Aspen plus simulation results for TOP and TAP plants at the base case production capacity 100,000 Mg^{-1} and torrefaction temperature of 270°C, 30 min.

	TOP	TAP
Feedstock flowrate, kg h^{-1}	34500	34500
Feed moisture content, %	50	50
Feed HHVd, MJ kg^{-1}	19.7	19.7
Final product, kg h^{-1}	13315	13153
Product moisture content, %	5.2	3.5
Final Solid product HHVd, MJ kg^{-1}	24	24
Torgas LHV, MJ kg^{-1}	6.4	6.8
Torrefaction mass yield, %	75	75
Feed to product ratio, wb	2.6	2.6
Energy yield of the torrefaction, %	93	92
Energy yield of the whole system, %	90	90
Drying [a], MJ kg^{-1} of product	3.09	3.12
Torrefaction [b], MJ kg^{-1} of product	0.77	0.71
Tor-cooling, MJ kg^{-1} of product	-0.39	-0.39
Pellet cooling, MJ kg^{-1} of product	-0.07	-0.09
Thermal energy requirement, MJ kg^{-1} of product	6.33	6.17
Torgas energy, MJ kg^{-1} of product	2.87	2.81
NG energy, MJ kg^{-1} of product	3.46	3.36
Electrical energy required, MJ kg^{-1} of product		
Drying and burning	0.14	0.12
Torrefaction	0.16	0.14
Tor-cooling	0.01	0.02
Grinding [c]	0.01	0.12
Pelletization (with binder)	0.54 (0.27)	0.29
Pellet cooling	0.01	0.01
Total energy required [d]	8.84 (8.21)	8.18
Torrefaction reactor dimension (ID x L), m	3 x 42	3 x 24

[a] The energy consumed in drying.

[b] The summation of energy required for heat-up and release from the reaction

[c] Grinding energy were calculated the based on the hammer mill power [27,37].

[d] Efficiency of electricity generation was assumed as 35%.

The experimental data of grinding the wood chips and torrefied woodchips in previous studies has shown a reduction around 90% in power consumption for grinding of the torrefied wood chips [18,24]. The estimated grinding energy consumptions were comparable to the experimental values reported in the literature [24,38,39]. The energy consumptions for pelletization was the input parameter for the simulation. Although the reported energy requirements of densification of torrefied biomass are much higher than that of raw biomass, the addition of binder might significantly reduce the energy consumption of pelletization of torrefied biomass [13,18]. It was assumed that pellet mill energy consumption might be halved by the proper binder addition. The electrical energy consumption related to the torrefaction system was slightly lower for the TAP model. In the TAP process, due to the higher bulk density of the inlet solid stream to the reactor, the volume of the reactor for a specific production capacity was significantly smaller than the TOP process torrefaction reactor. Despite the higher total bulk density, the porosity of every single densified biomass (e.g., pellet) is higher than the dense wood chip particles. The porosity of every single pellet is around 60%, and small sizes of particles within an individual pellet ensure the absence of internal heat transfer limitations (small Biot number). Moreover, the more uniform particle size distribution, facilitates the overall heat transfer within the bulk of solid materials, resulting in more uniform reaction rates, and thus avoiding hot spots and runaway reactions. Therefore, the energy requirement related to air injection blowers was lower in the TAP scenarios compared to the TOP. Also, the smaller volume resulted in the lower energy of roller drive motors.

The total energy consumption, considering 35% efficiency for electricity generation, was 8.84 and 8.18 MJ kg^{-1}, for TOP and TAP plants, respectively, which shows the marginal reduction

in the overall energy consumption for the TAP plants. However, the total energy consumptions for both TAP and TOP plants were almost similar in case of using appropriate binder addition.

Economic analysis

Capital investment

The capital expenditure on various equipment was obtained from literature and the base case results are shown in Table 6-3. The major parameters of capital costs for three processes of TAP, TOP, and WP at the base case capacity are given in Table 6-4. For all three cases studied, the total direct cost (TDC) contributed to 63% of the total capital investment (TCI). Considering the related direct cost and indirect of the reactor, torrefaction unit represents 34 and 25% of the TCI for TOP and TAP plant, respectively. The previous economic evaluations on the TOP plant performed by other researchers showed the higher contribution to the torrefaction reactor [13,40]. In the study performed by Pirraglia et al. the torrefaction reactor represented 60% of the total capital investment [40]. However, in their study, drying and torrefaction were taken place in the same equipment. Topell energy estimated the amount of 45% for the torrefaction reactor of the TCI for the same annual capacity production [13]. In this study, the TCI of the conventional torrefied pellet production (TOP) was about 15% higher than the TAP plant mainly due to the cost of the reactor. For a specific size of a torrefaction system, the increase in bulk density of feedstock would presumably increase the throughput of the reactor. This corresponds to lower capital investment for the higher bulk density feedstock to produce the same amount of final torrefied densified material.

Table 6-3. List of major equipment cost for the base case.

Equipment	Capacity [a]	Cost ($) 2017	Diesel usage/power [b]	Ref
Log loader	910 t/d	152,497	0.26 L/t diesel fuel	[41]
Debarking system	910 t/d	526579.3	2.1 L/t diesel fuel	[41]
Chipper	828 t/d	467,687	2.1 L/t diesel fuel	[41]
Dryer [c]		725,612		[14,27]
Extra facilities for biomass burner		463,331		[27]
Torrefaction reactor, TOP		4,604,435		[26,42]
Torrefaction reactor, TAP		2,983,620		
Grinding, raw wood chips	9.5 t/h	94921.52	300 hp	[14,15,27]
torrefied wood chips	19t/h	33,700	74 hp	
Pellet mill [d]	4.5 t/h	254,118	400 hp	[15,27]
Conditioner	4.5 t/h	48,282		[27]
boiler		55,087		[27]
Pellet cooler		105,452		
Screener/shaker (TAP :2)		41,422		[15,27]
Binder preparation facilities		10,000		
Conveyors		298,859		[27,43]
Tanks and hoppers		730,167		[27]
Feeders, filters, air systems, dust collectors, etc.		126,807		[27]
Site and site preparation		240,932		[27]
Paving		92,666		[27]
Pellet plant building and offices		1,101,732		[27]
Plant and office equipment and tools		108,013		[27]
Receiving station		140,417		[27]
Feedstock storage lot		388,847		[27]
Feedstock bare storage warehouse		302,436		[27]
Pellet storage warehouse		378,045		[27]

a The listed equipment price are for 100,000 Mg yr-1 pellet production capacity, otherwise it is specifically depicted.

b The electricity consumption for roller motor, blowers, etc. were obtained from Aspen Plus simulation and were considered in the operating costs.

c the dryer cost for the wood pellet production at the base case was assumed as $602,712 due to lower feedstock flow rate.

d The specific energy for pelletizing the raw wood is 55 kWh Mg^{-1}, while it is about 150 kWh Mg^{-1} for torrefied wood (without binder) [13]. The required power for pelleting 5 Mg h^{-1} torrefied wood were considered about 900 hp.

Table 6-4. Total capital investment for production of 100,000 Mg yr^{-1} torrefied pellets (in TAP and TOP plant), or wood pellets.

			TOP		TAP		Conventional Wood Pellet	
			M$	Breakdown	M$	Breakdown	M$	Breakdown
Direct Costs								
Log processing			2.29	8%	2.29	9%	1.70	10%
Drying			0.73	2%	0.73	3%	0.60	4%
Torrefaction			4.60	16%	2.98	11%		
Grinding and pelleting			1.24	4%	1.40	5%	1.40	8%
Others (Coolers, conveyors, tanks, etc.)			1.36	5%	1.40	5%	1.36	8%
Total			10.22	34%	8.80	34%	5.06	30%
Installation, Fraight, etc.			5.57	19%	4.77	18%	2.71	16%
Other direct costs			2.75	9%	2.75	11%	2.75	16%
Total Direct Equipment Cost (TDEC)			18.54	63%	16.32	63%	10.52	63%
Indirect Costs								
Engineering and supervision	0.06	of TDEC	1.11	4%	0.98	4%	0.63	4%
Construction Expenses	0.20	of TDEC	3.71	13%	3.26	13%	2.10	13%
Legal expenses	0.04	of TDEC	0.74	3%	0.65	3%	0.42	3%
Contractor's fee	0.10	of TDEC	1.85	6%	1.63	6%	1.05	6%
Contingency	0.20	of TDEC	3.71	13%	3.26	13%	2.10	13%
Total Indirect Equipment Cost	0.60		11.13	38%	9.79	38%	6.31	38%
Fixed Capital Investment (FCI)			29.67	88%	26.12	88%	16.84	88%
Working Capital	0.15	of FCI	4.04	12%	3.5	12%	2.22	12%
Total Capital Investment (TCI)			33.7	100%	29.6	100%	19.1	100%
Specific Investment ($/annual t of product)			340.2		302.8		190.6	
$/GJ			13.99		12.54		9.69	

The indirect costs contributed to 38% of the TCI in all cases. Different assumptions have been taken into account in various studies for the indirect costs percentage. The contingency factor has been varied in a range of 10% to 35% of TDC [28,44,45] and the total indirect costs has been reported between 32% to 128% of TDC [29,33,40,44,45]. An average value of 60% of TDC was considered in this study, and it was further explored in the sensitivity analysis.

The total capital investment for the base case capacity was $33.7, $29.6, and $19.1 million for the TOP, TAP, and WP, respectively. The TCI of the integrated torrefaction and pelletization plant was obviously increased compared to the wood pellet production plant. For an annual production of 100,000 Mg yr^{-1} torrefied pellets in the TAP plant, the total capital investment was 55% higher than a regular wood pellet plant, corresponding to extra $10 million for a torrefaction reactor, another set of cooler and other required equipment. However, this could be compensated through the increased co-firing share of the torrefied pellets in downstream processes such as power generation plants. Topell energy estimated the approximate extra costs of $35 Mg^{-1} for regular wood pellet at the power generation plant [13]. Their analysis showed the TCI of $29 million for 100,000 Mg^{-1} annual production TOP pellet and $19.5 million for 124,000 Mg yr^{-1} production of wood pellets [13]. Peng et al. reported a TCI in range of $22.1 to $31.0 million for a torrefied pellet plant (TOP) with 126,000 Mg^{-1} annual production capacity and $18.1 million for a 180,000 Mg yr^{-1}production of wood pellet [19]. These values were in the range of $23.4 million to $117.5 million for 50,000 to 500,000 Mg^{-1} production reported by Batidzirai et al. [14] and comparable with the estimated TCI in this study.

Production cost

Table 6-5 shows the summary of various production costs for the base case scenario of TOP, TAP, and wood pellet production plants. The feedstock cost was the most effective parameter in all three cases. The labor direct costs were about 9 to 12% of the total production costs (TPC), similar to Pirraglia et al. [40] study. However, considering the relevant benefits and overhead it resulted in 17 to 23% of TPC in all three cases, accounted for the second important parameter in the production costs evaluation.

Depreciation charge was also one of the effective factors, especially in the TOP plant due to the high cost of the torrefaction reactor. The depreciation charge was \$20.0, \$17.8, and \$9.9 Mg^{-1} for TOP, TAP, and WP plants, respectively. The total production cost of the integrated torrefaction and pelletization plants (\$172 Mg^{-1} for TOP and \$166 Mg^{-1} for TAP) was also increased compared to the conventional wood pellet production plant (\$114 Mg^{-1}). Considering the higher heating value of the final products, the production cost can be presented as \$7.1, \$6.9, and \$5.8 GJ^{-1} for TOP, TAP, WP pellets. The calculated production costs by Pirraglia et al. was \$199 Mg^{-1} for torrefied pellet production in a plant with 100,000 Mg^{-1} annual production capacity [40]. Peng et al. compared the economics of wood pellet production and torrefied pellet production from different feedstock. They reported the production costs of 65 to \$132 Mg^{-1} for conventional wood pellets and \$82 to \$152 Mg^{-1} for torrefied wood pellets [19]. Topell energy reported the cost of \$7.4 and \$6.8 GJ^{-1} for torrefied pellet and conventional wood pellet production, respectively [13].

Table 6-5. Operating costs parameter for TAP, TOP, and WP processes at the base case.

			TOP		TAP		Wood Pellet	
			$/t	Break down	**$/t**	Break down	**$/t**	Break down
Variable Costs								
Feedstock			64.06	37%	64.85	39%	42.7	37%
Natural gas fuel			11.6	7%	11.3	7%	9.0	8%
DM Water			0.0	0%	0.0	0%	0.1	0%
Water			0.1	0%	0.1	0%		0%
Electricity			17.9	10%	14.5	9%	8.9	8%
Diesel			12.4	7%	12.6	8%	9.1	8%
Other			6.5	4%	6.6	4%	3.2	3%
Total Variable costs			112.69	66%	110.0	66%	72.9	64%
Fixed Costs				0%				
Labor & supervision			15.2	9%	15.4	9%	13.8	12%
Benefits and general overhead	0.90	of Salaries	13.7	8%	13.8	8%	12.4	11%
Maintenance	0.03	of FCI	8.2	5%	7.2	4%	4.4	4%
Insurance and taxes	0.01	of FCI	1.9	1%	1.7	1%	1.0	1%
Total Fixed Operating Costs			38.92	23%	38.06	23%	31.7	28%
Depreciation			20.0	12%	17.8	11%	9.9	9%
Total Production cost ($ Mg-1)			171.6	100%	165.8	100%	114.5	100%
HHV (GJ/t)			24.3		24.1		19.7	
Production cost ($/GJ of product)			7.1		6.9		5.8	

Minimum selling price and profitability analysis

- Base case with and without binder

The minimum selling price (MSP) of the torrefied pellets at the base case was \$207 Mg^{-1} for the TOP process and \$197 Mg^{-1} for the TAP process, compared to \$135 Mg^{-1} for the conventional wood pellet as a result of the integration of the torrefaction reactor to the densification system. The corresponding MSP based on the energy content of the final pellets were \$8.5 GJ^{-1}, \$8.1 GJ^{-1}, and \$6.9 GJ^{-1}, respectively. These values were obtained considering 10% IRR for the NPV equal to zero and the period of 15 years for a plant lifetime. No transportation costs were accounted for in these calculations. The estimated gate price for the pellets in this study was lower than in previous studies. The initial estimation for TOP pellet gate price proposed by ECN, was \$202 to \$252 Mg^{-1} (\$258-323 Mg^{-1} based on 2017 with CEPCI factors), compared to \$164 to \$205 Mg^{-1} (\$209-261 Mg^{-1} based on 2017) for conventional wood pellets [12]. D. Agar reported the minimum selling price of \$211 Mg^{-1} for torrefied pellets (TOP) and \$183 Mg^{-1} for raw wood pellets including logistics and transportation costs (based on 2017) [46].

The MSP increased to \$218 Mg^{-1} (\$8.96 GJ^{-1}) and \$213 Mg^{-1} (\$8.84 GJ^{-1}) for TOP and TAP, respectively, in case of applying appropriate binder addition in the system. While the addition of a binder is almost substantial to produce pellets from torrefied biomass in the TOP process [18], the preliminary studies have shown the successful production of torrefied pellets in TAP method without adding any binder [18,23]. However, in order to improve the durability of the final products and prevent dust formation, further research has been suggested to study of binder addition impact on the quality of the final TAP pellets [17]. Pirraglia et al. estimated the price of \$261 Mg^{-1} for TOP pellets with binder [40].

- **Different type of auxiliary fuel: Bark biomass fuel instead of natural gas**

The minimum selling price of the TOP pellets at base case capacity with bark biomass as an auxiliary fuel was \$194 Mg^{-1} (\$7.98 GJ^{-1}), slightly lower than the case with natural gas fuel. Despite the small increase in the capital costs due to the requirement of the additional equipment for handling, feeding, and burning of the solid fuel, the operating costs decreased as a result of no extra charge for bark fuel. The MSP of the TAP pellets was reduced to \$189 Mg-1 (\$7.82 GJ^{-1}) with bark fuel. The bark separated in the debarking system, was more than sufficient to provide the required heat in the system. The usage of biomass bark would also benefit to reduce the NOx in the total emission from the plant [22].

- **Different production capacity and profitability study**

Figure 6-3 shows the variation of the specific capital investment, production costs, and minimum selling price by changing the production capacity in a TOP and TAP plant. It is obvious that the initial capital investment increases with the increase in the production capacity of the plant from 50,000 Mg yr^{-1} to 200,000 Mg yr^{-1}. However, conversely, the specific investment cost (cost per unit mass of the final product) decreases due to manufacturing more products. The increase in production capacity also cut down the production costs and minimum selling price, but with a slower slope compare to the specific capital investment cost. Since the current torrefaction systems have been mostly proposed at the pilot scale, the minimum selling price at all cases were comparable with reported values in the literature [12,40,46]. In all cases, the costs of the TAP plants were slightly lower than the TOP plants.

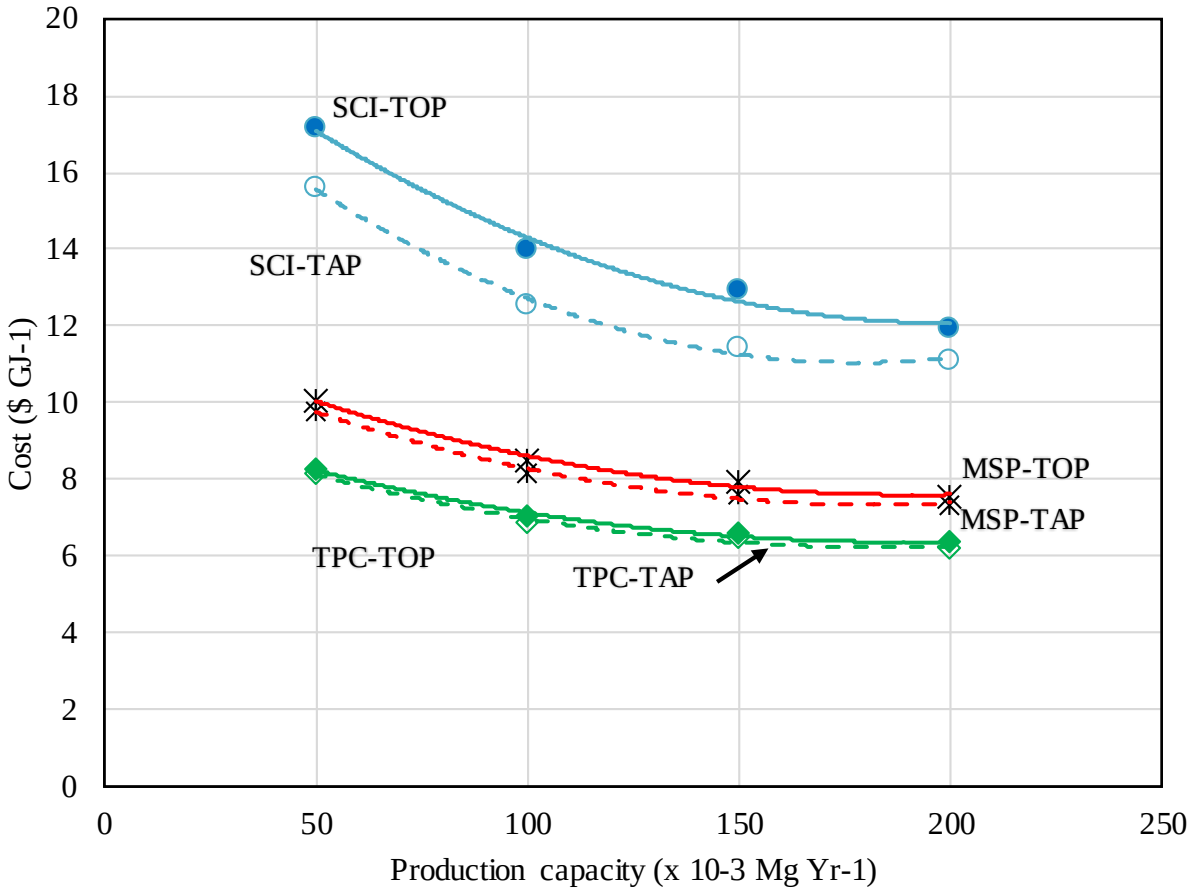

Figure 6-3.The variation of the specific capital investment (SCI), total production cost (TPC), and minimum selling price (MSP) by the annual production capacity of the integrated torrefaction and pelletization TOP and TAP plant.

It is worth noting that the reduction in plant costs by an increase in capacity is not linear and it depends on several parameters including capital investment, feedstock availability, operating parameters, and other factors such as climate, location, and logistics. The minimum selling price at 200,000 Mg yr^{-1}reduced to the lowest value of \$184 Mg^{-1} (\$7.6 GJ^{-1}) and \$178 Mg^{-1} (\$7.4 GJ^{-1}), for the TOP and TAP plant, respectively, which was 10% lower than the base case MSP. However, it is still not comparable with the delivered cost of the coal at the US electric power sector at the price of \$44.52 Mg^{-1} [47]. Batidzirai et al. reported that economically feasible TOP plants would be in the range of 200,000 to 250,000 Mg yr^{-1}, where it is comparable with traditional

wood pellets [14]. The average price of utility-grade wood pellets from the United States to global market reached to about \$199 Mg^{-1} in December 2017, although it dropped to about \$185 Mg^{-1} in the first two months of 2018 [48]. The MSP of the torrefied pellets at the base case were comparable with the price of regular wood pellets reported by EIA [48]. However, this is the breakeven price. The profitability study with ROI parameter showed that TOP pellets price ranging from \$210 Mg^{-1} (8.6 GJ^{-1}) to \$220 Mg^{-1} (\$9.1 GJ^{-1}) would lead to ROI of 5 to 20%. For the TAP pellets, the corresponding range is \$203 Mg^{-1} (8.3 GJ^{-1}) to \$209 Mg^{-1} (\$8.6 GJ^{-1}). The profitability analysis for the higher production capacity showed that the price of selling the TAP pellets is comparable with regular wood pellets with the ROI of 15% at the plant production capacity of 200,000 Mg yr^{-1}, which makes it a feasible production capacity similar to that reported by Batidzirai et al. [14].

- **Different torrefaction temperature**

Figure 6-4 presents the variation of the minimum selling price at two different torrefaction temperatures of 250 and 290°C. The torrefaction mass yield at the 250 and 290°C was about 87% and 53% compared to the base case torrefaction yield of 75% at 270°C. This resulted in the different total production capacity with the same amount of feedstock. Moreover, the energy consumption was changed mainly due to the different thermal energy requirement. Therefore, the minimum selling price at 250°C decreased to about \$183 Mg^{-1} and \$175 Mg^{-1}, for the TOP and TAP pellets, while it increased to \$277 Mg^{-1} and \$262 Mg^{-1} for the torrefied pellets at 290°C. However, the energy content of the torrefied pellets would change by torrefaction temperature as well. In case of evaluating the price of the final torrefied pellets based on the energy content, the MSP was \$8.3 GJ^{-1} and \$7.96 GJ^{-1} for T250 pellets, and \$9.7 GJ^{-1} and \$9.3 GJ^{-1} for T290, respectively for the TOP and TAP pellets.

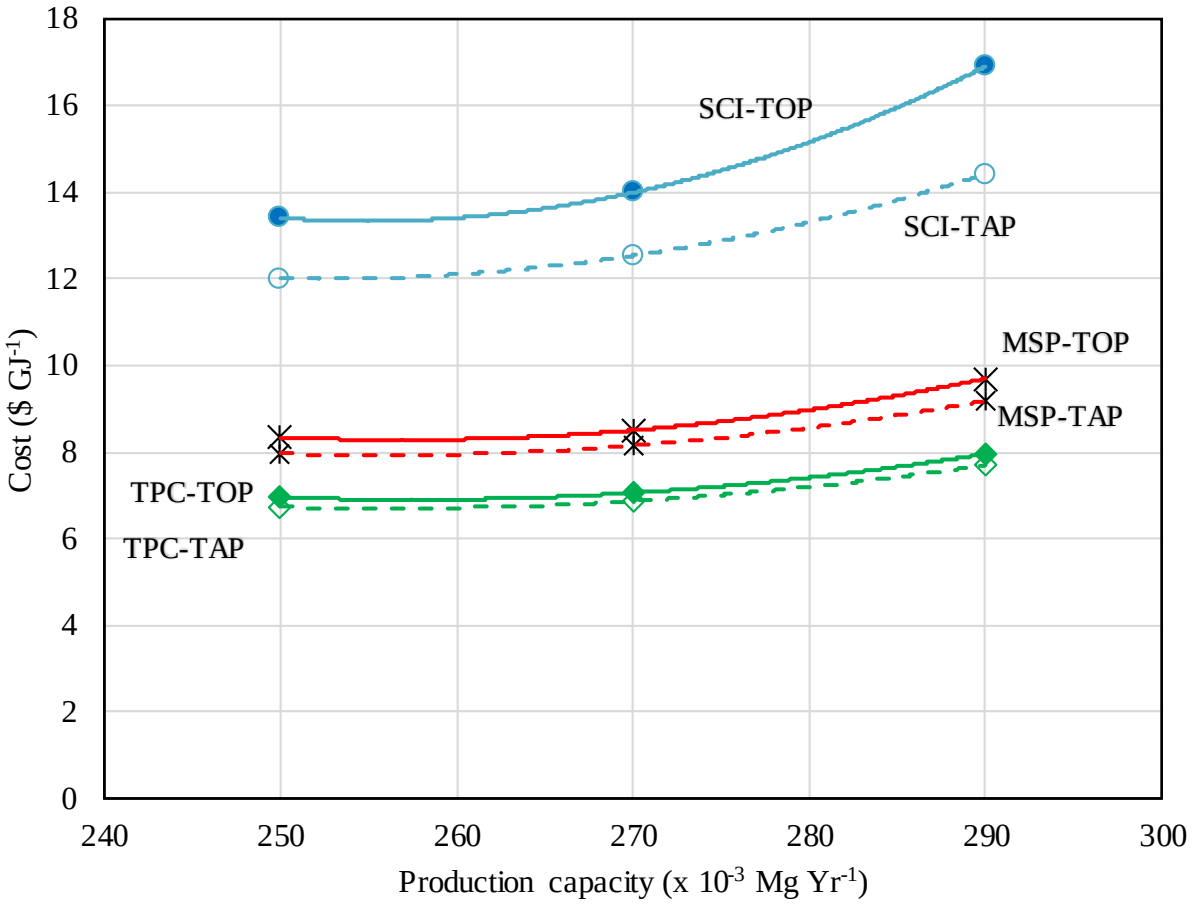

Figure 6-4.The variation of the specific capital investment (SCI), total production cost (TPC), and minimum selling price (MSP) by the torrefaction temperature of the integrated torrefaction and pelletization TOP and TAP plant.

Sensitivity analysis

Figure 6-5 shows the effects of the studied parameters on the minimum selling price of the TOP and TAP plant in the base case. The feedstock cost was the most sensitive parameter on the MSP. In this study, the wood logs were considered as feedstock to produce high quality and low ash content torrefied pellets. The cost of wood logs in literature varied from the low costs of $25 Mg^{-1} to $65 Mg^{-1} [19,49]. Therefore we investigate a ±50% changes on the base case cost. The 50% increase in feedstock costs, which might be due to the quality of feedstock or different

transportation distance, increased the final minimum price by about 15% and the MSP reached to at least \$229 Mg^{-1} for the TAP pellets. On the other hand, the lower feedstock cost (around \$25 Mg^{-1}) reduced the minimum selling price to \$164 Mg^{-1}. Although the torrefaction cost was the major parameter in the total capital investment, the impact on the TAP MSP was similar to the electrical energy consumption. The torrefaction cost was more important in case of the TOP pellets. The ±5% variation in the yield of the torrefaction system were also studied in both TOP and TAP pellets MSP. The increase in yield decreased the MSP to \$8.6 GJ^{-1} and \$ 8.1GJ^{-1} in the TOP and TAP, respectively. The similar 5% increase in the cost were obtained in case of decrease in the yield of both systems.

For the uncertainty of the cost model parameters, the internal rate of return (IRR) was a more important factor than indirect costs and income tax. A 25% change in the IRR, moved the MSP about 5% from the base case. The income tax variation by ±25 was almost similar to the electricity consumption effect. The indirect cost impact was slightly higher than the income tax, and it changes the MSP by 3 for 25% increase or decreases from the base case indirect cost, respectively.

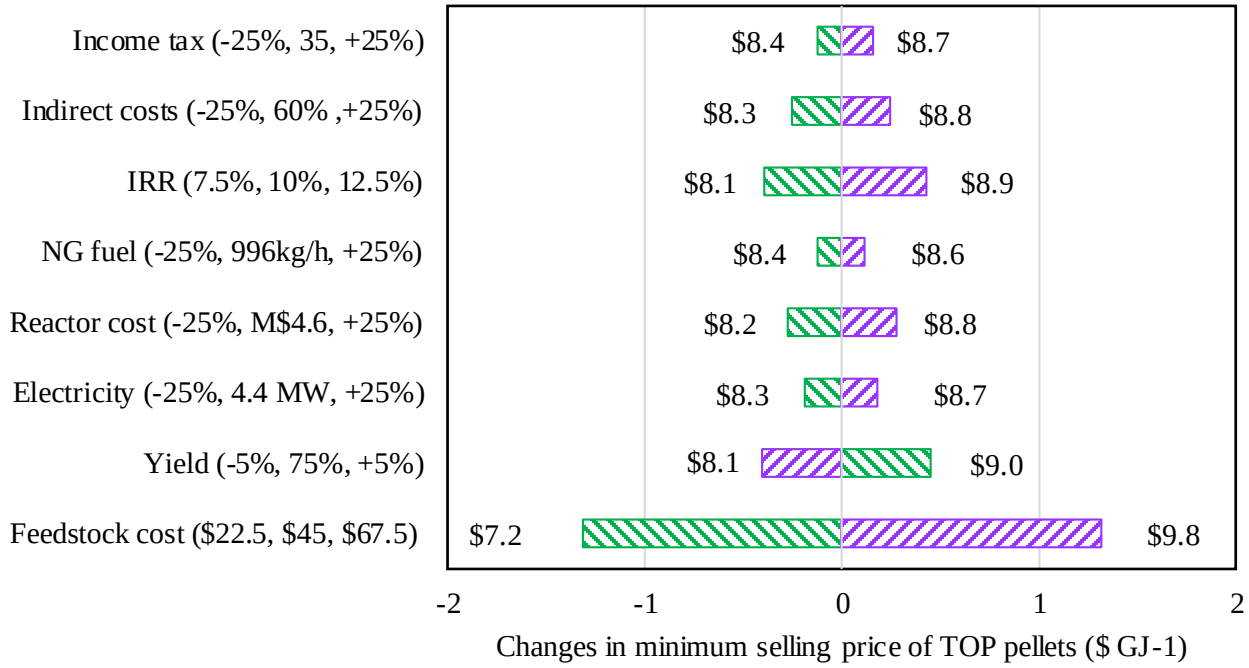

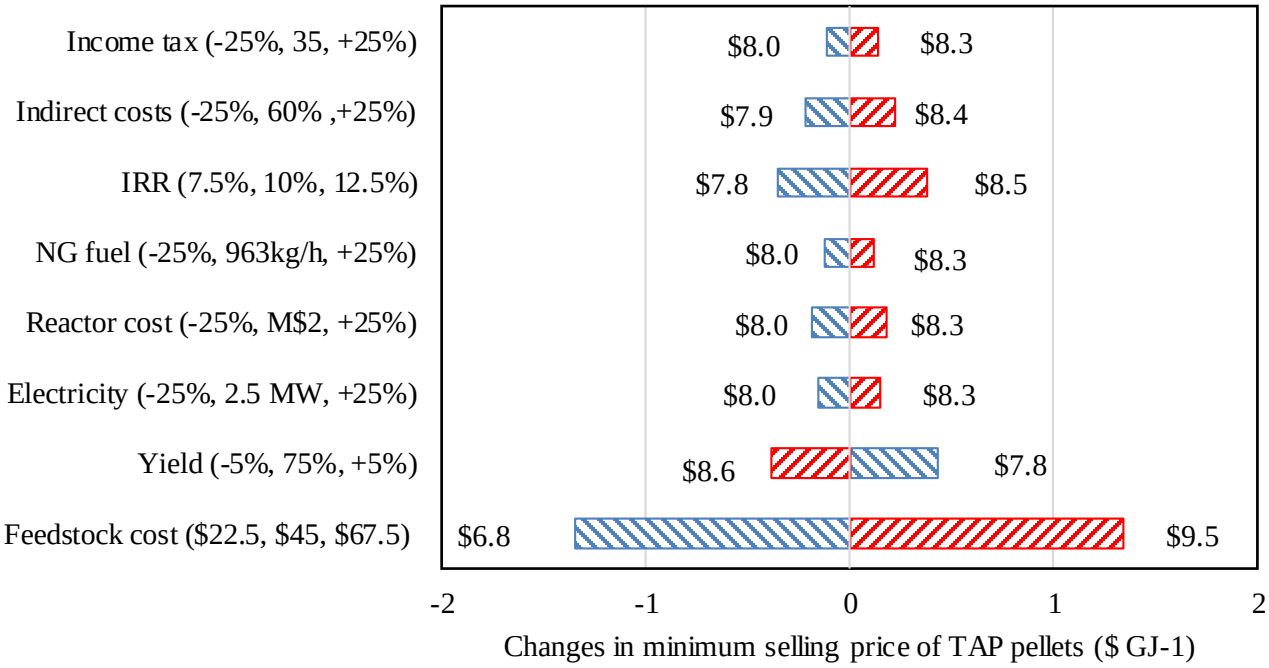

Figure 6-5. The sensitivity analysis of different parameter on the MSP of the TOP pellets (a) and TAP pellets (b).

Discussion

In this study, the minimum selling price of the torrefied wood pellets in both TOP and TAP pellet approach were not comparable with price of coal for power generation plant in the United States. The sensitivity analysis showed some of the assumed parameters including feedstock type and cost, indirect cost portion, auxiliary fuel type, and production capacity of the plant significantly impacted the MSP. In addition to those parameters, the bark separated in the preprocessing section is a valuable product that can be sold to the market. For instance, considering the 9% bark in the feedstock and price of \$25 Mg^{-1}, the MSP of the torrefied wood pellets at the base case can be reduced by \$6.5 Mg^{-1}, resulting in \$8.24 GJ^{-1} and \$7.9 GJ^{-1} for TOP and TAP pellets, respectively. Moreover, the torrefied pellets are carbon neutral fuels that can reduce the carbon foot print compared to the simple combustion of the other fuels. For instance, if the torrefied pellets with the same energy content of the coal were used for electricity generation purposes, it reduces about 2.3 Mg of CO_2eq emission per ever kWh generation [1]. If the carbon credit was considered for the CO_2 emission (e.g. \$20 Mg^{-1} of CO^2), there would be a great saving in usage of the torrefied pellets. Also, the renewable electricity production tax credit (PTC) can reduce the net price of the generated electricity even further, which is \$0.024 kWh^{-1} for the electricity generation from close-loop biomass resources [50].

Conclusion

Techno-economic analysis of an integrated torrefaction and pelletization process with a new pathway (torrefaction after pelletization (TAP)) was conducted and compared with the conventional TOP process. The mass and yield efficiency of the TAP and TOP process were almost similar. However, the total capital investment in a TAP with 100,000 Mg^{-1} production capacity (\$29.6 million) was reduced by about 12% compared to a TOP plant (\$33.7 million). Despite the

addition of a few equipment in the TAP (e.g., screener, conveyer, etc.), the capital investment of the reactor was reduced more than two folds, which was the main reason of the reduced total capital investment.

Although the addition of binder would significantly decrease the energy consumption of the densification in a TOP process, the total production cost of a conventional TOP plant was still slightly higher than a TAP pathway. The plant-gate minimum selling price at the base case was \$207 Mg^{-1} (\$8.5 GJ^{-1}) and \$197 Mg^{-1} (\$8.1 GJ^{-1}) for TOP and TAP, respectively. The evaluation of the production capacity showed that the delivered price of the TAP pellets from a 200,000 Mg yr^{-1} integrated plant, considering \$20 Mg^{-1} for shipping expenses, was comparable with the industrial utility grade regular wood pellet and providing more than 40% return of investment (ROI). The replacement of torrefied pellets with regular wood pellets would also lead to the extra saving of about \$35 Mg^{-1} at the power generation plants [13]. The feedstock cost was the most sensitive parameter on the selling price of the torrefied pellets.

Acknowledgments

This research was fully supported by the Consortium for Advanced Wood-to-Energy Solutions (CAWES) with funding provided by USDA Forest Products Laboratory (www.fs.fed.us) and U.S. Endowment for forestry and communities (www.usendowment.org). The authors thank the consortia members. CAWES is a public/private partnership initially formed by the USDA Forest Service, the U.S. Endowment for Forestry and Communities, and a number of innovative private companies and university partners committed to advancing sustainable, scalable, distributed wood-to-energy solutions that stimulate forest restoration and rural economic development.

References

[1] EIA Energy Information Administration- Independent Statistics and Analysis. International Energy Outlook 2017 Overview. US Energy Inf Adm 2017;IEO2017:143. doi:www.eia.gov/forecasts/ieo/pdf/0484(2016).pdf.

[2] Owusu PA, Asumadu-Sarkodie S. A review of renewable energy sources, sustainability issues and climate change mitigation. Cogent Eng 2016;3. doi:10.1080/23311916.2016.1167990.

[3] U.S. Environmental Protection Agency. Inventory of U.S. Greenhouse Gas Emissions and Sinks 1990-2016. n.d.

[4] Sami M, Annamalai K, Wooldridge M. Co-firing of coal and biomass fuel blends. Prog Energy Combust Sci 2001;27:171–214. doi:10.1016/S0360-1285(00)00020-4.

[5] Roni MS, Chowdhury S, Mamun S, Marufuzzaman M, Lein W, Johnson S. Biomass co-firing technology with policies, challenges, and opportunities: A global review. Renew Sustain Energy Rev 2017;78:1089–101. doi:10.1016/j.rser.2017.05.023.

[6] Goerndt ME, Aguilar FX, Skog K. Drivers of biomass co-firing in U.S. coal-fired power plants. Biomass and Bioenergy 2013;58:158–67. doi:10.1016/j.biombioe.2013.09.012.

[7] Nanou P, Carbo MC, Kiel JHA. Detailed mapping of the mass and energy balance of a continuous biomass torrefaction plant. Biomass and Bioenergy 2016;89:67–77. doi:10.1016/j.biombioe.2016.02.012.

[8] Koppejan J, Sokhansanj S, Melin S, Madrali S. Status overview of torrefaction technologies, a review of the commercialisation status of biomass torrefaction. IEA Energy Technol Network, IEA Bioenergy Task 32 2015.

[9] Chen WH, Peng J, Bi XT. A state-of-the-art review of biomass torrefaction, densification,

and applications. Renew Sustain Energy Rev 2015;44:847–66. doi:10.1016/j.rser.2014.12.039.

[10] Cao L, Yuan X, Li H, Li C, Xiao ZZ, Jiang L, et al. Complementary effects of torrefaction and co-pelletization: Energy consumption and characteristics of pellets. Bioresour Technol 2015;185:254–62. doi:10.1016/j.biortech.2015.02.045.

[11] Tumuluru JS, Sokhansanj S, Hess JR, Wright CT, Boardman RD. A review on biomass torrefaction process and product properties for energy applications. Ind Biotechnol 2011;5. doi:10.1089/ind.2011.0014.

[12] Bergman PCA. Combined torrefaction and pelletisation the TOP process. Energy Cent Netherlands, Rep No ECN-C-05-073, ECN, Petten, Netherlands 2005.

[13] Koppejan J, Sokhansanj S, Melin S, Madrali S. Status overview of torrefaction technologies. 2012.

[14] Batidzirai B, Mignot a. PR, Schakel WB, Junginger HM, Faaij APC. Biomass torrefaction technology: Techno-economic status and future prospects. Energy 2013;62:196–214. doi:10.1016/j.energy.2013.09.035.

[15] Pirraglia A, Gonzalez R, Denig J, Saloni D. Technical and Economic Modeling for the Production of Torrefied Lignocellulosic Biomass for the U.S. Densified Fuel Industry. Bioenergy Res 2013;6:263–75. doi:10.1007/s12155-012-9255-6.

[16] Chai L, Saffron CM. Comparing pelletization and torrefaction depots: Optimization of depot capacity and biomass moisture to determine the minimum production cost. Appl Energy 2016;163:387–95. doi:10.1016/j.apenergy.2015.11.018.

[17] Kumar L, Koukoulas AA, Mani S, Satyavolu J. Integrating torrefaction in the wood pellet industry: A critical review. Energy and Fuels 2017;31:37–54.

doi:10.1021/acs.energyfuels.6b02803.

[18] Ghiasi B, Kumar L, Furubayashi T, Lim CJ, Bi X, Kim CS, et al. Densified biocoal from woodchips: Is it better to do torrefaction before or after densification? Appl Energy 2014;134:133–42. doi:10.1016/j.apenergy.2014.07.076.

[19] Peng JH, Bi HT, Sokhansanj S, Lim JC, Melin S. An economical and market analysis of Canadian wood pellets. Int J Green Energy 2010;7:128–42. doi:10.1080/15435071003673518.

[20] Pirraglia A, Gonzalez R, Saloni D. Techno-economical analysis of wood pellets production for U.S. manufacturers. BioResources 2010;5:2374–90. doi:10.15376/BIORES.5.4.2374-2390.

[21] Mani S, Sokhansanj S, Bi X, Turhollow A. Economics of producing fuel pellets from biomass. Appl Eng Agric 2006;22:421–6. doi:10.13031/2013.20447.

[22] Manouchehrinejada M, Mani S. Process Simulation of Integrated Biomass Torrefaction and Pelletization (iBTP) plant. Energy 2018.

[23] Manouchehrinejad M, Mani S. Torrefaction after Pelletization (TAP): Evaluation of torrefied pellet quality and co-products. Biomass and Bioenergy 2018:1–38.

[24] Manouchehrinejad M, Giesen I Van, Mani S. Grindability analysis of torrefied wood chips and wood pellets n.d.:1–35.

[25] PFI Standards Committee. Pellet fuel institute (PFI) standard specification for residential/commercial densified fuel 2011;June.

[26] Bergman PCA, Boersma AR, Zwart RWR, Kiel JHA. Torrefaction for biomass co-firing in existing coal-fired power stations. Energy Cent Netherlands, Rep No ECN-C-05-013, Petten, Netherlands 2005.

[27] Campbell K. A feasibility study guide for an agricultural biomass pellet company. Agric Util Res Institute, St Paul, Minnesota 2007.

[28] Swanson RM, Satrio JA, Brown RC, Hsu DD. Techno-Economic Analysis of Biofuels Production Based on Gasification Techno-Economic Analysis of Biofuels Production Based on Gasification Alexandru Platon. Energy 2010;89:S11–9. doi:10.1016/j.fuel.2010.07.027.

[29] Dutta A, Talmadge M, Hensley J, Worley M, Dudgeon D, Barton D, et al. Techno-economics for conversion of lignocellulosic biomass to ethanol by indirect gasification and mixed alcohol synthesis. Environ Prog Sustain Energy 2012;31:182–90. doi:10.1002/ep.10625.

[30] Sultana A, Kumar A, Harfield D. Development of agri-pellet production cost and optimum size. Bioresour Technol 2010;101:5609–21. doi:10.1016/j.biortech.2010.02.011.

[31] Sahoo K, Mani S, Bilek EM (Ted). Techno-economic and environmental analysis of woodchips and pellets storage systems for a large-scale bioenergy conversion facility 2018:3–9. doi:10.1002/sia.3565.

[32] EIA Energy Information Administration- Independent Statistics and Analysis. Natural Gas Monthly, Selected national average natural gas prices Table 3. US Dep Energy, Washington, DC, Washington, DC 2017.

[33] Okeke IJ, Mani S. Techno-economic assessment of biogas to liquid fuels conversion technology via Fischer-Tropsch synthesis. Biofuels, Bioprod Biorefining 2017;11:472–87. doi:10.1002/bbb.1758.

[34] Li H, Chen Q, Zhang X, Finney K. Evaluation of a biomass drying process using waste heat from process industries: A case study. Appl Therm Enginering 2012;35:71–80.

doi:10.1016/j.applthermaleng.2011.10.009.

[35] Stelte W, Nielsen NPK, Hansen HO, Dahl J, Shang L, Sanadi AR. Pelletizing properties of torrefied wheat straw. Biomass and Bioenergy 2013;49:214–21.

[36] Phanphanich M, Mani S. Impact of torrefaction on the grindability and fuel characteristics of forest biomass. Bioresour Technol 2011;102:1246–53. doi:10.1016/j.biortech.2010.08.028.

[37] Hammer Mill | GEMCO Hammer Milling Grinder | Wood Crusher n.d. http://www.gemcopelletmills.com/hammer-mill.html (accessed August 3, 2018).

[38] Tapasvi D, Khalil R, Skreiberg Ø, Tran KQ, Grønli M. Torrefaction of Norwegian birch and spruce: An experimental study using macro-TGA. Energy and Fuels, vol. 26, 2012, p. 5232–40. doi:10.1021/ef300993q.

[39] Repellin V, Govin A, Rolland M, Guyonnet R, Vincent R, Alexandre G, et al. Energy requirement for fine grinding of torrefied wood. Biomass and Bioenergy 2010;34:923–30. doi:10.1016/j.biombioe.2010.01.039.

[40] Pirraglia A, Gonzalez R, Saloni D, Denig J. Technical and economic assessment for the production of torrefied ligno-cellulosic biomass pellets in the US. Energy Convers Manag 2013;66:153–64. doi:10.1016/j.enconman.2012.09.024.

[41] Polagye BL, Hodgson KT, Malte PC. An economic analysis of bio-energy options using thinnings from overstocked forests. Biomass and Bioenergy 2007;31:105–25. doi:10.1016/j.biombioe.2006.02.005.

[42] Peng JH. A study of softwood torrefaction and densification for the production of high quality wood pellets. Univeristy of British Columbia, Vancouver, Canada, 2012.

[43] Lamers P, Roni MS, Tumuluru JS, Jacobson JJ, Cafferty KG, Hansen JK, et al. Techno-

economic analysis of decentralized biomass processing depots 2015;194:205–13. doi:10.1016/j.biortech.2015.07.009.

[44] Doddapaneni TRKC, Praveenkumar R, Tolvanen H, Rintala J, Konttinen J. Techno-economic evaluation of integrating torrefaction with anaerobic digestion. Appl Energy 2018;213:272–84. doi:10.1016/j.apenergy.2018.01.045.

[45] Peters M, Timmerhaus K. Plant design and economics for chemical engineers. New York McGraw-Hill Chemical engineering Series; 2003.

[46] Agar DA. A comparative economic analysis of torrefied pellet production based on state-of-the-art pellets. Biomass and Bioenergy 2017;97:155–61. doi:10.1016/j.biombioe.2016.12.019.

[47] EIA Energy Information Administration- Independent Statistics and Analysis. Annual coal report 2016, Average Price of Coal Delivered to End Use Sector by Census Division and State, Table 34. US Dep Energy, Washington, DC 2017.

[48] EIA Energy Information Administration- Independent Statistics and Analysis. Densified biomass fuel manufacturing facilities in the United States by state, region, and capacity. US Dep Energy, Washington, DC 2017.

[49] Sahoo K, Bilek EM (Ted), Bergman R, Kizha AR, Mani S. Economic analysis of forest residues logistics options to produce quality feedstocks. Biofuels, Bioprod Biorefining 2018.

[50] IRS. Internal revenue bulletin, Notice 2017–33. Int Revenue Serv 2017.

CHAPTER 7

CONCLUSION AND RECOMMENDATIONS

Conclusion

The global concerns on the increasing rate of energy demand, climate change, fossil fuel depletion, and energy security have been stimulated the countries around the world to search for alternative, sustainable and renewable energy resources to substitute for the fossil fuels. Biomass is a promising carbon carrier resource that can be burned directly as a solid biofuel, or it can convert to other liquid or gaseous biofuels. One of the most attractive near-term applications of the lignocellulosic biomass is co-firing with coal in power generation plants. Electricity generation has the highest contribution to the GHG emission in the United States. Coal-fired power plants contribute about 30% of the total electricity production plants in the united states [1], which corresponds to the annual GHG emission of about 1208 million Mg CO_2 eq. Every metric tonne of enhanced biomass, with the same energy content of the coal, would reduce 2.3 Mg of CO_2eq emission. Nevertheless, the proper pretreatment processes are required to overcome the original biomass drawbacks and to improve its properties to be similar to those for coal. The wood pellet production process is a solely physical pretreatment method that has been widely developed and commercialized around the world. However, the low energy content and fibrous structure of the raw wood pellets impose extra challenges and expenses in downstream process operations, especially in existing coal power generation plants. The combined torrefaction and pelletization process is a proven, rather new technology to alleviate many of the biomass disadvantages such as heterogeneity, high moisture content, high oxygen content, hydrophilic nature, fibrous and difficult

to grind structure, and low energy density. The torrefied pellets as the final product of a combined torrefaction and pelletization process have a higher carbon content, better grindability, and higher energy density. Yet, the availability of biomass feedstock, the optimum energy consumption and expenses to produce torrefied wood pellets, and stringent environmental regulations need to compete with coal in power generation applications. While the conventional integrated torrefaction and pelletization, where biomass is initially torrefied and subsequently densified, has not yet fully developed, in this study we investigated the configuration of torrefied pellet production. In the proposed approach, **t**orrefaction takes place **a**fter **p**elletization (TAP). This approach provides the opportunity to integration torrefaction with the existing wood pellet production plants. The increased bulk density of pellets entering the torrefaction reactor, increases the throughput of the torrefaction system, improves the mass and heat transfer, and significantly reduces the size and capital costs of the torrefaction system. Nevertheless, the properties of the final product still need to be tested and standardized.

In order to investigate the properties of the torrefied pellets produced from the TAP approach, torrefaction experiments were performed on the two types of commercial wood pellets in the temperature range of 200 to 300°C, and chemical and physical properties of the final torrefied pellets, as well as the properties of the torrefaction by-products, were investigated in details. The data gathered from the experiments were directly applied to develop a comprehensive process simulation model to study the overall mass and energy balance, to verify the design parameters of different unit operations, and to determine system efficiencies at different operating conditions and scales. The developed process simulation was used to conduct a techno-economic analysis for different configurations of integrated torrefaction and pelletization processes and compared with the conventional approach.

The process simulation provided the framework to study the torrefaction of different lignocellulosic biomass in a wide temperature range. The several unit operations including combustion, drying, torrefaction, grinding, pelletizing, cooling, and screening were modeled in details and validated by experimental data and with available literature data. The model is applicable for the study any lignocellulosic biomass by incorporating the relevant kinetics and design parameters.

The experimental study on the torrefaction of wood pellets demonstrated the successful production of torrefied pellets even at high temperatures (around 300°C) without compromising the shape and integrity of the pellets. The properties of the torrefied wood pellets were improved at different levels including higher heating value, significant hydrophobicity, better grindability, and higher energy density compared with that of the raw wood pellets. However, the hardness and durability of the torrefied pellets still needed to be enhanced to prevent dust formation, particularly when long-distance transportation is required.

The techno-economic analysis of a TAP process at the production capacity of 100,000 Mg yr^{-1} and torrefaction temperature of 270°C (base case) required the total capital investment of $29.6 million with the total production cost of $166 Mg^{-1} ($6.9 GJ^{-1}), which respectively was about 12% and 3% lower than those of the conventional TOP process at the same capacity. The minimum selling price (MSP) of the TAP pellets at the base case considering 10% IRR for a 15 years period of plant life was $197 Mg^{-1} ($8.1 GJ^{-1}), which was 5% lower than the MSP of the conventional TOP pellets. The feasibility analysis of the different plant capacity (50 to 200 thousand Mg yr^{-1}) showed the non-linear reduction in the total capital investment, production cost, and the minimum selling price. The minimum selling price of the TAP torrefied pellets for a 200,000 Mg yr^{-1} plant capacity was about 177 $ Mg^{-1} and was comparable with the price of regular utility-grade wood

pellets ([2]) with 15% profitability (ROI - Return On Investment). The feedstock cost was the most sensitive parameters on the selling price of the torrefied wood pellets.

Recommendations

The goal of this study was to investigate the systems analysis of the combined torrefaction and pelletization with a new approach of torrefaction after densification. Although the expected objectives have been achieved, future research is recommended to strengthen our proposed approach:

1. To experimentally investigate the proper binder addition to improve the durability of the torrefied pellets. The type of the binder, the place of addition, and the method of the addition need to be optimized.
2. To study the different type of torrefaction reactors, to minimize the retention time, improve the durability, and optimize the final cost.
3. To investigate the impacts of the different type of torrefaction process such as wet torrefaction on the properties of the final products.
4. To improve the reaction simulation model by applying a more detailed FORTRAN compiler, and to investigate different types of torrefaction reactors.
5. To study on the solid densification, explore different effective parameters, and develop a relevant simulation model to consider the input parameters and estimate the energy consumption.
6. To explore for determining the specific grindability parameter for the fibrous biomass particle and study of the particle size impacts on the flowability and rheology of solid biomass on different downstream equipment such as pulverizer and furnaces.

7. To study the simulation of the integrated torrefaction and power generation system to explore the operating conditions, co-firing impacts at different percentage levels, design parameters of further required equipment, and possible optimizations.
8. To study the other applications of torgas (torrefaction by-product) in the potentially integrable systems (such as anaerobic digestion) or to produce valuable chemicals.
9. To explore the other application of torrefied biomass such as biocomposite production.
10. To study on different types of the biomass feedstock and the impacts on the torrefaction kinetics and the overall mass and energy balances.

References

[1] EIA Energy Information Administration- Independent Statistics and Analysis, International Energy Outlook 2017 Overview, U.S. Energy Inf. Adm. IEO2017 (2017) 143. doi:www.eia.gov/forecasts/ieo/pdf/0484(2016).pdf.

[2] EIA Energy Information Administration- Independent Statistics and Analysis, Densified biomass fuel manufacturing facilities in the United States by state, region, and capacity, U.S. Dep. Energy, Washington, DC. (2017). https://www.eia.gov/biofuels/biomass/?year=2017&month=12#table_data (accessed June 24, 2018).

APPENDICES

Supporting information: Torrefaction after Pelletization (TAP): Analysis of torrefied pellet quality and co-products

Water uptake analysis

The water uptake amount of the torrefied pellets at different temperature was studied by immersing each pellet (at least five replications) in water at approximately 1:20 solid to liquid ratio for a specific time at room temperature (Figure. S1.). The hydrophobicity and water stability of the torrefied pellets were improved with increase in the torrefaction temperature. The change in the color of the water was due to the leaching of some dissolved substances from the torrefied pellets at lower torrefaction temperatures.

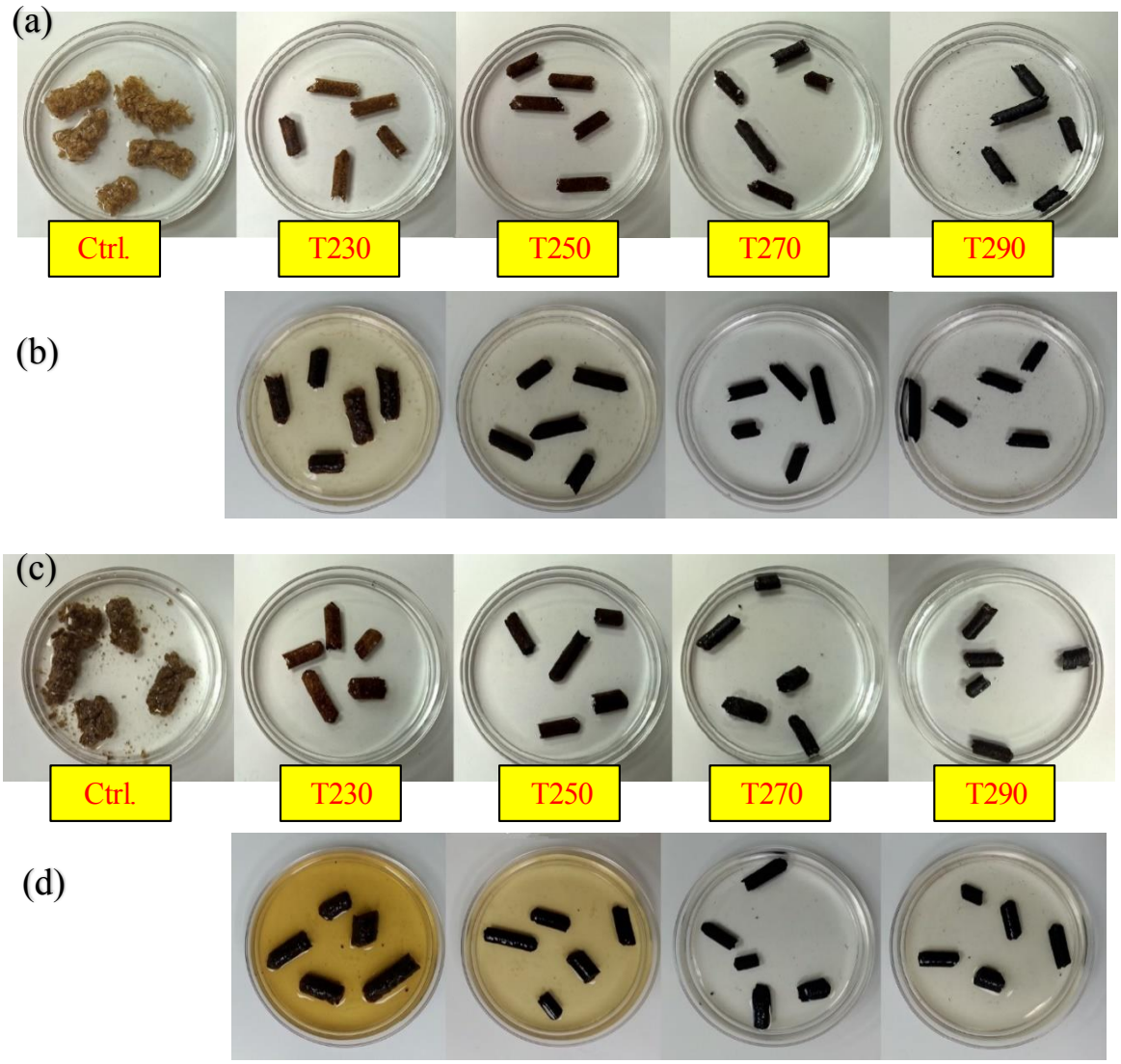

Figure S.1. Water uptake study of torrefied pellet; (a) CP1 pellets immediately after immersion, (b) CP1 pellets after one week, (c) CP2 pellets immediately after immersion, (d) CP2 pellets after one week.

The axial and radial expansion of the torrefied pellets after one-week water immersion

Table S.1. The leaching percentage, axial expansion, and radial expansion of CP1 and CP2 torrefied pellets after water immersion test.

Torrefaction Temperature	Initial density (kg m^{-3})		Density after immersion (kg m^{-3})		Axial expansion (%)		Radial expansion (%)		Mass leaching %	
	CP1	CP2	CP1	CP2	CP1	CP2	CP1	CP2	CP1	CP2
T230	832.6	838.1	722.6	789.8	7.7%	3.4%	-1.9%	-0.8%	3.4%	1.6%
	(218.3)	(116.6)	(61.6)	(74.1)	(12.1%)	(4.0%)	(6.1%)	(9.1%)	(2.8%)	(1.6%)
T250	923.7	952.3	837.2	849.0	9.4%	4.8%	-8.2%	0.0%	6.5%	3.8%
	(225.7)	(320.7)	(151.7)	(54.9)	(7.3%)	(17.2%)	(5.5%)	(1.0%)	(4.4%)	(2.3%)
T270	869.4	898.7	875.1	800.9	-0.7%	5.4%	1.0%	0.2%	0.2%	1.1%
	(48.7)	(217.7)	(54.3)	(139.5)	(4.6%)	(6.2%)	(2.1%)	(3.2%)	(0.5%)	(1.2%)
T290	906.1	700.3	792.0	696.9	4.8%	0.3%	3.6%	-0.1%	0.0%	0.3%
	(154.1)	(31.2)	(58.1)	(39.0)	(7.0%)	(1.5%)	(5.3%)	(0.9%)	(0.0%)	(0.8%)

Number enclosed in the parenthesis are standard deviations with n =5.

GC/MS analysis of the tor-liquid products

Table S.2. Area percentage of abundant components from GC/MS analysis.

	Components	T230		T250		T270		T290	
		CP1	CP2	CP1	CP2	CP1	CP2	CP1	CP2
Acid	Acetic acid	0.77	21.04	17.61	28.96	24.72	28.93	12.56	1.29
	Formic acid	-	-	-	-	6.11	-	1.40	-
	Benzeneacetic acid, 4-hydroxy-3-methoxy-	1.18	-	4.61	0.37	0.82	0.90	0.42	-
	Crotonic acid	-	-	-	-	-	1.64	-	0.46
	3,5-Dimethoxy-4-hydroxyphenylacetic acid	-	-	1.63	-	-	-	0.47	-
Ketone	Acetone	21.21	19.46	10.30	5.23	0.41	11.57	2.51	11.29
	2,3-Butanedione	4.60	0.66	1.49	0.69	2.47	0.57	-	1.14
	2,3-Pentanedione	0.46	-	0.31	-	0.26	0.14	0.23	0.31
	2-Butanone	-	-	-	-	-	0.33	0.22	-
	2-Butanone, 1-(acetyloxy)-	-	-	-	-	0.52	0.59	-	-
	2-Cyclopenten-1-one, 2-hydroxy-3-methyl-	-	1.31	0.35	0.38	2.47	-	-	-
	2-Furancarboxaldehyde, 5-(hydroxymethyl)-	-	-	2.85	-	1.24	-	2.22	-
	2-Furancarboxaldehyde, 5-methyl-	2.83	-	-	2.15	2.68	1.25	1.16	1.29
	2-Furanmethanol	-	-	0.64	0.84	6.11	-	0.00	-
	2-Propanone, 1-(4-hydroxy-3-methoxyphenyl)-	-	-	-	-	1.99	-	0.97	-
	2-Propanone, 1-hydroxy-	3.42	-	2.30	0.93	8.93	-	2.22	12.94
	1-Hydroxy-2-butanone	1.65	-	0.70	-	2.06	-	0.68	-
	Maltol			1.76	0.72	-	-	7.24	-
	5-Acetoxymethyl-2-furaldehyde	0.21	-	1.15	-	0.82	-	-	-
	N-(4-Methoxyphenyl)-2-hydroxyimino-acetamide	-	1.05	-	0.50	-	0.30	-	-
Phenol	Phenol, 2,6-dimethoxy-	0.42	1.60	1.90	3.36	1.72	2.99	2.32	7.29
	Phenol, 2,6-dimethoxy-4-(2-propenyl)-	-	-	0.26	2.43	0.35	2.12	-	3.76
	Phenol, 2-methoxy-	2.36	8.15	4.06	2.71	2.75	1.16	4.83	2.59
	Phenol, 2-methoxy-4-(1-propenyl)-, (E)-	0.94	3.42	-	3.92	-	2.51	-	-
	Phenol, 2-methoxy-4-methyl-	1.53	6.31	1.07	0.87	4.81	0.68	5.31	2.35
	Phenol, 2-methoxy-4-propyl-	-	-	0.80		0.34	-	1.01	-
	Phenol, 4-ethyl-2-methoxy-	0.54	1.47	0.65	0.62	1.17	0.71	5.80	1.29
	2-Methoxy-4-vinylphenol	-	1.05	-	1.03	0.52	0.29	2.32	0.86

	Components	T230		T250		T270		T290	
		CP1	CP2	CP1	CP2	CP1	CP2	CP1	CP2
	5-tert-Butylpyrogallol	0.24	0.84	-	1.21	-	1.35	1.93	3.18
Aldehyde	Furfural	18.86	20.25	14.90	10.28	1.03	14.46	5.80	8.23
	Vanillin	-	-	2.03	0.93	1.10	-	1.93	-
	Ethanone, 1-(4-hydroxy-3-methoxyphenyl)-	-	-	0.53	0.00	0.43	-	2.17	-
	Ethanone, 1-(4-hydroxy-3,5-dimethoxyphenyl)-	-	-	0.22	0.46	-	-	-	-
	3-Buten-2-one, 3-methyl-	-	-	-		-	-	0.18	0.32
	Total	61.22	86.62	72.12	68.60	75.82	72.48	65.90	58.60

Supporting information: Process Simulation of Integrated Biomass Torrefaction and Pelletization (iBTP) plant

Defining a biomass in Aspen Plus

A solid biomass is defined as a non-conventional solid in Aspen Plus software. In general, the thermodynamic properties of the non-conventional components are specified with appropriate enthalpy and density models. In this study, HCOALGEN and DCOALIGT were chosen as enthalpy and density model, respectively, from the existing database in the Aspen Plus. These models were basically proposed for coal but are valid for biomass with a good approximation. For the enthalpy model, there are four sub-models needed to be specified for calculating the Heat of combustion, Standard heat of formation, Heat capacity, and determining the basis condition for the enthalpy. The models, sub-models, and required input data chosen for this study are shown in Table S.3.

Table S.3. Thermodynamic property models chosen for the nonconventional biomass in Aspen Plus [1].

Solid thermodynamic property	Calculation method	Component attributes
Enthalpy model	HCOALGEN	Ul, Pr, Su[a]
Heat of combustion (HHV)	Boie correlation	Ul, Pr, Su
Standard heat of formation (H_f)	Heat of combustion-based correlation	Ul, Su
Heat capacity (cp)	Kirov correlation (1965)	Pr
Enthalpy basis	298.15 K and 1 atm	
Density model	Density of coal (IGT) (1976)	Ul, Su

a Ul: Ultimate analysis, Pr: Proximate analysis, Su: Sulfur analysis

b In this approach, the heat of formation is calculated based on the higher heating value of a nonconventional solid minus the heat of formation for CO_2, H_2O, HCl, and NO_2 at 298.15°K based on stoichiometric ratio.

The ultimate analysis and proximate analysis of raw wood chips and torrefied biomass were obtained from our previous studies [2,3]. The biomass (i.e., pine wood chips) higher heating values calculated based on the Boie correlation were comparable with experimental data (Table S.4).

Table S.4. The comparison of biomass experimental higher heating values with the calculated values based on Bioe correlation.

	Ctrl	T230[a]	T250[a]	T270[a]	T290[a]
Boie Correlation (MJ kg^{-1})[b]	19.66	20.61	21.09	23.26	25.64
HHV experimental (MJ kg^{-1})	20.42	21.38	22.05	22.97	27.1

a T#: Torrefied at #°C. e.g., T230: torrefied at 230°C.

b Boie (MJ kg^{-1}) = $(351.69*Yc+1162.46*Y_H-110.95*Y_O+104.67*Y_S+62.8*Y_N)/1000$.

The heat capacity of non-conventional biomass solid in Aspen Plus is calculated based on kirov correlation [4] using the proximate analysis. Therefore, the proximate analysis of the torrefied biomass should be modified in the simulation model. In order to estimate the proximate values, the higher heating value equation derived from the experimental proximate analysis were put into equal to the higher heating value obtained from the Boie correlation. Then, the volatile matters and fixed carbon were obtained by having the ash content from the elemental composition and constraining the summation of volatile matters, fixed carbon, and ash content to one. The HHV equation fitted on the experimental proximate analysis data is shown as Eq. (S1)

$$HHV\ (MJ\ kg^{-1}) = 1.533 \times VM + 1.878 \times FC - 138.4 \quad \text{(S1)}$$

Where VM is volatile matter (%) and FC is fixed carbon percentage (%).

Dryer: Input parameter calculations

Characteristic Drying Curve

In 1958, Van Meel [1] observed that the drying rate curves, during the falling-rate period, for a specific material often show the same shape at different gas temperature, humidity, and velocity. So, a single characteristic drying curve can be drawn for the material being dried. Many studies have been performed to investigate the different conditions, where characteristic drying curve might be applied [2–4]. Nevertheless, the concept is still to interpolate drying conditions within a particular system (with constant body geometry), and has been used to explore variations in drying behavior within a timber kiln, for example.

The normalized drying rate is defined as:

$$f = \frac{N}{N_m} \tag{S2}$$

Where N is the drying rate, Nm is the rate in the constant-rate period, and the characteristic moisture content becomes:

$$\Phi = \frac{X - X_e}{X_c - X_e} \tag{S3}$$

Where X is the volume-averaged moisture content, Xcr is the moisture content at the critical point, and Xe is that at equilibrium. Thus, the drying curve is normalized to pass through the point (1,1) at the critical point of transition in drying behavior and the point (0,0) at equilibrium. This representation leads to a simple lumped-parameter expression for the drying rate in the falling-rate period.

The defined normalized drying curve can be specified either by a tabular data for normalized solids moisture versus normalized drying rate, or by a shape factor for a drying curve function. The function has this form:

$$\text{Normalized drying rate} = 2F\frac{X}{X_c} - (2F-1)(\frac{X}{X_c})^2 \quad \text{(S4)}$$

Where F is the shape factor for the specified drying curve.

Drying kinetics

The function of the characteristic moisture content of the wood at different drying conditions has been investigated in several studies. In this study, we used the kinetics parameter of wood drying Phanphanich and Mani [5]. The calculated shape factor is 0.49.

$$\Phi = \frac{(X-X_e)}{(X_c-X_e)} = a.\exp(-k.t) \quad \text{(S5)}$$

At T= 80°C, a=0.9044, k= 0.024

X_c=1 (db)

X_e=0.007 (db) (Based on the ZuritZ's sorption isotherm [6]

The shape factor was calculated by fitting the Eq.3 over the experimental data from the Table S.5 which corresponds Eq. (S4).

Table S.5. Kinetics data for drying wood at T=80°C [5].

time (s)	(X-Xe)/(Xc-Xe)	X/Xc	N/Nc (Eq. 4)	Model (Eq. 3)
0	0.904	0.905	0.904	0.904
1	0.883	0.884	0.883	0.882
5	0.802	0.804	0.802	0.801
10	0.711	0.713	0.711	0.710
15	0.631	0.634	0.631	0.630
20	0.560	0.563	0.560	0.559
25	0.496	0.500	0.496	0.496
30	0.440	0.444	0.440	0.440
35	0.390	0.395	0.390	0.391
40	0.346	0.351	0.346	0.347
45	0.307	0.312	0.307	0.309
50	0.272	0.278	0.272	0.274

Mass transfer coefficient calculation

The relevant equation for calculating the mass transfer coefficient are as follows:

$$Re = \frac{u_G . d_P . \rho_G}{\mu_G} \quad \text{(S6)}$$

$$Sc = \frac{\mu_G}{\delta . \rho_G} \quad \text{(S7)}$$

$$Pr = \frac{\mu_G . c_{P,G}}{K_G} \quad \text{(S8)}$$

$$Sh_{lam} = 0.664 . \sqrt{Re} . \sqrt[3]{Sc} \quad \text{(S9)}$$

$$Sh_{turb} = \frac{0.037 . Re^{0.8} . Pr}{1 + 2.433 . Re^{-0.1} . (Pr^{2/3} - 1)} \quad \text{(S10)}$$

$$Sh_{av} = \sqrt{Sh_{lam}^2 + Sh_{turb}^2} \quad \text{(S11)}$$

The required properties of gas inside of the dryer were obtained from the Aspen Plus for calculating the dimensionless numbers of Re, Sc, and Pr. A calculation block with FORTRAN code was incorporated into the model to modify the initial guess for the Sh_{av} number based on Eq. (6) to Eq. (11).

Roller drive motor power

The total power required to drive a rotary drum dryer can be calculated by the Eq. (S12) [7]. The same amount of power was considered for rolling drive motor of the rotary kiln reactor.

$$bhp = \frac{\omega.(4.75.D.W_l + 0.1925.Dr.W_T + 0.33.W_T)}{100{,}000} \quad \text{(S12)}$$

Torrefaction: Input parameter calculations

RPlug mass and energy balance

The pre-defined RPlug reactor was chosen to define the torrefaction reactor. The main goal was conversion of the biomass solid based on the specified kinetics. In the RPlug reactor it is assumed that all reactions take place in the solid phase, therefore temperature and residence time of the solid were the main inputs for the conversion. RPlug uses an integral method over the length of the reactor to solve the mass and energy balance equations. The mass and energy balance of each component is calculated based on the Eq. (S13) and (S14), respectively:

$$\frac{dF}{dZ} = rate\ of\ reaction \times area \quad \text{(S13)}$$

$$\frac{dH}{dZ} = Heat\ transfered\ out\ or\ in\ , function\ of\ U \times \left(T_{process} - T_{thermal}\right).\pi.D \quad \text{(S14)}$$

RPlug integrates these equations using a variable -step-size Gear algorithm and keeping the integration error below a specified tolerance. In Aspen Plus, the components' enthalpies are calculated based on the enthalpy of formation, thus, the heat of reaction is included in the enthalpy difference over the length.

Since the filling grade of the rotary kiln drum and rotational speed are not considered in the RPlug input, it is necessary to modify the heat transfer coefficient and reactor volume.

Heat transfer coefficient calculations in the indirect heating rotary kiln

The heat transfer coefficient of the inside of rotary kiln was calculated based on the Li et al. [8] study. The main two pathways of heat transfer are i) heat transfer from wall to the bulk of the solid (conduction), ii) heat transfer from wall to the freeboard gas and from gas to the bulk of the solid (convection). The heat transfer through radiation mechanism was considered to be neglected since the torrefaction temperature is less than 527°C [9].

The effective heat transfer coefficient between rotating wall and the solid bed can be calculated based on the combination of thin gas film resistance and thermal resistance of the solid bed [8]. In this study we consider χ =0.1.

$$R1 = \frac{1}{h_{wb}} = \frac{\chi . d_p}{k_g} \tag{S15}$$

$$R2 = \frac{1}{h_{sb}} = \frac{0.5}{\sqrt{2. k_b . \rho_b . c_{pb} . \omega / \phi}} \tag{S16}$$

$$h_{ewb} = \frac{1}{Re1} = \frac{1}{R1 + R2} \tag{S17}$$

The heat transfer coefficient from wall to gas and from gas to bed can be written as bellow:

$$R3 = \frac{1}{h_{wg}} = \frac{d_e / k_g}{1.54\ Re_g^{0.575} Re_\omega^{-0.292}} \tag{S18}$$

$$R4 = \frac{1}{h_{gb}} = \frac{d_e / k_g}{0.46\ Re_g^{0.535} Re_\omega^{0.104} \eta^{-0.341}} \tag{S19}$$

$$h_{ewg} = \frac{1}{Re2} = \frac{1}{R3 + R4} \tag{S20}$$

According to the thermal resistance analogy, the total heat transfer coefficient of the rotary kiln inside is:

$$h = \frac{1}{Req} = \frac{1}{Re1} + \frac{1}{Re2} \tag{S21}$$

Residence time and length of the torrefaction reactor

Aspen Plus calculates the residence time of the RPlug reactors by dividing the total volume over the sum of constituents' molar volume flowrate (Eq. (S22)). Residence time is the main input for the reaction kinetics and it is an equal value for the all phases in the reactor. In the existing approach in Aspen Plus, since the molecular weight of non-conventional solid is assumed as one (1 g/gmole), residence time is calculated mainly based on the volume flowrate of the gas phase (torgas produce from the reactions) and not the solid phase. Although the calculated residence time is the equal value for both phases, it is required higher volume to reach the specified residence time (e.g. 30 min.). Therefore, the real length based on the volume flow rate of the solid need to be recalculated.

$$\tau_k = \frac{\pi . D^2}{4} . \int_{Z=0}^{Z=L} \frac{dZ}{F_Z . V_Z} \tag{S22}$$

The modified length of the reaction section was calculated based on the solid volume flow rate in the reactor and residence time of the reaction in the solid phase (Eq. (S23)). The Filling grade and rotational speed of the kiln have been already considered in the calculation of heat transfer coefficient Eq. (S21):

$$L_k = \frac{\left(\dot{M}_S/\rho_S\right)_{av} \times \tau_k}{(D_h^2 \times \pi \times 0.25 \times (1 - \varepsilon) \times \psi)} \tag{S23}$$

There is no reaction in the heat-up zone, and the relevant length is corresponding to the required area based on heat duty for heat-up and evaporation of water in the solids, heat transfer

coefficient, and logarithmic average of the temperature difference between the solid and external hot gas stream along the heating zone (LMTD). The relevant residence time can be estimated by Eq. (3) in the main text for the rotary kiln reactors. By keeping the LMTD at the high value and having the residence time, the heating rate of between 50 to 100°C min^{-1} (based on the temperature difference between torrefaction set-point and biomass input temperature) was achieved in all cases. The total length of the kiln reactor is the summation of length of heat-up zone and modified length from Eq. (S23).

Composition of pseudo components of V1 and V2

The composition of pseudo components of V1 and V2 are required to calculate the composition of intermediate and final solid products. In the Bates and Ghoneim [10] approach, the fractional composition of pseudo components of V1 and V2 are fixed within the range of torrefaction (usually between 200-300°C) and are calculated by fitting the model results (volatile yields) and experimental data (total torgas composition) through the least square solution [10,11]. For a pinewood feedstock the experimental data of torgas compositions and model yields (based on the Prins [12] kinetics) are shown in Table S.6.

$$\begin{bmatrix} W_{V1}^{230} & W_{V2}^{230} \\ W_{V1}^{250} & W_{V2}^{250} \\ W_{V1}^{270} & W_{V2}^{270} \\ W_{V1}^{290} & W_{V2}^{290} \end{bmatrix} \begin{bmatrix} Y_{a,V1} & Y_{b,V1} & \dots & Y_{l,V1} \\ Y_{a,V2} & Y_{b,V2} & \dots & Y_{l,V2} \end{bmatrix} = \begin{bmatrix} Y_a^{230} & Y_b^{230} & \dots & Y_l^{230} \\ Y_a^{250} & Y_b^{250} & \dots & Y_l^{250} \\ Y_a^{270} & Y_b^{270} & \dots & Y_l^{270} \\ Y_a^{290} & Y_b^{290} & \dots & Y_l^{290} \end{bmatrix}$$

The W_{V1}^{230} to W_{V2}^{290}, are normalized weight fractions of pseudo components based on the model at different torrefaction temperatures. The Y_a^{230} to Y_l^{290} are the normalized compositions of spices a to l (water to CH_4,) at different temperature experiment. The fixed compositions of pseudo components V1 and V2 including $Y_{a,V1}$ to $Y_{l,V2}$ were calculated based on the least square solution with the additional conditions as follow:

$$\sum_{j=a}^{j=l} Y_{j,V1=1} , \sum_{j=a}^{j=l} Y_{j,V2=1}, Y_{j,V1}, Y_{j,V2} \geq 0 \quad \text{(S24)}$$

Table S.6. Volatile composition of pine torrefaction at different temperature based on the experimental data from GC/TCD (for non-condensable products) and HPLC (for condensable products).

Torrefaction temperature	°C	230	250	270	290
Yields of pseudo components based on Prins et al. kinetics.					
Solid yield (%wt)	%wt	89.01	84.79	71.81	58.85
W_{V1}, yield (%wt)	%wt	10.31	13.97	21.25	26.90
W_{V2}, yield (%wt)	%wt	0.68	1.24	6.94	14.25
Volatile compositions from experiments for 30 min residence time of torrefaction					
Water	%wt	3.65	7.76	11.52	13.42
Levoglucosan	%wt	0.57	1.31	3.06	4.54
Formic acid	%wt	0.25	0.71	0.99	1.85
Acetic acid	%wt	0.11	0.26	0.31	0.49
Hydroxyacetone	%wt	0.07	0.22	0.77	1.43
Acetone	%wt	0.05	0.02	0.02	0.10
5-HMF	%wt	0.01	0.04	0.03	0.22
Furfural	%wt	0.06	0.18	0.60	2.32
2-methoxyphenol	%wt	3.18E-03	0.01	0.02	0.09
CO	%wt	0.93	1.06	3.66	5.92
CO_2	%wt	5.30	3.64	7.17	10.66
CH_4	%wt	0.00	0.00	0.05	0.12
Total Volatile	%wt	10.99	15.21	28.19	41.15
Solid yield	%wt	89.01	84.79	71.81	58.85

Dryer sensitivity analysis

Dryer length

Fixed parameters:		
Diameter	2.4	m
Feed flowrate	32900	kg h^{-1}
Inlet biomass MC	50	%
Inlet Biomass temperature	25	°C
NG mass flow rate	1011	kg h^{-1}
Inlet air RH	50	
Hot gas temperature	450	°C

Length	DRYSWOOD Temp	DRYSWOOD SOLID MC	TOCYC Gas Temp	EXHAUST Temp	TOCYC Gas RH	EXHAUST RH	Dryer Residence time	NTU
m	°C	Kg Kg Dry $^{-1}$	°C	°C	%	%	min	
10.0	71.0	0.1	86.6	93.8	36.9	29.5	5.7	2.7
11.0	70.6	0.1	83.4	90.5	42.3	33.6	5.7	2.8
12.0	70.2	0.1	80.7	87.9	47.3	37.5	5.7	2.9
13.0	69.8	0.1	78.6	85.7	51.9	41.0	5.7	3.1
14.0	69.4	0.1	76.8	83.9	56.1	44.3	5.7	3.2
15.0	69.1	0.1	75.3	82.3	59.9	47.2	5.7	3.3
16.0	68.7	0.1	74.0	81.1	63.4	49.9	5.7	3.4
17.0	68.4	0.1	73.0	80.0	66.5	52.3	5.7	3.4
18.0	68.1	0.1	72.0	79.0	69.3	54.4	5.7	3.5

Dryer diameter

Fixed parameters:		
Length	14	m
Feed flowrate	32900	kg h^{-1}
Inlet biomass MC	50	%
Inlet Biomass temperature	25	°C
NG mass flow rate	1011	kg h^{-1}
Inlet air RH	50	
Hot gas temperature	450	°C

Diameter	DRYSWOOD Temp	DRYSWOOD SOLID MC	TOCYC Gas Temp	EXHAUST Temp	TOCYC Gas RH	EXHAUST RH	Dryer Residence time	NTU
m	°C	Kg Kg Dry $^{-1}$	°C	°C	%	%	min	
1.4	71.8	0.2	95.4	102.8	25.9	20.8	5.7	2.4
1.7	71.0	0.1	86.5	93.8	37.0	29.5	5.7	2.7
2.0	70.4	0.1	81.6	88.8	45.5	36.1	5.7	2.9
2.2	69.8	0.1	78.4	85.5	52.2	41.3	5.7	3.1
2.4	69.4	0.1	76.8	83.8	56.1	44.3	5.7	3.2
2.5	69.3	0.1	76.2	83.3	57.5	45.4	5.7	3.2
2.7	68.9	0.1	74.6	81.6	61.8	48.7	5.7	3.3
2.8	68.5	0.1	73.3	80.4	65.4	51.4	5.7	3.4
3.0	68.2	0.1	72.3	79.3	68.4	53.7	5.7	3.5
3.2	67.9	0.1	71.5	78.5	71.0	55.7	5.7	3.6

Hot gas temperature

Fixed parameters:		
Geometry	2.4 x 14	m
Feed flowrate	32900	kg h^{-1}
Inlet biomass MC	50	%
Inlet Biomass temperature	25	°C
NG mass flow rate	1011	kg h^{-1}
Inlet air RH	50	

HOTGASIN Temp	DRYSWOOD Temp	DRYSWOOD SOLID MC	TOCYC Gas Temp	EXHAUST Temp	TOCYC Gas RH	EXHAUST RH	Dryer Residence time
°C	°C	Kg Kg-Dry $^{-1}$	°C	°C	%	%	min
200	53.3	0.2	58.7	65.6	57.0	43.7	5.7
250	57.5	0.2	63.2	70.1	57.8	44.7	5.7
300	61.0	0.1	67.1	74.0	58.1	45.2	5.7
350	64.1	0.1	70.5	77.6	57.8	45.2	5.7
400	66.9	0.1	73.8	80.8	57.1	44.9	5.7
450	69.4	0.1	76.8	83.9	56.1	44.3	5.7
500	71.8	0.1	79.6	86.7	54.9	43.5	5.7
550	73.9	0.1	82.4	89.5	53.5	42.6	5.7
600	76.0	0.1	85.0	92.1	51.9	41.5	5.7
650	77.9	0.1	87.6	94.7	50.3	40.4	5.7
700	79.7	0.1	90.0	97.2	48.7	39.2	5.7
750	81.4	0.0	92.4	99.5	47.1	38.1	5.7
800	82.9	0.0	94.7	101.9	45.5	36.9	5.7
850	84.4	0.0	96.9	104.1	43.9	35.7	5.7
900	85.7	0.0	99.1	106.3	42.4	34.6	5.7

Natural gas flow rate to the burner

Fixed parameters:		
Geometry	2.4 x 14	m
Feed flowrate	32900	kg h^{-1}
Inlet biomass MC	50	%
Inlet Biomass temperature	25	°C
Inlet air RH	50	
Hot gas temperature	450	°C

NATGAS mass flow	DRYSWOOD Temp	DRYSWOOD SOLID MC	TOCYC Gas Temp	EXHAUST Temp	TOCYC Gas RH	EXHAUST RH	Dryer Residence time	NTU
kg h^{-1}	°C	Kg Kg Dry $^{-1}$	°C	°C	%	%	min	
800.0	64.7	0.3	69.9	76.8	75.1	58.8	5.7	3.7
887.5	65.8	0.2	72.1	79.1	68.5	53.8	5.7	3.5
975.0	67.9	0.1	75.1	82.2	60.3	47.5	5.7	3.3
1011.2	69.4	0.1	76.8	83.9	56.1	44.3	5.7	3.2
1062.5	72.9	0.1	79.9	87.1	49.0	38.8	5.7	3.0
1150.0	85.8	0.0	89.2	96.5	33.2	26.6	5.7	2.6
1237.5	104.5	0.0	104.6	112.2	18.2	14.8	5.7	2.2
1325.0	120.1	0.0	120.1	128.0	10.4	8.6	5.7	1.8
1412.5	134.3	0.0	134.3	142.4	6.5	5.4	5.7	1.6
1500.0	147.3	0.0	147.3	155.7	4.3	3.6	5.7	1.5

Volume flowrate of hot gas in the dryer

Fixed parameters:		
Geometry	2.4 x 14	m
Feed flowrate	32900	kg h^{-1}
Inlet biomass MC	50	%
Inlet Biomass temperature	25	°C
NG mass flow rate	1011	kg h^{-1}
Inlet air RH	50	
Hot gas temperature	450	°C

Volume flowrate	DRYSWOOD Temp	DRYSWOOD SOLID MC	TOCYC Gas Temp	EXHAUST Temp	TOCYC Gas RH	EXHAUST RH	Dryer Residence time	NTU
m^3 h^{-1}	°C	Kg Kg-Dry $^{-1}$	°C	°C	%	%	min	
122297.0	67.6	0.1	70.7	77.6	73.7	57.8	5.7	3.7
123493.0	69.1	0.1	75.3	82.4	59.8	47.1	5.7	3.3
123866.0	69.4	0.1	76.8	83.9	56.1	44.3	5.7	3.2
124574.0	70.0	0.1	79.5	86.7	49.8	39.4	5.7	3.0
125565.0	70.6	0.1	83.4	90.6	42.2	33.6	5.7	2.8
126476.0	71.1	0.1	87.0	94.2	36.4	29.0	5.7	2.7
127325.0	71.4	0.1	90.3	97.6	31.7	25.4	5.7	2.5
128115.0	71.7	0.2	93.4	100.8	28.0	22.5	5.7	2.4
128860.0	71.8	0.2	96.3	103.8	25.0	20.1	5.7	2.4
129562.0	72.0	0.2	99.1	106.6	22.4	18.1	5.7	2.3

Nomenclature

A: Pseudo component
AS: Surface area (m^2)
B: Pseudo component
Bhp: Break horse power (hP)
BWI: Bond work index
C: Pseudo component
c_{pb}: Specific heat capacity of solid bed (J kg^{-1} K^{-1}). $c_{pb} = (1-\varepsilon).c_{ps} + \varepsilon.c_{pg}$
c_{pg}: Specific heat capacity of gas (J kg^{-1} K^{-1})
c_{ps}: Specific heat capacity of solid (J kg^{-1} K^{-1}).
d_e: Hydrodynamic diameter of the gas phase domain (m). $d_e = 0.5\ D\ (2\pi - 2\phi + sin2\phi)/(\pi - \phi + sin\phi)$
d_{gw}: Geometric mean diameter (mm)
d_p: Effective particle diameter (m)
db: Dry basis
D: Inside diameter of rotary kiln /drum (m)
D_h: Hydraulic diameter of the annulus rotary kiln (m)
Dr: Riding-ring diameter (ft). Dr= D +2
E_e: Electrical energy input
E_{th}: Thermal energy input
F: Shape factor for the specified drying curve.
H: bed height (m)
HHV: Higher heating value (MJ kg^{-1})
h: Heat transfer coefficient of rotary kiln inside (W m^{-2} K^{-1})
k: Reaction rate (s^{-1})
k: Thermal conductivity (W m^{-1} K^{-1})
k_b: Thermal conductivity of solid bed (W m^{-1} K^{-1}). $k_b = (1-\varepsilon).k_s + \varepsilon.k_g$
L: Length (m)
L_c: Characteristic length (m)
LHV: Lower heating value (MJ kg^{-1})
$\dot{M}$: Mass flow rate (kg h^{-1}), (kg s^{-1})
N: Drying rate
N_m: Drying rate in the constant-rate period
Q_{loss}: Rate of heat loss (W)
R: Universal gas constant (J mol^{-1} K^{-1}).
R_k: Kiln radius (m)
Re_g: Reynold number for gas in axial direction. $Re_g = \frac{u_g d_e}{\nu}$
Re_ω: Reynolds number for gas in rotational direction. $Re_{g\omega} = \frac{d_e^2 \omega}{\nu}$
RH: Relative humidity (%)
T: Temperature (°C or °K)
u_g: Gas velocity inside of the rotary kiln (m s^{-1})
V1: Pseudo component
V2: Pseudo component

V_d: Volume of dryer (m^3)
W_l: Live load (material) (kg or lb)
W_T: Total rotating load (equipment plus material) (kg or lb)
wb: Wet basis
X: Moisture content
X_c: Moisture content at the critical point
X_e: Moisture content at equilibrium
Y_M: Mass yield (%)
Y_E: Energy yield (%)
Greek symbols
α: Slope of the rotary kiln/drum (rad)
β: Kinetic ratio
β_G: Mass transfer between the surface of the particle and gas
γ: Kinetic ratio
δ: Diffusion coefficient of the vapor in the gas ($m^2\ s^{-1}$)
ε: Porosity
η: Relative fill level. $\eta = (2\phi - \sin(2\phi))/2\pi$
μ: Dynamic viscosity of gas/thermal fluid ($kg\ m^{-1}\ s^{-1}$)
ν: Kinematic viscosity of gas/thermal fluid ($m^2\ s^{-1}$)
ν: Kinetic ratio
ξ: Kinetic ratio
ρ_b: Bulk density of solid bed ($kg\ m^{-3}$)
ρ_g: Density of gas ($kg\ m^{-3}$)
ρ_p: Particle density ($kg\ m^{-3}$)
τ: Residence time (s or min)
ϕ : Half central angle of the solid bed section (rad). $\phi = cos^{-1}[\frac{(R_k - H)}{R_k}]$
Φ: Characteristic moisture content
χ : Thickness of the gas film between the wall and solid bed as the fraction of the particle diameter. In this study we considered χ =0.1.
ψ: Filling grade
ω: Rotation speed (s^{-1}), or rpm
Dimensionless numbers
Bi: Biot number
$P\acute{y}$: Pyrolysis number
Pe: Peclet number
Re: Reynolds number
Sc: Schmitt number
Pr: Prandtl number
Sh: Sherwood number

Subscripts
amb: Ambient (25°C)
av: Average
c: Critical
conv: Convection
k: Kiln
s: Solid
g: Gas
lam: Laminar
tor : Torrefaction/ torrefied
turb: Turbulent
wb: Wall to bed through thin gas film
sb: Wall to solid
ewb: Effective from wall to
wg: Wall to freeboard gas
gb: Gas to solid bed
ewg: Effective wall to bed through freeboard gas
NG: Natural gas